Novel Biomarkers for Arthritis

The role of P2X7 receptor in transglutaminase 2 export and activation

Rhiannon Griffiths, B.Sc.

School of Dentistry

Cardiff University

2017

Thesis submitted for the degree of Doctor of Philosophy

NOTICE OF SUBMISSION FORM

SECTION A: TO BE COMPLETED BY THE CANDIDATE AND SUBMITTED WITH THE THESIS			
Candidate's last name	Griffiths		
Candidate's first name(s)	Rhiannon		
Candidate's student number	C1345783		
School	DENTL		
Title of degree	Please circle appropriate degree title: DAHP, DClinPsy, DEdPsy, DHS, DSW, DNurs, EdD, EngD, MD, MPhil, MScD by Research, PhD, SPPD		
Full title of thesis	Biomarkers for Arthritis: The role of P2X7 receptor in transglutaminase 2 export and activation		
Is this a resubmission?	NO		
Is a Bar on Access or library deposit required?	Bar on Access: YES Library deposit: NO If YES, please attach your application form or approval confirmation. For guidance and forms, please see: http://learning.cf.ac.uk/quality/pgr/code/thesis-preparation-and-examination/uploading-your-thesis-to-orca-important-information/		
Candidate's signature	R Griffiths	Date	29/06/17

The completed form and all relevant supporting documentation should be returned to:

schoolrecords@cardiff.ac.uk or Student Records Team, Registry, 30-36 Newport Road, Cardiff, CF24 0DE.

ANNEX 1:
Specimen layout for Declaration/Statements page to be included in a thesis.

DECLARATION

This work has not been submitted in substance for any other degree or award at this or any other university or place of learning, nor is being submitted concurrently in candidature for any degree or other award.

Signed ..... (candidate) Date 29/06/17

STATEMENT 1

This thesis is being submitted in partial fulfillment of the requirements for the degree of PhD (insert MCh, MD, MPhil, PhD etc, as appropriate)

Signed ..... (candidate) Date 29/06/17

STATEMENT 2

This thesis is the result of my own independent work/investigation, except where otherwise stated, and the thesis has not been edited by a third party beyond what is permitted by Cardiff University's Policy on the Use of Third Party Editors by Research Degree Students. Other sources are acknowledged by explicit references. The views expressed are my own.

Signed ..... (candidate) Date 29/06/17

STATEMENT 3

I hereby give consent for my thesis, if accepted, to be available online in the University's Open Access repository and for inter-library loan, and for the title and summary to be made available to outside organisations.

Signed ..... (candidate) Date 29/06/17

STATEMENT 4: PREVIOUSLY APPROVED BAR ON ACCESS

I hereby give consent for my thesis, if accepted, to be available online in the University's Open Access repository and for inter-library loans **after expiry of a bar on access previously approved by the Academic Standards & Quality Committee.**

Signed ..... (candidate) Date 29/06/17

Acknowledgements

I would like to thank my supervisor, Professor Daniel Aeschlimann, for his advice and guidance throughout my PhD. I would also like to thank Professor Arwyn Jones for his support. I am grateful to have had a great group to work in, and thanks go especially to Dr Magdalena Adamczyk for her help throughout this project. Thanks to the other members of the group; Shannon Turberville, Ana Mafalda Jegundo dos Reis, and Dr Andreas Heil for their companionship and advice. Thanks also to Dr Vera Knauper and Dr Sharon Dewitt for their support and patience. Much of this work could not have been completed without the blood donors, I am thankful for their willingness to play an important role in my research.

I would like to gratefully acknowledge my funders, the Arthritis research UK Biomechanics and Bioengineering centre and the Cardiff University President's research scholarship for providing the grants allowing this work to be carried out.

I would like to thank family for being there for me throughout this process; My parents, for their encouragement and belief in me throughout, - Mum, it's nearly time to relax now – my brothers and their partners, Adam and Stef, Alex and Amy and Ewan and Holly, for providing support and distraction, I am looking forward to having more time to spend with you all. My grandparents, aunts and uncles have always been encouraging, but a special mention is reserved for Uncle Tom, who has provided invaluable support to my mum during my PhD, thanks for your advice and support.

I wouldn't have been able to do this without the unwavering support of my partner, John, thank you for always being there and making me laugh, even on the most stressful days. My second family, the Shea's, and friends, of whom there are too many to list, have all been part of a strong support network, providing encouragement and friendship. An especially big thank you goes to Rae, Rosie and Claire, keep your diaries free, I'll see you all soon

Abstract

Transglutaminase 2 (TG2)-mediated stabilization of extracellular protein assemblies has a pivotal function in tissue repair. However, aberrant TG2 activity has been linked to fibrosis and autoimmunity. There is also evidence that post-translational modification of proteins can occur in a manner that is specific to disease, for example citrullinated peptides seen in rheumatoid arthritis. TG2 modifies proteins in several ways, including through transamidation, esterification and deamidation of target glutamine residues. There is evidence of increased expression and activity of TG2 in osteoarthritis, potentially leading to the generation of protein modifications, which could act as biological markers of disease. The mechanism of TG2 release by cells controls its extracellular activity is unconventional and enigmatic. Our group has shown that TG2 export is linked to purinergic signalling, and implicated P2X7 receptor activation. P2X7R has several activation states; ATP stimulation causes ion channel opening, allowing membrane depolarization and Ca^{2+} entry into the cell. Prolonged stimulation leads to 'large membrane pore' activity, however the identity of this pore is unknown as there is conflicting evidence suggesting either dilation of the P2X7R channel itself or an interaction with an alternative plasma membrane channel.

The aim of this thesis is to elucidate mechanistically the process by which cells export TG2 and control its activation, alongside investigating the P2X7R pore. We have also looked at the involvement of GTP regulation of TG2 activity in its secretion and whether the TG2 activator, thioredoxin, can be secreted via the same pathway.

Through the use of pharmacological agents, we have shown that pannexin-1, a plasma membrane hemichannel proposed to interact with P2X7R, is unlikely to be the pore-forming component of P2X7R activation. A gain of function mutation in P2X7R expressed in HEK293 cells shows enhanced TG2 externalization from cells, correlating with increased pore activity, implicating P2X7R itself. Thioredoxin, a TG2 activator, is co-secreted. To confirm the transferability of our findings in this cell model to the innate immune response, human peripheral blood monocytes were differentiated into M1 macrophages and P2X7R mediated TG2 export assessed. Investigating this process will unravel a novel secretory pathway potentially used by select proteins, including potent signals regulating inflammation.

Table of Contents

List of Abbreviations

ADAMs	- a disintegrin and metalloproteinase proteins
ADP	- Adenosine 5'-diphosphate
AMP	- Adenosine 5'monophosphate
ATP	- Adenosine 5'-triphospate
BzATP	- 3'-O-(4-benzoyl)benzoyl adenosine 5'-triphosphate
CC2-DMPE	- Coumarin phospholipid
CNS	- Central nervous system
COMP	- Cartilage oligomeric protein
COPI/II	- Coat protein complex I/II
CTX-II	- Collagen type II C-telopeptide
DAPI	- 4',6-diamidino-2-phenylindole
$DiSBAC_2(3)$	- Bis-(1,3-Diethylthiobarbituric acid) trimethine oxonol
DMEM	- Dulbecco's modified Eagle's medium
DMSO	- Dimethyl sulfoxide
DTT	- Dithiothreitol
ECM	- extracellular matrix
EDTA	- ethylene diamine tetraacetic acid
EGFR	- Epidermal growth factor receptor
EGTA	- Ethylene glycol tetraacetic acid
ELISA	- Enzyme-linked immunosorbent assay
ER	- endoplasmic reticulum
FBS	- fetal bovine serum
FGF2	- Fibroblast growth factor 2

FRET - Fluorescence resonance energy transfer

FXIII - factor XIII

GDP - guanosine 5’ diphosphate

GFP - Green fluorescent protein

GM-CSF - granulocyte macrophage colony-stimulating factor

GPR56 - G-protein coupled receptor 56

GRASP - golgi reassembly-stacking protein

GRK3 - G-protein coupled receptor kinase 3

GTP - guanosine 5’ triphosphate

G protein - guanine nucleotide-binding proteins

HEK293 - Human embryonic kidney cells 293

HEPES - 4-(2-hydroxyethyl)-1-piperazineethanesulfonic acid

HLA - human leukocyte antigen

HRP - horseradish peroxidase

IL - interleukin

JSN - Joint space narrowing

LB - Luria-Bertani medium

LPS - Lipopolysaccharide

LRP1 - lipoprotein receptor-related protein 1

MDC - Monodansylcadaverine

MMP - Matrix metalloproteinase

MRI - Magnetic resonance imaging

MW - Molecular weight

NEM - N-ethylmaleimide

NFκB	- nuclear factor kappa-light chain enhancer of activated B cells
NLRP3	- NLR (NACHT, LRR and PYD) domain-containing protein 3
NMDG	- N-methyl-D-glucamine
NSAIDs	- non-steroidal anti-inflammatory drugs
OA	- osteoarthritis
OptiMEM	- modified eagle's minimum essential medium
P2XR	- ligand gated ion channel
PKCα	- Protein Kinase Cα
PMSF	- phenylmethylsulfonyl fluoride
PSS	- physiological salt solution
RA	- rheumatoid arthritis
RPMI 1640	- Roswell Park Memorial Institute 1640 medium
SDS	- sodium dodecyl sulphate
PAGE	- polyacrylamide gel electrophoresis
SH3	- Src homology 3 domain
SNP	- Single nucleotide polymorphism
SP1	- apoptotic transcription factor
TG	- transglutaminase
TGF-β	- transforming growth factor-β
TKR	- Total knee replacement
TLR	- Toll-like receptor
TM	- transmembrane
TNF-α	- Tumor necrosis factor-α
TRX	- Thioredoxin

TRXR - Thioredoxin reductaseUDP - Uridine 5’diphosphate

Chapter 1

1. Introduction

1.1 Arthritis

The two main forms of arthritis are rheumatoid arthritis (RA) and osteoarthritis (OA), with one quarter of the adult population affected by one of the many forms of arthritis (Barbour *et al.* 2017). RA is an autoimmune disease, in which the joints are infiltrated by activated immune cells causing inflammation, active tissue destruction and pain due to secretion of cytokines (van Kuijk *et al.* 2006). RA is the second most common joint disease in humans, affecting around 400 000 adults in the UK, with around three times as many women affected as men[1]. The symptoms commonly include joint pain and swelling and stiffness. Genetics play a role in the likelihood of someone developing RA, but lifestyle factors, such as obesity or smoking, also determine whether the disease will develop (Symmons *et al.* 2016). The strongest genetic driver of RA is the human leukocyte antigen (HLA)-DRB1, of which having certain alleles is more likely to result in RA (Newton *et al.* 2004). RA can be diagnosed using an anti-citrullinated peptide antibody test (Kastbom *et al.* 2004). Joint damage can be detected by x-ray to confirm the presence of joint disease as well as showing the progression. RA is treated through a combination of pain management (analgesics and non-steroidal anti-inflammatory drugs (NSAIDs)), steroids to reduce inflammation, disease modifying drugs, physical therapy, and surgery to replace joints if necessary.

OA on the other hand has historically been thought to be caused by gradual wearing away of the connective tissue in the joint, usually also causing pain and inflammation secondarily. OA affects approximately 250 million people worldwide, with prevalence increasing with age, however, 64% of people with OA are considered to be of working age (15-64 years) (Hunter *et al.* 2014). This fact, combined with the fact that 43% of people with arthritis have activity limiting symptoms, indicates that there will be a significant economic burden of OA, due to the loss of work hours (Hunter *et al.* 2014). The main cause is excessive joint loading (for example due to obesity) or joint injury (often seen in athletes) (Loeser *et al.* 2012). Therefore, the incidence is projected to increase with increasing obesity and as the average age of the population rises, also

[1]http://www.arthritisresearchuk.org/arthritis-information/conditions/rheumatoid-arthritis/causes.aspx

increasing the strain on healthcare services (Hunter *et al.* 2014). Although OA can be associated with these factors, there are also genetic factors that strongly contribute to predisposition to OA. These are often found to be single nucleotide polymorphisms (SNPs), which have been demonstrated to link to OA in a specific joint (Loughlin 2015). For example, a SNP in the 3' untranslated region of *ALDH1A2*, which codes for an enzyme involved in retinoic acid synthesis, was found to be connected to hand OA, but not OA at other sites (Styrkarsdottir *et al.* 2014). This SNP results in reduced expression of the enzyme, which may alter the retinoic acid levels (Styrkarsdottir *et al.* 2014). Retinoic acid is a signalling molecule with roles in skeletogenesis, which may relate to the involvement of this polymorphism in OA. Hip OA has been linked to a SNP upstream of two candidate genes in OA; nuclear receptor co-activator 3 (*NCOA3*, roles in DNA modification which can result in altered gene expression) shows reduced expression in OA cartilage and heparan sulfate 6-O endosulfatase 2 (*SULF2*, removes 6-O sulfate groups from heparan sulfate, affecting binding to signalling molecule, thereby altering the roles of heparan sulfate) shows increased expression in OA cartilage, indicating that expression level changes in these genes may contribute to OA (Otsuki *et al.* 2008; Evangelou *et al.* 2014). This indicates that different patients are likely to have different genetic factors driving the OA symptoms, suggesting that patient stratification based on these may be beneficial in treatment of the disease.

Although OA is the most common form of arthritis, there is currently no definitive molecular or biochemical diagnostic test, with symptoms, functional deficits and ultimately imaging being the only way to diagnose the disease (Lane *et al.* 2011). Current guidelines state that an OA diagnosis can be confirmed without further investigation if the person is 45 and over, has activity related joint pain and does not have morning-related joint stiffness (NICE 2014). As a result, OA is usually only diagnosed once the destruction of the joint tissue is irreversible, meaning that there is a requirement for identification of biomarkers specific to the early osteoarthritic process to aid much earlier diagnosis and intervention prior to tissue destruction (Lane *et al.* 2011). This medical need is compounded by the lack of effective therapies for progressing OA at present, with management of the disease currently being palliative i.e. by physiotherapy and painkillers prior to surgery to replace the affected joint with an implant (Lane *et al.* 2011). Patients are also advised to lose weight and exercise,

with the latter partly aimed at strengthening muscles local to the affected joint (NICE 2014). Identification of reliable biomarkers could also facilitate development of new approaches to therapy, through acting as reliable, measurable indicators of the success of therapeutic intervention (Lane *et al.* 2011). For example, currently, disease modifying OA drugs in clinical trials use radiographic joint space narrowing (JSN) as the measurable indicator of clinical efficacy (Hunter *et al.* 2014). This requires large sample sizes and a long period (2-3 years) to demonstrate the benefit of a new therapy. Discovery of an OA biomarker capable of demonstrating efficacy over a shorter time-period would therefore allow quicker analysis of potential therapeutics, possibly increasing the likelihood of discovery of a disease modifying therapeutic (Hunter *et al.* 2014).

1.2 Pathology of OA

OA affects all the structures of the joint and respective cells including chondrocytes, osteoblasts and overactive osteoclasts (degrading the bone), resulting in degradation of articular cartilage and remodelling of the underlying bone (Loeser *et al.* 2012). The clinically relevant features of OA are JSN, osteophyte formation, abnormalities in the subchondral bone or accumulation of synovial fluid driven by the inflammatory processes (Loeser *et al.* 2012). Due to changes in the environment of the damaged joint, the cells are functionally different and no longer perform the correct repair and maintenance functions thereby exacerbating the pathological process (Petersson and Jacobsson 2002; Findlay and Atkins 2014). OA is characterised by the gradual degradation of articular cartilage, inflammation of the synovium, joint stiffness and pain (Loeser *et al.* 2012). There can also be bony outgrowths formed around the edge of the joints, so called osteophytes (Orlandi *et al.* 2009). As in RA, these conditions can lead to pain and swelling in the joint, as well as joint stiffness. Patients also do not usually present in the clinic until significant joint damage has occurred, as this is when pain presents. This makes diagnosis of early OA difficult.

For a long time, OA was considered to occur due to ‘wear and tear’ of joints, as part of the aging process. It has, however, also been shown that there is an inflammatory component to OA (Fig. 1.1). It has been demonstrated that synovial inflammation occurs prior to articular cartilage damage, suggesting that this inflammation may cause or exacerbate the disease process (Wang *et al.* 2017). Immunohistochemistry of patient

synovial tissue samples showed severe inflammation in 31% of cases and a further 62.5% of patients had mild or moderate inflammation (Haywood *et al.* 2003). This indicates that inflammation plays an important role in the development of OA, as well as contributing to the pain experienced by patients.

Image removed due to copyright

Fig. 1.1 – Mechanical and immune mediated pathways leading to cartilage degradation in OA. Mechanical stress leads to the production of inflammatory mediators, such as IL-1 and TNF-α. This causes resident chondrocytes to produce cartilage degrading proteins, such as matrix metalloproteinases (MMPs, ADAM-TSs). Cartilage degradation causes release of antigens, to which an immune response can be mounted, further driving the release of inflammatory mediators and destruction of cartilage, leading to inflammation and pain. Reproduced from (Yuan *et al.* 2003).

The inflammation observed in OA causes swelling of affected joints, accumulation of synovial fluid and joint stiffness. The synovial fluid of most OA patients has an increased number of mononuclear cells, immunoglobulins and complement components, indicating an active immune response (Yuan *et al.* 2003). Normally cartilage has a degree of immune privilege, due to the lack of vasculature, however, infiltration of immune cells does occur in OA. For example, immunohistochemistry performed on synovial tissue samples of ten OA patients detected the presence of T- and B-lymphocytes, as well as dendritic-like cells, capable of antigen presentation (Lindblad and Hedfors 1987). In contrast, analysis of macroscopically non-inflamed areas demonstrated lower numbers of lymphocytes than the inflamed areas of the same patient. The lymphocytes are predominantly found in the synovial membrane, close to the damaged cartilage, however, there was also damaged cartilage with no nearby elevation in the number of immune cells, indicating that there can be cartilage loss in the absence of synovial inflammation (Lindblad and Hedfors 1987). There is also evidence of increased cytokine production by resident chondrocytes, such as IL-1β and TNF-α (Moos *et al.* 1999). IL-1β and TNF-α expression was localised to a proportion of the chondrocytes in the superficial zone of the cartilage, where more degeneration is observed. Analysis of the localisation of expression of these cytokines and matrix metalloproteinases (MMP-13, 1 and 8) and aggrecanase (ADAMTS-4/5) production demonstrates an association between expression of cytokines and MMPs (Tetlow *et al.* 2001). MMP-13 was found to have a more prominent extracellular

expression profile than MMP-1 and 8, which were mainly found intracellularly (Tetlow *et al.* 2001). MMP-13 preferentially degrades type-II collagen, which is a major component of articular cartilage, indicating that the expression of inflammatory cytokines in cartilage-resident chondrocytes drives production of molecules capable of contributing the cartilage degradation (Tetlow *et al.* 2001). Taken together, this evidence demonstrates an important role for inflammation in the OA disease process, highlighting that this is a more complex disease than simple wear-and-tear damage of the joint.

There is also a cellular component to the pathogenesis of OA, involving chondrocytes and immune cells (Fig. 1.1). As the articular cartilage lacks vasculature and therefore cannot be easily infiltrated by cells, it relies on resident chondrocytes to maintain the extracellular matrix (ECM) (Goldring and Marcu 2009). At an early stage of OA, it has been shown that chondrocytes can become larger and begin to proliferate, allowing them to accumulate into cell clusters (Goldring and Marcu 2009). The chondrocytes then show increased production of both matrix proteins and matrix degrading proteins, such as the MMPs and aggrecanases discussed above (Fig. 1.1) (Goldring and Marcu 2009). Chondrocytes also undergo hypertrophy, which results in matrix calcification. This can lead to osteophyte formation, through the differentiation of periosteal cells into chondrocytes at the joint margin, subsequently undergoing hypertrophy (Goldring 2000). At later stages of OA, it has been demonstrated that there are reduced numbers of cells in the cartilage, indicating that chondrocyte cell death occurs during disease progression. It is unclear whether chondrocyte apoptosis occurs because of cartilage destruction or whether it causes cartilage destruction (Goldring and Goldring 2007).

1.3 Current Biomarkers for OA

Biomarkers are defined as ‘a characteristic that is objectively measured and evaluated as an indicator of normal biologic processes, pathogenic processes or pharmacologic responses to therapeutic intervention’ by the National Institutes of Health (Lane *et al.* 2011). Although a variety of biomarkers have been identified for OA, none of these are sufficiently characterized for use as an end-point surrogate (Lotz *et al.* 2013). One of the current biomarkers for OA is imaging, i.e. using MRI to scan changes in cartilage volume, thickness or composition. This is a very expensive way to detect OA and x-ray is the current method of choice, but can only detect late stage OA. Therefore,

there is a preference for use of biochemical markers in blood, urine or synovial fluid. However, no reliable biochemical marker is currently available. This could be a molecule that is causing the joint damage or the presence of which is caused by joint damage. Currently, it is thought that molecules linked to joint damage relating to tissue degradation or synthesis are the most likely type to be identified. Patient studies have demonstrated that there are differences in levels of markers of tissue turnover between healthy controls and people with OA (Garnero *et al.* 2001). Some of the proteins analysed as biomarkers for OA will be discussed here.

As there is likely to be increased cartilage turnover in OA patients and degradation products of ECM can be released into the synovial fluid and blood serum, the levels of these may indicate the presence of disease or progression. The collagen type II C-telopeptide (CTX-II, a degradation product of collagen type II) can be detected in urine using an ELISA with a monoclonal antibody to CTX-II (Christgau *et al.* 2001). Where there is increased cartilage turnover, there is an increase in CTX-II C-telopeptide release, which suggests that measuring this protein can reflect elevated cartilage destruction, but the levels were not significantly reduced after 3 months of rehabilitation (Garnero *et al.* 2001). The knee lesion severity was found to correlate with urine CTX-II levels in older patients, but not in younger patients (Christgau *et al.* 2001).

There is also a possible role for analysing ADAMTS-5 degradation of aggrecan, which is an important proteoglycan component of cartilage with roles in the compressive strength and in chondrocyte cell-cell and cell-matrix interactions. Degradation of aggrecan by ADAMTS-5 produces an ARGS neo-epitope This protease has been shown to drive cartilage loss in preclinical models of arthritis and higher serum levels of ARGS epitope were found in OA patients who had undergone total knee replacement (TKR) (Germaschewski *et al.* 2014). There was, however, no difference in serum concentration of ARGS between OA patients without TKR and healthy controls (Germaschewski *et al.* 2014). Again, as this biomarker cannot identify all OA patients, especially those at early stages of OA, it is not an ideal biomarker for early diagnosis and is instead likely to indicate disease burden (Bay-Jensen *et al.* 2016).

Cartilage oligomeric protein (COMP) is a degradation product of articular cartilage (Verma and Dalal 2013). Serum COMP levels were found to be significantly higher in

knee OA patients than in the control group (without knee OA) and this elevation was seen throughout the first 3 years of disease (Verma and Dalal 2013). However, 17% of tested knee OA patients showed serum COMP levels that overlap with control, with this overlap more likely in younger, female OA patients (44-48 years) (Verma and Dalal 2013). This indicates that while serum COMP levels may be useful in diagnosing early OA, they are not able to identify all cases of OA.

As an alternative to cartilage degradation products, the involvement of inflammation suggests that the presence of inflammatory mediators could be used as biomarkers. Interleukin 1 receptor antagonist (IL-1Rα) is an inhibitor of IL-1 signalling, which mediates its effect through binding to the IL-1 receptor on the surface of the cell but not initiating signalling and preventing IL-1 binding (Arend *et al.* 1994). There is a modest association between IL-1Rα and severity or progression of OA (Attur *et al.* 2015). Higher levels of IL-1Rα gave increased JSN after 24 months (Attur *et al.* 2015). This suggests that IL-1Rα could therefore be used as a prognostic indicator, but has not been shown to be a useful early stage OA diagnostic biomarker. Another study showed that higher levels of IL-6 or TNF-α in synovial fluid was associated with increased osteophyte development and increasing levels of either gave progressive JSN (Larsson *et al.* 2015). This presents cytokines and immune modulators as potential targets for monitoring or modifying disease progression, but again is likely to show later in the disease process, once significant damage has already occurred.

Due to the considerable overlap between the groups (healthy vs disease or between patients with different pathology) in all of the biomarkers tested to date, these tests are not diagnostic in individual patients even though clear differences sometimes exist between the groups. These biomarkers are also likely to be more useful for confirming OA at later stages of disease. This demonstrates that current biomarkers are not sufficiently selective of patients to be useful in clinically diagnosing OA. Most of the biomarkers studied to date use quantitative difference for diagnosis as they are related to tissue turnover. This explains why this cross-over between healthy controls and patients can occur as tissue turnover is often affected by other underlying conditions (Lotz *et al.* 2013). Therefore, there is a need for a qualitative biomarker, the presence or absence of which could give a definitive diagnosis of OA.

1.4 TG2 in OA

Transglutaminase 2 (TG2) is an enzyme capable of modifying glutamine side chains of target proteins, with roles in stabilising extracellular assemblies and important functions in tissue repair. The gene for TG2 has been found to be up-regulated in OA, and TG2 is the dominant catalytically active TG in the extracellular matrix of the cartilage (Fig. 1.2) (Summey *et al.* 2002; Tarantino *et al.* 2013). The Hartley Guinea Pig model is a well-characterised model of spontaneous knee OA. In these animals it has been shown that both TG2 and the isopeptide bonds formed by TG2 are abundant in the early stages of disease (Huebner *et al.* 2009). The levels of TG2 in this model also correlate to the severity of the disease, at both the mRNA level in the chondrocytes and the protein level in the synovial fluid (Huebner *et al.* 2009). Another model of OA (surgically induced knee joint instability in mice) has also implicated TG2 in the disease process by demonstrating that TG2 knock-out mice have decreased cartilage destruction (Orlandi *et al.* 2009). This shows that increased expression of TG2 in the osteoarthritic joint is part of the disease process or indirectly exacerbates the disease process. TG2 is present extracellularly and involved in cross-linking in this disease (Orlandi *et al.* 2009).

Image removed due to copyright

Fig. 1.2 TG2 expression in normal and OA cartilage. Histology of serial sections of human head femur articular cartilage shows a smooth surface and normal cartilage in a, with low TG2 expression in b. Osteoarthritic cartilage staining shows increased destruction in c and an increase in TG2 expression in d. Figure reproduced from Tarantino *et al*, 2013.

In the growth plate TG2 has been found to be a marker for chondrocyte hypertrophy and is required for chondrocyte maturation and differentiation resulting in calcification (Aeschlimann *et al.* 1993; Aeschlimann *et al.* 1996). This is possibly through regulation of extracellular matrix-cell communication (Johnson and Terkeltaub 2005). Chondrocyte hypertrophy and calcification of joint cartilage is part of OA pathology, resulting in the formation of osteophytes. N-ε (γ-glutamyl) lysine cross-links are abundant in the bone matrix and correlate with mineralisation seen in OA, supporting a role for TG2 in the pathogenesis of this disease (Johnson and Terkeltaub 2005). This means that reaction products of TG2 could provide a novel biomarker in the form of a protein in the extracellular matrix of the joint that has been modified by TG2 in a way

specific to the disease. It has been demonstrated that the extracellular activity of TG2 is important to its role in OA (Johnson and Terkeltaub 2005). Therefore, to understand the role of TG2 in OA and to identify disease relevant reaction products, it is important to understand the mechanism by which it is released from cells. Externalisation of TG2 is linked to transamidation reactions via Ca^{2+}-dependent activation of the enzyme (Johnson and Terkeltaub 2005).

1.5 Transglutaminases

The transglutaminase (TG) family has nine members, all with related structures and enzymatic functions (Grenard *et al.* 2001). All of the members, except band 4.2 protein, are protein-glutamine γ-glutamyltransferases, which perform post-translational modification of glutamine side chains of proteins in a calcium dependent manner. These enzymes belong to the papain-like superfamily of cysteine proteases due to the structural homology of the catalytic domain of TGs to these cysteine proteases (Makarova *et al.* 1999). The TG family comprises factor XIII, keratinocyte TG (TG1), tissue TG (TG2), epidermal TG (TG3), prostate TG (TG4), TG5, TG6 and TG7 and there is one catalytically inactive homologue (erythrocyte band 4.2). These different members of the TG family are likely to have arisen due to gene duplication and rearrangement (Grenard *et al.* 2001; Deasey *et al.* 2012; Thomas *et al.* 2013). Each member of the transglutaminase family has a specific expression pattern and can selectively cross-link proteins (Beninati and Piacentini 2004).

Factor XIII is expressed in megakaryocytes, platelets, macrophages, dendritic cells, chondrocytes and osteoblasts (Kiesselbach and Wagner 1972; Henriksson *et al.* 1985; Cerio *et al.* 1989; Nurminskaya *et al.* 2002; Nakano *et al.* 2007). FXIII exists in different forms, whether it is intracellular or circulating in blood plasma. Plasma FXIII is a tetramer, consisting of two FXIIIA subunits, which are capable of being active, and two FXIIIB subunits, which are inhibitory (Aeschlimann and Paulsson 1994). In cells, FXIII is a dimer of two FXIIIA subunits (Aeschlimann and Paulsson 1994). FXIII is activated by thrombin dependent proteolysis, cleaving off the activation peptide on the FXIIIA subunit (Aeschlimann and Paulsson 1994). In the presence of Ca^{2+}, the FXIIIB subunits then dissociate, leaving the active FXIIIa enzyme (Aeschlimann and Paulsson 1994). In the blood, FXIIIa is responsible for stabilizing fibrin clots to facilitate blood coagulation (Lorand 2001). In humans, a deficiency in

FXIIIA results in a bleeding disorder that can lead to premature death due to haemorrhage (Anwar and Miloszewski 1999). FXIIIA deficient mice also have clotting disorders, which leads to reduced survival of pregnant females due to spontaneous haemorrhage (Lauer *et al.* 2002). There is also reduced survival of male mice due to fibrosis (Souri *et al.* 2008).

TG1, TG3 and TG5 are skin and hair transglutaminases, with roles in maintaining these structures. All have roles in the formation of the stratum corneum (the outermost layer of the skin, formed of dead cells) during terminal keratinocyte differentiation. TG1 is expressed at low levels in proliferating keratinocytes, with an increase in expression during keratinocyte differentiation, cross-linking cornified envelope proteins (Steinert *et al.* 1996). TG1 is membrane associated and hence essential for binding the proteinaceous cornified membrane to the lipid membrane (Steinert *et al.* 1996). TG1 knockout mice demonstrate the importance of this enzyme in the function of this membrane and have defects in cornified envelope formation and in development of the skin permeability barrier (Kuramoto *et al.* 2002). TG3 is expressed in epidermal cells and also has roles in formation of the stratum corneum and can also cross-link structural proteins in the hair follicle (Tarcsa *et al.* 1997). TG3 knockout mice demonstrate the role of this protein in hair structure, having a curled structure of their hair and whiskers due to alterations to the crosslinking of structural proteins (Iismaa *et al.* 2009). TG5 expression has been identified during the early stage of epidermal differentiation (Candi *et al.* 2002). TG5 knockout mice have not been generated, but deficiency in humans causes acral peeling skin syndrome, demonstrating an important role in the integrity of the skin (Cassidy *et al.* 2005). These TGs are activated by proteolysis; TG1 is processed by cathepsin D to form a 10/67/33kDa complex (Steinert *et al.* 1996; Egberts *et al.* 2004), TG3 is processed by cathepsin L into a 50/27kDa complex (Kim *et al.* 1990; Cheng *et al.* 2006) and TG5 activation may require processing, however the exact nature of this is unclear (Pietroni *et al.* 2008).

TG6 expression has been shown to be widespread in neuronal cells of the brain, spinal cord and the retina, but has also been identified in the skin (Thomas *et al.* 2013). TG6 has been implicated in neurological conditions, specifically those induced by gluten (Thomas *et al.* 2013). TG6 appears to have a role in gluten ataxia, where

autoantibodies are generated to TG6, allowing gluten sensitivity to have effects on the central nervous system (CNS) (Hadjivassiliou *et al.* 2008; Hadjivassiliou *et al.* 2013). Mutations in the gene coding for TG6 have also been identified in spinocerebellar ataxia type 35, where mutations in TG6 reduce its stability or activity, resulting in cell death (Guan *et al.* 2013).

There is little information regarding the functions of TG4 and TG7 in humans. In mice, deficiency in TG4 results in defects in copulatory plug formation, resulting in reduced fertility (Dean 2013). It has been suggested that an increase in TG4 expression could be related to aggressive prostate cancer (Jiang and Ablin 2011). TG7 has also been linked to poor cancer prognosis, in this case where increased expression of TG7 is seen in breast cancer cells (Jiang *et al.* 2003).

The inactive TG homologue, erythrocyte band 4.2 is expressed in red blood cells (Zhu *et al.* 1998). This protein is inactive due the substitution of the active site residues (Iismaa *et al.* 2009). This protein plays a mainly structural role, as a major component of the erythrocyte membrane skeleton, binding ankyrin and the cytoplasmic domain of anion exchanger 1 and linking the membrane to the cytoskeleton to maintain membrane shape and stability (Iismaa *et al.* 2009). Deficiency in erythrocyte band 4.2 therefore leads to structural problems with red blood cells, whereby the cells are smaller due to membrane loss and are more spherical, lacking some of the characteristic biconcavity of the cell (Iismaa *et al.* 2009).

1.6 Expression of TG2

TG2 is the most ubiquitously expressed member of the TG family, and is constitutively expressed in endothelial cells, smooth muscle cells, fibroblasts, and many organ-specific cell types, for example chondrocytes (Thomazy and Fesus 1989; Aeschlimann and Paulsson 1991; Aeschlimann *et al.* 1993). Due to this widespread expression, TG2 is found in many cells of the immune system including cells of the myeloid and lymphoid lineages (Eckert *et al.* 2014). In these cells, TG2 may regulate differentiation, for example TG2 expression increases substantially during monocyte differentiation into macrophages (Murtaugh *et al.* 1984). The gene for TG2, TGM2, has response elements for NF-κB, retinoic acid, TGF-β and IL-6 (Aeschlimann and Thomazy 2000). TNF-α treatment of liver cells also increased the TG2 mRNA levels and cross-linking, indicating an increase in the amount of active TG2, mediated

through NF-κB (Kuncio *et al.* 1998). TG2 is also present in a variety of cell compartments, including the cytoplasm, mitochondria and nucleus, as well as being present at the cell surface (Nurminskaya and Belkin 2012). The sub-cellular localisation can have effects on the function of TG2, through allosteric regulation of conformational changes by various cofactors, including Ca^{2+}, nucleotides and thioredoxin or proteins that it interacts with. For example, TG2 can form a complex with retinoblastoma (Rb) which in the cytoplasm has a pro-apoptotic function and in the nucleus has an anti-apoptotic function (Milakovic *et al.* 2004).

1.7 Types of reactions performed by TGs

Transglutaminases perform post-translational modification through three different reaction types; transamidation, esterification and hydrolysis (Folk *et al.* 1968). These result in one of five different post-translational modifications shown in fig. 1.3. These reactions require a glutamine containing protein or peptide (the acceptor substrate), which reacts with the active site cysteine forming the γ-glutamylthioester, the acyl-enzyme intermediate, and releasing ammonia. This is followed by a deacylation step, which can be through one of the three reaction types. There can be hydrolysis of the substrate (Fig. 1.3 e), binding of the second substrate, which can be an amine to give a transamidation reaction (Fig. 1.3 a-c) or alcohol giving esterification (Fig. 1.3 d). These all result in cleavage of the thioester bond and regeneration of the active enzyme. The detailed mechanism for a cross-linking reaction is shown in fig. 1.4 (Lorand and Graham 2003). The result of a transamidation reaction between proteins is cross-linking where the glutamine containing protein is cross-linked to a lysyl residue by an N^{ε}-(γ-glutamyl)lysine isopeptide bond (Fig. 1.3 a). Amine incorporation occurs where an amine is incorporated into a glutamine side chain of the acceptor protein (Fig. 1.3 b). The lysine side chain of a donor protein can also be acylated by a glutamine-containing peptide of suitable sequence (Fig. 1.3 c). Esterification is fatty acid modification of an acceptor-protein glutamine side chain and has been described in the context of cornified envelope formation (Fig. 1.3 d) (Nemes *et al.* 1999). Finally, hydrolysis results in either deamidation when using H_2O as a donor whereby the NH_2 group on the acceptor protein glutamine side chain is replaced with an OH group to form a glutamate (Fig. 1.3 e) or isopeptide cleavage, involving a H_2O molecule acting

as a donor, breaking the isopeptide bond cross-linking two proteins (Fig. 1.3 f) (Iismaa *et al.* 2009).

Image removed due to copyright

Fig. 1.3 – Post-translational modifications performed by TGs (Lorand and Graham 2003)

Image removed due to copyright

Fig. 1.4 – Cross-linking reaction mechanism. Substrate 1 (glutamine containing) forms a complex with the cysteine of the TG2 active site, then the oxyanion intermediate forms through hydrogen bonding between the Cys nitrogen and the nitrogen of the active site Trp, which stabilizes the interaction. Acylation causes release of NH_3 and formation of the acylenzyme intermediate. There is then nucleophilic attack by substrate 2, forming the oxyanion intermediate. Finally, deacylation occurs and the cross-linked product is released and TG is regenerated (Iismaa *et al.* 2009).

There are several defining features of TGs; they have a papain-like Cys-His-Asp catalytic triad and a crucial tryptophan residue 36 residues upstream of this Cys, which is necessary for the proper interaction of the enzyme active site Cys with the substrate (Hettasch and Greenberg 1994; Pedersen *et al.* 1994) (Fig. 1.4). They also show saturable binding of the second substrate to the acylenzyme intermediate, making this likely to be the rate limiting step (steps shown in fig. 1.4) (Curtis *et al.* 1974). The acylenzyme intermediate has different specificity for certain amine containing substrates, when examined experimentally, it has lower binding affinities putrescine and n-butylamine (which occur physiologically) than the affinity for dansylcadaverine (which is used experimentally), demonstrating that there are likely to be differences in the affinity for physiological substrates, leading to preferential use of certain substrates (Curtis *et al.* 1974).

1.8 Unique characteristics of TG2

As well as having a latent transamidation activity TG2 has several other unique characteristics, including ubiquitous expression in mammalian tissues. In the cell, TG2 can be found in the cytosol as well as associated with the cell membrane and nuclear membrane. TG2 has been shown to interact with phospholipids (Fesus *et al.* 1983; Zemskov *et al.* 2011) or be membrane bound indirectly by interacting with integral membrane proteins such as integrins, GPR56 (G-protein coupled receptor 56) and

syndecan 4, among other plasma membrane proteins (Akimov *et al.* 2000; Xu *et al.* 2006; Telci *et al.* 2008). TG2 has a nucleotide binding site and interacts with GTP with high affinity (Begg *et al.* 2006a). GTP-bound TG2 is capable of GTP hydrolysis, acting as a G-protein, for example through an interaction with the α1-adrenergic receptor, which can then initiate downstream signalling (Nakaoka *et al.* 1994). TG2 also has a variety of extracellular roles, these are predominantly in the cell stress response and tissue repair, and relate to its transamidation activity, but it also has roles in cell migration, differentiation and tissue mineralisation (such as endochondral ossification) amongst others (Aeschlimann *et al.* 1993; Aeschlimann *et al.* 1996; Akimov and Belkin 2001; Stephens *et al.* 2004). TG2 is also involved in stabilising the dermo-epidermal junction (Raghunath *et al.* 1996) and having a role in activating TGF-β in inflammation (Nunes *et al.* 1997).

1.9 Structure and allosteric regulation of TG2

TG2 is a ~78kDa protein, comprising four domains (common to all TGs); an N-terminal β-sandwich domain, a catalytic core and two C-terminal β-barrel domains (Liu *et al.* 2002). These domains adopt different positions in relation to each other, depending on whether the molecule is in its Ca^{2+}-facilitated active form or GTP-bound inactive conformation (Fig. 1.5). Transglutaminase activity of TG2 is latent, so it is activated by calcium binding to at least 3 sites on the molecule (Ahvazi *et al.* 2003; Kiraly *et al.* 2009), and is inhibited by GTP binding at an allosteric site (Begg *et al.* 2006a). Ca^{2+} binding causes a relaxation of the molecule to allow substrate access to the active site through a channel which then triggers it to adopt the 'open' conformation (Pinkas *et al.* 2007). GTP, GDP and to a lesser extent ATP inhibit transamidation activity through formation of a 'closed' structure (Fig. 1.5). In this conformation the substrate is unable to access the active site. In the intracellular environment there is a high level of GTP (100-200μM) and a low level of Ca^{2+} (<1μM) meaning that TG2 is likely to be in the closed conformation. Once TG2 has been released from cells it is more likely to be in the open conformation as in the extracellular environment there are higher levels of Ca^{2+} (1.5-2.5mM) and very low levels of GTP, so the enzyme has transamidation activity. During cell stress, it is likely that the levels of Ca^{2+} inside the cell rise, potentially allowing activation of TG2 inside the cell and hence cross-linking of intracellular proteins occurs (Pinkas *et al.* 2007).

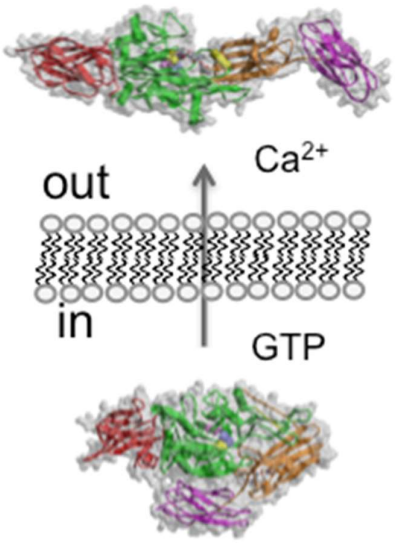

Fig. 1.5 – Peptide inhibitor bound (transamidation intermediate) and GTP bound conformations of TG2. Inside the cell there is a higher level of GTP, so TG2 is in the closed conformation. Outside the cell there is a higher level of Ca^{2+} and TG2 can adopt the open conformation (Reproduced from Professor Daniel Aeschlimann).

1.10 GTP binding pocket

The GTP binding pocket of TG2 is located at the interface of the catalytic core domain and β-barrel 1 (Liu *et al.* 2002; Jang *et al.* 2014). Within the β-barrel 1 domain, amino acids 476 to 482 and 580 to 583 have been shown to be important for GTP and GDP binding (Liu *et al.* 2002; Jang *et al.* 2014) (Fig. 1.6). In the core domain, K^{173} and F^{174} are required for GTP binding (Liu *et al.* 2002). There are several important residues thought to be required for hydrolysis of GTP in addition to binding (Fig. 1.6). These include R^{580} in human TG2, substitution of which to alanine abolishes GTP binding (Begg *et al.* 2006a; Ruan *et al.* 2008).There are also two further arginine residues – R^{476} and R^{478} – which bind the phosphate groups of the GTP (Liu *et al.* 2002), as does R^{580}. Several residues are required for binding the nucleoside group of GTP, including F^{174} (Liu *et al.* 2002). K^{173} extends over the bound GTP to stabilize the interaction between the TG2 and GTP (Johnson and Terkeltaub 2005).

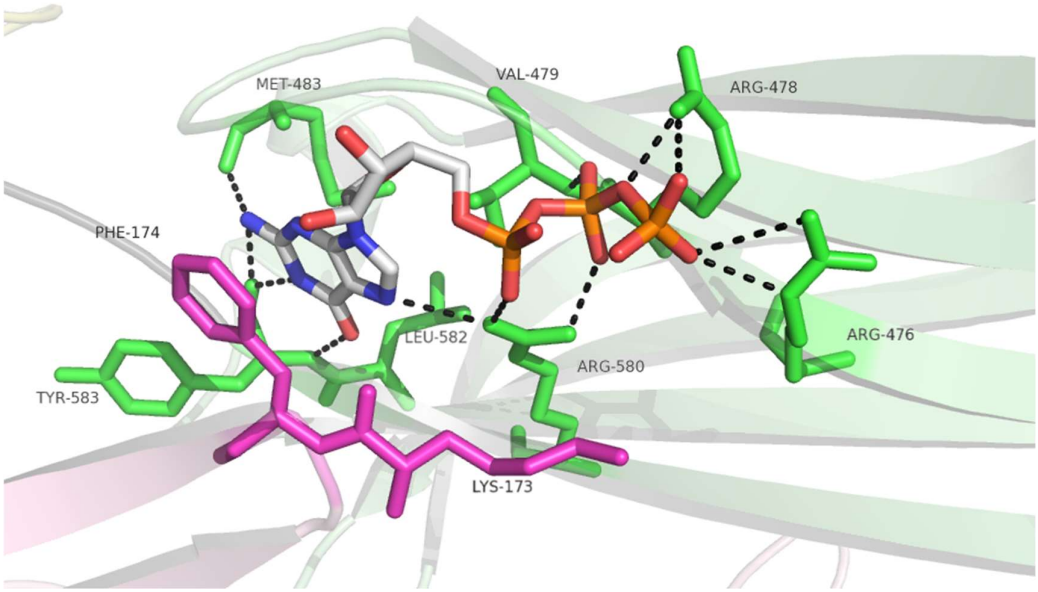

Fig. 1.6 – Important residues in the GTP binding pocket of human TG2. Figure was generated based on the x-ray crystal structure of the TG2-GTP complex (Jang *et al.* 2014) by Shannon Turberville. Residues forming the GTP binding pocket are highlighted and labelled. Green residues are those from the β-barrel 1 domain of TG2, pink residues are from the core domain. Dashed lines indicate that the positions of charges are close enough for an interaction of that residue with GTP, i.e. less than 3.5Å in distance.

1.11 Further mechanisms of TG2 activity regulation

In addition to regulation by GTP and Ca^{2+} binding, the activity of TG2 can also be regulated by other mechanisms, including binding to another protein and oxidation resulting in disulphide bond formation (Stamnaes *et al.* 2010). Protein-protein interactions can regulate TG2 activity by affecting the access of substrates to the active site. For example, the heparan sulfate binding site is located on the closed conformation of TG2, thereby modulating other activities of TG2 when it is bound to heparan sulfate (Lortat-Jacob *et al.* 2012).

In the extracellular environment, despite high levels of Ca^{2+}, TG2 is often inactive due to oxidation causing a disulphide bond to form initially between C^{230} and C^{370}, which can then facilitate formation of a disulphide bond between C^{370} and C^{371} (Fig. 1.7) (Stamnaes *et al.* 2010). These disulphide bonds can form when TG2 adopts the Ca^{2+}

bound, open conformation and inactivate TG2 (Stamnaes *et al.* 2010). This mechanism appears specific to TG2 as these Cys residues are not conserved in other TG isoforms. Thioredoxin-1 has been suggested to reactivate oxidized enzyme (Jin *et al.* 2011). Thioredoxin-1 acts on a broad range of protein targets to modulate their activity in response to the redox environment, by reversible reduction of disulphide bonds (Arner and Holmgren 2000). Reduced thioredoxin-1 has a hydrophobic surface area, allowing binding to an oxidised substrate protein (in this case, TG2 with a disulphide bond) (Eklund *et al.* 1984). Thioredoxin-1-$(SH)_2$ contains two active site cysteines, one of which acts as the attacking nucleophile, forming a covalently linked transition state between the two proteins (Holmgren 1995). The first proton is transferred to TG2, then the deprotonated cysteine can attack the second cysteine of thioredoxin-1, causing its proton to also transfer, and formation of a disulphide bond in thioredoxin-1, resulting in thioredoxin-1-$(S)_2$ and reduced substrate, in this case TG2 (Holmgren 1995). Thioredoxin reductase can then reactivate thioredoxin-1 by another reduction reaction (Arner and Holmgren 2000). Thioredoxin reductase contains a selenocysteine and a cysteine in its active site, which, along with NADPH, reduce the disulphide bond of thioredoxin-1, resulting in reactivation of thioredoxin-1 (Arner and Holmgren 2000).

Image removed due to copyright

Fig. 1.7 – Schematic of the oxidation of TG2 leading to inactivation. Figure adapted from (Stamnaes *et al.* 2010).

1.12 Physiological Functions of TG2

Given that TG2 has been investigated for over 4 decades, it is not possible to comprehensively cover all of the available information. A brief summary of relevant aspects is given and the reader referred to in depth review articles for further detail (Aeschlimann and Thomazy 2000; Nurminskaya and Belkin 2012). There are many roles for the modified substrates of TGs. For example, TG2 transamidation is important for matrix stabilization needed for wound healing, angiogenesis and bone remodelling (Aeschlimann and Thomazy 2000). For these roles, it is essential that TG2 is released from the cells into the ECM. Once TG2 has been externalized, besides crosslinking target proteins, it also has structural roles as it forms a complex with fibronectin, bridging binding to syndecan 4 (Stephens *et al.* 2004; Telci *et al.* 2008). This subsequently activates PKCα which can then translocate to the membrane and

bind to the intracellular region of β1 integrin, triggering signalling, which is involved in wound healing (Stephens *et al.* 2004; Telci *et al.* 2008). TG2 also has important roles in the intracellular environment, mainly in protein cross-linking during apoptosis where TG2 can specifically cross-link SP1, a transcription factor, to induce apoptosis (Tatsukawa *et al.* 2009). TG2 can also act as a scaffold protein, regulating actin cytoskeleton organization (Yi *et al.* 2009).

TG2 expression and activity increase in inflammation due to regulation of the gene by proinflammatory cytokines, in particular IFN-γ (Bayardo *et al.* 2012). Tgm2 has a TGFβ-1 response element in its promoter, with different cells responding to this stimulus differently, for example, TGFβ-1 results in upregulation in fibroblasts and downregulation in epithelium (Ritter and Davies 1998). TG2 expression can also be increased by NFκB (Ai *et al.* 2012), IL-1 (Johnson *et al.* 2003a) and IL-6 (Suto *et al.* 1993), with increased expression enhancing cross-linking activity (Johnson *et al.* 2003a). There is also increased TG2 expression in macrophages infiltrating wounds (Murtaugh *et al.* 1983; Murtaugh *et al.* 1984), which accounts for the increase in phagocytic capacity of macrophages in comparison to monocytes (Seiving *et al.* 1991). Due to increased amounts of surface TG2, macrophages also show increased adhesion to fibronectin, with cells not expressing TG2 having reduced adhesion (Akimov and Belkin 2001). TG2 is also involved in differentiation of immune cells, for example dendritic cell differentiation induced by lipopolysaccharide (LPS) (Matic *et al.* 2010) and neutrophil granulocytes (Balajthy *et al.* 2006). This indicates the important role of TG2 in the correct functioning of the immune system.

In bone, TG2 plays an important role in endochondral ossification, where the hyaline cartilage formed in the embryo is replaced by bone (Nurminskaya and Belkin 2012). This replacement is termed osteogenesis and it is during this process that chondrocyte proliferation stops and chondrocyte hypertrophy begins. Hypertrophic chondrocytes secrete type X collagen and differentiate further to deposit mineral into the surrounding matrix, after which the cells undergo apoptosis (Long and Ornitz 2013). TG2 and FXIIIA expression is upregulated in these hypertrophic chondrocytes (Johnson and Terkeltaub 2005). Addition of TG2 exogenously increases mineralisation and chondrocyte hypertrophy and the induction of chondrocyte hypertrophy is enhanced by GTP binding to TG2 (Johnson and Terkeltaub 2005).

However, TG2 knockout mice do not have serious skeletal developmental abnormalities, indicating that TG2 is dispensible for this process. Deficiencies do become apparent once the mice become injured or in experimental models of disease, having delayed tissue repair. It has been suggested that FXIIIa, which is also involved in this process, can compensate for the lack of TG2 expression, however TG2 and FXIIIA knockout mice also have no serious skeletal abnormalities (De Laurenzi and Melino 2001).

1.13 G-protein functions of TG2

When TG2 is GTP bound, which is likely to occur intracellularly due to high GTP concentrations, it can function as a G-protein (Nakaoka *et al.* 1994). This activity occurs in the absence of transglutaminase activity and Ca^{2+} bound TG2 has no GTPase activity (Kiraly *et al.* 2009). Inside the cell, TG2 is associated with calreticulin, which may regulate TG2 activity by suppressing GTP binding/hydrolysis and transamidating activities, meaning that it is inactive for signalling (Fig. 1.8) (Feng *et al.* 1999). When an agonist binds a relevant G-protein coupled receptor (GPCR), the receptor induces exchange of GDP for GTP in TG2, causing dissociation from calreticulin (Feng *et al.* 1999). In this way intracellular TG2 is capable of responding to and passing on extracellular signals, through interactions with transmembrane receptors including α1 adrenergic, thromboxane A2 and oxytocin receptors (Baek *et al.* 1993; Park *et al.* 1998; Vezza *et al.* 1999). For example, epinephrine binding of the α1 adrenergic receptor induces TG2 interaction with the receptor and TG2 binding to PLCδ1 (Nakaoka *et al.* 1994; Feng *et al.* 1996). This leads to phosphoinositide hydrolysis and an increase in intracellular Ca^{2+} (Kang *et al.* 2002), which will have a variety of downstream effects in different cells, in some cases through protein kinase C (PKC) activation (Fig. 1.8) (Almami *et al.* 2014). This pathway can also activate ERK and MEK in cardiomyocytes and induce cell proliferation in hepatocytes (Lee *et al.* 2003). PLCδ1 can also act as a guanine nucleotide exchange factor (GEF) for TG2 and as a GTP hydrolysis inhibitory factor (GDI), amplifying the signal from TG2 binding to the receptor (Fig. 1.8) (Baek *et al.* 2001).

Image removed due to copyright

Fig. 1.8 - TG2 G protein activity. Activation of a G-protein coupled receptor (GPCR) induces GTP binding by TG2, resulting in calreticulin (CRT) dissociation (1) from TG2 complex, activating G-

protein function of TG2 and PLCδ1 binding (2). TG2 binding activates PLCδ1, allowing it to catalyse phosphatidylinositol 4,5-bisphosphate (PIP_2) conversion to diacylglycerol (DAG) (6) and release of inositol 1,4,5-triphosphate (IP_3), which increases intracellular Ca^{2+} levels. PLCδ1 stabilises GTP binding by TG2 and stimulates GDP release from TG2, acting as a GEF (5) and slows down GTP hydrolysis, acting as a GDI (3), although GTP hydrolysis can still occur. GDP bound TG2 can then be inhibited by CRT binding (4) and either enter the cycle again at (1) or bind to Ca^{2+}, inhibiting TG2 G-protein functions. Adapted from (Eckert *et al.* 2014).

1.14 Non-enzymatic roles of TG2

TG2 also has roles that do not involve any of its enzymatic activities or G-protein functions, which can have effects on cell adhesion, migration and the formation of focal adhesions between different cell types (Lorand and Graham 2003; Stephens *et al.* 2004). These involve non-covalent interactions with other proteins. For example, TG2 can interact with fibronectin to form fibronectin matrix fibrils, thereby stabilising the ECM, without needing cross-linking activity (Turner and Lorand 1989). TG2 can also interact with integrins, which are cell surface receptors capable of interacting with ECM and with a connection to the cytoskeleton (Akimov *et al.* 2000) although no direct interaction between these molecules has been demonstrated and this therefore may be an indirect interaction. TG2 is able to simultaneously interact with both proteins, allowing cells to interact with fibronectin, thereby promoting cell adhesion and spreading (Akimov *et al.* 2000). Interaction with heparan sulfate allows TG2 to participate in signalling, as heparan sulfate can act as a signalling co-receptor affecting tissue distribution and cellular trafficking. An interaction with heparin is essential for cell adhesion to the TG2-fibronectin matrix, thereby affecting the interaction between the cell and the extracellular matrix (Lortat-Jacob *et al.* 2012). These interactions can also play a role in pathological situations, for example, the TG2-GPR56 interaction aids cell adhesion and prevents cancer metastasis (Xu *et al.* 2006).

1.15 Pathological functions of TG2

Given its many roles it is not surprising that TG2 has also been implicated in pathological processes, a small number of these will be discussed here. For example, in normal circumstances TG2 can cross-link collagen I giving it resistance to degradation by proteases, whereas this can lead to tissue fibrosis when TG2 is excessively released from cells due to damage and is no longer properly regulated (Johnson *et al.* 2003b; Huang *et al.* 2009). Another example is celiac disease where

TG2 has been identified as the main autoantigen, with α, γ-gliadins (gluten proteins) being a preferred substrate for TG2 modification (Dieterich *et al.* 1997). TG2 mediated deamidation of gliadin peptides, leads to the generation of T-cell epitopes and autoantibodies directed to either TG2 or the modified gliadin (Skovbjerg *et al.* 2004; Iversen *et al.* 2013). In OA, chondrocyte hypertrophy occurs pathologically, involving TG2 due to an increase in its expression and ultimately, activity (Johnson and Terkeltaub 2005). An increase in expression of TG2 has also been observed in osteoarthritic tissues in humans and mice (Orlandi *et al.* 2009). Surgical induction of knee OA in wild-type and TG2 knockout mice has revealed that TG2 knockout leads to a reduction in cartilage destruction and an increase in osteophyte formation (Orlandi *et al*. 2009), confirming a role for TG2 in OA and indicating opposing effects on different pathologies of OA. The role of TG2 in OA is discussed in more detail in section 1.4.

1.16 Conventional protein secretion

In conventional protein secretion, proteins with an *N*-terminal or internal signal peptide are directed through the endoplasmic reticulum (ER)/Golgi pathway to subsequently be released from the cell (Fig. 1.9) (Nickel and Rabouille 2008). The signal peptide targets the protein into the ER, through a signal peptide recognition particle (Nickel and Rabouille 2008). Within the ER, proteins are folded (with the help of chaperones) and unfolded or incorrectly folded proteins are redirected for degradation and protein modification, such as N-linked glycosylation, is initiated (Wang and Kaufman 2016). The proteins are then transported from the ER to the Golgi apparatus in COPII coated vesicles (Nickel and Rabouille 2008). Inside the Golgi, further protein modification, for example O-linked glycosylation, occurs (Ohtsubo and Marth 2006). Proteins may also be processed, then proteins are sorted for transport to the correct location in the cell. Proteins to be secreted by cells are packaged in COPI coated vesicles, which can mediate transport back to the ER or towards the plasma membrane (Nickel and Rabouille 2008). There are however, also secreted proteins that lack a signal peptide and/or lack the glycosylation characteristic of the ER/Golgi secretory pathway, indicating that they are secreted through an alternative mechanism.

Image removed due to copyright

Fig. 1.9 Conventional protein secretion. The pathway for conventional protein secretion involves directing the protein into the ER, due to the presence of a signal peptide in the protein. The protein is then transported from the ER to the Golgi in COPII coated vesicles. Proteins pass through the Golgi and those that are secreted from the cell are then transported to the surface of the cell in COPI coated vesicles. (Nickel and Rabouille 2008)

1.17 Mechanisms of unconventional protein secretion

There are many different pathways for secretion beyond the conventional ER/Golgi secretory pathway, although some have overlap with the conventional protein secretion process and use part of its machinery. There are also many proteins that do not undergo conventional secretion, in some cases this may be because this pathway would be detrimental to the function of either the protein or the cell (Nickel and Rabouille 2008). For example, signalling molecules and their receptors could interact in the ER or Golgi when being synthesised by cells at the same time, resulting in undesired signalling. In the case of thioredoxin, the oxidative environment could cause protein misfolding, which would have detrimental effects on function (Nickel and Rabouille 2008).

Proteins with signal peptides are directed into the ER and can then bypass the Golgi, in some cases being taken to the plasma membrane in COPII vesicles, formed in the ER (Wang *et al.* 2004). If these proteins had passed through the Golgi, the modifications present would be different, thereby affecting protein function. Proteins in COPII vesicles can also be transported into an endosomal or lysosomal compartment, which can then fuse with the plasma membrane for protein secretion (Nickel and Rabouille 2008). Transmembrane proteins can trigger stress in the ER, leading to export bypassing the Golgi. One mechanism involving ER stress can involve GRASPs (golgi reassembly stacking protein), proteins involved in maintaining the structure and function of the Golgi. For example, GRASP55 under conditions of stress becomes phosphorylated and localises to the ER (Kim *et al.* 2016), where is recognises the PDZ domain of the protein to be secreted, aiding its encapsulation and transport to the plasma membrane (Gee *et al.* 2011).

Protein secretion can also occur independently of either ER or Golgi, and proteins using this alternative route are termed cytoplasmic or nuclear secretory proteins. For

example, FGF2 (fibroblast growth factor 2) has been shown to translocate directly across the plasma membrane (Schafer *et al.* 2004). FGF2 is recruited to the plasma membrane by ATP1A1 (Zacherl *et al.* 2015), a component of the Na/K-ATPase, then FGF2 interacts with $PI(4,5)P_2$ (a phosphoinositide), which aids FGF2 oligomerisation at the cell membrane (Muller *et al.* 2015). The oligomer formed by FGF2 adopts a toroidal structure, with FGF2 in the centre and $PI(4,5)P_2$ interaction sites on the outside (Steringer *et al.* 2012; Muller *et al.* 2015; Steringer *et al.* 2015). This FGF2 oligomer inserts into the plasma membrane, forming a pore. Following this, FGF2 could be directly translocated across the plasma membrane either by disassembly of the oligomer and release of components outside the cell or the pore of the oligomer itself regulating the secretion of FGF2 monomers (La Venuta *et al.* 2015). This is a novel, regulated, secretory mechanism involving direct translocation across the plasma membrane of an intracellular protein.

IL-1β is also secreted through several different non-conventional secretory pathways, under tight regulation due to its role in inflammation. IL-1β has been proposed to enter the endolysosome, under conditions of starvation, where it can be processed and released when the endolysosome fuses with the plasma membrane (Andrei *et al.* 1999). IL-1β secretion also occurs during the process of cell death known as pyroptosis (He *et al.* 2015). Activation of caspase-4/5, due to inflammasome formation on toll-like receptor 2 (TLR2) activation, or capsase-1 through cross-talk with the NLRP3 inflammasome, leads to processing of gasdermin D (Kayagaki *et al.* 2015). The gasdermin D N-terminal fragment then translocates to the plasma membrane, through an interaction with PIP2, where is forms a pore through which IL-1β can be secreted (Chen *et al.* 2016). It has also been shown that IL-1β secretion in macrophages occurs when TLR4 and P2X7R are both activated (Fig. 1.10) (Netea *et al.* 2009). These conditions lead to formation of the NLRP3 inflammasome, which activates caspase-1 (Netea *et al.* 2009). Caspase-1 activation leads to cleavage of pro-IL-1β, forming IL-1β, which is then released from cells in microvesicles (Pizzirani *et al.* 2007; Netea *et al.* 2009). This mechanism of regulated secretion is likely to occur in inflammation, due to the presence of ATP extracellularly, leading to activation of purinergic receptors including P2X7R (Bodin and Burnstock 1998), which are discussed in detail below. P2X7R has also been implicated in the release of IL-6, a pro-inflammatory cytokine which contains a signal peptide but has multiple different pathways for secretion

(Solini *et al.* 1999). It is clear that TG2 secretion must occur in a regulated manner, as the secretion occurs under specific circumstances, for example in chondrocyte hypertrophy (Aeschlimann *et al.* 1993). However, it is unclear which mechanism or parts of a known mechanism of unconventional secretion is relevant to TG2 secretion.

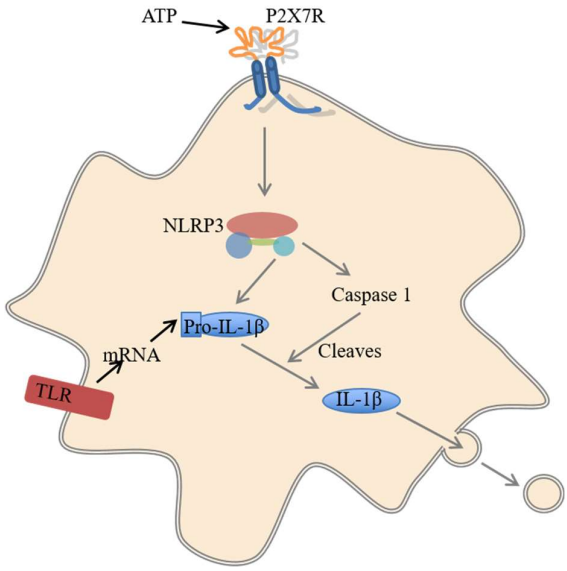

Fig. 1.10 IL-1β secretion from macrophages involving P2X7R. In macrophages, activation of TLR4 has been shown to increase production of IL-1β mRNA and P2X7R activation has been shown to activate the NLRP3 inflammasome, leading to caspase-1 activation and cleavage of pro-IL-1β to IL-1β and its secretion via microvesicles.

1.18 Externalisation of TG2

TG2 lacks a signal peptide and is therefore not directed into the ER (Aeschlimann and Paulsson 1994). TG2 also lacks the glycosylation characteristic of the ER/Golgi secretory pathway, despite harbouring multiple target sequences, indicating that it follows an alternative mechanism for secretion (Aeschlimann and Paulsson 1994). All TGs lack the N-terminal hydrophobic leader sequence typical of most secreted proteins, but TG2 and FXIIIa are released into the extracellular matrix by cells and have well established extracellular functions (Aeschlimann and Paulsson 1994). This leader sequence normally directs proteins through the ER and Golgi to then be transported out of the cell as discussed above. Therefore, it is likely that TG2 is released via an ER/Golgi independent pathway.

Several mechanisms for TG2 externalisation have been suggested. Zemskov *et al.* proposed that TG2 is imported into recycling endosomes by phospholipid-dependent binding to the vesicle, then delivery inside the vesicle. The vesicle then fuses with the plasma membrane, exposing TG2 to the extracellular environment. This is suggested to be a route for constitutive TG2 externalisation (Zemskov *et al.* 2011). However, the implied mechanism for membrane translocation into the endosomes remains

undefined. It has also been suggested in experiments using smooth muscle cells that TG2 release could be via microparticles as a TG2/eGFP fusion protein could be identified inside these vesicles (van den Akker *et al.* 2012). Both of these studies suggested that a local increase in Ca^{2+} was required for TG2 externalisation. However, we hypothesised that TG2 could be released in a pathway similar to that of IL-1β (Fig. 1.10). Our group has shown that, consistent with this hypothesis, TG2 can be released in response to P2X7R stimulation by ATP (Adamczyk 2013; Adamczyk *et al.* 2015). However, we have also shown that TG2 could be released from cells (other than myeloid cells) that lack some components of the inflammasome, formation of which is required for the externalisation of IL-1β, indicating some differences between the two pathways (Adamczyk 2013; Adamczyk *et al.* 2015). Furthermore, TG2 was released as free protein and not in vesicles, despite P2X7R inducing abundant microvesicle shedding (Adamczyk *et al.* 2015).

1.19 ATP in inflammation

As we have demonstrated TG2 secretion can be induced by P2X7R activation, extracellular ATP is clearly involved in the process of TG2 export by cells. ATP can be released by a variety of cells during inflammation, including immune cells such as activated platelets and leukocytes and non-immune cells, including epithelial and endothelial cells (Fitz 2007; Cauwels *et al.* 2014). This release can occur in a regulated manner or through leakage from damaged cells, as well as being released from cells that are exposed to mechanical stress such shear stress but are not irrecoverably damaged (Lazarowski *et al.* 2003). Apoptotic cells have been shown to release ATP through pannexin-1 channels, acting as a signal to phagocytic cells to attract them to the location of the dying cell (Chekeni *et al.* 2010). Release of ATP allows it to accumulate extracellularly, particularly when combined with downregulation of ectonucleotidases, resulting in the activation of ATP-sensitive receptors (Eltzschig *et al.* 2012). This suggests that ATP is a mediator of inflammation at an early stage of the process (Bodin and Burnstock 1998). ATP has a variety of pro-inflammatory roles, mainly mediated through NLRP3 inflammasome formation and activation (McDonald *et al.* 2010), occurring at high extracellular ATP concentrations (millimolar range). This includes aiding cytokine and chemokine secretion following tissue injury

(Cauwels *et al.* 2014), and also, as our laboratory have recently demonstrated, possibly TG2 secretion (Adamczyk 2013; Adamczyk *et al.* 2015).

1.20 Purinergic Receptors

Purinergic receptors are plasma membrane receptors capable of responding to the purine nucleotide ATP, as well as its metabolites ADP, AMP and adenosine to varying degrees (Burnstock 2007). There are two main classes of purinergic receptors, P1 receptors and P2 receptors. The main agonist for P1 receptors is adenosine, where P2 receptors respond to ATP (Burnstock 2007). The P2 receptors are further divided into two families, P2Y receptors, which are G-protein coupled and P2X receptors, which are ionotropic, forming cation selective channels (Burnstock and Kennedy 1985; Burnstock 2007). Primarily, this difference in response type leads to comparatively slow signalling from P2Y receptors and very fast signalling from P2X receptors (Khakh 2001). P2Y receptors expressed in macrophages are critical for chemotaxis in response to ATP, for example in the attraction of macrophages to the site of cell death or tissue damage (Kronlage *et al.* 2010). P2X receptors are more involved in mediating the immune response, through secretion of cytokines (Gabel 2007). This appears to occur at the site of tissue damage due to an increased responsiveness of P2X7 receptor to ATP when ionic conditions (Na^+ and K^+ concentrations) are altered, which would likely occur *in vivo* in damaged tissues (Gudipaty *et al.* 2001). Cell lysis results in release of the contents of the cell, including ATP and increasing the concentration of K^+ and organic ions due to their higher concentration intracellularly. This would alter the ion concentrations most significantly in tissues with high cell density and a large number of damaged or dying cells, resulting in increased P2X7R activation (Gudipaty *et al.* 2001). Both P2Y and P2X receptor activation results in elevation of Ca^{2+} concentrations in the cells. In the case of P2Y receptors, this is through release of Ca^{2+} from intracellular stores, such as in the ER (Cowen *et al.* 1989). P2X receptors also cause release of Ca^{2+} from intracellular stores, but this is overwhelmed by extracellular Ca^{2+} influx (Alonso-Torre and Trautmann 1993). The Ca^{2+} increase in P2Y receptor expressing cells is capable of increasing transcription of proinflammatory cytokines, for example IL-6 (Hanley *et al.* 2004).

1.21 P2X receptors

There are 7 members of the P2X family, all of which are stimulated by ATP to form channels selective for monovalent cations, or in some cases also allowing passage of Ca^{2+} or anions (North 2002). P2X receptors have a widespread tissue distribution, including expression throughout many tissues of the body, including, but not limited to, those of the central nervous system, the musculo-skeletal system, the gastrointestinal system and the immune system (Surprenant and North 2009). Due to the initial discovery of P2X receptors in the CNS, their role in mediating excitatory synaptic transmission is now well-established (Surprenant and North 2009). The generation of P2X receptor knockout mice has enabled further understanding of their roles both physiologically and in pathology (Surprenant and North 2009).

Activation of P2X receptors by ATP leads to receptor trimerisation, predominantly as homotrimers, however heterotrimers have been identified (Nicke *et al.* 1998; Kawate *et al.* 2009). These include P2X1/2, P2X1/4 P2X2/3, P2X2/5 P2X1/5, P2X 1/6, P2X2/6 and P2X4/6, which have been shown to coimmunoprecipitate in these combinations following expression in either oocytes or HEK293 (human embryonic kidney cells 293) cells (Torres *et al.* 1999; Aschrafi *et al.* 2004; Nicke *et al.* 2005; Brederson and Jarvis 2008; Jiang 2017). Receptor activation results in formation of the ion channel, which is permeable to small cations in all P2X receptors, and receptors also form signalling complexes through interactions with membrane components and other receptors (Surprenant and North 2009). Activation of P2X receptors can, in some cases lead to permeability to larger cations, such as Tris, NMDG, ethidium ions and YO PRO-1, a DNA binding dye that has been used to study this property in P2X receptors (Evans *et al.* 1996; Virginio *et al.* 1999b; Smart *et al.* 2003). This effect is most pronounced in P2X7R, although it has also been suggested that P2X2, P2X4, and P2X2/3 and P2X2/5 heterotrimers are also capable of forming the membrane pore, however results with these receptors show inconsistencies (Khakh *et al.* 1999; Compan *et al.* 2012).

P2X1 receptors (P2X1R) form a cation selective channel in response to ATP application, with a low permeability to larger cations such as NMDG and tris (Evans *et al.* 1996) . This suggests that P2X1R forms an ion channel, which does not widen to also form a membrane pore. P2X1R was identified in platelets, and a deletion of a

leucine (one of a run of four leucine residues at position 351-353) was found in an individual with deficient platelet aggregation, which resulted in bleeding diathesis due to deficient blood clotting (Oury *et al.* 2000). This mutation resulted in normal receptor plasma membrane expression and therefore likely disrupts the channel structure or conductance/opening, causing a lack of P2X1R function (Clifford *et al.* 1998; Oury *et al.* 2000). In the immune system, P2X1R is involved in neutrophil chemotaxis, aiding migration towards the site of inflammation or infection (Lecut *et al.* 2009). This receptor also has a role in the nervous system, primarily in stimulation of the sympathetic nerve, involved in contraction of the vas deferens (Mulryan *et al.* 2000). P2X1R also interacts with members of the cytoskeleton, for example actin and β-tubulin (Lalo *et al.* 2011), which is essential for its role in arterial vasoconstriction (Vial and Evans 2005).

P2X2 receptors (P2X2R) also form a cation selective ion channel, which has been suggested to be either impermeable to larger cations (Such as NMDG) or to gradually expand, increasing permeability, during prolonged activation of the receptor (Ding and Sachs 1999; Eickhorst *et al.* 2002). P2X2R has a role in digestion, through enteric neurotransmission and peristalsis of the small intestine (Ren *et al.* 2003), alongside roles in neuronal signalling in the brain, including mediating excitatory signals to the interneurons in the hippocampus and at the neuromuscular junction on skeletal muscles (Khakh *et al.* 2003; Ryten *et al.* 2007).

P2X3 receptors (P2X3R) have a highly restricted expression pattern, being expressed in sensory neurons (Chen *et al.* 1995). They therefore have a role in pain sensation through mediation of stimulation of sensory neurons, as well as taste and temperature sensation (Cockayne *et al.* 2000; Finger *et al.* 2005; Shimizu *et al.* 2005). However, P2X3R knockout mice have shown both reduced and enhanced responses to thermal stimuli, suggesting that there may be some compensation for the loss of P2X3R (Shimizu *et al.* 2005). These receptors are highly responsive to ATP, requiring only nanomolar concentrations to be activated (Sokolova *et al.* 2006), where other P2X receptors require micromolar or even millimolar concentrations to be activated (North 2002) . P2X2/3R heterotrimers show some traits that are more in common with P2X2R; they are inhibited by high calcium concentrations, whereas P2X3R have been shown to be insensitive to high calcium. Furthermore, they show a gradual increase in

permeability to larger cations following activation, again a feature not seen in P2X3R but present in P2X2R (North 2002).

P2X4 receptors (P2X4R) induce permeability to larger cations, such as NMDG over a period of tens of seconds (approx. 50-100s) of continuous stimulation, suggesting that they are capable of inducing membrane pore formation to a degree (Soto *et al.* 1996; Virginio *et al.* 1999b), although this could also relate to complexing with P2X7R. P2X4R aids intracellular trafficking of vesicles, through roles in vesicle fusion with the plasma membrane and lysosome fusion, acting by increasing Ca^{2+} concentration inside the cell to allow activation of Ca^{2+} dependent processes (Cao *et al.* 2015). They have been implicated in flow induced changes in vascular tone and remodelling (Yamamoto *et al.* 2005), as well as having a role in the brain, through mediating brain derived neurotrophic factor (BDNF) release in microglia which encourages growth of new neurons and sustains existing neurons (Ulmann *et al.* 2008). Pathologically, they have been demonstrated to have a role in neuropathic pain (Ulmann *et al.* 2008).

P2X5 receptors (P2X5R) in humans exist only as a non-functional splice variant, which lacks exon 10 (Lê *et al.* 1997). A human specific polymorphism appears to result in expression of this non-functional receptor, absence of which in other species results in functional receptor expression (Kotnis *et al.* 2010). In other species, P2X5R do show some activity, although there is some diversity in the levels of response. For example, in chick and bullfrog, a good response is measured in terms of Cl^- permeability (chick) and membrane potential changes (chick and bullfrog) (Jensik *et al.* 2001; Ruppelt *et al.* 2001). However, in rodents and zebrafish, the response is minimal despite good levels of protein expression (Garcia-Guzman *et al.* 1996; Diaz-Hernandez *et al.* 2002). P2X5R knockout mice show normal early bone development and homeostasis, but have a diminished osteoclast response to inflammatory conditions *in vivo*, suggesting a role in this process (Kim *et al.* 2017). In humans, P2X5R can form a functional heterotrimer with P2X1R, which was isolated from cortical astrocytes and is capable of producing currents in response to ATP (Lalo *et al.* 2008). P2X1/5R however show significant differences to either of the homomeric receptors; they are more sensitive to ATP, and in contrast to P2X5R they are not affected by increased extracellular calcium concentrations (although this effect is also seen in P2X1R). They are also less permeable to calcium than P2X1R, however the

calcium permeability cannot be compared to that of P2X5R as this has not been characterised, and they give larger currents than those seen with P2X5R alone (North 2002). This indicates that a heterotrimer of certain receptor monomers is capable of modulating the response of both of the respective receptor monomers to ATP.

P2X6 receptors (P2X6R) are not capable of producing currents in response to ATP application when expressed in HEK293 cells or oocytes, possibly due to insufficient glycosylation in these cell systems (North 2002). P2X6R forms functional heterotrimers, however these reflect the activity of the alternative receptor subunit in the trimer; P2X2/6R show little difference in response to P2X2R and P2X4/6R show little difference to P2X4R (Le *et al.* 1998; King *et al.* 2000). This suggests that the presence of P2X6R in the heterotrimer does not prevent activity of the other receptor, but this does also not imply that P2X6R itself gains any functionality. P2X6R knockout mice have no apparent defects under physiological conditions, with no change in the expression of other P2XRs, which could compensate for its absence (de Baaij *et al.* 2016). These mice have not been tested under pathological conditions, where defects may become apparent.

1.22 P2X7 Receptor

The P2X7 receptor (P2X7R) requires high concentrations of ATP for activation (in excess of 1mM) (McLarnon 2005). The end-point of receptor activation is cell death by apoptosis if stimulation with agonist is persistent (~30 min) or at very high agonist concentrations (≥300μM BzATP, 3'-O-(4-benzoyl)benzoyl adenosine 5'-triphosphate) (Wiley *et al.* 2011). BzATP is an ATP analogue that is a P2X7R selective agonist with higher potency than ATP. As with the other members of this family, P2X7R activation leads to the formation of a cation selective channel, however, prolonged activation leads to the formation of a membrane pore, which allows passage of larger cationic molecules, otherwise only consistently observed in P2X4R (Virginio *et al.* 1999a; Virginio *et al.* 1999b). P2X7R also exhibits responses to BzATP that are unlikely to be connected to channel formation; membrane blebbing and microvesicle release. Membrane blebbing begins after ~30 seconds of continuous application of ≥30μM BzATP (an ATP analogue that is around 10-fold more potent than ATP as an agonist of the P2X7R) (North 2002). This process requires contractile forces generated by the cytoskeleton, specifically of actin and myosin (Morelli *et al.* 2003). P2X7R can

activate protein kinase C (PKC) and Rho-associated kinase, which may activate ROCK1, which mediates the cytoskeletal rearrangement (Morelli *et al.* 2003; Noronha-Matos *et al.* 2014). Membrane blebbing has not been observed on activation of other members of the P2X receptor family. Activation of the P2X7R also leads to shedding of microvesicles (with a diameter of less than 1μm) within seconds of activation (Pizzirani *et al.* 2007; Adamczyk *et al.* 2015).

P2X7R transcription has been shown to be under regulation by specificity protein 1 (Sp1) (García-Huerta *et al.* 2012). This can be controlled through the PI3K/Akt pathway activated by EGFR, and activation of this pathway upregulates P2X7R expression (Gomez-Villafuertes *et al.* 2015). Inhibition of this pathway reduces nuclear levels of Sp1, suggesting that activation of this pathway is allowing Sp1 to activate P2X7R expression (Gomez-Villafuertes *et al.* 2015). Abundant P2X7R expression has been demonstrated in cells of the haematopoietic system, including monocytes/macrophages, lymphocytes and microglia (Di Virgilio *et al.* 2001). It has also been shown in bone cells, such as osteoblasts and osteoclasts. In the central nervous system, expression has been demonstrated on neurons, Schwann cells and astrocytes (Coddou *et al.* 2011). In the gut, P2X7R expression has been demonstrated in the intestinal epithelial cells as well as antigen presenting cells, indicating a role in the immune response in the gut (Cesaro *et al.* 2010; Lees *et al.* 2010; Huang *et al.* 2016).

The expression of P2X7R in the CNS has been linked to physiological functions in sleep and in memory formation, and pathological functions in hyperalgesia and in depression (Dell'Antonio *et al.* 2002; Lucae *et al.* 2006; Labrousse *et al.* 2009; Davis *et al.* 2016). P2X7R is thought to be involved in neurological pain, whereby increased P2X7R expression has been demonstrated in the spinal cord after nerve injury, and administering a P2X7R inhibitory drug prevents the development of mechanical allodynia (Kobayashi *et al.* 2011). The induction of neuropathic pain by P2X7R may involve its ability to mediate release of TNFα, iNOS, PGE2 and BDNF, all of which have been associated with neuropathic pain (Tsuda *et al.* 2012). It has also been demonstrated in rats that administering P2X7R-specific inhibitors reduces tactile allodynia (Honore *et al.* 2006). P2X7R has also been shown to be upregulated in patients with Alzheimer's disease and Huntington's disease, as well as a variety of

other neurological diseases (Parvathenani *et al.* 2003; Chessell *et al.* 2005; Diaz-Hernandez *et al.* 2009). It has been shown that a polymorphism in P2X7R (481C>T) results in 4-fold decrease in the probability of developing Alzheimer's disease (Sanz *et al.* 2014). Analysis of the microglia and astrocytes surrounding the β-amyloid plaques in the brains of mice show increased P2X7R expression (Parvathenani *et al.* 2003). It is possible that P2X7R is involved through a role in α-secretase activity, which stimulates SAPPα release, leading to plaque formation (Diaz-Hernandez *et al.* 2012). Polymorphisms in P2X7R have also been linked to major depressive disorder and anxiety disorders, although these links have not been confirmed in other studies (Lucae *et al.* 2006; Erhardt *et al.* 2007). The P2X7R has also been linked to some cancers, in particular through a possible upregulation of VEGF expression, allowing survival of the tumour (Fang *et al.* 2013).

An increased response to ATP has also been measured in peripheral blood monocytes from RA patients in comparison to a control group, indicated by an increase in IL-1β secretion from these cells (Al-Shukaili *et al.* 2008). Specific receptor polymorphisms linked to OA and RA in genetic studies. In RA, a gain-of-function polymorphism in P2X7R (1068G<A) is two-fold more prevalent in RA patients than in controls. This polymorphism may therefore increase the inflammatory response due to increased receptor activity (Al-Shukaili *et al.* 2011). The P2X7R has also been linked to pain in OA, with patients expressing a hypoactive version of the P2X7R being less likely to have clinically relevant pain (Fuller *et al.* 2009). The loss-of function polymorphism ($R^{270}H$) is linked to a reduction in chronic pain sensitivity in OA patients (Sorge *et al.* 2012). ATP can be released as a consequence of cell death, damage or alternatively, from plasma membrane stretching, via a process involving connexins (Bao *et al.* 2004). Therefore, the mechanical stress that can result from tissue damage, e.g. in OA, could also induce ATP release from chondrocytes at a level sufficient to activate P2X7R (Genetos *et al.* 2005). Chondrocytes have been shown to express both connexins and P2 receptors, including P2X7R and can therefore respond to the presence of ATP in the extracellular environment (Knight *et al.* 2009) and can also release ATP in response to mechanical stimulation (Millward-Sadler *et al.* 2004). It has also been shown that in response to ATP, chondrocytes can secrete increased levels of PGE2, which is itself released in response to IL-1, suggesting that activation of P2X7R by ATP is responsible for enhanced release of inflammatory mediators, either

directly or indirectly (Koolpe *et al.* 1999). This suggests that it is possible that P2X7R becomes over-activated in the OA joint, therefore, it is possible that stimulation of the P2XR by ATP in chondrocytes could induce excessive secretion and extracellular accumulation of TG2 in OA. This evidence implicates P2X7R activity in OA pathology, and suggests its involvement could go beyond the known role in pain sensation.

1.23 Domain Organisation of P2X7R

The P2X7R comprises five domains, an intracellular *N*-terminal domain, two transmembrane domains, an extracellular domain and a long intracellular *C*-terminal domain (Fig. 1.11) (Torres *et al.* 1998). Each of these has an important role in the function of the receptor, for example the extracellular domain interacts with ATP to allow receptor stimulation and there are several glycosylation sites essential for receptor function (Torres *et al.* 1998). For example, N187 is an important glycosylation site, mutation of which prevents correct receptor localisation to the membrane of the cell, which provides a possible explanation of the decreased receptor function seen in the $N^{187}A$ mutant receptor (Lenertz *et al.* 2010).

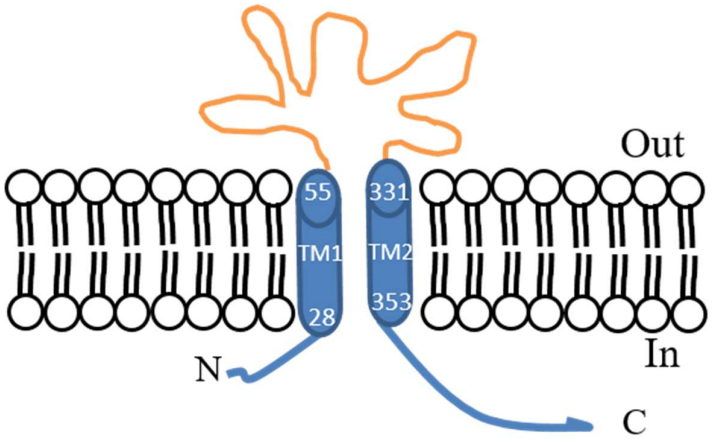

Fig. 1.11 – Transmembrane structure of the P2X7R. Transmembrane domains are indicated as TM1 and TM2. Residues of TM1 and TM2 for human P2X7R are also indicated.

The P2X7R is unique amongst P2 receptors in having a very long intracellular *C*-terminus, thought to be important for membrane pore formation by the receptor (Costa-Junior *et al.* 2011), a channel permeable to larger cationic molecules. The *C*-terminus is approximately 200 amino acids longer than the *C*-termini of the other P2XRs (Costa-Junior *et al.* 2011). There is at present no structural information

available for the *C*-terminus and there are no proteins with extended homologies to this sequence in the protein database. However, there are several regions with sequences correlating to known domains in other proteins. There is an SH3 (Src homology 3) binding motif at residues 441-460, which can interact with Src tyrosine kinase. This suggests that the *C*-terminus may be able to participate in ion channel-independent signalling (Denlinger *et al.* 2001). Src tyrosine kinase is thought to be responsible for activating pannexin 1, which has been suggested to be the membrane pore that associates with this receptor (see section 1.26), in response to P2X7R activation. This is supported by the discovery that the $P^{451}L$ mutation in mouse P2X7R, which is in the SH3 binding domain prevents pore formation (Sorge *et al.* 2012). The $P^{451}L$ substitution could therefore prevent pore formation by preventing the interaction between the P2X7R and Src tyrosine kinase so Pannexin 1 cannot be activated (Iglesias *et al.* 2008). There are also other regions of the *C*-terminus that are possibly important for membrane pore formation, where mutations cause a loss of pore functionality. However, as the *C*-terminus is also important for receptor expression at the surface of the cell, some of these mutations clearly affect trafficking of the receptor and this may result in the apparent decrease in pore formation (Costa-Junior *et al.* 2011). Finally, expressing a receptor that lacks the *C*-terminus causes an apparent loss of larger dye molecule uptake but not cation transport, such as Ca^{2+} or K^{+}, demonstrating a lack of pore formation but no effect on other functions of the receptor (Adinolfi *et al.* 2010). Further functions of the P2X7R attributed to the *C*-terminus include the internalization and recycling of the receptor (see section 1.24). The residues responsible for this are likely to be between positions 357-360, 508-510 and 540-543 in the *C*-terminus, because these residues are in a β-arrestin binding motif, allowing phosphorylation and internalisation of the receptor, possibly mediated by GRK3 (Costa-Junior *et al.* 2011). Receptor internalization occurs following ATP activation, resulting in either degradation to an 18kDa form of the receptor or recycling back to the cell membrane (Feng *et al.* 2005).

The second transmembrane domain has been demonstrated to be important for surface expression in experiments that substituted the TM2 of the P2X7R with the TM2 of P2X1R or P2X4R (Sun *et al.* 2013). Site directed mutagenesis as well as allelic variations in the population have also shown that channel function of the receptor is highly sensitive to sequence changes in the TM2 (Stokes *et al.* 2010; Sun *et al.* 2010).

Combined with structural studies this suggests that positioning of TM2 relative to TM1 in the membrane is critical for ion channel definition. Furthermore, by substituting single residues in the TM2, a decreased dye uptake can be seen, as can a decrease in membrane blebbing associated with P2X7R activation (Sun *et al.* 2013).

1.24 Turnover of the P2X7R

ATP stimulation can induce internalisation of the P2X7R (Feng *et al.* 2005). It has been shown that the recycling process begins with phosphorylation of tyrosine, threonine and serine residues, possibly in part by the kinase GRK3, which has been shown to co-localise with the receptor (Feng *et al.* 2005). There is also an increased binding of β-arrestin-2, which may target the receptor to dynamin and clathrin-coated pits, allowing endocytosis of the receptor into clathrin-coated endosomes (Feng *et al.* 2005). From these endosomes, the receptor can either be exported to lysosomes or recycled back to the membrane (Feng *et al.* 2005).

1.25 Activation of P2X7R: Ion channel formation

P2X7R is activated by binding of ATP; as the functional receptor in the cell membrane is a trimer, three ATP molecules can bind the extracellular region of the receptor trimer, activating it (one ATP molecule per subunit) (Yan *et al.* 2010). Different states of ligand occupancy have been suggested to be associated with different extents of pore dilation (Jiang *et al.* 2013). It has been proposed that the receptor trimers may cluster at later stages of activation, for example when the pore is formed (Connon *et al.* 2003). When low concentrations of ATP (less than 100μM) are applied for a short period, the receptor becomes permeable to monovalent and divalent cations (Surprenant *et al.* 1996). ATP binding in these conditions leads to an influx of Ca^{2+} and membrane depolarization due to K^+ leaving the cell and Na^+ entering the cell. This is driven by the osmotic gradient across the cell membrane. Ca^{2+} entering the cell can initiate calcium signaling, having a variety of effects on cellular processes.

1.26 Activation of P2X7R: Membrane pore formation

Prolonged stimulation of the P2X7R (seconds to minutes of ATP application) or higher concentrations of ATP can lead to the formation of a larger, non-selective, cation permeable pore, which will allow passage molecules up to 900Da into the cell (Virginio *et al.* 1999b). This includes dyes such as ethidium bromide and YO PRO-1. This pore could be formed by the receptor itself (an extended pore) by dilation of the channel or acquisition of additional subunits or by coupling to other channels following receptor activation (Fig. 1.12) (Alberto *et al.* 2013). Experiments by Virginio et al have suggested that as the pore dilates it passes through a series of smaller size pores before reaching the final size permeable to NMDG (Virginio *et al.* 1999a). Alternatively, this pore could be formed through coupling of the receptor to another protein in the membrane, for example pannexin hemichannels (Iglesias *et al.* 2008). Pannexins are capable of forming a channel through the plasma membrane to the extracellular environment, which is permeable to ions of up to 900Da, consistent with the observed capabilities of the 'pore' formed by the P2X7R (Alberto *et al.* 2013). Suadicani *et al.* have demonstrated that the use of antagonists of gap junction channels can inhibit the 'P2X7R pore' activity, suggesting a role for pannexins. Furthermore, the use of pannexin 1 antagonists have been shown to decrease 'pore' formation by the P2X7R in some cells (Suadicani *et al.* 2006). However, experiments in

macrophages have also demonstrated that the pannexin 1 knock-out has no effect on dye uptake when the P2X7R is activated, suggesting that pannexin may not be the single pore-forming component (Qu *et al.* 2011). Recent experiments by Browne *et al* using a version of the P2X7R with the $G^{345}C$ mutation have further supported a channel dilation theory. Introduction of the cysteine at a position in the transmembrane domain which forms part of the ion permeation pathway allows the channel to be blocked using large cysteine-reactive molecules (Browne *et al.* 2013). When modified, the current induced by ATP was inhibited, and ethidium ion entry was reduced, indicating that pore formation was also reduced (Browne *et al.* 2013). This suggests that the dyes enter the cell through the P2X7R ion channel.

Image removed due to copyright

Fig. 1.12 – Representation of the potential models explaining the larger pore formed by the P2X7R. A. demonstrates a widening of the ion channel of P2X7R itself to form an intrinsic pore that is permeable to NMDG or YO PRO-1. B. represents the alternative hypothesis, where the C-terminus of the P2X7R interacts with an extrinsic membrane channel (North 2002).

1.27 New insights from crystal structure of the P2X7R

In general, all available crystal structures have shown that there is a characteristic architecture associated with P2XRs. All P2X receptors have intracellular *N*- and *C*-termini, with two transmembrane domains and a large extracellular domain, rich in glycosylation and disulphide bridges (Kawate *et al.* 2009; Hattori and Gouaux 2012;

Karasawa and Kawate 2016; Mansoor *et al.* 2016). This was initially demonstrated by crystallization of a modified P2X4 protein at resting state to 3.1Å resolution, that was generated using a construct lacking both *N*- and *C*- termini and containing three point mutations (ΔzfP2X4-B; C51F, N78K, N187R) (Kawate *et al.* 2009). Since then, a second P2X4 structure has been published, resolved to a higher resolution (in complex with ATP to 2.8Å, in the absence of ATP to 2.9Å), based on a construct with *N*- and *C*-terminal truncations, and containing 4 amino acid changes; ΔN27, ΔC24, N78K and N187R (Hattori and Gouaux 2012). This structure revealed the ATP binding motif and the open channel conformation. A structure for P2X3R has also been published, which retains more of the *N*- and *C*- termini than the P2X4R structures. This may provide a more accurate structure and relative positioning of the transmembrane domains as the absence of N- and C- termini in the truncated P2X4R proteins may change the positioning of the transmembrane domains (Mansoor *et al.* 2016). This construct also contained 3 amino acid changes; T13P, S15V and V16I (hP2X3-MFC). P2X3 receptors have some properties which differ significantly to P2X2, P2X4, P2X5 and P2X7 receptors, but which are in common with P2X1 receptors. These are that P2X1 and P2X3 show a rapid, nearly complete desensitization and a nanomolar affinity for 2',3'-*O*-(2,4,6-Trinitrophenyl)adenosine-5'-triphosphate, TNP-ATP, (an ATP analogue which acts as a selective P2X1 and P2X3 antagonist) (Mansoor *et al.* 2016). P2X2, P2X4, P2X5 and P2X7 have a 1000-fold decreased affinity for TNP-ATP and show slow, incomplete desensitization (Mansoor *et al.* 2016). This indicates that there are likely to be some differences between P2X3 and P2X7, structurally, to account for these functional differences. The P2X3 structure also demonstrated that a cytoplasmic cap exists, which is made up of two β-strands from the *N*-terminus and one β-strand from the *C*-terminus, which sits beneath the cytoplasmic domain, capping the surface of the pore (Mansoor *et al.* 2016) (Fig. 1.13). As the residues that would be required to perform this function in other P2XRs were not present in crystallised proteins, it is not known if an analogous cap exists in other P2XRs. Finally, a crystal structure of the P2X7R has recently become available, using panda P2X7R, which has a high degree of homology to human P2X7R (Karasawa and Kawate 2016). The construct used for crystallization lacks the majority of the *N*- and *C*- termini (truncation at position 360), as well as having 5 additional mutations; $N^{241}S$, $N^{284}S$, $V^{35}A$, $R^{125}A$ and $E^{174}K$

(Karasawa and Kawate 2016). Due to the lack of *C*-terminal portion of the receptor in this structure, the conformation of this is still unknown.

Image removed due to copyright

Fig. 1.13 - Cartoon representation of hP2X3 structure. hP2X3R is shown in open state, with the position of the cytoplasmic cap indicated. Structure shown a) in side view, b) from above (the extracellular side) and c) the ion permeation pathway (Mansoor *et al.* 2016).

The structure of P2X receptors has been likened to the shape of a dolphin, where the transmembrane helices and the extracellular domain make up flukes and body of the dolphin, and the head, both flippers and dorsal fin are also present (Fig. 1.14) (Kawate *et al.* 2009). This structure has been confirmed to be consistent across all published P2X receptor structures (Hattori and Gouaux 2012; Karasawa and Kawate 2016; Mansoor *et al.* 2016).

Image removed due to copyright

Fig. 1.14 – Structure of P2X7R subunits. The P2X7R structure has been likened to the shape of a dolphin. In green, the transmembrane domains make up the fluke of the dolphin, the extracellular domain makes up the body and head and has structures similar to the left and right flippers and the dorsal fin. Figure adapted from (Kawate *et al.* 2009).

The first published P2X4R structure revealed that in the closed conformation, the large extracellular domain adopts a chalice shape, with 6 alpha helices (two from each subunit) making up the transmembrane domain (Kawate *et al.* 2009). These alpha helices are angled through the membrane, crossing each other to constrict the transmembrane pore. The open state structure predicts that activation of the receptor results in an iris-like movement of the transmembrane domains, which results in them moving away from the central axis by 3Å, widening the pore (Fig. 1.15) (Hattori and Gouaux 2012). This opens lateral fenestrations of the extracellular domain, allowing

ions to enter (Fig. 1.16) (Hattori and Gouaux 2012). The acidity of the central vestibule means that cations are attracted and anions are repelled, leading to an accumulation of cations at the entrance to the ion channel (Hattori and Gouaux 2012). In the pdP2X7R structure, this conformation is proposed to reflect the open, undilated state of the receptor (ion channel formation, but no membrane pore present) (Karasawa and Kawate 2016).

Image removed due to coypright

Fig. 1.15 - Transmembrane helices move in an iris-like manner. a and b) The transmembrane regions of the closed (grey) and open states of P2X4R are superimposed, with black arrows and bars indicating the rotation of the transmembrane helices. A) indicates that TM1 rotates by ~10º and TM2 by ~55º anticlockwise about the pore centre and perpendicular to the membrane. B) demonstrates the orientation of the transmembrane helices, whereby TM2 is shown to tilt by ~8º parallel to the membrane (Hattori and Gouaux 2012).

Image removed due to copyright

Fig. 1.16 - Section of an electrostatic potential surface of P2X4R demonstrating the position of the lateral fenestrations. Red indicates a negative electrostatic potential (-10kT) and blue indicates a positive electrostatic potential (+10kT, dielectric constant: 80) demonstrating the position of the lateral fenestrations, which allow ions to enter and exit the receptor (Hattori and Gouaux 2012).

The published P2X7R structure reveals some differences to the P2X4R structures, although the general architecture is the same (Karasawa and Kawate 2016). One of the major differences is that a cavity in between subunits is larger in P2X7R (Fig. 1.17), and is a site of drug binding (Karasawa and Kawate 2016). This cavity narrows on ATP binding, indicating that P2X7R-specific drugs prevent receptor activation through preventing this conformational change. This also indicates why these drugs show some degree of specificity for P2X7R, as they would be too large to fit in the cleft of other P2X receptors, specifically P2X4R. Hence, this provides a potential target for specific drug design (Karasawa and Kawate 2016). The narrowing of this cavity also allows the lower body to widen further, opening the P2X7R channel (Karasawa and Kawate 2016). Other P2X receptors have a narrower cleft to begin with, possibly explaining some of the functional differences seen with P2X7R, possibly accounting for how P2X7R membrane pore formation occurs, but the absence of an ATP bound open structure prevents any conclusions being drawn regarding this (Karasawa and Kawate 2016).

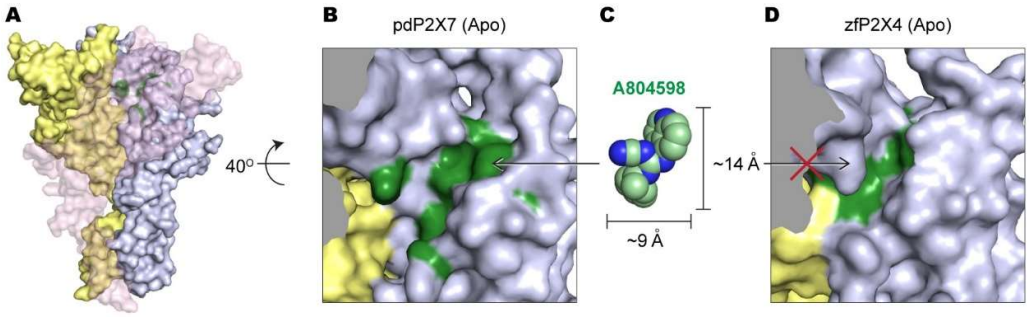

Fig. 1.17- Difference in the shape of the cavity of P2X7R and P2X4R. A) P2X7R receptor (no ligand bound) shown from the side, one subunit of the trimer is coloured yellow, one grey and the other pink. The cavity zoomed in in B (P2X7R) and D (P2X4R) narrows during receptor activation, and is a site of P2X7R specific drug binding. Structures demonstrate that this cavity is narrower in P2X4R than P2X7R, indicating that the drug is unable to access the site in P2X4R. Green residues in B are the drug binding resides (drug shown in C is A804958, magnified in scale with the zoomed structures) and green residues in D are the equivalent residues in P2X4R (Karasawa and Kawate 2016).

1.28 Aims of the Thesis

. Our group have demonstrated a regulated mechanism for TG2 secretion from cells, involving P2X7R activation by ATP. The pathway for externalisation of TG2 is critical

for regulating its transamidation activity and hence controls the formation of modifications in extracellular proteins and peptides, which could act as biomarkers for diseases such as OA. Therefore, this thesis aims to further our understanding of how TG2 secretion is regulated and the mechanistic steps involved.

The following questions are investigated in this thesis:

1. Is ‘membrane pore’ formation induced upon P2X7R activation required for TG2 secretion, and if so, what is the identity of the respective membrane pore?
2. What activities or conformational states of TG2 are required for its secretion and is the TG2 activating oxidoreductase thioredoxin mechanistically tied in to the secretion?
3. Is this pathway of physiological relevance, i.e. do cells of the immune system release TG2 through this pathway?
4. How do polymorphisms in the human P2X7R affect TG2 secretion?

Addressing these questions will allow us to elucidate a new pathway for secretion of TG2 and potentially other unconventionally secreted proteins involving thioredoxin. The translation of these findings from a HEK293 cell model to primary human macrophages will allow us to demonstrate that this is a physiologically relevant pathway for protein secretion and importantly, the innate immune response. Investigating the impact of polymorphisms in P2X7R on this novel secretory pathway may have wider implications in regards to susceptibility to disease, including OA.

Chapter 2

2. Methods

General Methods

2.1 Cell Culture

2.1.1 Maintenance of HEK293 Cells

Human embryonic kidney cells with a Flp-In site for DNA integration (HEK293 Flp-In, Invitrogen, Thermo Fisher, Leicestershire, UK) were maintained in Dulbecco's modified Eagle's medium (DMEM, Gibco, Thermo Fisher) supplemented with 10% heat inactivated foetal bovine serum (hiFBS, Gibco), 2mM L-glutamine (Invitrogen, Thermo Fisher) 100µg/ml penicillin, 100U/ml streptomycin (pen/strep, Invitrogen) and 100µg/ml Zeocin (Gibco). HEK293 cells expressing either the wild-type P2X7R (obtained from Dr Magdalena Adamczyk), P2X7R with the $A^{348}T$ mutation (HEK293 $A^{348}T$) or $P^{451}L$ mutation (HEK293 $P^{451}L$) or the truncated version of P2X7R (P2X7R variant B) or the V5-tagged P2X7R were maintained in DMEM supplemented as above, as well as with 100µg/ml hygromycin B (Invitrogen). Approximately every 5 days, confluent cells (at approximately 90% confluency) were passaged 1:10. Media was removed, cells washed in 5ml PBS (Oxoid, Cheshire, UK) and trypsinised (addition of 1.5ml 1% trypsin and 0.48mM EDTA, Gibco) at 37°C for several minutes until they were easily removed from the surface of the flask by gentle tapping. 5ml of DMEM supplemented with 10% hiFBS was added to block the trypsin and the cells were collected by centrifugation at 350x g for 5 minutes. Supernatant was removed and the cell pellet re-suspended in 10ml DMEM containing 10% hiFBS. 1ml of the cell suspension was added to 13ml of DMEM supplemented as above and seeded in a T75 flask (Sarstedt, Leicestershire, UK).

2.1.2 Extraction of human PBMCs

Human blood was taken from healthy volunteers with informed consent under Ethics Approval DS REC 15/37a (Cardiff University Dental School Research Ethical Committee) and Wales REC3 10/MRE09/28: AR UK BBC Multi-project ethical submission (for experiments involving DNA sequencing of P2X7R from white blood cells). All experiments were performed in accordance with relevant guidelines and regulations. There were no exclusion criteria, although individuals with a history of inflammatory joint disease, gluten sensitivity, or taking anti-inflammatory medication

were requested to decline to take part in the study. Up to 35ml peripheral blood was taken, after consent was taken. Peripheral blood was drawn into a vacutainer containing 10U/ml heparin (Vacuette, Greiner Bio One, Stonehouse, UK), with final volumes between 12ml and 40ml. Blood was diluted to at least 1:1 ratio of Blood:PBS and 35ml of this mix was layered over 15ml sterile Ficoll Paque premium (Thermo Fisher) and centrifuged at 18-20°C for 30 min at 400x g (no brake). Plasma was removed to 1cm from the white cell interface and the white cell interface was taken into a fresh 50ml tube. PBS was added to at least double the volume of white cell interface and centrifuged at 18-20°C for 10 min at 380x g (medium brake applied). The supernatant was removed from the white cell pellet and the pellet re-suspended in 50ml PBS. The cells were centrifuged at 18-20°C for 10 min at 200x g (medium brake applied). Supernatant was removed and cells re-suspended in 1ml RPMI 1640 (RPMI, Lonza, Tewkesbury, UK) containing 10% FBS, 2mM l-glutamine, 100U/ml penicillin and 100µg/ml streptomycin. 50µl of the cells were added to 450µl 2% acetic acid to lyse any remaining erythrocytes and 10µl of this was used for counting as described in section 2.1.4. Cells were seeded in RPMI containing 10% FBS, 2mM l-glutamine, 100U/ml penicillin and 100µg/ml streptomycin and 20ng/ml rhGM-CSF (recombinant human granulocyte macrophage colony-stimulating factor, Immunotools, Germany) to direct monocytes to differentiate into M1 macrophages.

2.1.3 M1 macrophage culture

Cells extracted as described in Section 2.1.2 were incubated at 37°C with 5% CO_2 for 7 to 10 days with a media change every third day. On day 7 or day 10, macrophages were trypsinised, as described previously (Section 2.1.1), at 37°C for several minutes until the cells become more rounded. The cells then required gentle scraping to remove them from the surface of the flask. 5ml RPMI containing 10% FBS was added to inactivate the trypsin and cells were centrifuged at 350x g for 5 minutes. The supernatant was removed and the cells re-suspended in 2ml RPMI containing 10% FBS, 2mM l-glutamine, 100U/ml penicillin and 100µg/ml streptomycin and 20ng/ml rhGM-CSF. Cells were then counted as described in section 2.1.4 and used in experiments as outlined in section 2.1.11.

2.1.4 Counting cells

When required, cells suspended in medium after trypsinisation were counted using a Neubauer Haemocytometer (Thermo Fisher). 10µl of cell suspension was mixed with 10µl Trypan Blue (0.4%, T8154, Sigma). 10µl of this mixture was loaded into the haemocytometer by capillary force and unstained (therefore viable) cells were counted according to the manufacturers' protocol and the number of cells per ml calculated as follows:

$$\left(\frac{total\ number\ of\ cells\ counted \times dilution\ factor}{number\ of\ squares\ counted}\right) \times 10000$$
$$= number\ of cells/ml$$

2.1.5 Total cell protein extraction

Cells were lysed with cell extraction buffer (20mM HEPES/NaOH pH7.4, 150mM NaCl, 1mM EGTA, 1% Triton-X-100 and 0.25% deoxycholic acid containing 1mM phenylmethylsulfonyl fluoride (PMSF), 1mM N-ethylmaleimide (NEM) and 10% glycerol), and lysate was centrifuged at 15 000x g for 15 minutes at 4°C and supernatant stored frozen for analysis.

2.1.6 Determination of protein concentration

The BCA protein assay kit (Pierce, Thermo Fisher) was used to determine the protein concentration of cell lysates. This assay uses the principle of reduction of Cu^{2+} to Cu^{1+} which can then react with bicinchoninic acid (BCA) to give a purple product in the presence of protein. Samples were diluted 1:5 in TBS and 25µl of this was mixed with 200µl of working reagent (reagent A and reagent B in a ratio of 50:1) and incubated for 30 minutes at 37°C, followed by a 10 minute incubation to equilibrate the plate to room temperature and absorbance was read at 562nm. The samples were compared to known concentrations of bovine serum albumin (BSA) standards. Concentrations of samples were derived using linear regression to fit the values for the standards.

2.1.7 SDS PAGE

SDS PAGE separation of proteins was performed to assess purity of purified TG2 and to enable transfer of proteins onto a nitrocellulose membrane for Western blotting. Equal volumes of cell lysate and 2x sample buffer (25mM Tris/HCl pH6.8, 3.9mM

EDTA, 4% SDS, 30% glycerol, 0.3% bromophenol blue) containing 2% β-mercaptoethanol (Sigma, Suffolk, UK) were mixed and boiled for 3 minutes at 98°C. Lyophilised conditioned media was re-suspended in 50µl of the following solution: 1000µl 8M urea, 980µl 2X sample buffer and 20µl β-mercaptoethanol (1%). 10µg of the protein or 10µl of re-suspended conditioned media were loaded into Novex 4-20% Tris-Glycine polyacrylamide gels (Invitrogen) or 16% Tricine gels (for thioredoxin probing, Invitrogen) alongside 30µg low molecular weight marker (GE, Hertfordshire, UK). The gel was run for 2 hours at 125V (constant voltage) in SDS PAGE running buffer (25mM Tris/HCl, pH8.8, 192mM glycine, 0.1% SDS). For analysis of protein purity, the gel was then stained using Coomassie brilliant blue R. Where required, the gel was then used to transfer proteins onto a nitrocellulose membrane (Amersham protran NC, Thermo Fisher) to allow probing with antibodies for the desired protein.

2.1.8 Western Blotting

Sponges, blotting paper and nitrocellulose membrane were soaked in ice-cold transfer buffer (25mM Tris, 192mM glycine, 20% methanol) and a blotting sandwich assembled. Proteins were transferred onto the nitrocellulose membrane for 2 hours at 125mA constant current in transfer buffer. Nitrocellulose membrane was briefly stained with Ponceau S solution (0.1% Ponceau S, 5% acetic acid in H_2O) to visualize transfer efficiency and mark the protein marker positions and was then washed with TBS (20mM Tris/HCl, pH7.4, 150mM NaCl) to remove the stain. Membrane was blocked in 5% non-fat milk powder (Sigma, unless indicated otherwise in Table 2.1) in TBS for 1 hour, to prevent non-specific binding of antibody to the membrane. Primary antibodies were diluted in 5% non-fat milk powder in TBS (unless indicated otherwise in table 2.1) and incubated with the membrane as listed in table 2.1. Membrane was washed 3 times for 5 minutes in TBS-T (TBS containing 0.05% Tween-20). Secondary antibody was diluted and incubated as listed in table 2.2 in 5% milk in TBS-T (unless indicated otherwise in table 2.2). Then membrane was washed 3 times for 5 minutes with TBS-T and once for 5 minutes with TBS. ECL prime (GE) was diluted in a 1:1 ratio of solution A: solution B and spread over the membrane for 2 minutes. Excess was removed and membrane exposed to Amersham Hyperfilm (GE) for the required amount of time (ranging from several seconds to 30 minutes).

Table 2.1 Details of primary antibodies used in Western blotting and immunostaining.

*Antibody diluted in 3% Casein in TBS, appropriate secondary antibody diluted in 3% Casein in TBS-T. Blocking also performed in 3% Casein in TBS.

Name Clone	**Species**	**Final Concentration (WB)**	**Final Concentration (immunostaining)**	**Catalogue number manufacturer**
Anti TG2 CUB7402	Mouse Monoclonal	200ng/ml 1.5h, RT	2µg/ml 1h, RT	MS-224-P1 Thermo scientific
Anti TG2 β-sheet	Mouse Monoclonal	200ng/ml 2h, RT	-	A034 Zedira
Anti TG2 β-barrel	Mouse Monoclonal	200ng/ml 2h, RT	-	A037 Zedira
Anti P2X7R	Rabbit Polyclonal	1µg/ml ON, 4°C	2µg/ml ON, 4^0C	Sc-25698 Santa Cruz
Anti P2X7R extracellular domain	Rabbit Polyclonal	1.6µg/ml ON, 4^0C	4µg/ml ON, 4^0C	APR-008 Alomone labs
Anti β-Tubulin TUB2.1 (primary)	Mouse Monoclonal	2.6µg/ml 1h, RT	1.3µg/ml 1h, RT	T4026 Sigma
Anti IκBα	Rabbit Polyclonal	1µg/ml 2h, RT	-	Sc-371 Santa Cruz
Anti thioredoxin*	Rabbit Polyclonal	1µg/ml 2h, RT	-	FL-105 Santa Cruz
Anti Caspase-3	Rabbit Polyclonal	0.04µg/ml ON, 4^0C	-	9662 Cell Signalling Technology

Table 2.2 Secondary antibodies used in Western blotting and immunostaining

Name	Species	Final Conc. (WB)	Final Conc. (immunostaining)	Catalogue number manufacturer
HRP conjugated anti mouse	Rabbit	2µg/ml 1 hour, RT	-	P0260 Dako
HRP conjugated anti rabbit	Swine	2µg/ml 1 hour, RT	-	P0399 Dako
Alexa Fluor 488 conjugated anti mouse	Goat	-	10µg/ml 1 hour, RT	A11001 Invitrogen
Alexa Fluor 488 conjugated anti rabbit	Donkey	-	10µg/ml 1 hour, RT	A21206 Invitrogen
Alexa Fluor 594 conjugated anti rabbit	Goat	-	10µg/ml 1 hour, RT	A11037 Invitrogen

2.1.9 TG2 secretion from HEK293 cells

To investigate the release of TG2 by cells expressing different variants of the P2X7R or assess the release of TG2 GTP binding mutants, P2X7R expressing HEK293 cells were transfected with the pcDNA3.1 vector encoding TG2 (plasmid obtained from Professor Daniel Aeschlimann) and stimulated using BzATP (Adamczyk 2013). HEK293 cells expressing P2X7R stop, P2X7R $A^{348}T$, P2X7R $P^{451}L$ or P2X7R variant B were seeded at $1.2x10^5$ cells/well in a 24 well plate (Sarstedt) in 0.5ml DMEM containing 10% hiFBS without antibiotics. 24 hours later, cells were transiently transfected with pcDNA 3.1 WT TG2 or TG2 GTP binding mutants also in pcDNA 3.1 using Fugene-6 transfection reagent (Promega) according to the manufacturers' instructions. A 1.5µl Fugene-6:0.5µg DNA ratio was used. Appropriate amounts of Fugene-6 and antibiotic-free medium were mixed, then TG2 plasmid was added and the mixture incubated at room temperature for 30 minutes for DNA-lipid complexes to form. Medium was changed to fresh DMEM containing 10% hiFBS without antibiotics. 100µl of the Fugene-6/DMEM/DNA mix was added drop-wise to each well. 48 hours post-transfection, HEK293 P2X7R expressing HEK cells were used for stimulation. OptiMEM was left in the incubator overnight to be pre-warmed and pre-gassed with CO_2. BzATP was used for stimulation at a final concentration of 0.1mM,

diluted in OptiMEM. Cells were washed for 5 minutes at 37°C, 5% CO_2 with pre-warmed OptiMEM (200µl/well), and where required the cells were pre-treatment was applied to cells, as indicated in Table 2.3, then 0.1mM BzATP or OptiMEM only was added and incubated for 10 minutes at 37°C, 5% CO_2. Media was collected and centrifuged at 1 500x g for 10 minutes and the supernatant was kept for analysis. Cells were washed with pre-warmed OptiMEM, then fresh pre-warmed OptiMEM was added for a 30 minute chase period at 37°C, 5% CO_2. Media was collected and centrifuged at 1 500x g for 10 minutes as before and supernatant was kept for analysis. Remaining cells were lysed with cell extraction buffer (20mM HEPES/NaOH pH7.4, 150mM NaCl, 1mM EGTA, 1% triton-X-100 and 0.25% deoxycholic acid containing 1mM PMSF, 1mM NEM and 10% glycerol), and lysate was centrifuged at 15 000x g for 15 minutes at 4°C and supernatant stored frozen for analysis. Media was lyophilised and reconstituted at 10-fold higher concentration, to allow loading of the equivalent of 150µl of sample into the SDS PAGE gel (section 2.1.7). 10µg of total cell protein, as determined by BCA assay (section 2.1.6) was loaded for cell lysate samples. A Western blot was then performed, probed using an anti TG2 antibody (as described in section 2.1.8).

Table 2.3 Treatments applied to cells

Compound	Target	Concentration	Stage applied
A740003 (Tocris, Bristol, UK)	P2X7R	5μM	Present at all times 10 minute preincubation
Calmidazolium chloride (Merck, NJ, USA)	P2X7R ion channel	1μM	Present at all times 10 minute preincubation
^{10}Panx (Tocris)	Pannexin-1	100μM	Present at all times 30 minute preincubation
Trovafloxacin (Sigma)	Pannexin-1	100μM	Present at all times 30 minute preincubation
2.5mM Ca^{2+}	P2X7R	2.5Mm $CaCl_2$	Present at all times 10 minute preincubation
Ac-YVAD-cmk (Sigma)	Caspase-1	100μM	Present at all times different preincubation times
EDTA	TG2	5mM	Present at all times 10 minute preincubation
Pitstop 2 (Abcam, Cambridge, UK)	Endocytosis	20μM	Present at all times 10 minute preincubation
E64 (sigma)	Cysteine proteases	100μM	Present at all times 10 minute preincubation
Aprotinin (Sigma)	Serine proteases	10μg/ml	Present at all times 10 minute preincubation
Apyrase (Sigma)	degrades ATP		15 minute preincubation
DNCB (Sigma)	Thioredoxin	10μM 30μM	Present at all times 30 minute preincubation
PX-12 (Sigma)	Thioredoxin	50μM	Present at all times 30 minute preincubation

2.1.10 TG2 secretion from M1 macrophages

M1 macrophages derived from human peripheral blood mononuclear cells (PBMCs) were seeded at a density of $1x10^5$ cells/well in 0.5ml RPMI containing 10% FBS, 2mM l-glutamine, 100U/ml penicillin and 100μg/ml streptomycin and 20ng/ml rhGM-CSF in a 24-well plate. 4 wells were required per condition. Cells were allowed to adhere to the plate for 24 hours prior to the experiment. Media was removed and cells were washed in 0.2ml OptiMEM for 5 minutes. Where pre-incubation with inhibitors was required, this was performed in OptiMEM and is described in table 2.3. BzATP was used for stimulation at a final concentration of 0.1mM, diluted in OptiMEM. Cells were washed for 5 minutes at 37°C, 5% CO_2 with pre-warmed OptiMEM (200μl/well), then 0.1mM BzATP or OptiMEM only was added and incubated for 10 minutes at 37°C, 5% CO_2. Media was collected and centrifuged at 1 500x g for 10 minutes and the supernatant was kept for analysis. Cells were washed with pre-

warmed OptiMEM, then fresh pre-warmed OptiMEM was added for a 30 minute chase period. Media was collected and centrifuged at 1 500x g for 10 minutes and supernatant was kept for analysis. Remaining cells were lysed with cell extraction buffer (20mM HEPES/NaOH pH7.4, 150mM NaCl, 1mM EGTA, 1% triton-X-100 and 0.25% deoxycholic acid containing 1mM PMSF, 1mM NEM and 10% glycerol), and lysate was centrifuged at 15 000x g for 15 minutes at 4°C and supernatant stored frozen for analysis or prior to cell lysis, cell surface protein was extracted as described in section 2.12. Media samples were concentrated by ethanol precipitation by addition of 3x volume of ice cold ethanol absolute and stored at -20°C overnight. Samples were then centrifuged at 15 000x g for 10 minutes at 4°C and the pellet re-suspended in sample buffer (as described in section 2.1.10). This allowed loading of the equivalent of 400µl media sample into an SDS PAGE gel (section 2.1.7). Cell lysate concentration was determined by BCA assay (section 2.1.6) and 10µg total cell protein loaded. A Western blot was then performed and probed using an anti-TG2 antibody (section 2.1.8).

Methods in Chapter 3

2.2 Generating P2X7R variant expressing HEK293 Cells

2.2.1 Cloning P2X7R Variants

The wild-type P2X7R DNA in a version of the pcDNA5/FRT vector modified to include the multiple cloning site from pcDNA4/V5-His was provided by Dr Magdalena Adamczyk (Adamczyk 2013). Primers for introducing a point mutation giving a hyperactive P2X7R; $A^{348}T$ P2X7R (Stokes *et al.* 2010), or an inactive receptor; $P^{451}L$ P2X7R (Sorge *et al.* 2012) or a truncated form of P2X7R (Variant B) which lacks the final 249 amino acids of the C terminus of the receptor (Adinolfi *et al.* 2010), were designed as is shown in table 2.4 and ordered from Eurofins MWG. PCR reaction mixes contained 10µl 5x Phusion buffer (Finnzymes, Thermo Fisher, final concentration of 1.5mM $MgCl_2$), 0.3µg template DNA, 2µM each of forward and reverse primers as listed in table 2.4, 2 units Phusion polymerase (Finnzymes), 0.8mM dNTPs and MilliQ H_2O up to a final volume of 50µl. PCR cycles are shown in table 2.5.

Table 2.4 Primer sequences for mutagenesis. Underlined region of the forward primer for variant B will introduce a KpnI restriction site. Underlined region of the variant B reverse primer will introduce an XhoI restriction site. Nucleotides differing from the wild-type sequence are given in red.

P2X7R Variant	Forward Primer	Reverse Primer
$A^{348}T$	5'-GTCTGGCCACTGTGTTCATCG-3'	5' GAACACAGTGGCCAGACCGAAG 3'
$P^{451}L$	5'-GACACACCCCTGATTCCTGGAC-3'	5'-CAGGAATCAGGGGTGTGTCATGG-3'
Variant B	5'-TTAGGTACCTTCACCATGCCGGCCTGCTGC-3'	5'-TTCTCGAGTTAGTCACTTCCTTCTCCAAACCATTTTCCTAAAGCATGGAAAAGAGAATCTCTTACCGAAGTAGGAG-3'

Table 2.5 PCR cycles for P2X7R constructs *Extension time reduced to 3 minutes for variant B.

Stage	Temperature (°C)	Time	Repeats
	94	2 minutes	
Denaturing Annealing Extension	94 55, 57, 60.2 or 62 72	1 minute 45 seconds 7 minutes*	X 16
	72	10 minutes	

Successful amplification of the desired products was determined using agarose (1%) gel electrophoresis both before and after DpnI digestion. DpnI digest was performed after purification of PCR products using a QIAgen gel extraction kit (QIAgen, Manchester, UK), following the manufacturers' protocol and elution in 50µl MilliQ H_2O. The original template was removed from the PCR product by addition of 6µl Promega buffer B (6mM Tris/HCl pH7.5, 6mM $MgCl_2$, 50mM $NaCl_2$, 1mM DTT), 10 units Dpn1 (Promega, Southampton, UK) and 3µl H_2O followed by incubation at 37ºC overnight. Where amplification had occurred (indicated by a band of the correct size on a 1% agarose gel that is resistant to DpnI digest), the product was purified again as above. Giga competent cells (*E. coli* DH5α, Invitrogen) were transformed with the purified DNA by heat shock at 42°C for 45 seconds, placed on ice for 2 minutes, then SOC media (Invitrogen) was added and cells incubated at 37°C for 1 hour prior to spreading on LB agar plates containing 100µg/ml ampicillin (Sigma) to select for bacteria that have taken up the plasmid. Bacteria were grown on plates overnight at 37°C, then single colonies were picked and transferred into 3ml LB media containing 100µg/ml ampicillin. Bacteria were collected by centrifugation at 6 800x g for 3 minutes and plasmid DNA purified using the QIAquick miniprep kit (QIAgen) according to the manufacturers' instructions. The plasmid DNA was sequenced to confirm desired substitutions have been made using primers P2X7R forward 3, P2X7R reverse 3, PCR3.1-BGH reverse and T7 sequencing primer (Table 2.6) and the service facility of Cardiff University.

Table 2.6 Sequencing primer sequences

Name	Sequence
P2X7R forward 3	5'-GTGCTCATCAAGAACAATATCGAC-3'
P2X7R reverse 3	5'-CTCCCTAGTAGCTGCTGGTTCA-3'
PCR3.1-BGH reverse	5'-TAGAAGGCACAGTCGAGG-3'
T7	5′-TAATACGACTCACTATAGGG-3'

The variant B fragment was transferred into the pcDNA5/FRT vector. Initially, the fragment was sequenced using P2X7R forward 3 primer as shown in Table 2.6 to confirm the sequence was as expected. Both the fragment and the vector were cut with restriction enzymes Acc65I and XhoI (Promega), using 30µl purified DNA, 5µl Promega buffer D, 1µl each enzyme and made up to a final volume of 50µl in MilliQ H_2O and incubated at 37°C, overnight. A 1% agarose gel was run to confirm the presence of the correct bands, and these were purified using the QIAgen gel extraction kit, according to the manufacturers' protocol. The vector was CIPed following digestion, using alkaline phosphatase (Promega), incubated for 1 hour at 37°C. A ligation was set up, using a 3:1 ratio of insert:vector in a final volume of 20µl, containing 1µl T4 DNA ligase (Promega) and 2µl 10x ligase buffer and incubated at 14.5°C overnight. Ligations were transformed into Dh5α as described previously, and colonies picked and grown to allow miniprep cultures to be generated, as described above. The miniprep DNA from 8 clones was digested using Acc65I and XhoI as described above and a 1% agarose gel run to enable selection of clones containing the correct size insert for sequencing. Clones were sequenced at the Cardiff university service facility using primers as shown in Table 2.6, sequencing alignment for the successful generation of P2X7R variants are shown in the appendix (supplement S1).

2.2.2 Generating Stable P2X7R expressing HEK293 cell lines

Plasmids containing the P2X7R with either the $A^{348}T$ or $P^{451}L$ mutation or Variant B were transfected into HEK293 Flp-In cells to allow stable expression of the receptor. A 6-well plate (Sarstedt) was coated with 100µg/ml poly-L-lysine for 5 minutes at 37°C, washed with PBS and allowed to air dry. $7.6x10^5$ cells were seeded per well and were allowed to grow for 24 hours. The medium was then replaced with DMEM containing 10% hiFBS and no antibiotics. For each well 0.2µg of the desired plasmid

plus 6µl Fugene-6 and 1.8µg of the pOG44 Cre recombinase expression vector were incubated for 30 minutes at room temperature to form DNA-lipid complexes and was then added to the cells. Control cells were transfected with pOG44 plasmid only. After 48 hours, media was replaced every day for approximately 2 weeks with fresh DMEM containing 10% hiFBS and 100µg/ml hygromycin B to select for transfectants (until colonies began to form and most of the pOG44 only transfected cells had died). Cells were grown to confluency in the presence of hygromycin B, initially in a 24-well plate and the trypsinisation and re-seeding procedure repeated in progressively larger plates/flasks until there were enough cells to be grown in a T75 flask. Cells were then maintained as described in section 2.1, and frozen stocks of resulting cell strains prepared (At high cell density, in DMEM containing 50% hiFBS and 15% DMSO, stored in liquid nitrogen).

2.2.3 qPCR analysis of P2X7R variant RNA expression

RNA was extracted from two confluent wells of a 24-well plate per cell line, using the Direct-Zol RNA miniprep kit (Zymo Research, Germany). Briefly, cells were lysed in 200µl trizol (Invitrogen) and an equal volume of ethanol was added. This mixture was transferred to a Zymo-Spin IIC column and centrifuged at 13 000x g for 30 seconds and flow through discarded. 400µl Direct-zol RNA prewash buffer was added to the column and centrifuged at 13 000x g for 30 seconds. This step was repeated once. 700µl RNA wash buffer was added to the column and centrifuged at 13 000x g for 2 minutes. The RNA was eluted by adding 50µl nuclease free H_2O to the column and the column was centrifuged at 13 000x g for 1 minute. RNA was stored at -80°C.

To synthesise cDNA from RNA extracted from HEK293 cells expressing P2X7R variants, cDNA was synthesised using a reverse transcription PCR 2-step protocol. 1µl oligo dT (5µg/ml, Promega), 1µl dNTPs (10mM each), 4µg mRNA and nuclease-free H_2O up to 20.5µl were mixed, and PCR performed as shown in table 2.7.

Table 2.7 RT PCR protocol for cDNA synthesis

65°C	5 min
4°C	2 min
Pause	Add 4µl 5X first strand buffer 2µl 0.1M DTT
Mix and centrifuge briefly	
42°C	2 min
Pause	Add Superscript II RT 0.5ul
Mix	
42°C	50 min
95°C	2 min
4°C	2 min
42°C	2 min
Pause	Add Superscript II RT 0.5ul
42°C	50 min
70°C	15 min

qPCR was performed using SYBR green PCR core reagents (Applied Biosystems, Thermo Fisher), as follows; 2µl 10x SYBR green PCR reaction buffer, 1.2µl 25mM $MgCl_2$, 1µl dNTPs, 0.25µl AmpliTaq DNA polymerase, made up to 20µl in nuclease free H_2O. PCR cycles performed as in table 2.8 using Applied Biosystems QuantStudio 6 Flex.

Table 2.8 qPCR reaction cycles

Polymerase activation	95ºC	10 min	
Denature	95ºC	15 sec	40 cycles
Anneal/Extend	60ºC	1 min	

2.2.4 Transient P2X7R transfections

Due to issues with P2X7R variant B stable expression, transient expression of the P2X7R was tested. P2X7R was transfected to determine whether transient expression

would be possible for TG2 release assays. A 12-well plate was coated with 100µg/ml poly-l-lysine for 5 minutes at 37°C, then washed with PBS and left to air dry in the sterile hood. HEK293 Flp In cells were seeded at a density of $1.2x10^5$ cells/well in 3ml DMEM supplemented with 10% FBS and 100U/ml penicillin and 100µg/ml streptomycin. 24 hours later, cells were transfected with P2X7R (wild type or variant B). P2X7R plasmid (wild type P2X7R or variant B) and fugene-6 were mixed with DMEM in a 1.5µl:1µg ratio of Fugene-6:DNA. 48 hours later, cells were lysed with cell extraction buffer (20mM HEPES/NaOH pH7.4, 150mM NaCl, 1mM EGTA, 1% triton-X-100 and 0.25% deoxycholic acid containing 1mM PMSF, 1mM NEM and 10% glycerol), and lysate was centrifuged at 15 000x g for 15 minutes at 4°C and supernatant stored frozen for analysis. Concentration was determined by BCA assay (section 2.1.6) and samples run on SDS PAGE (section 2.1.7) and Western blotting performed (section 2.1.8). For membrane depolarisation measurements with transient transfections, $2x10^4$ cells per well were seeded into a poly-l-lysine coated black optical bottom 96 well plate. Transfections were performed 48 hours, 36 hours and 24 hours prior to measurements, using a 1:1.5 ratio of fugene-6:DNA, as described above.

2.2.5 Establishing a membrane depolarisation assay

Membrane depolarisation can be measured using a plate based assay, using $DiSBAC_2(3)$ (Bis-(1,3-Diethylthiobarbituric Acid) Trimethine Oxonol, Molecular Probes, Invitrogen). This is a voltage sensitive probe, which enters depolarised cells and binds proteins to give a fluorescent signal. $DiSBAC_2(3)$ can be used alone, or in conjunction with a FRET (fluorescence resonance energy transfer) partner, CC2-DMPE (a coumarin-phospholipid, Invitrogen). CC2-DMPE acts as the FRET donor and is inserted in to the outer leaflet of the plasma membrane. $DiSBAC_2(3)$ is the FRET acceptor, and is a negatively charged bis-oxonol compound which can bind to either the outer or inner leaflet of the plasma membrane. When cells are at resting potential, $DiSBAC_2(3)$ is present at the outer leaflet, therefore energy is transferred from CC2-DMPE to $DiSBAC_2(3)$ and the emission is read at the wavelength for $DiSBAC_2(3)$ emission. When cells become depolarised, $DiSBAC_2(3)$ moves to the inner leaflet of the plasma membrane and FRET does not occur. This means that a decrease in fluorescence is read from $DiSBAC_2(3)$ and an increase in the emission from CC2-DMPE.

2.2.6 Membrane depolarisation measurements using DiSBAC$_2$(3) only

Black, optical-bottom 96-well plates were coated with 100µg/ml poly-l-lysine for 5 minutes at 37°C, then washed with PBS and left to air-dry in the sterile hood. HEK293 P2X7R cells were seeded at a density of 5x10^4 per well. Once cells were 80% confluent, they were washed with voltage sensor probe buffer-1 (VSP-1, 160mM NaCl, 4.5mM KCl, 0.9mM $CaCl_2$, 1mM $MgCl_2$, 10mM glucose, 10mM HEPES pH7.4), then 90µl VSP-1 containing 10µM DiSBAC$_2$(3) was added and incubated for 30 minutes to allow loading of the cells. After pre-incubation, fluorescence was measured using the FLUOstar omega by scanning a 4mm orbital section at the centre of the well, using excitation at 540-10nm and emission at 590-20nm, with measurements every 15 seconds for 10 minutes with a gain of 1300. Baseline fluorescence was read for 5 cycles, then BzATP (final concentration 0.1mM) or KCl (final concentration 30µM) was injected. The baseline was subtracted from the data, then the control curve was subtracted and the data plotted on an XY graph using GraphPad Prism .

2.2.7 Determining optimum excitation and emission wavelengths for DiSBAC$_2$(3) and CC2-DMPE

Emission and excitation spectra were measured for DiSBAC$_2$(3) and CC2-DMPE using the spectrofluorimeter (Fluoromax-3, Horiba, Jobin Yvon). It was determined that optimum excitation of CC2-DMPE occurs using the 420-10nm filter and emission should be read at 460-20nm (CC2-DMPE) and 550-10nm (DiSBAC$_2$(3)).

2.2.8 Membrane depolarisation measurements using DiSBAC$_2$(3) and CC2-DMPE

Black, optical-bottom 96-well plates (Nunc, New York, USA) were coated with 100µg/ml poly-L-lysine for 5 minutes at 37°C, then washed with PBS and left to air-dry in the sterile hood. HEK293 P2X7R cells were seeded at a density of 5x10^4 per well (or for transient transfections as described in section 2.5.3). Once cells were 80% confluent, they were washed with VSP-1. Equal volumes of 5mM CC2-DMPE and 20% pluronic-F127 were mixed and diluted to 5µM CC2-DMPE in VSP-1. 100µl CC2-DMPE was added to the cells and incubated protected from the light at room temperature for 30 minutes. CC2-DMPE was removed and cells were washed briefly twice with 100µl VSP-1. 100µl 10µM DiSBAC$_2$(3) was added and incubated for 30

minutes with the plate protected from light. Where used, 5 minutes prior to the end of this incubation, quenchers were added (ESS-2; 40mM Tartrazine, 60mM Acid Red 37 and 40mM Acid Fuchsin, or each of these independently or 0.08% Bromophenol Blue. (Knapp *et al.* 2001)). After pre-incubation, fluorescence was measured using the Fluostar omega, using three cycle sections; 1) 5 readings with 5 flashes per well every 2 seconds, after which 0.1mM or 0.5mM BzATP was injected or KCl to a final concentration of 82µM. 2) 10 readings with 5 flashes per well every 1.16 seconds, then 3) 25 readings with 10 flashes per well every 1.26 seconds. Filters used were excitation at 420-10nm and emission at 460-20nm and 550-10nm with a gain of 2200 and 2400 respectively. The baseline was measured from a well containing no cells and was subtracted from the data from wells containing cells. The first 5 readings (cycle section 1) were taken to give average fluorescence emission from $DiSBAC_2(3)$ and CC2-DMPE, then the 6 readings between 29 and 36 seconds (cycle section 3) were taken to give the after-stimulation average fluorescence emission from $DiSBAC_2(3)$ and CC2-DMPE. These readings were used to give the initial and final ratios of $DiSBAC_2(3)$:CC2-DMPE fluorescence by calculating fluorescence at 460nm/fluorescence at 550nm. The response ratio was calculated as follows: Final $DiSBAC_2(3)$:CC2-DMPE/Initial $DiSBAC_2(3)$:CC2-DMPE. A higher response ratio indicates more depolarisation of the cells.

2.2.9 Immunolocalisation of P2X7R variants

Immunolabelling was performed to enable imaging by confocal microscope of the P2X7R to confirm its expression on the surface of the cells. HEK293 Flp In, wild-type P2X7R, P2X7R $A^{348}T$, P2X7R $P^{451}L$ or P2X7R variant B cells were seeded at a density of $1x10^4$ cells into separate wells of a chamber slide in 200µl DMEM containing 10% hiFBS and allowed to grow for one day (to around 80% confluency). Cells were washed with PBS, fixed with 4% paraformaldehyde for 10 minutes and washed three times for 5 minutes in PBS. Cells were permeabilised with 0.1% triton-X-100 for 10 minutes in PBS containing 0.5% paraformaldehyde, then washed three times for five minutes in PBS. Blocking for non-specific binding was performed using 1% BSA in PBS for 30 minutes at room temperature. Primary antibody was diluted in 1% BSA as shown in table 2.1 and added to the appropriate wells and 1% BSA without antibody was added to negative control wells. Cells were incubated for 2 hours at room

temperature then washed 3 times for 5 minutes with PBS. Fluorescently labelled secondary antibody was diluted in 1% BSA as shown in table 2.2 to all wells and incubated for 1 hour at room temperature. Chambers were removed and slides washed 3 times for 5 minutes in PBS. Coverslips were mounted using Vectashield with DAPI (Vector Laboratories) to stain the nucleus. Cells were imaged using a Leica confocal microscope with the 63x/1.4 NA oil objective. AlexaFluor 488 excitation is at 458nm (using the argon ion laser) and emission captured at 494-535nm. AlexaFluor 594 excitation is at 590nm (using the 590nm laser) and emission captured at 600-620nm. DAPI nuclear stain can be visualized by excitation at 405nm (using the 405nm diode laser) and emission collected at 430-512nm.

2.2.10 Calcium flux measurements

Activation of P2X7R by BzATP leads to ion channel formation and Ca^{2+} influx into the cell. This can be measured using the calcium indicator Fluo-4 (Invitrogen). Black optical bottom 96-well plates were coated with 100µg/ml poly-L-lysine for 5 minutes at 37°C, then washed with PBS and left to air-dry in the sterile hood. HEK293 P2X7R cells were seeded at a density of $5x10^4$ per well. Once cells were 80% confluent, they were washed with 200µl pre-warmed OptiMEM (Gibco). OptiMEM containing 3µM Fluo-4 (reconstituted in DMSO containing 12% w/v pluronic-F127 (Invitrogen)) was added to the cells and incubated at 37°C, 5% CO_2 for 20 minutes. Cells were washed once in OptiMEM and 90µl fresh OptiMEM was added. Fluo-4 fluorescence was measured using the bottom optics of the FLUOstar omega, scanning a 4mm orbital area in the centre of the well. Experiment was performed at 37°C, 5% CO_2. Excitation was at 480-10nm and emission at 520-10nm, with a gain of 2600. Baseline fluorescence for each well was read for 5 seconds, then BzATP was injected to a final concentration of 0.1mM. The change in Fluo-4 fluorescence was read for 20 seconds after injection. The baseline was subtracted from the data, then the control curve was subtracted and the mean of eight repeats plotted on an XY graph using GraphPad Prism. To calculate the rate of Ca^{2+} uptake by the cells, data from the 10 seconds immediately following BzATP treatment was fitted using non-linear regression, assuming pseudo first order kinetics, using the following equation; Y=(Ymax-Ymax*exp(-k*x))+f.

2.2.11 Measuring pore formation by YO PRO-1 uptake

The pore formed by the P2X7R is permeable to the DNA binding dye YO PRO-1, meaning that the pore formation ability of cells expressing the P2X7R can be assessed by measuring YO PRO-1 uptake (Adamczyk 2013). Black optical bottom 96-well plates were coated with 100µg/ml poly-L-lysine (Sigma) for 5 minutes at 37°C, then washed with PBS and left to air-dry in the sterile hood. HEK293 P2X7R cells were seeded at a density of $3x10^4$ per well. Once cells were 80% confluent, they were washed with 200µl pre-warmed physiological salt solution (PSS; 147mM NaCl, 10mM HEPES/NaOH, pH7.4 12mM glucose, 0.9mM $CaCl_2$, 2mM KCl, 1mM $MgCl_2$,). When inhibitors were employed, cells were pre-incubated with inhibitor diluted in PSS as stated in table 2.3. PSS containing 1µM YO PRO-1 (Invitrogen) was added to the cells, and fluorescence was measured using the bottom optics of the FLUOstar Omega, scanning a 4mm orbital area in the center of the well. Experiment was performed at 37°C, 5% CO_2. Excitation was at 480-10nm and emission at 520-10nm, with a gain of 2100. Baseline fluorescence was read every 40 seconds for 6 cycles. After 6 cycles, either H_2O (control) or BzATP at 0.1mM or 0.5mM final concentration was added using the injectors of the FLOUstar Omega, then YO PRO-1 uptake was measured for 60 minutes in 40 second intervals. The baseline was subtracted from the data, then the control curve was subtracted and the mean of three repeats ± SEM plotted on an XY graph using GraphPad Prism.

Methods in Chapter 4

2.3.1 Cloning TG2 GTP binding variants

The wild type TG2 DNA pcDNA3.1 vector was provided by Professor Daniel Aeschlimann. The TG2 $R^{580}A$ in pcDNA3.1 was provided by Dr Siri Iismaa. Primers for introducing $K^{173}L$ and $K^{173}N/F^{174}D$ were designed as shown in table 2.7 and ordered from Eurofins MWG. PCR reaction mixes contained 5µl 10x Phusion HF buffer, 0.5µg template DNA, 2µM each of forward and reverse primers as listed in table 2.9, 2 units Phusion polymerase, 0.8mM dNTPs and MilliQ H_2O up to a final volume of 50µl. PCR cycles are shown in table 2.10.

Table 2.9 Primer sequences for mutagenesis. Mutated bases are highlighted in red.

TG2 Variant	Forward Primer	Reverse Primer
$K^{173}L$	5'-CAGGGCTCGGCCTTATTCATCAAGAACATACC-3'	5'-GTTCTTGATGAATAAGGCCGAGCCCTGGTAG-3'
$K^{173}N/F^{174}D$	5'-CCAGGGCTCGGCCAATGACATCAAGAACATACCT-3'	5'-GGTATGTTCTTGATGTCATTGGCCGAGCCCTGGTAG-3'

Table 2.10 PCR cycles for TG2 constructs

Stage	Temperature (°C)	Time	Repeats
	94	2 minutes	
Denaturing Annealing Extension	94 55, 58, 62 or 65 72	30 seconds 45 seconds 7 minutes	X 16
	72	10 minutes	

Successful amplification of the desired products was determined using agarose (1%) gel electrophoresis both before and after DpnI digestion. DpnI digest was performed after purification of PCR products using a QIAgen PCR purification kit, following the manufacturers' protocol and elution in 50µl MilliQ H_2O. The original template was removed from the PCR product by addition of 6µl Promega buffer B (6mM Tris/HCl pH7.5, 6mM $MgCl_2$, 50mM $NaCl_2$, 1mM DTT), 10 units Dpn1 (R6231, Promega) and 3µl H_2O followed by incubation at 37°C overnight. Where amplification had occurred

(indicated by a band of the correct size on a 1% agarose gel that is resistant to DpnI digest), the product was purified again as above. Giga competent cells (*E. coli* DH5α) were transformed with the purified DNA by heat shock at 42°C for 45 seconds, placed on ice for 2 minutes, then SOC media (Invitrogen) was added and cells incubated at 37°C for 1 hour prior to spreading on LB agar plates containing 100µg/ml ampicillin to select for bacteria that have taken up the plasmid. Bacteria were grown on plates overnight at 37°C, then single colonies were picked and transferred into 3ml LB media containing 100µg/ml ampicillin. Bacteria were collected by centrifugation at 6 800x g for 3 minutes and plasmid DNA purified using the QIAquick miniprep kit according to the manufacturers' instructions. The plasmid DNA was sequenced to confirm desired substitutions have been made using the primers in table 2.11 and the service facility of Cardiff University, sequencing alignment of the successful generation of TG2 variants is shown in the appendix (Supplement S2).

Table 2.11 Sequences of primers used for TG2 GTP binding variant sequencing

Name	Sequence	Mutations used for
hTG2 up102	5'-GCTCTTCAACGCCTGGTGCC-3'	$K^{173}N$, $K^{173}L$, $K^{173}N/F^{174}D$
hTG2 down103	5'-GGCGTTCTTCAGGAACTTGG-3'	$K^{173}N$, $K^{173}L$, $K^{173}N/F^{174}D$
hTG2 up106	5'-CATGACCAGAACAGCAACC-3'	$R^{580}A$
hTG2 rev	5´-CAGCTTGCGTTTCTGCTTGG-3'	$R^{580}A$

2.3.2 Expression and purification of TG2 GTP binding variants

Recombinant TG2 was purified from *E. coli* culture using affinity chromatography with a nickel column followed by ion exchange chromatography as previously described (Hadjivassiliou *et al.* 2008). 1L of *E. coli* culture expressing TG2 was grown to OD 0.6 at 600nm and then expression of TG2 induced with Rhamnose (0.5% w/v final concentration, Genaxxon bioscience, Germany) and grown at 20°C overnight with shaking at 150rpm. Bacteria were pelleted by centrifugation at 24 471x g for 30 minutes at 4°C, then re-suspended in 30ml buffer A1 (20mM Tris/HCl pH7.5, 300mM NaCl, 1mM EDTA). Cells were homogenized using the Stansted pressure cell homogenizer. The homogenized sample was cleared by centrifugation at 47 808x g for 30 minutes at 4°C. The lysate was applied to a nickel column (His-TRAP HP column, 5ml, GE) as TG2 binds to the column because of a N-terminal His-tag that was

engineered. The column was washed using several volumes of buffer A1 to remove any proteins that had not bound to the column. Weakly bound proteins were removed by washing with 10% buffer B1 (20mM Tris/HCl pH7.5, 300mM NaCl, 1mM EDTA, 300mM imidazole). Approximately 12ml of 50% Buffer B1 was used to elute the TG2 and fraction sizes of 1ml were collected. The protein containing fractions were pooled and diluted 1:3 with buffer A2 (20mM Tris/HCl pH7.5, 1mM EDTA) to reduce salt concentration, and loaded onto an ion exchange column (Source Q15, 6ml column) equilibrated in buffer A2. After washing with buffer A2, the TG2 was eluted using a linear gradient of buffer B2 (20mM Tris/HCl pH7.5, 1mM EDTA, 1M NaCl) increasing to 100% over 60 minutes. There is a large peak in absorbance at 280nm at approximately 50% buffer B2 indicating that the TG2 was being eluted. The fractions corresponding to the peak were collected and pooled. Protein was stored at -20°C. Protein concentration was determined as described in section 2.1.6 and activity was measured using the isopeptidase assay described in section 2.3.3 or the MDC (monodansylcadaverine) activity assay described in section 2.3.4.

2.3.3 Isopeptidase activity assay

TG2 can hydrolyse the isopeptide bond formed during the cross-linking reaction and this property has been used in quantitative assays (Adamczyk *et al.* 2013). This assay uses a quenched fluorescent probe (Abz-APE(γ-cad-Dnp)QEA, A102, Zedira, Germany) that mimics the cross-linked TG2 product and hydrolysis of this isopeptide bond releases the quencher to allow an increase in light emission. Black, optical-bottom 96-well plate, buffers and $CaCl_2$ solution were warmed to 37°C before the experiment. FLUOstar Omega injectors were primed with 20mM $CaCl_2$ (final concentration in each well of 2mM) for enzyme activation or H_2O for the control reaction. 3mM DTT was added to each well, and where required, GTP (Sigma, G5884) at the following final concentrations in each well: 660µM, 300µM, 150µM, 75µM, 37.5µM, 18.8µM, 9.4µM, 4.7µM, 2.3µM, 1.2µM and 0µM in a volume of 10µl. Control well contained 0mM GTP. TG2 was diluted to 25µg/ml in assay buffer (60mM Tris/HCl, pH7.5, 125mM NaCl, 12.5mM glycine methylester) plus 62.5µM A102 and 80µl of this was added to the required wells. Excitation was at 320nm and emission at 440-10nm. A 15 minute pre-incubation time was allowed before cycle 1, then readings were taken every 40 seconds for 10 cycles before enzyme activation to establish a

baseline. Following Ca^{2+} (or H_2O) injection, readings were taken for one hour at 40 second intervals. Baseline fluorescence was subtracted from the data, then the control curve was subtracted and data plotted using GraphPad Prism. The rate of enzyme activity at each GTP concentration was determined by performing linear regression analysis in GraphPad Prism. The results of this analysis were plotted and fitted to a sigmoidal dose response curve and the K_D determined.

2.3.4 MDC activity assay

As an alternative to the isopeptidase activity assay, the monodansylcadaverine assay was used to measure TG2 activity as a measure of transamidation activity (Lorand *et al.* 1971). This assay allows real-time measurement of the amount of monodansylcadaverine incorporated into N,N-dimethylcasein by TG2. A 1:10 ratio of TG2:Assay buffer (v/v) (50mM Tris/HCl, pH8, 10mM $CaCl_2$, 10mM glutathione (reduced), 2.5% glycerol, 2.5% DMSO, 20µM N,N-dimethyl casein (Sigma) and 25µM monodansylcadaverine (Fluka, Sigma-Aldrich) was used. Reagents were pre-warmed to 37°C and the reaction started by addition of enzyme. The plate (Black optical bottom, Nunc) was read using the bottom optics of the FLUOstar Omega every 40 seconds with excitation at 332nm and emission at 515nm.

2.3.5 Native PAGE

Native Page was performed to show differences in conformational changes between wild type TG2 and GTP binding variants of TG2 in the presence of GTP. 4µg purified recombinant TG2 was mixed with an equal volume of 2x sample buffer (100mM Tris/HCl pH 6.8, 15% glycerol, 0.02% bromophenol blue, 10mM DTT). Samples where GTP was required were incubated with 25µM GTP for 10 minutes in sample buffer. 0.25µM GTP was also included in the running buffer (25mM Tris/HCl pH7.8, 192mM glycin) for these samples. Samples were run on Novex 10% polyacrylamide tris-glycine gels (Invitrogen) both with and without GTP at 100V, 35mA for 3 hours on ice.

Methods in Chapter 5

2.4.1 Investigating the ability of caspase-1 to cleave TG2

To assess the ability of caspase-1 to cleave TG2, recombinant TG2 processing by recombinant caspase-1 was tested. Recombinant caspase-1 (Abcam) was reconstituted in PBS containing 15% glycerol (1unit/µl). 0.25µg, 0.5µg and 1µg purified recombinant TG2 was incubated with 1 unit caspase-1 at 37ºC for 1 hour, made up in caspase-1 reaction buffer (50mM HEPES pH7.4, 50mM NaCl, 0.5mM EGTA, 10% glycerol, 5mM DTT). Recombinant TG2 was also incubated at 37ºC for 1 hour in caspase-1 reaction buffer, without caspase-1 to account for any degradation that may occur due to experimental conditions. Samples were then run on an SDS PAGE gel and Western blotting was performed for TG2.

2.4.2 Investigating the ability of M1 macrophage conditioned media to cleave TG2

To investigate the possibility that TG2 processing occurs in the conditioned medium of the M1 macrophages, recombinant TG2 was incubated with conditioned medium. $1x10^5$ M1 macrophages were seeded per well in 24 well plate and 24 hours later, cells were used for P2X7R stimulation. OptiMem was pre-warmed and pre-gassed with CO_2 in the incubator overnight. Cells were washed with 0.2ml/well OptiMem, then 0.25ml per well of 0.1mM BzATP in OptiMem was added to the cells and incubated for 10 minutes at 37ºC with 5% CO_2. 0.25ml conditioned media were collected from each well (1ml conditioned media in total) and centrifuged at 1 500x g for 10 minutes to remove cell debris. 5mM tris/HCl pH7.4 was added prior to storage at -20ºC. 2µg of TG2 was added to 20µl conditioned medium, or fresh OptiMem as a control. The following protease inhibitors and their relevant vehicle controls were added to the medium, to assess the roles of different families of proteases: GM6001 (50µM, 0.5% DMSO), EDTA (5mM, 2% H_2O), PMSF (1mM, 1% ethanol), NEM (1mM, 1% H_2O), Aprotinin (10µg/ml, 0.1% H_2O), E64 (10µM, 10% H_2O), benzamidine (10mM, 3.04% H_2O), bestatin (40µM, 4% methanol), leupeptin (10µg/ml, 0.1% H_2O), pepstatin A (1µM, 0.1% DMSO), phosphoramidon (5µM, 0.5% H_2O) and chymostatin (100µM, 1% DMSO). Reaction was incubated at 25ºC, overnight, then samples were run on SDS PAGE and Western blotting was performed for TG2.

2.4.3 Immunoprecipitation of TG2

To investigate the nature of processing of the cleaved form of TG2, immunoprecipitation was performed to extract TG2 from conditioned medium and lysate of M1 macrophages. For P2X7R stimulation, $1x10^5$ M1 macrophages were seeded per well in 24 well plate and 24 hours later, cells were used for P2X7R cell stimulation experiments. OptiMem was pre-warmed and pre-gassed with CO_2 in the incubator overnight. Cells were washed with 0.2ml/well OptiMem, then 0.25ml per well of 0.1mM BzATP in OptiMem was added to the cells and incubated for 10 minutes at 37ºC with 5% CO_2. 0.25ml conditioned media were collected from each well (5ml conditioned media in total) and centrifuged at 1 500x g for 10 minutes to remove cell debris. 5mM tris/HCl pH7.4 was added, alongside protease inhibitors AEBSF, NEM and EGTA. Cell lysates were also collected in cell extraction buffer (50mM HEPES pH 7.4, 150µM NaCl, 1% Triton, 1% Na Deoxycholate, 0.1% SDS, 10% glycerol, 1.5mM MgCl, 1mM EGTA, AEBSF and NEM), as a positive control. Protein G sepharose beads (GE) were prepared by taking 100µl of 75% bead slurry and washing 3 times in 1ml PBS. Beads were settled by spinning at 500xg for 1 minute. The sample was pre-cleared by adding media to the prepared beads, and incubating at 4ºC for 1 hour with shaking. Beads were settled by spinning at 16 000xg, 4ºC for 10 minutes, then the supernatant was kept and beads disposed of. 1µg CUB7402 anti-TG2 antibody was added to the supernatant (5ml conditioned media) and also to 850µg of total cell lysate and incubated 4ºC, overnight, with shaking. 100µl of 75% bead slurry prepared as previously, then conditioned media and lysate added to beads and incubated at 4ºC, 2 hours with mixing. Beads were collected at 500xg for 1 minute and the supernatant removed and kept. The beads were washed 3 times in 800µl wash buffer (50mM HEPES pH7.4, 150mM NaCl, 0.1% triton, 10% glycerol). The beads were collected by centrifugation at 5 000x g for 15 seconds between each wash. The beads were boiled for 5 minutes in 50µl sample buffer and centrifuged at 16 000x g for 10 minutes to elute the bound protein. 15µl of eluted protein was run on SDS PAGE for subsequent analysis by ms/ms (performed by the Cardiff University service facility) and 15µl of eluted protein was used for Western blotting, probing for TG2, to confirm successful extraction of the protein.

2.4.4 Biotin labelling of cell surface proteins

Cell surface proteins were extracted using the Pierce cell surface protein isolation kit (Thermo Scientific). Cell surface proteins were labelled with Thermo Scientific EZ-link Sulfo-NHS-SS-Biotin by addition of this as an ice-cold solution and incubation for 30 minutes at 4°C with gentle agitation. Any un-reacted EZ-link Sulfo-NHS-SS-Biotin was quenched by addition of quenching buffer and mixing, then the cells were scraped into solution and centrifuged at 500x g for 3 minutes, then the supernatant was discarded. The provided lysis buffer was then used to lyse the cells, with a 30 minute incubation on ice, with brief vortexing every 5 minutes. Lysates were then centrifuged at 10 000x g for 2 minutes at 4°C and supernatant collected. The biotin labelled proteins were isolated using Thermo Scientific NeutrAvidin agarose by addition of the clarified lysate to a provided column and incubated with end-over-end mixing for 1 hour at room temperature. The column was centrifuged at 1 000x g for 1 minute and the flow through discarded. 200µl 1x SDS PAGE sample buffer (as described in section 2.1.7) containing 5mM DTT was added to the column and incubated with end-over-end mixing for 1 hour at room temperature. The column was centrifuged at 1 000x g for 2 minutes and the flow through collected. 20µl of the flow through was run on SDS PAGE gel and Western blotting performed as described previously (section 2.1.7 and section 2.1.8 respectively).

Methods in Chapter 6

2.5.1 Genomic DNA extraction from peripheral blood samples

Genomic DNA was extracted using the Wizard genomic DNA purification kit (Promega). A minimum of 5ml blood was used for DNA extraction, performed according to the manufacturers' protocol, as follows. 15ml cell lysis solution was mixed with 5ml blood and incubated for 10 minutes, with inversion 2-3 times once during the incubation, to lyse the red blood cells. This was then centrifuged at 2 000x g for 10 minutes. The supernatant was removed, without disturbing the pellet, leaving approximately 1.5ml liquid and then vortexed for 10-15 seconds to re-suspend the pellet. 5ml of nuclei lysis solution was added to the cells and pipetted up and down five or six times to lyse the white blood cells. 1.65 ml of protein precipitation solution was added to the nuclear lysate and vortexed for 10 to 20 seconds, then centrifuged at 2 000x g for 10 minutes at room temperature. The supernatant was collected and added to 10ml room temperature isopropanol and gently mixed by inversion until DNA forms a visible small white pellet then centrifuged at 2 000x g for 1 minute. The supernatant was removed and 10ml room temperature 70% ethanol was added to the DNA. The tube was inverted to wash the DNA pellet, then centrifuged at 2 000x g for 1 minute. The ethanol was removed and pellet air dried for 10 to 15 minutes. 400µl DNA rehydration solution was added and incubated at 65°C for 1 hour. DNA was stored, awaiting further analysis, at 4°C.

2.5.2 Amplification of *P2RX7* exons for sequencing

P2RX7 gene amplification, to allow genomic DNA sequencing and identification of polymorphisms, was performed by PCR, using the primers shown in table 2.12. The alignment of these primers with *P2RX7* reference sequence is shown in the appendix (supplement S3). PCR was set up using 10µl GC buffer (Finnzymes), 1µl 10mM dNTPs, 2.5µl each of forward primer and reverse primer (10µM), 2µl human genomic DNA (5ng/µl), 0.5µl Phusion high-fidelity DNA polymerase and made up to 50µl with RNase free H_2O. PCR was performed as outlined in table 2.13. PCR reactions were run on a 1% agarose gel and where prominent bands were present, these were extracted using the QIAgen gel extraction kit. Where the bands were faint, they were cut out of the gel and PCR repeated as previously to further amplify the band. DNA was

sequenced using the Cardiff University service facility and the primers shown in table 2.12.

Table 2.12 Primers used for P2X7R PCR amplification and sequencing analysis

Exon	Forward Primer	Reverse Primer
Exon 1	5'-CCCTGTCAGGAAGAGTAGAGC-3'	5'-GCTGTCGTGTCTTTCGGGGTC-3'
Exon 2	5'-CATCCTCCAACGCCTGCATCC-3'	5'-GAGCAGCGACCAGTGGCAGCG-3'
Exon 3	5'-GGAGAGGTTCGCCCAGCAAGC-3'	5'-CCACGTTCAGCCTTCTTCGTC-3'
Exon 4	5'-GGATATCGAATCACTTCTCCACG-3'	5'-CAGACCGTAGAACCACTGTAAACA-3'
Exon 5	5'- CGCAGTTCTTTCACATCTGTGG-3'	5'-CTGGTCTACTCCGGAACGGCT-3'
Exon 6	5'-CCAAGCCAAGAAACCAGAAGC-3'	5'-GACCGACAGAATCAATAGATGACG-3'
Exon 7	5'-CAGATCTGTTTTCAATCGAGATG-3'	5'-CAGATCCCTACCTCCTACAGTTT-3'
Exon 8	5'-AGGGAGATGTCTGGCGGTTGC-3'	5'-GGTCACCGACTTAGCGTAAGG-3'
Exon 9	5'-CCAGCACTTTCAAAGGGATCT-3'	5'-CTGACACAGGTTAATGACGACAC-3'
Exon 10 and 11	5'-GCACGTTGAAGCAAAAGAGCG-3'	5'-CAAGTGTCCTGTGGTTCTGTAC-3'
Exon 12	5'-GAGCCAGCTTGTTCAATAGTCTATC-3'	5'-GATCGTCCTCAGGGAAAATACG-3'
Exon 13	5'-GAACCTGAGGGCTTGTCATGG-3'	5'-GCCTGACTTCGGTCCGTGGCACCG-3'

Table 2.13 PCR cycles for amplifying P2X7R exons

Stage	Temperature (°C)	Time	Repeats
	98	30 seconds	
Denaturing	98	10 seconds	
Annealing	60	30 seconds	X 40
Extension	72	1 minute	
	72	7 minutes	

Chapter 3

3. Dissecting the role of P2X7R activities in TG2 secretion: Is enzyme externalization linked to membrane pore formation?

3.1 Introduction

Stimulation of P2X7R induces different stages of receptor activation. Initially, with a short period of ATP activation (seconds), an ion channel forms, giving membrane depolarisation through Na^+ and Ca^{2+} influx and K^+ efflux (Surprenant *et al.* 1996). The Ca^{2+} influx will also lead to calcium signalling inside the cell. Prolonged receptor activation (tens of seconds to minutes, mM concentration of ATP) leads to formation of a membrane pore, allowing passage of larger cationic molecules (Coutinho-Silva and Persechini 1997). There are three ATP binding sites on the P2X7R, it has been proposed that binding of two molecules of ATP induces ion channel opening. Saturation (binding at all three ATP binding sites) leads to membrane pore formation (Yan *et al.* 2010; Hattori and Gouaux 2012).

The identity of the P2X7R membrane pore is unknown, however, there are two main hypotheses as to how the membrane pore is formed. The pore formed by P2X7R could be 1. through an interaction with another plasma membrane channel or 2. formed by dilation of the ion channel formed by the receptor itself. Application of colchicine (a microtubule disruptor) to cells prevented dye uptake, but had no effect on ion channel formation (Marques-da-Silva *et al.* 2011). This implicates separate pathways for membrane pore formation and ion channel formation. Pannexin -1 is one such pore that has been implicated, however, membrane pore formation can also be seen in cells lacking pannexin-1 expression (Sun *et al.* 2013) and inflammasome formation and IL-1β secretion in pannexin-1 null mouse macrophages has been demonstrated (Qu *et al.* 2011). There is substantial evidence for either hypothesis, with neither being more convincingly demonstrated and distinct mechanisms may be involved in different cell types. In the following, I will briefly outline the supporting evidence for the two hypotheses.

The separate pore forming component is often thought to be the plasma membrane protein pannexin-1 (Locovei *et al.* 2007; Iglesias *et al.* 2008). Pannexins are structurally similar to connexins and are comprised of four transmembrane domains with two extracellular loops and a cytoplasmic tail. Pannexin-1 monomers can form hexamers, often termed ‘pannexons’, which form a cation selective channel between

the cell and the extracellular environment (hemichannels) (Bruzzone and Dermietzel 2006). This pore formed by pannexin-1 has been shown to be permeable to cations up to 900Da, consistent with the observed capabilities of the membrane pore formed by P2X7R (Bruzzone *et al.* 2005). Suadicani *et al* have demonstrated that the use of antagonists of gap junction channels can inhibit P2X7R membrane pore activity, implicating pannexins (Suadicani *et al.* 2006). On the other hand, it has been demonstrated that bone marrow derived macrophages lacking pannexin-1 expression are capable of secreting IL-1β and IL-18, which requires P2X7R membrane pore formation (Qu *et al.* 2011).

The second hypothesis for P2X7R membrane pore formation is that the P2X7R ion channel itself can dilate to form a larger membrane pore. It has been demonstrated that HEK293 cells expressing P2X7R are capable of dye uptake (Browne *et al.* 2013; Sun *et al.* 2013). These cells express pannexin-1, however, inhibition of pannexin-1 using the peptide mimetic inhibitor ^{10}Panx had no effect on dye uptake. Stimulating P2X7R in cells which lack pannexin-1 expression can still induce membrane pore formation (Sun *et al.* 2013). Taken together, this implicates an alternative channel to pannexin-1 or P2X7R itself as the essential membrane pore forming component. The same group identified several residues within the second transmembrane domain of the P2X7R that are required for membrane pore formation. These residues could contribute by either affecting the size of the pore formed by P2X7R itself or through interacting with other proteins (Sun *et al.* 2013). Structural modelling of P2X7R has demonstrated that the P2X7R ion channel/membrane pore could dilate due to successive ATP binding events causing conformational changes. Each molecule of ATP binding to the trimeric receptor could cause additive conformational changes. When the first ATP molecule binds, a small conformational change may occur, and on binding of a second ATP molecule a conformational change large enough to induce ion channel formation may occur. When the third ATP molecule binds, the receptor is fully activated, possibly meaning that a more dilated channel is formed due to a final conformational change (Yan *et al.* 2010). It has also been experimentally shown that the P2X7R pore passes through a series of smaller intermediate stages as it dilates, before reaching the fully dilated size, which is permeable to NMDG (Virginio *et al.* 1999a). While these studies could implicate dilation of the P2X7R itself in membrane pore formation, it has also been shown that ion channel activity can be blocked without affecting pore formation

(for example, by calmidazolium (Virginio *et al.* 1997)). This does not preclude P2X7R itself as the pore forming component but suggests that the membrane pore is not a dilated ion channel.

Our group has demonstrated that TG2 release occurs on P2X7R activation and can be inhibited by application of a specific P2X7R inhibitor (A740003) (Adamczyk *et al.* 2015). We have shown that TG2 release is mechanistically separate from calcium signalling and ion channel formation, by application of an inhibitor (calmidazolium) that block these P2X7R activities (Adamczyk *et al.* 2015). When calmidazolium is used, TG2 secretion still occurs. However, inhibition of calcium signalling prevents flotillin-2 secretion, a lipid raft protein which is often used as a marker of microvesicle release, also suggesting that TG2 secretion does not occur through microvesicles. Separation of microvesicles from conditioned media of P2X7R stimulated cells showed TG2 absent from microvesicle fractions and present in soluble fractions (Adamczyk *et al.* 2015). This separates TG2 release from these activities of the P2X7R, suggesting that it is membrane pore formation that leads to TG2 secretion.

In this chapter, the relationship between the P2X7R membrane pore and TG2 secretion is investigated in more detail by pharmacological inhibition of pannexin-1 and introduction of mutations into the P2X7R using HEK293 cells expressing P2X7R as a model.

Aims for this chapter:

1. Investigate whether pannexin-1 is the membrane pore forming component of P2X7R in our cell model.
2. Establish a membrane depolarisation assay to investigate whether the *C*-terminally truncated P2X7R variant B forms a functional cell surface receptor.
3. Generate cells stably expressing selected P2X7R variants.
4. Investigate the role of P2X7R membrane pore formation in TG2 secretion.

3.2 Results

3.2.1 Is pannexin-1 involved in membrane pore formation upon P2X7R activation in the HEK293 cell model?

To establish whether membrane pore formation is the essential step for TG2 secretion following P2X7R activation, the identity of the membrane pore needed investigating. One theory suggested that the membrane pore was formed by interaction with another plasma membrane channel, thought to be pannexin-1 (Locovei *et al.* 2007; Iglesias *et al.* 2008). Here, I used pannexin-1 inhibitors to assess the role of pannexin hemichannels in pore formation and TG2 secretion.

YO PRO-1 is a cell-impermeable fluorescent cationic compound that can be taken up through the membrane pore formed by P2X7R activation. Once taken up by cells, DNA binding by the dye leads to enhanced fluorescence emission, giving an indication of the membrane pore forming capabilities of cells expressing P2X7R. This assay has been previously established in our laboratory (Adamczyk 2013; Adamczyk *et al.* 2015). HEK293 cells expressing wild-type P2X7R were treated with pannexin-1 inhibitors; trovafloxacin (trova) (Poon *et al.* 2014) and ^{10}Panx (a pannexin-1 mimetic peptide, sequence: WRQAAFVDSY) (Pelegrin and Surprenant 2006). When P2X7R expressing cells were stimulated with 0.1mM or 0.5mM BzATP neither trova or ^{10}Panx had any inhibitory effect on YO PRO-1 uptake and therefore the membrane pore forming capabilities of these HEK293 cells (Fig. 3.1 A and C). Analysis of the rates of YO PRO-1 uptake confirm that there is no significant decrease in membrane pore activity in the presence of these inhibitors (T-test $p>0.05$) (Fig. 3.1 B and D). Concentrations of ligand that induce receptor activation (0.1mM BzATP) or receptor ligand binding site saturation (0.5mM BzATP) were examined as at least two components contribute to YO PRO-1 uptake, activated by different states of P2X7R ligand occupancy (Adamczyk 2013). This indicates that pannexin-1 is unlikely to be the membrane pore forming component in this cell model, even under conditions of full ligand occupancy of P2X7R.

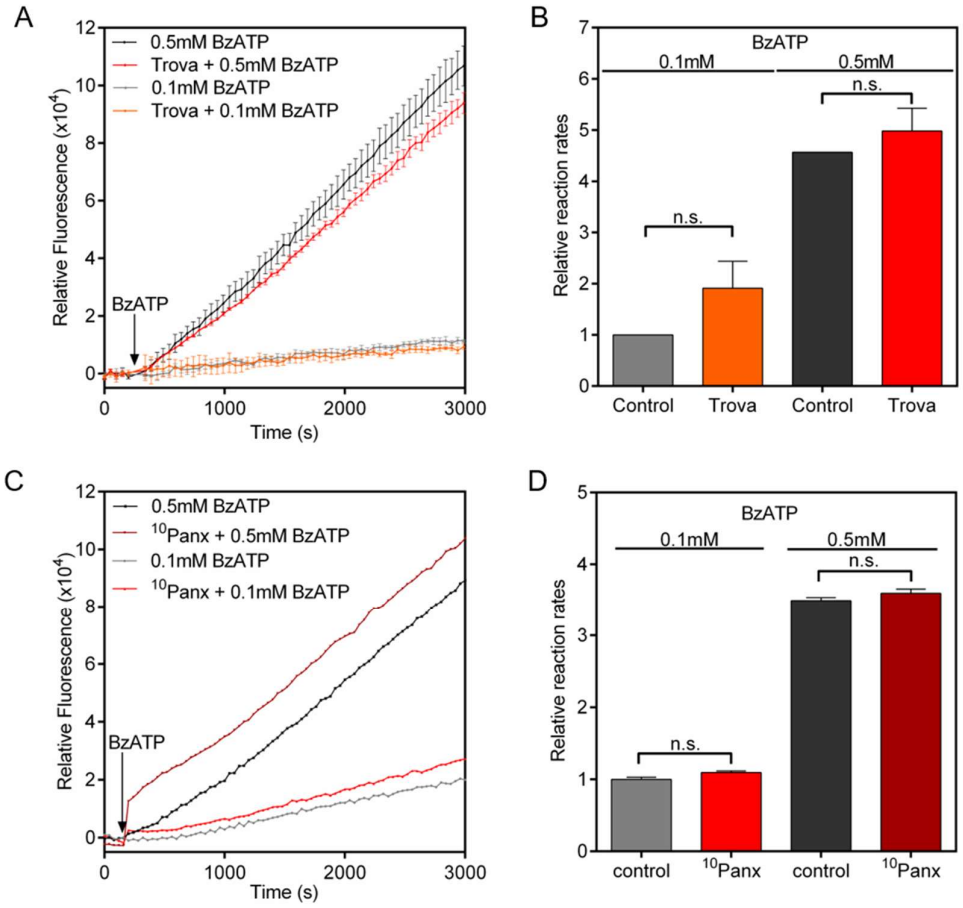

Fig. 3.1 YO PRO-1 uptake in the presence of pannexin-1 inhibitors. HEK293 cells expressing wild type P2X7R were seeded in a 96 well plate at a density of $3x10^4$ cells/well. Once cells were 80% confluent, cells were washed and pre-treated for 30 minutes with or without 100µM ^{10}Panx or 100µM trovafloxacin (trova). After pre-incubation, 1µM YO PRO-1 in PSS was added to the cells, and cells were stimulated with 0.1mM BzATP or 0.5mM BzATP. YO PRO-1 uptake was measured (excitation 480nm, emission 520-10nm) in the presence of A) 100µM Trovafloxacin or vehicle control (0.1% DMSO). Each point is the mean fluorescence ± SEM of three wells, with the non-stimulated control subtracted to account for fluorescence bleaching. Graph is representative of five independent experiments. C) Experiment performed in the presence of 100µM ^{10}Panx or vehicle control (H_2O). Each point is fluorescence from a single well, with the non-stimulated control subtracted to account for fluorescence bleaching. Graph is representative of four independent experiments. B and D) YO PRO-1 uptake rates were calculated from linear regression analysis of initial response (between 200 and 800 seconds following BzATP injection) in the presence of these inhibitors or vehicle control. The vehicle control treated with 0.1mM BzATP was set to 1 and all other data in the relevant experiment adjusted according to this control to allow comparison of uptake rates between experiments. n.s. indicates result is not significant as determined by t-test ($p>0.05$).

3.2.2 TG2 release is not affected by the pannexin-1 hemichannel inhibitor trovafloxacin

Although pannexin-1 does not appear to be involved in membrane pore formation by HEK293 cells, as indicated by YO PRO-1 uptake, it is possible that YO PRO-1 uptake and TG2 secretion occur through distinct membrane pore components. To assess whether pannexin-1 could be involved in TG2 secretion, HEK293 cells transiently transfected to express TG2 were treated with trova. The P2X7R was stimulated using 0.1mM BzATP and conditioned media collected and the presence of TG2 assessed by Western blotting using a previously established protocol (Adamczyk *et al.* 2015). As we found previously that TG2 secretion occurs in the initial 10 minute pulse of BzATP and continues during a 30 minute chase in the absence of BzATP, I used these conditions to ensure that pannexin-1 involvement was detected at either of these times. I tested 0.1mM BzATP and not 0.5mM BzATP as this concentration is sufficient for TG2 secretion so inhibition of pannexin-1 in these conditions would prevent TG2 secretion if it was involved. The presence of trova did not affect TG2 secretion (Fig. 3.2), therefore pannexin-1 is unlikely to be the pore forming component involved in TG2 release from cells. This indicates that an alternative membrane pore forming component, or a membrane pore formed by the P2X7R itself is required for TG2 secretion.

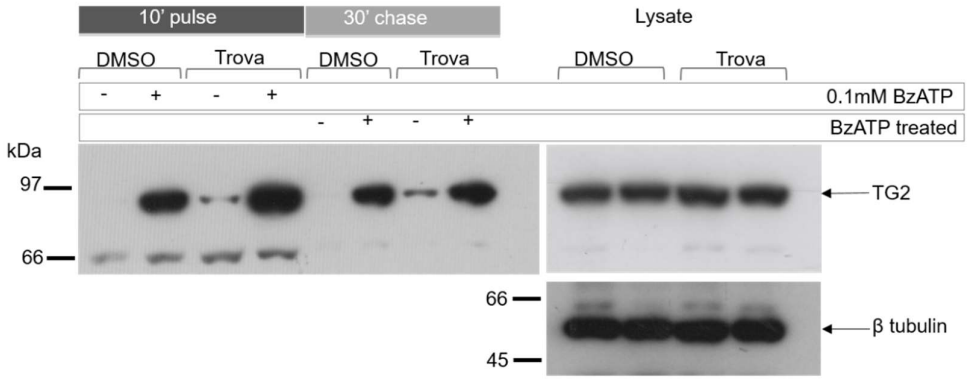

Fig. 3.2 TG2 secretion in the presence of pannexin-1 inhibitor. WT P2X7R HEK293 cells were transfected to express TG2 transiently, after 48 hours cells were pre-incubated with 100µM trovafloxacin (trova) or DMSO (0.1%) as a control for 30 minutes and trovafloxacin and DMSO were present during the subsequent steps of the experiment. Cells were stimulated with 0.1mM BzATP or left without agonist in OptiMEM as a control for 10 minutes as indicated. The conditioned media were collected and cells further incubated for 30 minutes in OptiMEM without BzATP. Conditioned media were again collected and cells lysed to allow assessment of TG2 expression levels. 150µl of conditioned media or 10µg total cell protein (as determined using BCA assay) were run for each sample on a 4-20% SDS PAGE gel under reducing conditions. Western blotting for TG2 (CUB7402, 200ng/ml) and β-tubulin (TUB2.1, 2.6µg/ml) was performed. Result shown is representative of 3 independent experiments.

3.2.3 Selecting P2X7R variants for expression in HEK293 cells

The selected mutations were chosen as they have previously been shown to modify P2X7R membrane pore formation specifically, and not other activities of the P2X7R. The $A^{348}T$ mutation was identified in human genomic screening, and shown to be present as the critical polymorphism for hyperactive P2X7R membrane pore formation (Stokes *et al.* 2010). The $P^{451}L$ mutation was identified in a genetic screen of mice with different pain sensitivities. Membrane pore formation was shown to be abolished in mice carrying leucine at position 451 (Adriouch *et al.* 2002). As there is a high degree of homology between the mouse and human receptor sequences in the respective sequence motif (an SH3 domain binding motif), it was expected that this amino acid exchange would have the same effect in both species (Fig. 3.3). Finally, a truncated version of the P2X7R, P2X7R variant B, was selected as a second variant deficient in pore formation. P2X7R variant B is a naturally occurring human splice variant, which leads to inclusion of an early stop codon from an intron between exons

10 and 11. This prevents translation of the final 249 amino acids from the *C*-terminus of the receptor and adds 18 amino acids from this intron (Adinolfi *et al.* 2010). The *C*-terminus is known to be important for membrane pore formation (Costa-Junior *et al.* 2011).

Mouse (L451) 445-SLHDSPLTPGQ-455
Mouse (P451) 445-SLHDSPPTPGQ-455
Human 445-ALHDTPPIPGQ-455
Rat 445-SLHHSPPIPGQ-455

Fig. 3.3 Sequence alignment of mouse, human and rat P2X7R. The SH3 domain binding motif X-P-P-X-P containing the residue at 451 are highlighted in yellow. Residues differing from the mouse sequence are underlined.

3.2.4 Detection of the extracellular domain of P2X7R for immunostaining

HEK293 Flp In cells were stably transfected to express P2X7R variant B, a truncated form of the receptor which lacks 249 amino acids from the intracellular *C*-terminus as well as two variants carrying a single amino acid exchange, P2X7R $A^{348}T$ and P2X7R $P^{451}L$. As transfectants were generated using Cre-mediated site-specific integration, transgene expression levels were expected to be comparable. Nevertheless, to demonstrate successful transfection with all plasmids, qPCR was performed. The expression of the P2X7R gene in cells transfected with plasmids for expression of wild type P2X7R, P2X7R $A^{348}T$, P2X7R $P^{451}L$ and P2X7R variant B was found to be similar (Fig. 3.4 A). Both P2X7R $A^{348}T$ and P2X7R $P^{451}L$ appear to show slightly increased mRNA expression levels in comparison to wild type P2X7R, however, this is likely to be within experimental error and appears to have little effect on the amount of protein expression (Fig. 3.4 B). qPCR data therefore demonstrates successful transfection of HEK293 cells with all plasmids, including P2X7R variant B. Western blotting demonstrated a very low level of P2X7R variant B in the stable cell line in comparison to wild type P2X7R, whereas P2X7R $A^{348}T$ and P2X7R $P^{451}L$ expressed at similar levels to the wild type (Fig. 3.4 B). As site-specific integration with Cre was used to generate stable cell lines, positional effects of transgene expression were not expected. Nevertheless, the experiment was conducted six times with similar outcomes, i.e. very low to no expression of P2X7R variant B. As the most specific antibody for P2X7R is directed to the *C*-terminus (Sc-25698) and P2X7R variant B

lacks much of the *C*-terminus present in wild type P2X7R, it was not possible to use this antibody to detect surface expression of P2X7R variant B. The antibody to the extracellular domain of P2X7R (Alomone labs, APR008) was therefore tested for suitability for immunostaining. An initial experiment labelling fixed parental HEK293 Flp In cells, which do not express P2X7R, and wild-type P2X7R expressing HEK293 cells with this antibody showed non-specific staining of the parental cells (Fig. 3.4 C). This was shown to not be due to secondary antibody issues, as cells incubated with secondary antibody only did not show any staining (Fig. 3.4 C). To address whether this was due to autofluorescence from the fixative, which can be present when the fluorescent label is in the green range (such as AlexaFluor 488), the secondary antibody was changed to an AlexaFluor 594 conjugated antibody. Staining of both HEK293 Flp In parental cells and HEK293 wild type P2X7R expressing cells was seen under these conditions, indicating that there is some non-specific binding of this antibody. To remove antibody that may recognise undesirable membrane proteins, the primary antibody was cross-absorbed by incubation with parental HEK293 Flp In cells prior to use in immunostaining experiments. The parental HEK293 Flp In cells stained using this antibody showed reduced staining in comparison to wild type P2X7R expressing cells, although staining was still visible in both cell lines. The signal for wild type P2X7R expressing cells was very low, therefore higher concentrations of primary antibody were cross-absorbed in the same way and used to stain parental HEK293 Flp In cells and wild type P2X7R expressing cells. It was important to establish a protocol giving a high level of specific staining of wild type P2X7R as the expression of P2X7R variant B was shown by Western blotting to be much lower than that of wild type P2X7R. These conditions resulted in staining of both parental HEK293 Flp In cells and wild type P2X7R expressing cells, meaning that these conditions resulted in non-specific antibody binding. Therefore, the lower primary antibody concentration was used for staining of parental HEK293 Flp In, wild type P2X7R and P2X7R variant B expressing cells. Due to similar levels of staining seen in the parental HEK293 Flp In cells as wild type P2X7R expressing cells, the conditions tested for this antibody were not able to demonstrate surface expression of P2X7R. The staining seen in HEK293 wild type P2X7R cells and HEK293 Flp In cells was, however, higher than the staining seen in HEK293 P2X7R variant B expressing cells, suggesting that these cells do not express functional P2X7R on the cell surface.

As it was not possible to demonstrate surface expression of P2X7R variant B using immunostaining, a plate-based assay for membrane depolarisation was established. This assay has the advantage of being able to demonstrate whether receptor is functional, as well as being cell surface expressed.

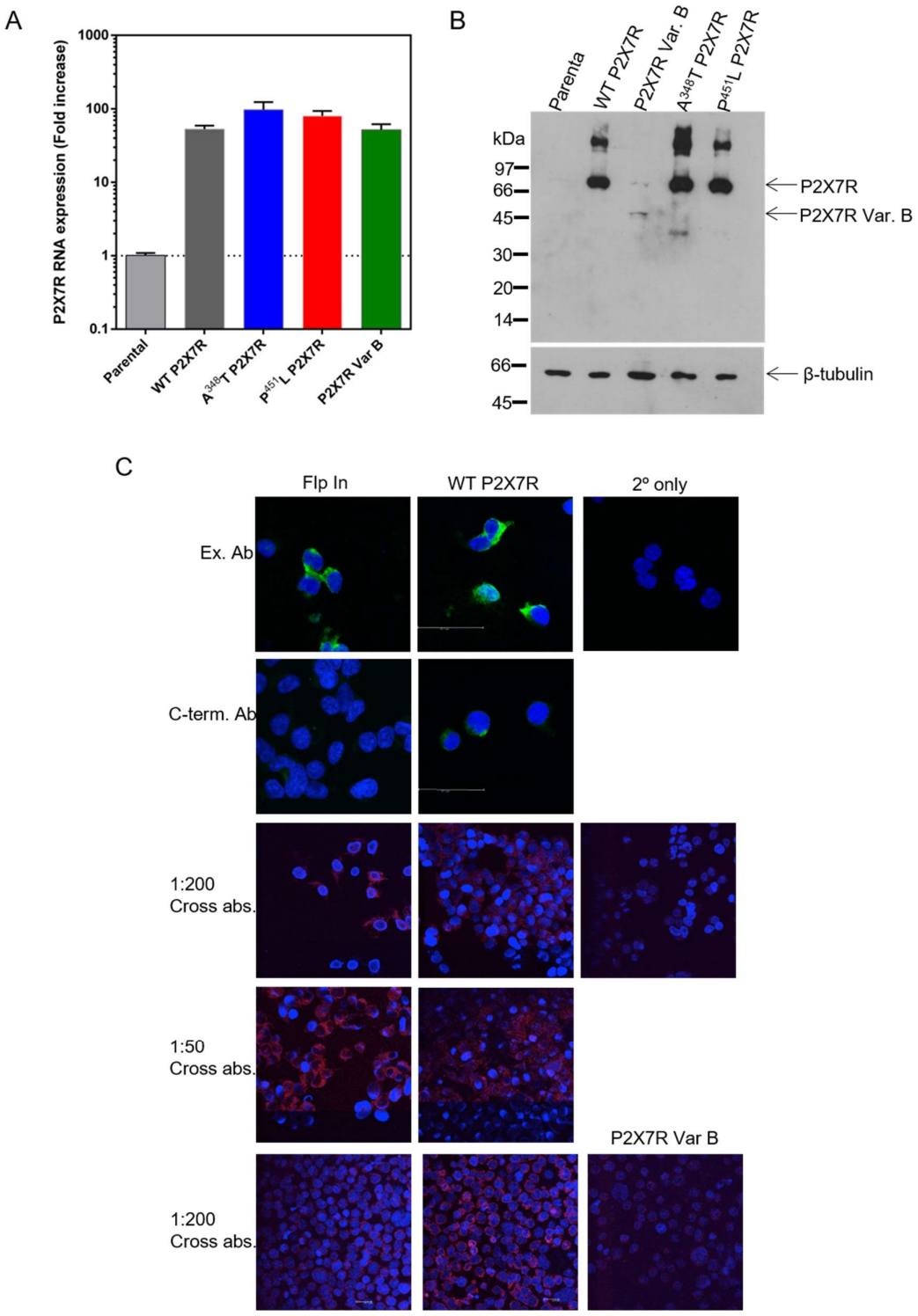

Fig. 3.4 Western blotting and Immunostaining using an antibody to the extracellular domain of the P2X7R. A) qPCR was performed in duplicate and analysed using the ΔΔCt method, normalised to the housekeeping gene control, H36B4 and given relative to *P2RX7*

expression in HEK293 Flp In cells. Data are presented as mean ± SEM. B) Cell lysates were run on a 4-20% SDS PAGE gel under reducing conditions and probed using an antibody to the extracellular domain of the P2X7R (APR008, 1.6µg/ml). C) Immunostaining was performed using the extracellular antibody described above at either 1:200 or 1:50 dilution. An example of P2X7R staining with the C-terminus antibody (Sc-25698, 2µg/ml) is also included. Where cross-absorption of the antibody is indicated (cross abs.), prior to P2X7R staining the antibody was pre-incubated with fixed HEK293 Flp-in cells to remove any cross-reacting or non-specific antibodies.

3.2.5 Establishing a plate based membrane depolarisation assay to assess ion channel activity of P2X7R and selected variants

The P2X7R is also capable of inducing membrane depolarisation, through formation of an ion channel. Membrane depolarisation can therefore be used as a measure of P2X7R activation and hence functional protein expression on the surface of the cell. As an antibody for the extracellular domain of P2X7R was found to be unsuitable for use in immunostaining, this assay can be used as an alternative to demonstrate expression of the *C*-terminally truncated P2X7R variant B that has been reported to have ion channel activity but not membrane pore activity (Adinolfi *et al.* 2010).

Membrane depolarisation can be measured using $DiSBAC_2(3)$ alone (Adinolfi *et al.* 2010), however, it is more sensitive when used in conjunction with FRET partner CC2-DMPE (Hoffman *et al.* 2005). CC2-DMPE has a lipid domain, which allows its insertion into the outer leaflet of the plasma membrane (Fig. 3.5). $DiSBAC_2(3)$ is capable of translocating from the outer leaflet to the inner leaflet of the plasma membrane. At resting potential, $DiSBAC_2(3)$ is present at the outer leaflet, causing energy transfer from CC2-DMPE to $DiSBAC_2(3)$, and emission can be measured from $DiSBAC_2(3)$. When cells become depolarised, $DiSBAC_2(3)$ moves to the inner leaflet and energy transfer no longer occurs, so emission is measured from CC2-DMPE and a drop in the emission from $DiSBAC_2(3)$ can be measured, indicating membrane depolarisation of the cells.

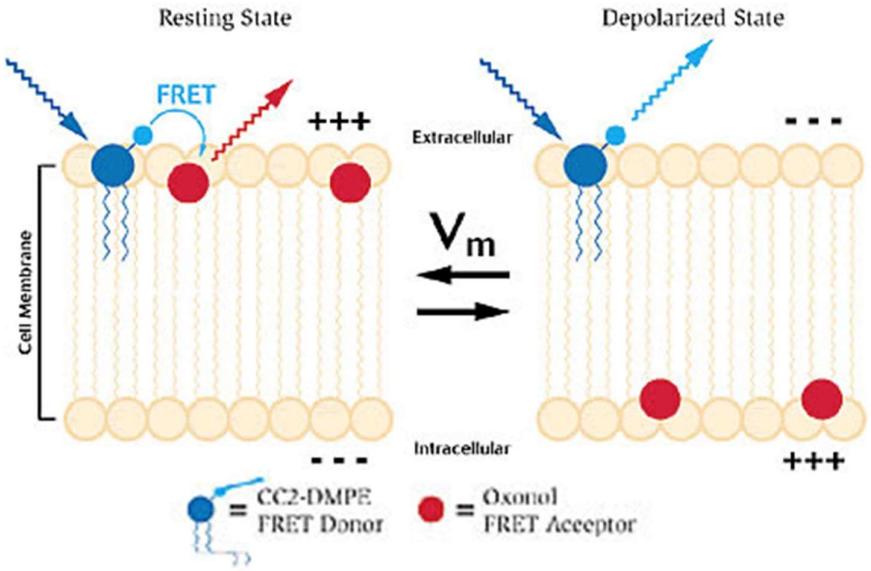

Fig. 3.5 FRET interaction between CC2-DMPE and DiSBAC2(3). At resting state, both CC2-DMPE (blue circle, listed as CC2-DMPE FRET Donor) and DiSBAC2(3) (red circle, listed of Oxonol FRET Acceptor) are present on the outer leaflet of the cell membrane, allowing a FRET interaction to occur. When cells become depolarised, the DiSBAC2(3) moves to the inner leaflet of the plasma membrane, so no FRET occurs and fluorescence from CC2-DMPE can be measured. Figure adapted from Hoffmann *et al*, 2005.

3.2.6 Measuring changes in membrane potential using DiSBAC$_2$(3)

Initially, membrane depolarisation measurements were done using DiSBAC$_2$(3) alone, essentially following previously published work (Adinolfi *et al.* 2010). High extracellular K^+ concentrations are known to induce membrane depolarisation therefore this was used as a positive control to ensure that the probe was capable of indicating depolarisation. HEK293 cells stably expressing P2X7R were stimulated in the presence of DiSBAC$_2$(3) with 0.1mM BATP or 30mM KCl. In this experiment, membrane depolarisation could be seen when 30mM KCl was injected (Fig. 3.6 A). When 0.1mM BzATP was injected, membrane depolarisation could not be measured. The level of fluorescence measured when KCl was injected was low, and membrane depolarisation in these conditions should be high. As BzATP induces a lower level of depolarisation than KCl, and therefore a lower fluorescent signal from the probes, this experimental set up was not sensitive enough to detect this. Intracellular Ca^{2+} was measured using Fluo-4, a membrane permeable dye, where fluorescence occurs on calcium binding to demonstrate that HEK293 P2X7R cells were capable of forming an ion channel in response to either 0.5mM BzATP or 0.1mM BzATP, and membrane

depolarisation should therefore be possible to measure (Fig. 3.6 B). As a more sensitive assay was required, DiSBAC$_2$(3) was used in conjunction with CC2-DMPE in future experiments.

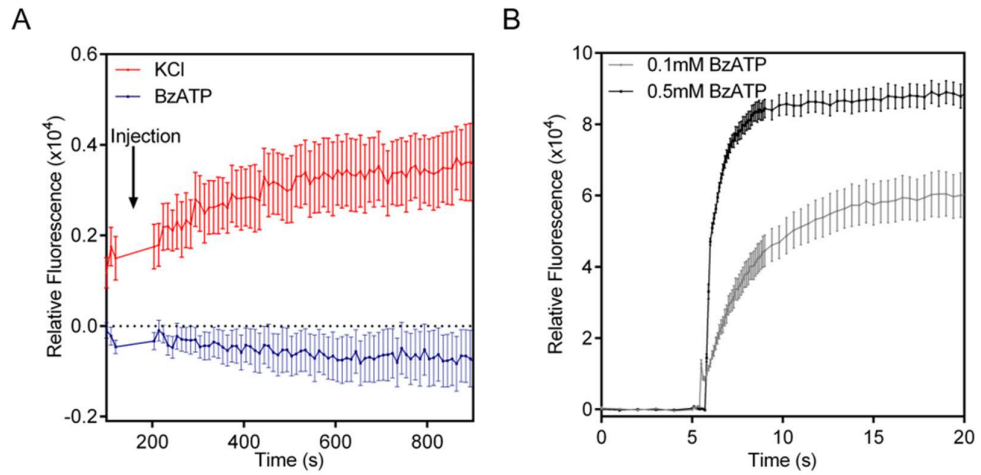

Fig. 3.6 Membrane depolarisation measured in HEK293 P2X7R cells using DiSBAC$_2$(3). A) HEK293 cells stably expressing P2X7R were seeded in a 96 well plate at a density of 5x10^4 cells/well. When cells reached 80% confluency, cells were washed in VSP-1 then incubated in VSP-1 containing 10µM DiSBAC$_2$(3) for 30 minutes. Cells were then stimulated with 0.1mM BzATP or 30mM KCl and fluorescence was measured for 1000 seconds (excitation: 540-10, emission: 590-20nm). Each point is mean fluorescence from 4 wells ± SEM with the control curve (cells with no KCl or BzATP added) subtracted. Representative of four independent experiments B) HEK293 cells stably expressing P2X7R were seeded in a 96 well plate at a density of 5x10^4 per well. Once cells were 80% confluent, cells were loaded with Fluo-4 and stimulated with 0.1mM or 0.5mM BzATP. Fluorescence was measured using the FLUOstar Omega (excitation 480nm, emission 520-10nm). The well specific fluorescence was subtracted from the data, then the control curve was subtracted (cells with H_2O added, instead of BzATP). Data are the mean of 8 wells ± SEM, representative of two experiments.

3.2.7 Measuring membrane depolarisation using DiSBAC$_2$(3) and CC2 DMPE

As DiSBAC$_2$(3) fluorescence measured at 590-20nm was not sensitive enough to measure membrane depolarisation induced by 0.1mM BzATP, CC2-DMPE was used in conjunction with DiSBAC$_2$(3). To ensure that the correct filters were being used for excitation and emission to give the maximum collection of the fluorescence, the excitation and emission spectra were measured for both CC2-DMPE and DiSBAC$_2$(3). CC2-DMPE fluorescence excitation was found to be highest between 390nm and

420nm, so the chosen excitation filter was 420-10nm (Fig. 3.7 A). CC2-DMPE emission was found to peak at 460nm, so the chosen emission filter was 460-20nm. The 460nm emission from CC2-DMPE is capable of exciting $DiSBAC_2(3)$ as it overlaps at the low end of its excitation curve (Fig. 3.7 B). $DiSBAC_2(3)$ fluorescence emission was found to peak at 560nm, therefore the 550-10nm filter was more appropriate than the 590-20nm filter used previously (Fig. 3.7 B). The final filters used were; excitation 420-10nm, emission 460-20nm and 550-10nm. Using these filters, an initial test of membrane depolarisation showed that the combination of CC2-DMPE and $DiSBAC_2(3)$ was sensitive enough to measure membrane depolarisation in HEK293 P2X7R cells in response to KCl or BzATP (T-test KCl vs control $p>0.05$, BzATP vs control $p=0.0251$) (Fig. 3.7 C). Membrane depolarisation measured was higher for BzATP than for KCl, although this was not a significant difference (T-test, $p>0.05$). The response ratio measured was still modest, which could relate to the high concentration of $DiSBAC_2(3)$ present extracellularly as the measurements were performed in the presence of this fluorophore (in the medium). Fig. 3.7 D shows that the increase in fluorescence from CC2-DMPE can be measured, but an expected decrease in fluorescence from $DiSBAC_2(3)$ could not be detected. The high extracellular $DiSBAC_2(3)$ concentration could be giving a high background, masking any change in signal from $DiSBAC_2(3)$ that has moved from the outer leaflet of the plasma membrane to the inner leaflet. Therefore, different concentrations of $DiSBAC_2(3)$ in the media were investigated next.

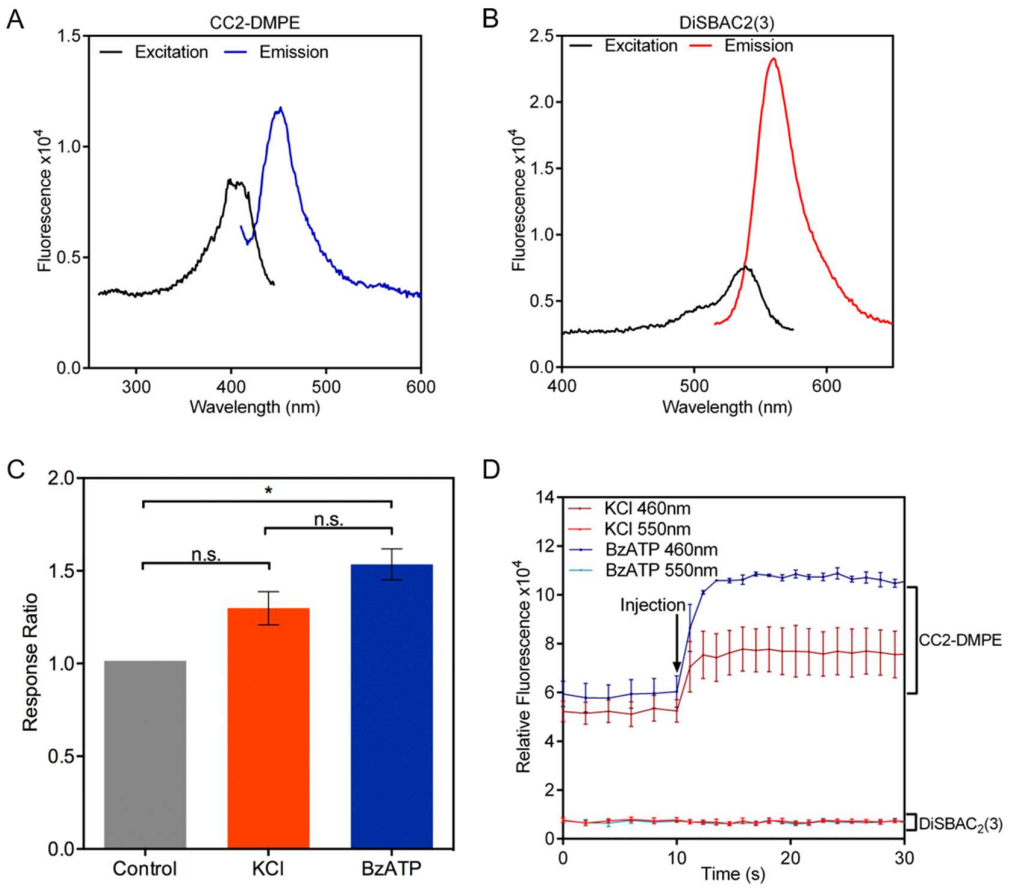

Fig. 3.7 Measuring membrane depolarisation using CC2 DMPE and DiSBAC$_2$(3).

A) and B) Excitation and emission spectra were measured using a fluorimeter to establish the correct filters to gain the maximum signal from the cells. C) and D) HEK293 cells stably expressing P2X7R were seeded at a density of 5x10^4 in a 96 well plate. Once cells were 80% confluent, they were pre-loaded with 5µM CC2-DMPE for 30 minutes, then excess CC2-DMPE was removed and cells washed. Cells were then pre-incubated with 10µM DiSBAC$_2$(3) for 30 minutes in VSP-1. Cells were then stimulated with either 0.1mM BzATP or 82mM KCl. Fluorescence was measured using the FLUOstar omega (excitation 420-10nm, emission 460-20nm and 550-10nm). C) Shows the response ratio calculated from 3 wells ± SEM with blank (no cells) subtracted. Response ratio was calculated by taking the mean of the first five baseline readings (0 to 5 seconds) and the mean of five post-stimulation readings (29 to 35.5 seconds) for each well after baseline (no cells) subtraction. The initial ratio was calculated by dividing the baseline mean reading at 460nm by baseline mean reading at 550nm and the final ratio was calculated by dividing the post-stimulation mean reading at 460nm by the post-stimulation mean reading at 550nm. The response ratio was then calculated by dividing the post-stimulation ratio by the initial ratio and the mean of these values for each condition was calculated. Representative of two independent experiments D) Shows membrane depolarisation curves as a mean from 3 wells ± SEM, with blank (no cells) subtracted. * t-test $p<0.05$.Representative of two independent experiments.

3.2.8 Effect of changing DiSBAC$_2$(3) concentration on membrane depolarisation measurements

As DiSBAC$_2$(3) is present extracellularly at high concentration relative to the FRET donor during the experiment, it is possible that this is masking the decrease in fluorescence that should be observed as a consequence of changes in level of FRET upon membrane depolarisation. Lower concentrations of DiSBAC$_2$(3) were tested, to see whether this allowed the decrease in fluorescence emission from the FRET acceptor to be seen. 10μM DiSBAC$_2$(3) was also included (concentration used previously) and present during the experiment or washed out after the pre-incubation step and replaced with fresh VSP-1 prior to the fluorescence measurements, to establish whether DiSBAC$_2$(3) is inserting into the plasma membrane at a sufficient level to be able to indicate depolarisation. Removing the DiSBAC$_2$(3) from the cell supernatant may then allow this change in fluorescence to be seen, as the excess DiSBAC$_2$(3) would not be present to mask the signal. The increase in fluorescence from CC2-DMPE could be measured in all of the conditions tested (Fig. 3.8 A), however the decrease in fluorescence from DiSBAC$_2$(3) was not measurable at any of the DiSBAC$_2$(3) concentrations used (Fig. 3.8 B). Fig. 3.8 C shows that reducing DiSBAC$_2$(3) concentration does not significantly alter the response ratio measured (T-test $p>0.05$), except at 2μM DiSBAC$_2$(3) (T-test $p=0.0192$). However, 10μM DiSBAC$_2$(3) will continue to be used, as the manufacturer recommends, and different quenchers will be investigated.

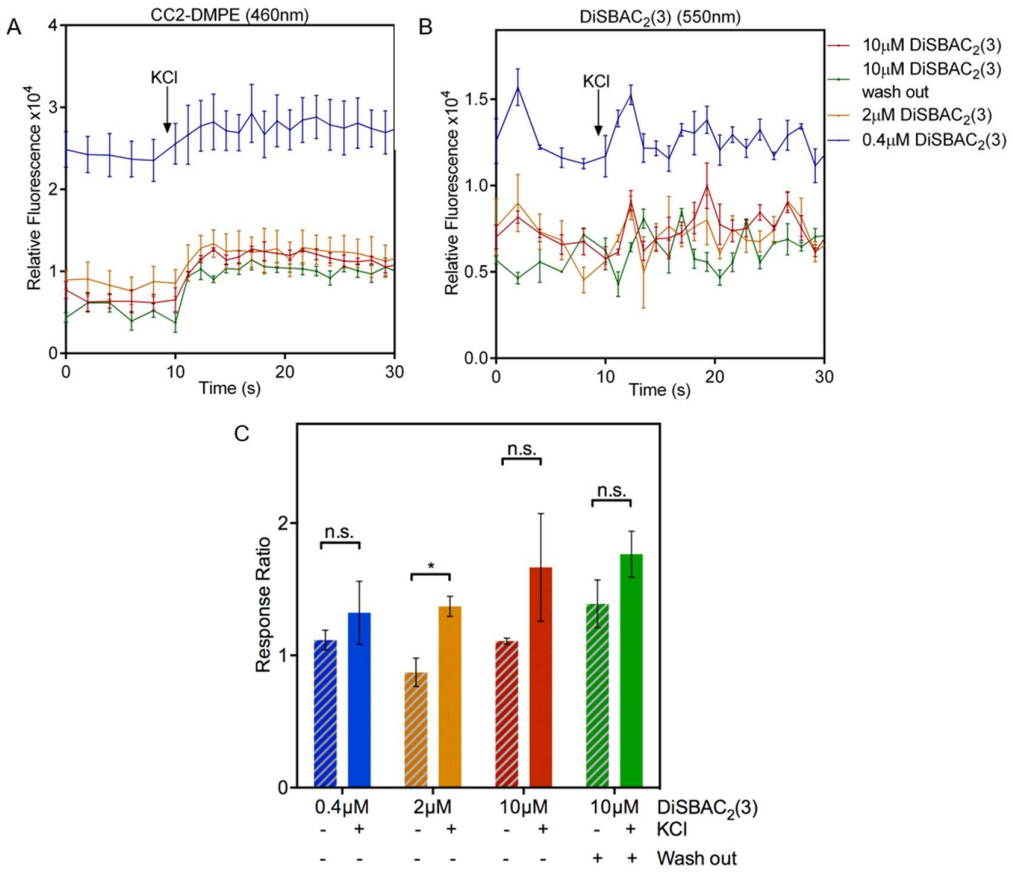

Fig. 3.8 Effect of different DiSBAC2(3) concentrations on membrane depolarisation measurements. Membrane depolarisation experiments were performed as outlined in fig. 3.7 C, using the following $DiSBAC_2(3)$ concentrations: 10µM, 2µM or 0.4µM as indicated. For one of these conditions (10µM $DiSBAC_2(3)$ wash out), after the 30 minute incubation the $DiSBAC_2(3)$ was washed out and replaced with fresh VSP-1 without $DiSBAC_2(3)$. A) shows fluorescence emission at 460-20nm (emission from CC2-DMPE) for KCl treated cells. B) shows fluorescence emission at 550-10nm (emission from $DiSBAC_2(3)$) for KCl treated cells. Data are the mean fluorescence of 3 wells ± SEM with control curve (no cells) subtracted. C) shows response ratios calculated as described in fig. 3.7 C. Data are mean fluorescence of 3 wells ± SEM. Control (H_2O) response ratio shown in striped bars and 82mM KCl response ratio shown in solid bars. Significance was determined by t-test, n.s. indicates not significant ($P>0.05$), * indicates $p<0.05$. Experiment performed once.

3.2.9 Effect of different quenchers on membrane depolarisation measurements

As changing the concentration of $DiSBAC_2(3)$ did not yield the desired result, different quenchers were tested to suppress solution-derived $DiSBAC_2(3)$ fluorescence. The quenchers selected were ESS-2 (40mM tartrazine, 60mM acid red 37, 40mM acid fuchsin, 2% of this solution added to each well), individual components of ESS -2; 60mM acid red 37, 40mM acid fuchsin or 40mM tartrazine (2% of each of these solutions added to each well), and 0.08% bromophenol blue (final concentration in the well) (Knapp *et al.* 2001). Cell experiments were conducted as in previous section. Fig. 3.9 A demonstrates that the increase in fluorescence from CC2-DMPE can be seen in all conditions, however Fig. 3.9 B demonstrates that the decrease in fluorescence from $DiSBAC_2(3)$ cannot be measured in any of these conditions. Calculation of response ratios showed that inclusion of tartrazine improved the membrane depolarisation measurements in comparison to control more than the other quenchers (T-test $p=0.002$ KCl vs H_2O treated cells in the presence of tartrazine, $p=0.0223$ in the absence of any quencher, $p=0.0367$ in the presence of bromophenol blue and $p=0.0309$ in the presence of acid fuchsin, $p>0.05$ in the presence of ESS2 and acid red 37) (Fig. 3.9 C). Therefore, different concentrations of tartrazine were tested to optimise the concentration for quenching the undesired signal. Tartrazine at a final concentration of 1.2mM (2% of 60mM tartrazine in each well) was found to have the most beneficial effect on the membrane depolarisation measurements (T-test $p<0.0001$ KCl vs H_2O treated cells in the presence of 1.2mM tartrazine) (Fig. 3.9 D). In the presence of 1.2mM tartrazine, when BzATP was applied, it was possible to measure a significant response (T-test $p=0.0055$). The response measured when 82mM KCl was applied was higher than the response measured when 0.1mM BzATP was used, as expected (T-test, $p=0.00655$ KCl vs BzATP treated cells, $p=0.0029$ KCl vs H_2O treated cells in the presence of 1.2mM tartrazine) (Fig. 3.9 E). In future experiments, 10µM $DiSBAC_2(3)$ and 1.2mM tartrazine was used.

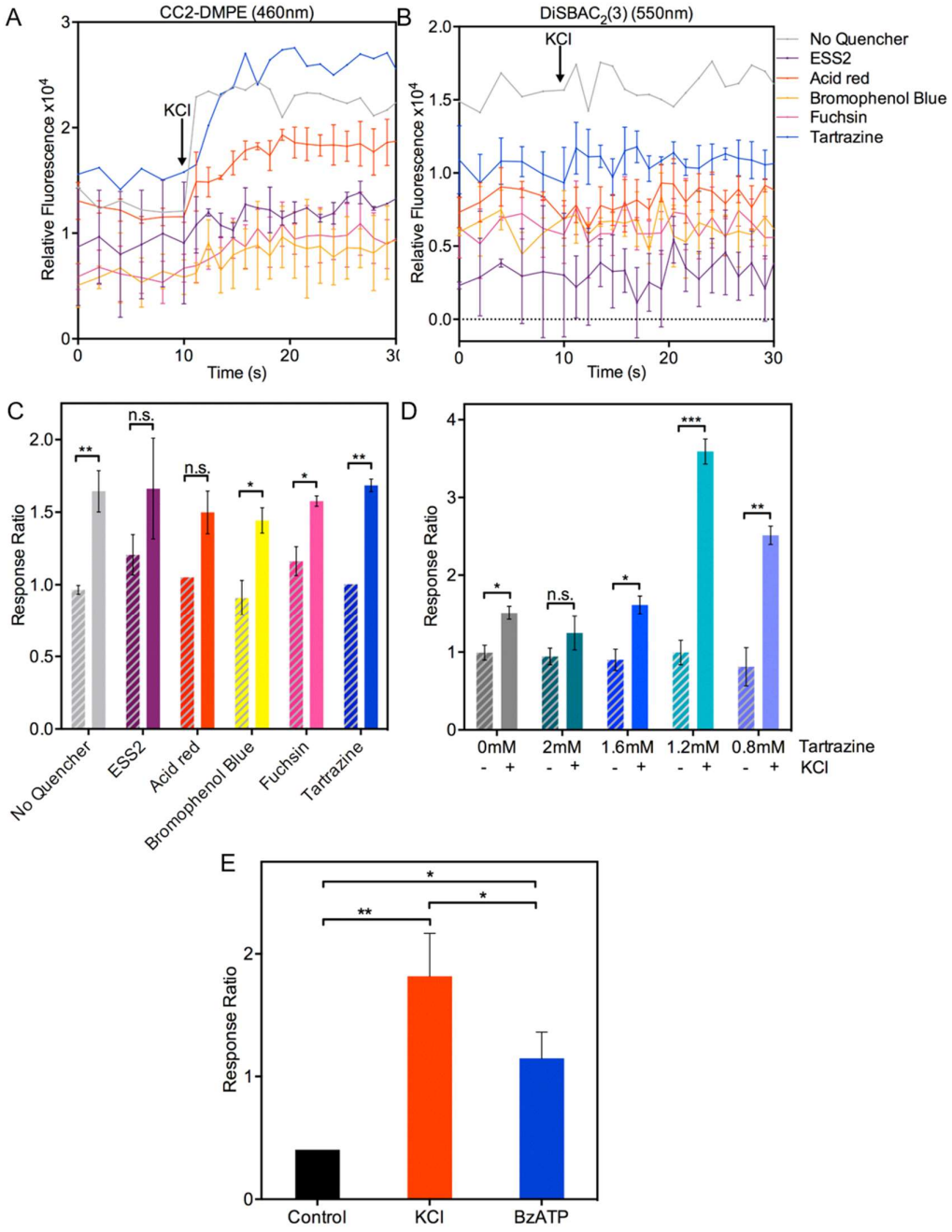

Fig. 3.9 Effect of different quenchers on membrane depolarisation measurements. Membrane depolarisation experiments were performed as outlined in fig. 3.7 C. For the final 5 minutes of the 30 minute incubation with $DiSBAC_2(3)$, quenchers were added at the following final concentrations; ESS-2 (60mM acid red 37, 40mM tartrazine and 40mM acid fuchsin, 2% in each well), 60mM acid red (2% in each well), 0.08% bromophenol blue, 40mM acid fuchsin (2% in each well) and 40mM tartrazine (2% in each well) or 2mM, 1.6mM, 1.2mM, 0.8mM tartrazine (final concentrations in each well). A) shows fluorescence emission at 460-20nm (emission from CC2-DMPE) for KCl treated cells with blank (no cells) subtracted, data are the mean of 2 wells ± SD. B)

shows fluorescence emission at 550-10nm (emission from $DisBAC_2(3)$) for KCl treated cells with blank (no cells) subtracted, data are the mean of 2 wells ± SD. Experiment performed once. C) shows response ratio ± SD calculated as in fig. 3.7 C in the presence of quenchers. D) Tartrazine was added for the final 5 minutes of the $DiSBAC_2(3)$ at the indicated concentrations (final concentration in each well) and response ratios ± SD calculated as in fig. 3.7 C. Experiment performed once. E) Membrane depolarisation was measured in the presence of 1.2mM tartrazine in response to 82mM KCl or 0.1mM BzATP and response ratios ± SD calculated as in fig. 3.7 C. T-test performed to determine significance, *p<0.05, **p<0.005, ***p<0.001, n.s. not significant. Representative of two repeat experiments.

3.2.10 Assessing the presence and functionality of P2X7R variant B on the cell surface

It has been reported previously that P2X7R variant B is capable of ion transport on ligand binding (Adinolfi *et al.* 2010), so the plate-based membrane depolarisation assay established here could be used to confirm the presence of the receptor on the cell surface. Using stable cell lines of wild type P2X7R or P2X7R variant B, membrane depolarisation could be detected in response to KCl in both cell lines (wild-type P2X7R t-test p=0.009, P2X7R variant B t-test p=0.0133) (Fig. 3.10 A). This indicated that the cells were capable of depolarisation and the assay was working correctly for both cell lines. A response to 0.1mM BzATP could be detected in the wild type P2X7R expressing cells (T-test p=0.0129, but not in the cells expressing P2X7R variant B (T-test p>0.05), although this response was not found to reach significance in all experiments (Fig. 3.10 A and C). This indicates that P2X7R variant B may not be expressed at the surface of the cells or not expressed at sufficient levels to depolarise the cell.

To exclude adaptive changes of the cells to transgene overexpression, the wild type P2X7R and P2X7R variant B were transiently transfected into the HEK293 Flp In cell line to assess whether P2X7R variant B could be expressed at a higher level under these conditions. Western blotting demonstrated that P2X7R variant B was expressed at a similar level to wild type when transient transfection was performed (Fig. 3.10 B). For membrane potential measurements, cells were transiently transfected with P2X7R variant B or wild type P2X7R and expression was allowed to continue for 24, 36 and 48 hours prior to conducting the analysis. Results were compared to the HEK293 parental Flp In cell line and wild type P2X7R expressing stable cell line. All cell lines responded to KCl. As expected, HEK293 parental Flp In cells did not respond to

BzATP and membrane depolarisation was seen in wild type P2X7R expressing cells (stable cell lines). Transient transfections of wild type P2X7R showed a response but this did not reach significance when 0.1mM BzATP was applied (T-test $p>0.05$). This highlights that variability introduced by transient transfection is not conducive to these measurements due to a lack of sufficient sensitivity. Cells transiently transfected with P2X7R variant B also did not respond to 0.1mM BzATP (T-test $p>0.05$), suggesting that P2X7R variant B is not present on the cell surface or if present, is not functional (Fig. 3.10 C).

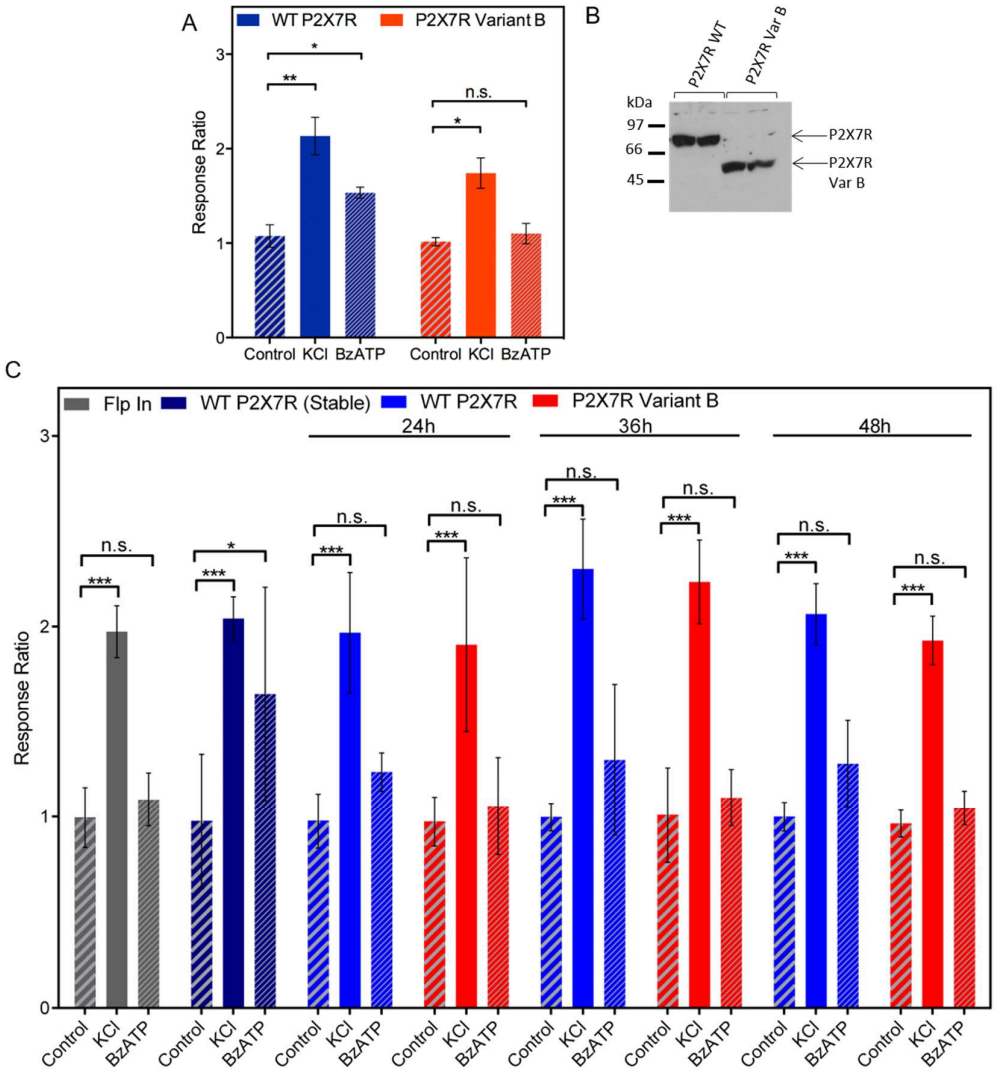

Fig. 3.10 Assessing membrane depolarisation of cells expressing wild type P2X7R and P2X7R variant B. A) Membrane depolarisation experiments were performed as described in Fig. 3.9 E. The response ratio was calculated and is shown as the mean of 3 wells ± SEM. Representative of two independent experiments B) HEK293 Flp In cells were seeded at a density of $1.2x10^5$ cells/well in a 24 well plate. After 24 hours, cells were transfected with plasmids for expression of wild-type P2X7R or P2X7R variant B. Western blotting was performed as in Fig. 3.4 A, using the extracellular antibody for P2X7R (APR008). C) Parental HEK293 Flp In cells or HEK293 cells stably expressing wild type P2X7R were seeded at a density of $2x10^4$ cells/well in a 96 well plate. Cells were transfected to transiently express wild type P2X7R or P2X7R variant B where indicated, and membrane depolarisation experiments were performed 24, 36 or 48 hours later, as described in Fig. 3.9 E. Response ratio was calculated and is shown as the mean of 2 wells ± SD. Experiment performed once. Data were analysed using T-test, *$p<0.05$, **$p<0.005$, ***$p<0.001$, n.s. not significant.

3.2.11 P2X7R $P^{451}L$ and $A^{348}T$ variants: impact of mutations on membrane pore formation and TG2 secretion

As pannexin-1 does not seem to be involved in membrane pore formation or TG2 secretion by P2X7R in the HEK293 cell system, mutations expected to affect pore formation were introduced into the P2X7R. The $A^{348}T$ mutation was identified in human genomic screening and has been shown to result in enhanced membrane pore activity (Stokes *et al.* 2010). The $P^{451}L$ mutation was identified in the mouse P2X7R and has been shown to give a receptor incapable of pore formation (Adriouch *et al.* 2002). As there is a high degree of homology between the human and mouse P2X7R in the respective sequence motif (Fig. 3.3), it was expected that the $P^{451}L$ mutation would have a similar effect on pore formation in the human receptor as seen in the mouse receptor. These amino acid exchanges were introduced into the P2X7R expression plasmid using site directed mutagenesis and stable cell lines were established, using the HEK293 Flp In cells and co-transfection with Cre for site-specific DNA integration.

Western blotting was used to demonstrate P2X7R expression and assess total protein levels (Fig. 3.4 A and Fig. 3.11 A). The parental HEK293 Flp-In cell line does not express P2X7R. Both P2X7R $A^{348}T$ and P2X7R $P^{451}L$ were expressed at a similar level to wild-type P2X7R. To confirm that the P2X7R variants were present at the cell membrane, immunostaining was performed using the specific P2X7R antibody to the intracellular C-terminus (Sc-25698). Both P2X7R mutants were expressed at the cell surface, as was the wild-type P2X7R (Fig. 3.11 B). Parental HEK293 Flp In cells show very little (background) staining, indicating that the cell surface staining seen in transfected cells is specific to P2X7R. The antibody used for staining is directed to the C-terminus of the P2X7R, which P2X7R variant B is lacking, therefore staining was not possible for this receptor variant.

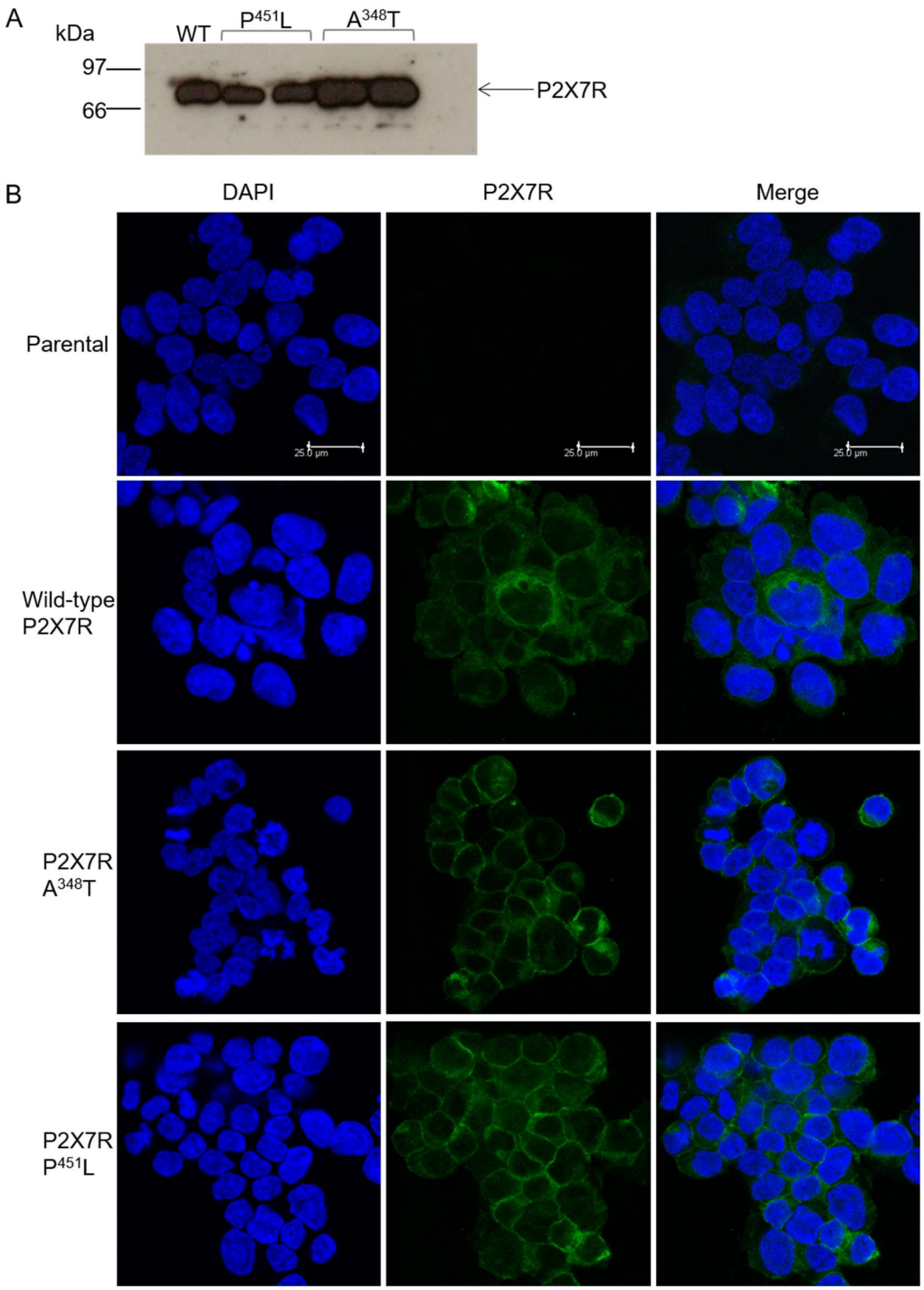

Fig. 3.11 Demonstrating overall and cell surface expression of P2X7R in HEK293 cells. A) Western blotting was performed as described in Fig. 3.4 A, but using the anti-P2X7R C-terminus antibody (Sc-25698, 1µg/ml). B) HEK293 Flp-In, wild-type P2X7R, P2X7R A348T and P2X7R P451L cells were seeded at a density of 1x104 cells into separate wells of a chamber slide in DMEM containing 10% FBS and allowed to grow for 1 day. Cells were fixed with 4%

paraformaldehyde and permeabilised with 0.1% triton-X-100. Primary antibody (anti-P2X7R C-terminus, Sc-25698, 2 µg/ml) binding was detected using fluorescently labelled secondary antibody (AlexaFluor 488). Coverslips were mounted using Vectashield with DAPI (Vector Laboratories) to stain the nuclei. Cells were imaged using a Leica confocal microscope with the 63x/1.4 NA oil objective. AlexaFluor 488 excitation is at 458nm (using the argon ion laser) and emission captured at 494-535nm. DAPI nuclear stain can be visualized by excitation at 405nm (using the 405nm diode laser) and emission collected at 430-512nm. Images are representative of three independent experiments.

3.2.12 Characterising the properties of P2X7R variants $A^{348}T$ and $P^{451}L$

To assess functionality of the mutant receptors, P2X7R $A^{348}T$ and P2X7R $P^{451}L$, calcium flux was measured using Fluo-4, as described previously. P2X7R cells were stimulated with 0.1mM BzATP and change in fluorescence measured. The calcium response measured in wild-type P2X7R and P2X7R $P^{451}L$ cells is comparable (T-test $p>0.05$), indicating that this mutation does not have a significant effect on calcium flux in the cells (Fig. 3.12 A). The calcium response in P2X7R $A^{348}T$ expressing cells appears increased in comparison to wild-type P2X7R, although this was not found to be significant (T-test $p>0.05$). Analysis of the rate of this response shows that the k' (apparent rate constant) for wild type P2X7R, P2X7R $A^{348}T$ and P2X7R $P^{451}L$ fall within the 95% confidence intervals (Fig. 3.12 B). Therefore, the calcium response is not substantially changed in these cells. The slight increase in response rate in P2X7R $A^{348}T$ cells may also relate to a slight elevation in the amount of P2X7R expressed (3.11 A). Taken together these data show that functional receptor is present in all three cell lines and that agonist treatment induces a robust ion channel response with both variant receptors.

A

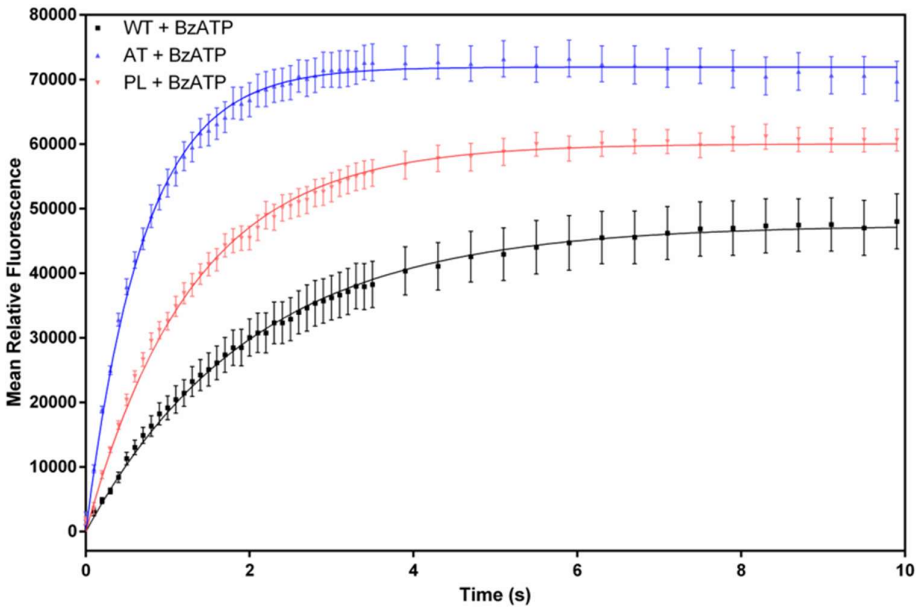

B

Experiment		WT	A348T	P451L
1	k' (s-1)	0.74	0.95	0.64
	CI	0.58 to 0.91	0.77 to 1.14	not calc
2	k' (s-1)	0.49	1.41	0.77
	CI	0.44 to 0.54	1.32 to 1.51	0.71 to 0.83
3	k' (s-1)	1.18	1.26	0.54
	CI	1.10 to 1.25	1.18 to 1.34	0.49 to 0.58
	Mean k' (s-1) ± SEM	0.80 ± 0.25	1.21 ± 0.17	0.65 ± 0.082

Fig. 3.12 Calcium response in P2X7R variant expressing cells. To measure intracellular calcium, HEK293 P2X7R cells were seeded at a density of $5x10^4$ per well in a 96 well plate. After 48 hours cells were pre-loaded with 3µM Fluo-4, then stimulated with 0.1mM BzATP. Fluo-4 fluorescence was measured using the FLUOstar Omega (excitation: 480-10nm and emission: 520-10nm). A) Data were normalised for baseline fluorescence, then the control curve (H_2O treated cells, instead of BzATP) was subtracted. Data are the mean of eight repeats, representative of two experiments ± SEM. B) Rate of calcium uptake by the cells was calculated using the 10s immediately after BzATP injection and data fitted assuming pseudo first order kinetics and using the following equation: Y=(Ymax-Ymax*exp(-k'*x))+f. Values given as rate per second (k' (s^{-1}) where k'=k*[P2X7R]. f represents a constant.

To investigate membrane pore forming properties of the P2X7R variants, YO PRO-1 uptake was measured as before. Surprisingly, the P2X7R P451L mutant gives pore formation comparable to wild-type P2X7R (Fig. 3.13 A). The P2X7R A348T mutant shows enhanced membrane pore forming properties, in comparison to the wild-type P2X7R (Fig. 3.13 A). At 0.04mM BzATP, activation of P2X7R A348T is seen. In contrast, the wild type P2X7R shows minimal YO PRO-1 uptake when stimulated

with 0.04mM BzATP, as does P2X7R $P^{451}L$ (Fig. 3.13 B). Analysis of the rate of YO PRO-1 uptake at different BzATP concentrations indicates that the apparent ligand binding activity of P2X7R $A^{348}T$ is unchanged in comparison to wild type P2X7R and P2X7R $P^{451}L$ (P2X7R $A^{348}T$ K_D 60 ± 10μM, P2X7R $P^{451}L$ K_D 70 ± 10μM) (Fig. 3.13 C). Taken together, these data show that P2X7R $P^{451}L$ behaves like wild type P2X7R, whereas the P2X7R $A^{348}T$ has a potentiated response but unchanged ligand affinity.

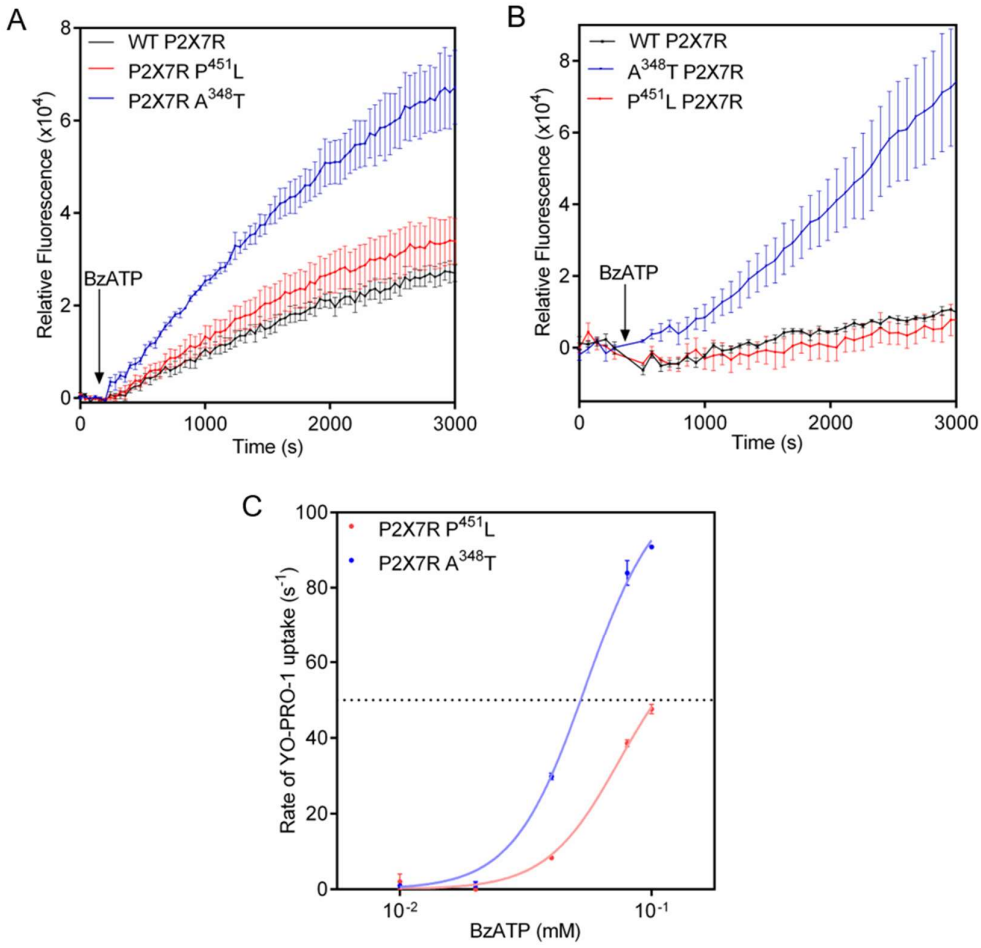

Fig. 3.13 Characterising P2X7R membrane pore forming properties by measuring YO PRO-1 uptake. A) To measure pore formation, YO PRO-1 uptake was used. HEK293 cells expressing wild type or mutant P2X7R were seeded in a 96 well plate at a density of $3x10^4$ cells/well. Once cells were 80% confluent, 1µM YO PRO-1 in PSS was added to the cells, and cells were stimulated with 0.1mM BzATP. YO PRO-1 uptake was measured (excitation 480nm, emission 520nm) for 1 hour. Each point is the mean of three wells, ± SEM. Graphs are representative of three independent experiments. B) YO PRO-1 uptake performed as in A), with cells stimulated with 0.04mM BzATP. C) YO PRO-1 uptake was performed as in A), with cells stimulated with 0.01mM, 0.02mM, 0.04mM, 0.08mM and 0.1mM BzATP. Linear regression analysis was performed using the initial response (from 700 to 1600 seconds) to determine the YO PRO-1 uptake rate which was then plotted against the concentration of BzATP and K_D determined by fitting the data with sigmoidal dose-response curve.

3.2.13 Is TG2 Secretion altered in P2X7R $A^{348}T$ or $P^{451}L$ expressing cells?

TG2 presence in the media of cell lines expressing wild type or mutant P2X7R, with and without stimulation of the P2X7R, was analysed by Western blotting. The P2X7R was stimulated using 0.1mM BzATP and conditioned media collected both after 10 min of stimulation and after an additional 30 min chase period without agonist (3.14 A). The P2X7R $A^{348}T$ expressing cells showed a significant increase in TG2 secretion, correlating with the increase in membrane pore formation. This was evident already within the 10 min stimulation period, suggesting faster kinetics. The P2X7R $P^{451}L$ expressing cells showed a similar level of TG2 secretion to the wild-type receptor expressing cells consistent with the two receptors having comparable pore formation activity. There was a lack of TG2 secretion from P2X7R variant B expressing cells, however this could be due to a lack of cell surface expression of the respective receptor variant, as already discussed in detail in section 3.2.10. Densitometry analysis of TG2 in the media from 3 experiments confirms the increase in TG2 secretion when the P2X7R $A^{348}T$ is compared to wild type P2X7R (Fig. 3.14 B).

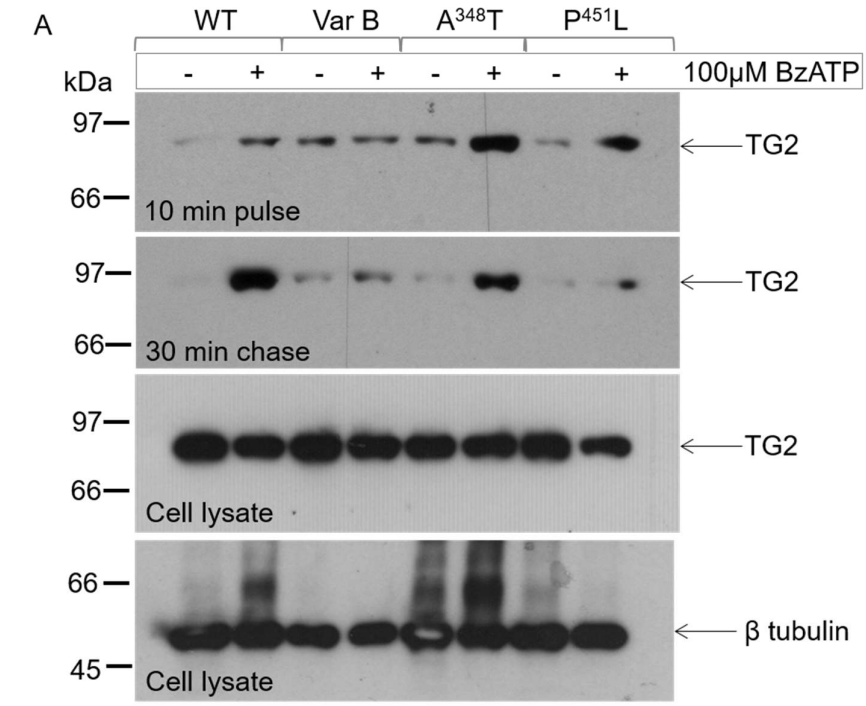

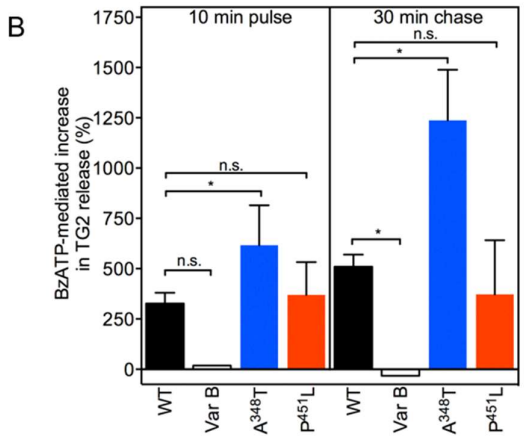

Fig. 3.14 TG2 secretion by P2X7R variant expressing cells. HEK293 cells expressing P2X7R variants were seeded at a density of $1.2x10^5$ cells/well in a 24 well plate. After 24 hours, cells were transfected with TG2. After a further 48 hours, cells were stimulated with 0.1mM BzATP in OptiMEM for 10 minutes and conditioned media collected (pulse). Fresh OptiMEM was applied for a further 30 minutes, without BzATP and conditioned media were collected (chase). At the end of the experiment, cells were lysed with cell extraction buffer to assess levels of TG2 in cells (cell lysate). 150µl concentrated conditioned media or 10µg of total cell lysate protein were run on a 4-20% SDS PAGE gel under reducing conditions and Western blotting performed using anti-TG2 antibody (CUB7402, 200ng/ml) and anti-β-tubulin antibody (TUB2.1, 2.6µg/ml). A) Western blot is representative of five experiments. B) Densitometry performed on three TG2 release experiments. Data

shown are mean ± SD. Significance was determined using repeated measures ANOVA followed by Tukey's post-hoc test, *p<0.05.

3.3 Discussion

The work performed in this chapter aimed to investigate the role of membrane pore formation in response to P2X7R activation in externalisation of TG2. This included assessing the involvement of pannexin-1 in pore formation and the use of P2X7R mutants in an attempt to dissect various activities of the receptor. Pore formation itself was monitored using YO PRO-1 uptake and TG2 secretion was assessed by Western blotting. This work demonstrates that pore formation in HEK293 cells does not involve pannexin-1. Other groups have also found that pannexin-1 is not involved in pore formation in HEK293 cells (Browne *et al.* 2013; Sun *et al.* 2013). However, it has also been reported that HEK293 cells require pannexin-1 to form pores (Pelegrin and Surprenant 2006). As it is possible that multiple mechanisms exist that could account for membrane pore formation by P2X7R, I have analysed membrane pore formation in response to different agonist concentrations and also used two mechanistically different ways to inhibit pannexin-1. Furthermore, TG2 secretion could occur through a pannexin-1 channel, despite YO PRO-1 uptake being unaffected. I therefore tested whether TG2 secretion occurred in the presence of pannexin-1 inhibitors, and found this was also unaffected. Taken together, our evidence suggests that pannexin-1 is not involved in pore formation or TG2 secretion by P2X7R (Adamczyk *et al.* 2015).

To further investigate the mechanism of pore formation in these cells, P2X7R variants were generated. These included a truncated version of the P2X7R, P2X7R splice variant B, lacking the final 249 amino acids of the *C*-terminus due to the inclusion of an intron between exons 10 and 11, which introduces a premature stop codon. The *C*-terminus of the P2X7R has been shown to be important for cell surface expression of the receptor. Smart et al (2003) demonstrated that truncation of the *C*-terminus of the rat receptor between residues 551 and 581 prevents ethidium ion uptake (a measure of membrane pore formation), as well as ion channel function and cell surface expression. This group also found that truncated receptors with wild type-like pore formation and ion channel activity had similar levels of expression to the wild type receptor. Whereas when these functions were lost, the respective truncated receptors

showed no cell surface expression. However, a truncation at position 380 allowed the receptor to still function as an ion channel but not to form membrane pores, therefore it was concluded that (95% of) the *C*-terminus was required for pore formation (Smart *et al.* 2003). The P2X7R variant B used here is a naturally occurring human splice variant. Adinolfi et al (2010) reported cell surface expression of this variant by immunostaining and showed it responded to BzATP treatment by membrane depolarisation and Ca^{2+} influx, but not ethidium ion uptake (Adinolfi *et al.* 2010). As I was unable to find an antibody able to give specific P2X7R binding by immunolabelling of cells, other than one generated to an epitope in the *C*-terminus, I used membrane depolarisation to establish whether the receptor was expressed on the cell surface and functional. I was unable to measure a change in membrane potential in response to BzATP stimulation, despite using a more sensitive probe than Adinolfi *et al*, suggesting that P2X7R variant B was not expressed on the cell surface or not functional. qPCR demonstrated that RNA levels of P2X7R variant B were comparable to wild-type receptor, and Western blotting showed much reduced levels of protein. As transient expression, similar to stable expression, of P2X7R variant B did not yield functional cell surface receptor, it is not due to negative selection. This suggests that receptor protein in the cell is degraded, possibly due to trafficking or folding issues. I was also unable to detect an increase in TG2 in the conditioned media of P2X7R variant B expressing HEK293 cells stimulated with BzATP, however this may be due to a lack of surface expression of the truncated receptor, not due to the effect of truncation on larger-membrane pore formation. My finding that this truncated P2X7R variant was not expressed at significant levels by HEK293 cells or displayed demonstrable activity is consistent with the work outlined above by Smart et al (2003), as P2X7R variant B lacks the majority of the *C*-terminus, including the region between 551 and 558, thought to be vital for cell surface expression of the receptor.

Expression levels of the $A^{348}T$ and $P^{451}L$ P2X7R variants was demonstrated by Western blotting to be similar to wild type P2X7R and both variants were found on the cell surface by immunolabelling. P2X7R $P^{451}L$ cells show similar calcium uptake to wild type P2X7R expressing cells, suggesting that ion channel function in this mutant is unaffected. P2X7R $A^{348}T$ however shows an increase in calcium uptake rate in response to BzATP, suggesting that the ion channel has increased activity. Analysis of the ligand binding to P2X7R showed that this was unchanged in P2X7R $A^{348}T$,

suggesting that the increase in ion channel activity may be due to the state of channel dilation. The $A^{348}T$ variant also shows enhanced pore formation. The $P^{451}L$ variant shows pore formation similar to wild type P2X7R, which was unexpected. The $P^{451}L$ mutation was identified in mouse (Adriouch *et al.* 2002) where a genomic screen showed that mice with L^{451} show reduced pain sensitivity in comparison to mice with P^{451} (Sorge *et al.* 2012). The authors of this study were able to demonstrate that this was due to a lack of membrane pore formation by this variant. As there is a high degree of homology between the mouse and the human P2X7R and conservation of the respective sequence motif (Fig. 3.15), this mutation was expected to have similar consequences in the mouse and human receptor. However, in our cell model membrane pore formation of the human receptor was unaffected. This highlights that even though the receptors in these two species are very similar, there are some mechanistic differences in membrane pore formation between human and mouse. Sorge et al (2012) also found that inhibition of pannexin-1 in mice expressing the P^{451} receptor prevented pore formation (Sorge *et al.* 2012). As I did not see any involvement of pannexin-1 in pore formation in HEK293 cells expressing wild type P2X7R, it is possible that I don't see any change in pore formation because the P^{451} is involved in an interaction with pannexin-1 in mouse macrophages that does not occur in the cells I was using. This could indicate that different pathways are involved either because of species or cell type. However, it has also been shown that pannexin-1 deficient macrophages are competent in P2X7R-dependent IL-1 secretion (Qu *et al.* 2011).

_N_-terminal domain:

```
hX7v1    MPACCSC SDV   FQYETNKV  TRIQSMN YGTIK                          30
mX7      MPACCSW   NDV   LQYETNKV  TRIQSTN YGTVK
hX4v1    MAGCCAALAAFL  FEYDTPRI  VLIRSRK VGLMN
```

Transmembrane 1:

```
hX7v1    WFFHVIIFSY VC  FALVS                                          47
mX7      WVLHMIVFSY IS  FALVS
hX4v1    RAVQLLILAY VI  GCYHPHLA EVEMESPRR WVFVW
```

Extracellular domains:

```
hX7v1    DKL YQRKEPVISS VHTKVKGIAE VKEEIVENGV KKLVHSVFDT ADYTFPLQG NSF
mX7      DKL YQRKEPVISS VHTKVKGIAE VTENVTEGGV TKLGHSIFDT ADYTFPLQG NSF
hX4v1    EKG YQETDSVVSS VTTKVKGVAV TNT        SKLGFRIWDV ADYVIPAQEENSL

hX7v1    FVMTNFLK TEGQEQRLCP EYPTRRTLCS SDRGCKKGWM DPQSKGIQTG          140
mX7      FVMTNYVK SEGQVQTLCP EYPRRGAQCS SDRRCKKGWM DPQSKGIQTG
hX4v1    FVMTNVIL TMNQTQGLCP EIPDATTVCK SDASCTAGSA GTHSNGVSTG

hX7v1    RCVVYEGNQK TCEVSAWCPI EAVEEAPRPA LLNSAENFTV LIKNNIDFPG        200
mX7      RCVPYDKTRK TCEVSAWCPT EEEKEAPRPA LLRSAENFTV LIKNNIHFPG
hX4v1    RCVAFNGSVK TCEVAAWCPV EDDTHVPQPA FLKAAENFTL LVKNNIWYPK

hX7v1    HNYTTRNILP GLNITCTF HK T      QNP QCPIFR LGDIFRETGD           240
mX7      HNYTTRNILP TMNGSCTF HK T      WDP QCSIFR LGDIFQEAGE
hX4v1    FNFSKRNILP   NITTTY LK SCIYDAKTDP FCPIFR LGKIVENAGH

hX7v1    NFSDVAIQGG IMGIEIYWD CNLDRWFH HCRPKYSFR RLDD                  280
mX7      NFTEVAVQGG IMGIEIYWD CNLDSWSH HCRPRYSFR RLDD
hX4v1    SFQDMAVEGG IMGIQVNWD CNLDRAAS LCLPRYSFR RLDT

hX7v1    KTTNVSLYPG YNFRYAKYYK EN NVEKRTLI KVFGIRFDIL VFGTGGKFD        329
mX7      KNTDESFVPG YNFRYAKYYK EN NVEKRTLI KAFGIRFDIL VFGTGGKFD
hX4v1    RDVEHNVSPG YNFRFAKYYR DLAGNEQRTLI KAYGIRFDII VFGKAGKFD
```

Transmembrane 2:

```
hX7v1    IIQLVVYIGST LSYFGLAAVF IDFLI                                  355
hX7vB    IIQLVVYIGST LSYFGLVRDS LFHAL
mX7      IIQLVVYIGST LSYFGLATVC IDLLI
hX4v1    IIPTMINIGSG LALLGMATVL CDIIV
```

_C_-terminal domain:

```
hX7v1    DTYSS NCCRSHIYPW CKCCQPCVVNE YYYRKKCES IVEPKPT                397
hX7vB    GKWFGEGSD
mX7      NTYSS AFCRSGVYPY CKCCEPCTVNE YYYRKKCES IMEPKPT
hX4v1    LYCMKKR LYYREKKYK YVEDYEQGL ASELDQ

hX7v1     LKY VSFVDESHIR MVNQQLLGRS LQDVKGQEVP RPAMDFTDLS RLPLALHDTP   450
mX7       LKY VSFVDEPHIR MVDQQLLGKS LQVVKGQEVP RPQMDFSDLS RLSLSLHDSP
hX4v1

hX7v1    PIPGQPEEIQ LLRKEATFRS RDSPVWCQCG SCLPSQLPES HRCLEELCCR        508
mX7      PTPGQSEEIQ LLHEEVAPKS GDSPSWCQCG NCLPSRLPEQ RRALEELCCR

hX7v1    KKPGACITTS ELFRKLVLSR HVLQFLLLYQ EPLLALDVDS TNSRLRHCAY        566
mX7      RKPGRCITTS KLFHKLVLSR DTLQLLLLYQ DPLLVLGEEA TNSRLRHRAY

hX7v1    RCYATWRFGS QDMADF AILP SCCRWRIRKE FPKSEGQYSG FKSPY            595
mX7      RCYATWRFGS QDMADF AILP SCCRWRIRKE FPKTEGQYSG FKYPY
```

Fig. 3.10 Alignment of the mouse and human P2X7R with human P2X4R. Alignment of the P2X7R amino acid sequence with the P2X4R sequence highlights the overall homology but differences with regards to the C-terminus. The position of the P451L and A348T mutations are shown in red. The P451L mutation lies within an SH3 domain binding motif (highlighted in blue). The *C*-terminal sequence of the truncated P2X7R variant B differs after transmembrane 2

domain, highlighted in red. Green regions are those thought to be involved in the internalisation and recycling of the receptor (Costa-Junior *et al.* 2011).

In line with the receptor properties with regards to pore formation, the P2X7R $A^{348}T$ variant shows enhanced TG2 secretion and the secretion of TG2 by P2X7R $P^{451}L$ is unchanged from wild type P2X7R. These findings, along with our previous work demonstrating that TG2 secretion is not linked to P2X7R ion channel formation or microvesicle release implicate the pore of the P2X7R in TG2 secretion (Adamczyk *et al.* 2015). The hyperactivity of P2X7R $A^{348}T$ does not relate to a decreased threshold of agonist concentration required to induce pore formation and may instead relate to the size of the ion channel and membrane pore formed by this receptor variant. Sun et al (2003) have suggested that binding of individual molecules of ATP to the P2X7R gradually changes the conformation of the P2X7R to open an ion channel once two ATP molecules have bound and full receptor activation and pore formation occurring once three ATP molecules bind (Sun *et al.* 2013). It is possible that the $A^{348}T$ mutation distorts the receptor so that two molecules of ATP binding leads to formation of a larger ion channel and full receptor occupancy by ATP leads to formation of a larger membrane pore than seen in wild type P2X7R. This would support the ion channel dilation theory of P2X7R activation being responsible for larger membrane pore formation. This theory is supported by data demonstrating that the $G^{345}C$ mutant in the second transmembrane domain can be used to block pore formation, using cysteine-reactive compounds which act to block the channel formed by P2X7R (Browne *et al.* 2013).

In summary, our data from our previous publication (Adamczyk et al. 2015) and this thesis show that TG2 release involves the membrane pore formed upon P2X7R activation. It remains to be shown whether membrane translocation occurs via this pore or whether the pore transmits a signal that leads to enzyme export. I have shown that the pore formed in this HEK293 cell model does not require pannexin-1 hemichannel activity and is therefore likely to involve P2X7R itself and be formed by higher order receptor oligomers or large conformational changes, or both. However, I can also not entirely exclude an interaction with another as yet unidentified membrane channel.

Chapter 4

4. Is there a link between regulation of conformational changes in TG2 that control enzymatic activity and TG2 secretion?

4.1. Introduction

Activity of several TGs including TG2 is under allosteric regulation by Ca^{2+} and GTP (Liu *et al.* 2002; Ahvazi *et al.* 2003; Begg *et al.* 2006a). Intracellularly there are high levels of GTP (100-200μM) and low levels of Ca^{2+} (<1μM), which causes TG2 to adopt a GTP-induced closed conformation (Fig. 4.1), inactivating transglutaminase activity (Liu *et al.* 2002). If the cell becomes compromised, a rise in intracellular Ca^{2+} can lead to Ca^{2+} binding to TG2 and a switch to the open conformation, activating transglutaminase activity (Pinkas *et al.* 2007). TG2 is also likely to be active extracellularly under normal circumstances due to the high Ca^{2+} concentrations (1.5-2.5mM) and low GTP concentrations, favouring Ca^{2+} binding. Having established that TG2 was secreted on P2X7R activation, I was interested in assessing whether the GTP binding ability of TG2 was required for this mechanism of secretion. TG2 unable to bind GTP has previously been shown to not be secreted via other pathways, as discussed in this chapter, therefore it was important to investigate this in the context of P2X7R activation.

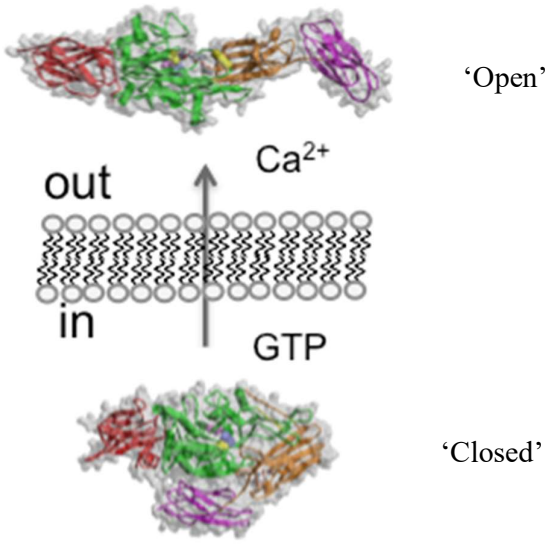

Fig. 4.1 Ca^{2+} and GTP bound conformations of TG2. Inside the cell there is a higher level of GTP, so TG2 is in the closed conformation. Outside the cell there is a higher level of Ca^{2+} and TG2 is in the open conformation. Structural representations of TG2 were created based on x-ray structures: 1KV3C, 2Q3ZA (Reproduced from Professor Daniel Aeschlimann).

The GTP binding site of TG2 is located at the interface of the β-barrel 1 domain and the catalytic core domain (Liu *et al.* 2002; Jang *et al.* 2014). Within the β-barrel 1 domain, amino acids 476 to 472 and 580 to 583 have been shown to be important for GTP binding, through both resolution of an x-ray crystal structure of GDP-bound TG2 (Liu *et al.* 2002) and GTP-bound TG2 (Jang *et al.* 2014) and a mutation based approach (Iismaa *et al.* 2000; Begg *et al.* 2006b). It has also been demonstrated that K^{173} and F^{174} in the core domain are required for GTP binding (Liu *et al.* 2002). These approaches were able to delineate the roles of specific residues in GTP binding. The x-ray crystal structure demonstrated that R^{580} forms two ion pairs with the α- and β-phosphates of GTP (Fig. 4.2), stabilising the interaction with GTP (Jang *et al.* 2014). R^{478} and V^{479} main chains are also positioned near the β-phosphate of GDP, with a hydrogen bond formed with V^{479} (Liu *et al.* 2002). V^{479}, along with F^{174}, M^{483}, L^{582} and Y^{583} form a hydrophobic pocket, within which the guanine base sits (Liu *et al.* 2002). The F^{174} may also stabilise the interaction by forming aromatic stacking interactions with the guanine ring (Fig. 4.2) (Liu *et al.* 2002). K^{173} and R^{476} form a positively charged area to stabilise the negative charges on the γ-phosphate during

hydrolysis, and H_2O hydrogen bonded to either of these residue side chains may act as the nucleophilic attacking group in GTP hydrolysis (Liu *et al.* 2002).

In the closed conformation, the access of the Gln donor substrate to the active site is blocked. This has become apparent through the position of several loops of the β-barrel 1 domain in the GDP/GTP-bound TG2 structure (Liu *et al.* 2002; Jang *et al.* 2014). A loop connecting the third and fourth β-strands and another loop connecting the fifth and sixth β-strands are positioned to block access to the active site (Liu *et al.* 2002). The first loop contains a tyrosine residue (Y^{516}) which can form a hydrogen bond with the active site cysteine (C^{277}) (Liu *et al.* 2002; Begg *et al.* 2006b). This prevents C^{277} from participating in reactions, indicating that Y^{516} must move to make the active site accessible to substrates (Liu *et al.* 2002). Therefore, GTP binding does not only block access of the substrate to the active site due to conformational constraints, but also inactivates an essential active site residue.

The GTP bound form of TG2 has been demonstrated to have important activities both physiologically and pathologically, for example in osteoarthritis and cancer (Johnson and Terkeltaub 2005; Tee *et al.* 2010). In cancer, a splice variant of TG2 (TG2-S), lacking 149 amino acids present on the *C*-terminus of full length TG2 (TG2-L), but with 10 alternative amino acids at the *C*-terminus was found to have protective effects against cancer (Tee *et al.* 2010). TG2-S was found to have much reduced transamidation activity, as well as being unable to bind GTP, where TG2-L is capable of GTP binding. TG2-L bound to GTP contributed to resistance to certain cancer therapeutics (Antonyak *et al.* 2006; Tee *et al.* 2010). This therefore presents inhibitors of GTP binding or TG2 activating agents as possible cancer therapies (Tee *et al.* 2010).

To investigate the role of GTP binding by TG2 in osteoarthritis, Johnson and Terkeltaub (2005) transfected wild type TG2 and different mutant forms of TG2 into chondrocytes. Wild type TG2 was capable of inducing chondrocyte hypertrophy, indicated by an increase in type X collagen expression and matrix calcification (Johnson and Terkeltaub 2005). This was found to be dependent on TG2 interaction with β1 integrin, which would induce intracellular signalling events within the chondrocyte, in particular through p38 mitogen activated protein kinase, shown to be involved in chondrocyte hypertrophy *in vitro* (Johnson and Terkeltaub 2005). The GTP binding mutant $K^{173}L$, however, was found to have a decreased capacity to induce p38

phosphorylation and therefore chondrocyte hypertrophy, but still showed similar transamidation activity to wild type TG2 (Johnson and Terkeltaub 2005). These data suggest that GTP binding by TG2 is important for chondrocyte hypertrophy. It is possible that GTP bound TG2 can interact differently with cell surface receptors or extracellular matrix components, altering the interaction with chondrocytes (Johnson and Terkeltaub 2005). This indicates a role for extracellular GTP-bound TG2 in important biological processes, independent of transamidation activity. The GTP-bound TG2 conformation may indeed be stabilised by interaction with heparin at the cell surface (Scarpellini *et al.* 2009).

Given the critical role nucleotides play not only in regulating TG2 conformation but also in its biological function it is essential to understand how nucleotide binding or exchange relates to a possible export mechanism. Furthermore, despite extracellular TG2 being likely to be in the open conformation due to Ca^{2+} binding, TG2 has been found to be abundantly present in an inactive form extracellularly (Stamnaes *et al.* 2010). TG2 has been demonstrated to be inactivated by the formation of a disulphide bond between neighbouring cysteine residues in the oxidising extracellular environment (Stamnaes *et al.* 2010). A disulphide bond forms initially between C^{230} and C^{370} (Ca^{2+}-bound enzyme), which then facilitates formation of a disulphide bond between C^{370} and C^{371}, inactivating the enzyme (Stamnaes *et al.* 2010). This disulphide bond has been shown to be reduced by thioredoxin-1, reactivating TG2 (Jin *et al.* 2011). This gives a second regulatory step for TG2 activation, whereby the large quantity of extracellular TG2 is apparently regulated by thioredoxin-1 externalisation (Jin *et al.* 2011).

Thioredoxin-1 is a redox protein, which is ubiquitously expressed and can act as a protein chaperone (Arner and Holmgren 2000). Thioredoxin-1 has roles in modulation of the immune system (being important for activation of defensins), as well as redox roles in regulation of transcription factors (e.g NFκB) and regulating apoptosis (Arner and Holmgren 2000). Thioredoxin-1 can act extracellularly, for example, in the immune system it can act as a chemokine, causing migration of neutrophils, monocytes and T-cells (Bertini *et al.* 1999). The mechanism of thioredoxin-1 release from cells is unconventional as it has been shown that thioredoxin-1 is not released through the classical ER/Golgi secretory pathway, and similarly to TG2 lacks a leader

sequence (Rubartelli *et al.* 1992). Initially, it was suggested that thioredoxin-1 secretion had similar features to IL-1β secretion; however, it was later found not to be associated with membrane bound particles released from cells, thereby differing from Il-1β secretion (Rubartelli *et al.* 1992). In parallel with our work (Adamczyk *et al.* 2015), it was recently found that thioredoxin-1 could be secreted through activation of the P2X7R in mouse bone marrow macrophages, not requiring inflammasome activation, however the precise mechanism of protein export remains unknown (Rothmeier *et al.* 2015). Given the similarity in regulation of thioredoxin-1 secretion to TG2 secretion, it is possible that it is secreted through the same pathway as TG2. As thioredoxin-1 has a role in TG2 activation extracellularly and is a known chaperone protein, it is also possible that it also has a functional role during protein secretion *per se*.

The work presented in this chapter assesses the involvement of GTP binding to TG2 in its secretion through the pathway regulated by P2X7R. I was also investigating here the potential co-release of thioredoxin-1 through this pathway and a possible functional role for thioredoxin-1 in TG2 secretion. These data are a step towards a mechanistic understanding of the export process.

Aims for this chapter:

1. To assess secretion of TG2 GTP binding variants in response to activation of P2X7R.
2. To analyse TG2 variants for changes in enzymatic activity by assessing transamidation activity and its regulation by GTP.
3. To investigate the effect of inhibitors of different functions of P2X7R on the secretion of thioredoxin-1.
4. To evaluate a potential functional role for thioredoxin-1 in this pathway of TG2 secretion by application of thioredoxin-1 inhibitors.

4.2. Results

4.2.1. Is TG2 externalisation regulated by the conformational change induced upon GTP binding or by GTP hydrolysis?

The mutations shown in the structural model of TG2 in fig. 4.2 were selected for analysing the requirement of GTP binding to TG2 for its secretion. Four mutants were generated for these studies, $K^{173}N$, $K^{173}L$, $K^{173}N/F^{174}D$ and $R^{580}A$. K^{173} participates in hydrogen bonding to stabilise the interaction with the γ-phosphate of GTP and may also participate in GTP hydrolysis by stabilising an intermediate state (Iismaa *et al.* 2000; Liu *et al.* 2002). Therefore, mutations $K^{173}L$ and $K^{173}N$ at this position were chosen as they were likely to have an effect on GTP hydrolysis, with TG2 still likely to be capable of GTP binding, $K^{173}N$ being a more conservative amino acid exchange, whereas $K^{173}L$ removes the ability for hydrogen bonding to GTP entirely. F^{174} forms part of the hydrophobic pocket for the guanine base and can stabilise the interaction through aromatic stacking interactions. Mutation $F^{174}D$ is therefore likely to be disruptive for binding of GTP to TG2, as it lacks the aromatic ring and introduces a negative charge. Finally, R^{580} interacts with the α- and β- phosphates of the GTP molecule, thereby making a critical contribution to the interaction (Liu *et al.* 2002). Mutation to $R^{580}A$ removes the ability for hydrogen bonding and will therefore affect the binding of GTP, as has been shown previously (Iismaa *et al.* 2000). These mutations were introduced into TG2 in the pMAG plasmid for recombinant TG2 expression in *E. coli* (N-terminally His-tagged TG2 (Hadjivassiliou *et al.* 2008)) and the pCDNA3.1 plasmid for transient expression in HEK293-P2X7R cells (native TG2 (Stephens *et al.* 2004)).

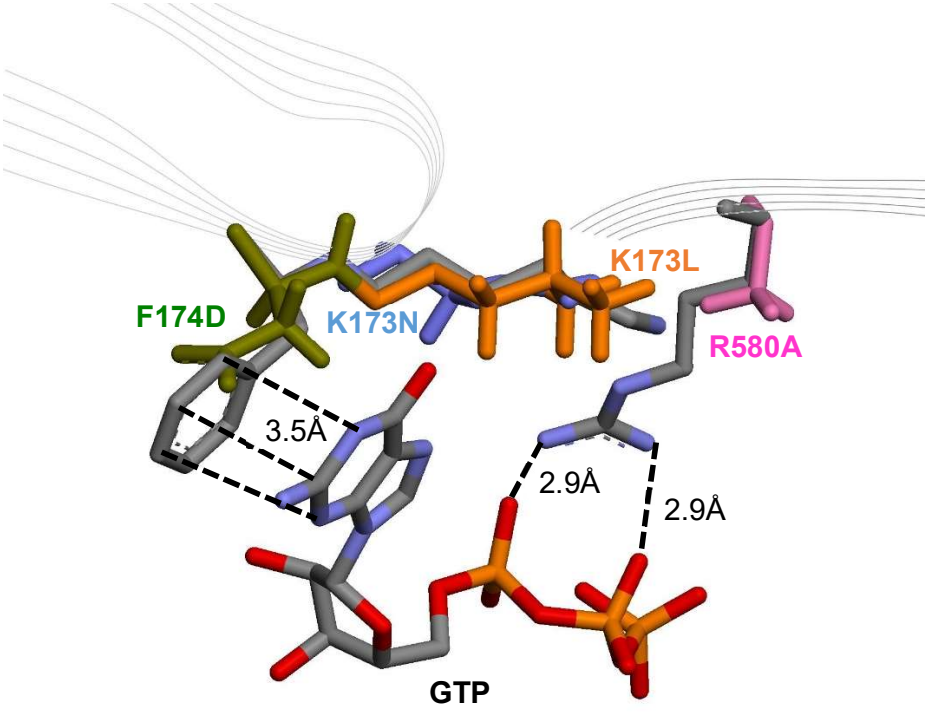

Fig. 4.2 Mutations in the GTP binding pocket used in this chapter. **The introduced amino acids are superimposed over original amino acids, shown as follows; D^{174} is in green, N^{173} is shown in blue, L^{173} is shown in orange and A^{580} is shown in pink. Carbons shown in grey, with nitrogens in blue, oxygens in red, and phosphate groups in orange. Potential hydrogen bonds are indicated with black dashed lines. Residues highlighted as being important in TG2-GTP binding by Liu et al and Jang et al (Liu *et al.* 2002; Jang *et al.* 2014) were arranged around a GTP molecule. Figure generated by Dr Konrad Beck and Professor Daniel Aeschlimann.**

4.2.2. Secretion of TG2 GTP binding site variants by HEK293-P2X7R cells

HEK293 cells expressing wild-type P2X7R were transiently transfected with expression vectors for TG2 GTP binding site variants. After 48h, P2X7R was stimulated with 0.1mM BzATP. Conditioned media were collected after 10 minutes of BzATP treatment, and again after a 30 minute chase period in the absence of BzATP. Western blotting of conditioned media showed that wild-type TG2 is secreted under these conditions as expected (6.6-fold increase over baseline in 10 minute pulse, 6.2-fold increase over baseline in 30 minute chase) (Fig. 4.3). TG2 $K^{173}N$ is also secreted, to a similar level as wild-type TG2, confirmed by densitometry (5.1-fold increase over baseline in 10 minute pulse, 3.1-fold increase over baseline in 30 minute chase,

repeated measures ANOVA and Tukey's post-hoc test $p>0.05$ in comparison to wild-type TG2 secretion) (Fig. 4.3). Conditioned medium from cells expressing TG2 $K^{173}L$ and TG2 $K^{173}N/F^{174}D$ collected after 10 minute pulse and 30 minute chase shows significantly decreased secretion of these in comparison to wild-type (TG2 $K^{173}L$; no increase over baseline at 10 minute pulse, 1.1% increase over baseline at 30 minute chase, TG2 $K^{173}N/F^{174}D$; 1.6% increase over baseline at 10 minute pulse, no increase over baseline at 30 minute chase, repeated measures ANOVA and Tukey's post-hoc test $p<0.05$ in comparison to wild-type TG2) (Fig. 4.3). $R^{580}A$ TG2 is not released in response to P2X7R stimulation, the secretion over 3 experiments was found to be significantly reduced in 10 minute pulse conditioned medium (repeated measures ANOVA and Tukey's post-hoc test $p<0.05$), and no bands were detected in 30 minute chase medium. (Fig. 4.3). These results indicate that either GTP binding and hydrolysis or the conformational change in TG2 upon GTP binding is required for TG2 secretion, therefore the exact nature of the interaction of GTP with these TG2 mutants needed further investigating.

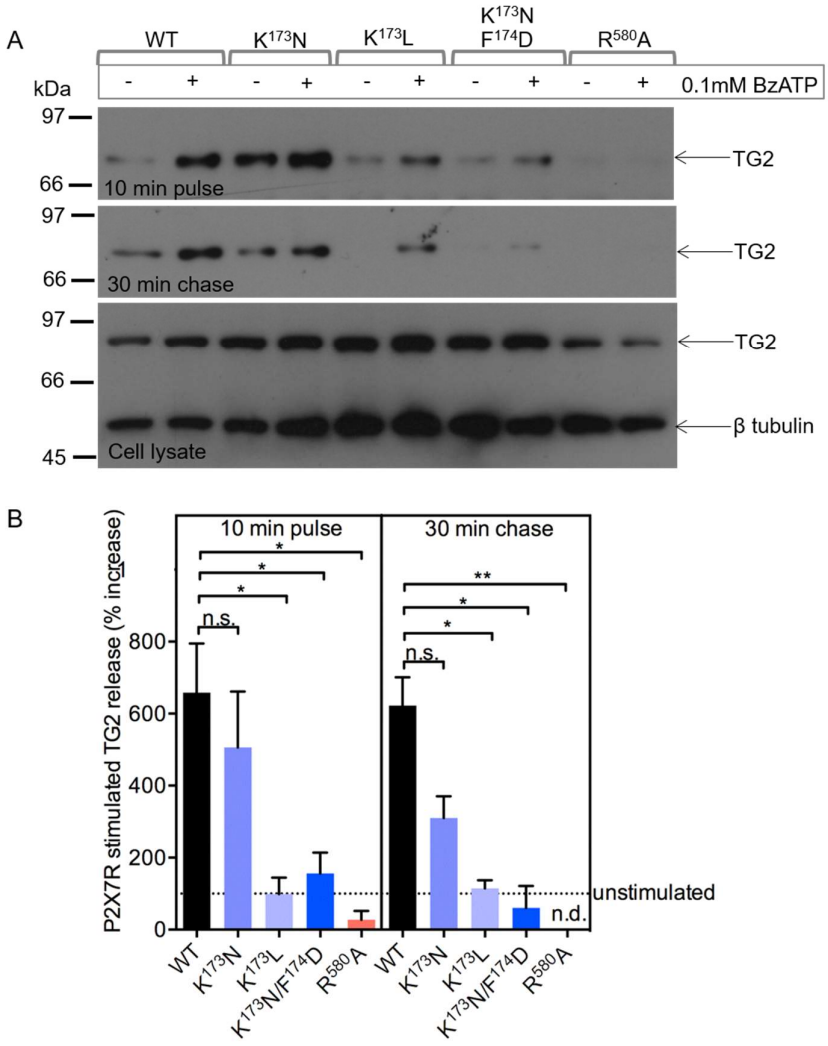

Fig. 4.3 Secretion of TG2 GTP binding site variants by HEK293 P2X7R cells. HEK293 P2X7R cells were seeded at a density of $1.2x10^5$ cells/well in a 24 well plate. After 24 hours, cells were transfected with TG2 variants. 48 hours later, cells were treated with 0.1mM BzATP or vehicle control in OptiMem for 10 minutes (pulse). The conditioned media were collected and cells were incubated for a further 30 minutes in OptiMEM without BzATP (chase) and conditioned media collected. Cell lysates were prepared at the end of the experiment to allow assessment of TG2 expression levels. 150µl of conditioned media (concentrated) or 10µg total protein for cell extracts were run for each sample on a 4-20% SDS PAGE gel under reducing conditions. Western blotting for TG2 (CUB7402, 200ng/ml) and β-tubulin (TUB2.1, 2.6µg/ml) was performed. A) Western blot result shown is representative of at least 3 independent experiments for each of the TG2 variants. B) Densitometry analysis was performed on each of the three experiments for each variant. Density of the bands was measured using Gel Doc EZ System and Image Lab software (BioRad) and the increase in TG2 secretion in BzATP stimulated cells calculated as a percentage increase relative to unstimulated cells expressing the same mutant. Data shown are mean ± SEM. Repeated measures ANOVA performed to test significance, followed by Tukey's post-hoc test n.s. = not significant, *p=<0.05, **p<0.005.

4.2.3. Expression and purification of TG2 GTP binding site variants

To enable biochemical analysis, TG2 GTP binding site variants were produced recombinantly in *E. coli* and purified using Ni^{2+} affinity chromatography followed by anion exchange chromatography. Protein purification was performed in parts by Shannon Turberville. SDS-PAGE gel analysis of purified proteins showed that the purification results in a highly pure TG2 preparation (Fig. 4.4 A). The intact His-tagged protein runs at an apparent molecular mass of 78kDa in line with what was reported by us and others previously (Hadjivassiliou *et al.* 2008). Bands that were not at the expected molecular weight for TG2 (smaller than 78kDa) have been assessed in our lab previously using mass spectrometry and were found to be degradation products of TG2. TG2 activity assays show that all the mutants were active, however both TG2 $K^{173}N/F^{174}D$ and TG2 $R^{580}A$ show substantially reduced activity in both transamidation (Fig. 4.4 B) and isopeptidase (Fig. 4.4 C) activity assays in comparison to wild type TG2. TG2 $K^{173}L$ shows a comparable level of activity to wild type in the transamidation assay, but shows reduced activity in the isopeptidase assay. The TG2 $K^{173}N$ mutant is either as active or more highly active than wild type TG2 in the respective assays. As these reactions were carried out in the presence of reducing agent, it appears unlikely that oxidative enzyme inactivation is the reason for this reduced activity observed for some mutants. It therefore appears that GTP-binding although controlling enzyme activity allosterically also has a role in keeping the enzyme in a conformation that allows for rapid activation through Ca^{2+}-binding. No changes in secondary structure were evident for TG2 $K^{173}N$, TG2 $K^{173}L$ and TG2 $K^{173}N/F^{174}D$ when compared to wild-type TG2 using circular dichroism spectroscopy (personal communication with Shannon Turberville), confirming that the overall fold of the protein is not disrupted by the mutations.

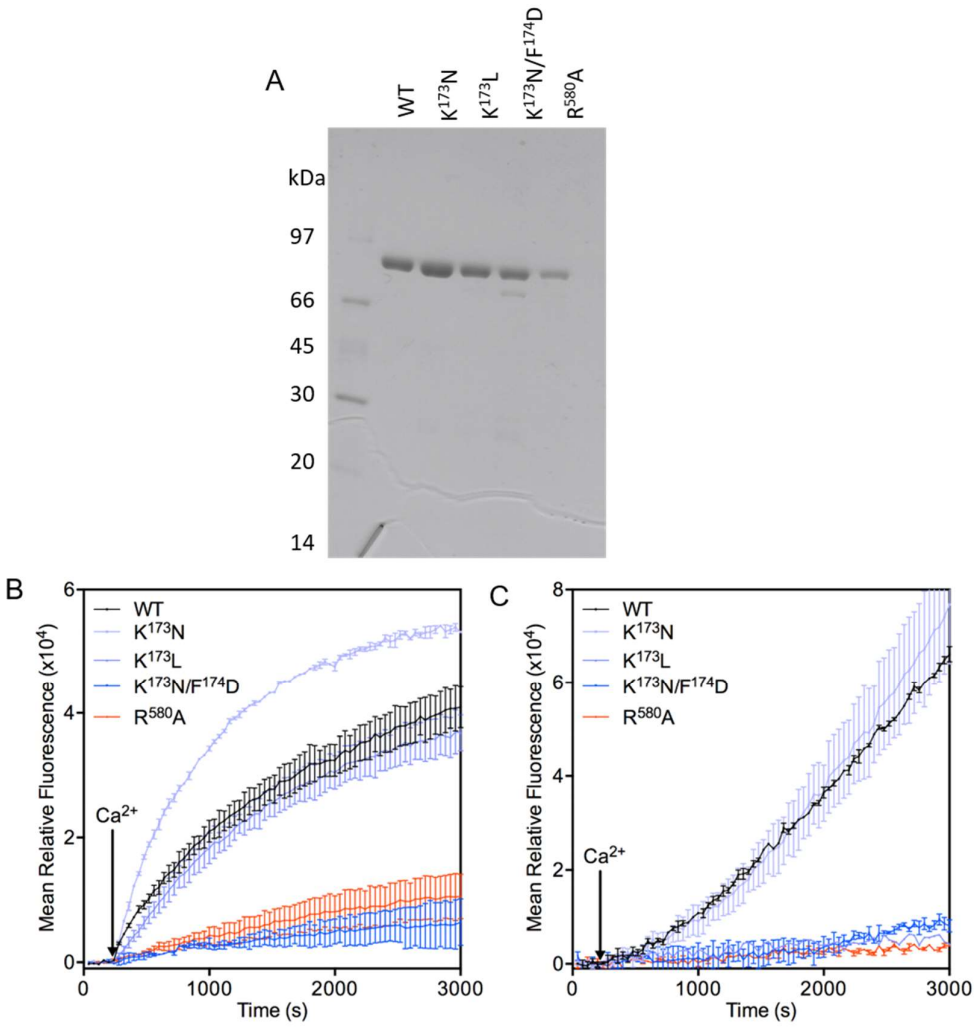

Fig. 4.4 Characterisation of purity and activity of preparations of TG2 variants.

A) 1µg purified protein for each of the TG2 variants were run on a 4-20% SDS PAGE gel under reducing conditions, then stained using Coomassie brilliant blue R. B) Transamidation activity of TG2 variants (20µg/ml) was assessed by MDC incorporation assay. Fluorescence as a result of monodansylcadaverine incorporation into N,N-dimethylcasein was measured for 1 hour (excitation 320-10nm, emission 520-10nm). The reaction was initiated by injection of Ca^{2+} (2mM, arrow); data are the mean of 2 wells ± SD, and representative of 2 independent experiments. C) Isopeptidase activity of TG2 variants (20µg/ml) was assessed by measuring the fluorescence increase as a result of cleavage of the intramolecularly quenched A102 substrate for 1 hour (excitation 320-10nm, emission 440-20nm) as previously described (Adamczyk *et al.* 2013). Data are the mean of 2 wells ± SD, and representative of 2 independent experiments.

4.2.4. Regulation of the conformation and activity of TG2 variants by GTP

The conformational change that occurs on GTP binding can be seen by running TG2 variants on a native PAGE gel, whereby the compact conformation of the GTP-bound enzyme produces a faster migrating species (Murthy *et al.* 1999). The shift in mobility of the detected species is clear when wild type TG2 is assessed in the presence or absence of an excess of GTP, where the absence of GTP gives a less mobile band ('open' conformation of TG2) (Fig. 4.5 A) and the presence of GTP gives a more mobile band ('closed' conformation of TG2) (Fig. 4.5 B). However, enhanced migration is in parts due to the additional negative charges of the TG2-GTP complex. This shift is also seen for the TG2 $K^{173}N$ and TG2 $K^{173}L$ mutants, showing that GTP binding still induces a conformational change in these mutants. With the TG2 $K^{173}L$ mutant, however, the proportion of protein in the GTP-bound state appears to be reduced in comparison to wild-type TG2. This suggests the apparent binding affinity of this mutant for GTP is lower. TG2 $K^{173}N/F^{174}D$ and TG2 $R^{580}A$ do not show the shift in band position seen in wild-type TG2. This suggests that these mutants were not capable of binding GTP, or that GTP binding does not induce the conformational change from open to closed conformation.

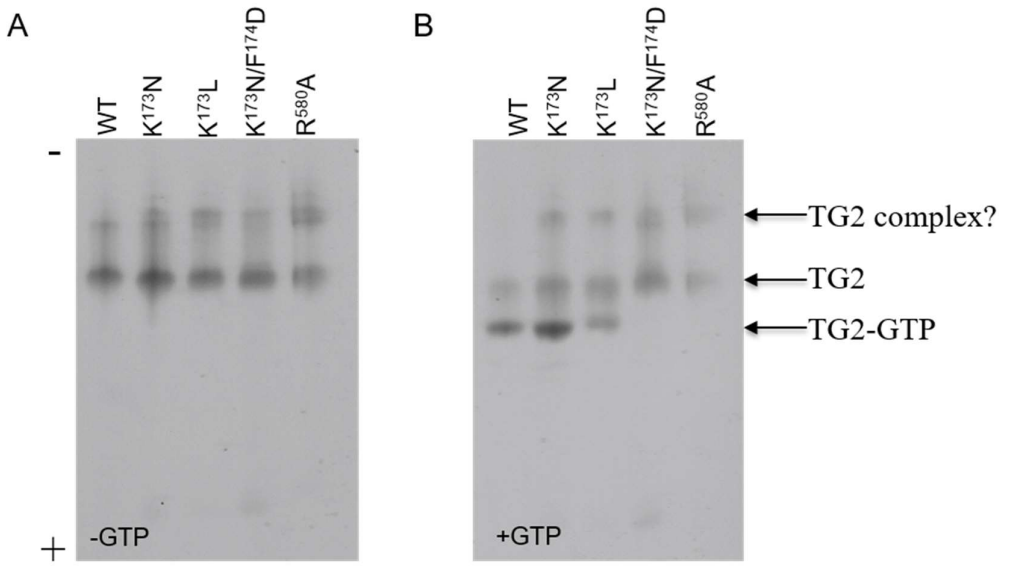

Fig. 4.5 Analysis of GTP binding of TG2 variants using native PAGE. A) For native PAGE, TG2 variants (4µg) were run on a 10% tris-glycine gel under native conditions at 100V, 35mA for 3 hours on ice (cathode and anode use indicated). Gels were stained using Coomassie brilliant blue R. B) TG2 variants were incubated with 25µM GTP for 10 minutes, then gels run as in A but in the presence of 25µM GTP.

The influence of GTP binding on transamidation activity of TG2 mutants was assessed by isopeptidase assay, as described in section 4.2.3. The assay was carried out in the presence of a GTP concentration series (0.25µM to 600µM). Our laboratory has previously shown that the apparent K_d of wild-type TG2 for GTP using this assay is 2.9µM (Adamczyk *et al.* 2013). The isopeptidase activity assay showed that the activity of the TG2 $R^{580}A$ mutant was not inhibited, even at high levels of GTP (600µM) (Fig. 4.6). The TG2 $K^{173}N/F^{174}D$ mutant had a significantly shifted K_D in comparison to wild type TG2 (K_D>600µM, TG2 wild-type K_D=22 ± 4µM), indicating a much reduced affinity for GTP. The TG2 $K^{173}N$ (K_D=41 ± 14µM) and TG2 $K^{173}L$ (K_D=26 ± 24µM) mutants showed comparable sensitivity to GTP inhibition in comparison to wild-type TG2 (K_D=22 ± 4µM), indicating that these mutations do not have very large effects on apparent GTP binding. Taken together with results on specific activity in isopeptidase assay and native PAGE analysis, this could indicate that only a fraction of the $K^{173}L$ is in a conformation competent to bind GTP.

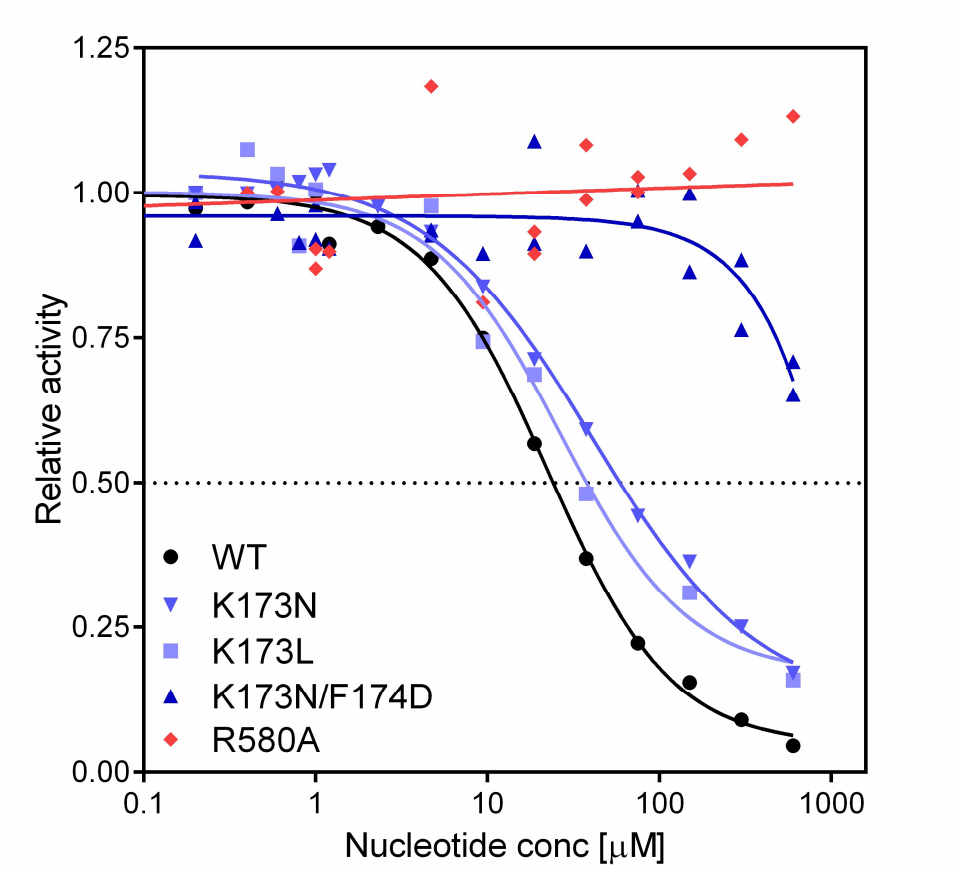

Fig. 4.6 Apparent binding affinity of TG2 variants for GTP. Isopeptidase activity of TG2 variants was measured as in fig. 4.4 in the presence of GTP from 0μM to 600μM. The control curve (TG2 with no Ca^{2+}) was subtracted to account for time dependent fluorescence bleaching. Reaction rates were then derived by linear regression (From 1000 seconds to 2500 seconds). Data shown are the mean of two wells. Data were fitted with a sigmoidal dose response curve ($Y=Y_{min}+(Y_{max}-Y_{min})/1+10^{(logEC50-X)}$) to allow the apparent K_D to be determined (half maximal inhibition).

The results outlined here show that either GTP binding or hydrolysis or the conformational change in TG2 that occurs on GTP binding is essential for TG2 secretion. The release of the TG2 $K^{173}N$ mutant being similar to wild-type TG2 suggests that it is GTP binding that is essential for efficient TG2 secretion as opposed to GTP hydrolysis, as the binding of GTP by TG2 $K^{173}N$ is similar to wild-type TG2, the hydrolysis of GTP, however, has been reported to be reduced in TG2 $K^{173}N$ in comparison wild-type TG2 (Datta *et al.* 2007). The mutants TG2 $K^{173}L$, $K^{173}N/F^{174}D$ and $R^{580}A$ show substantially reduced release, with the release of TG2 $K^{173}N/F^{174}D$ and TG2 $R^{580}A$ being indistinguishable from background. It has been reported that the

TG2 $R^{580}A$ mutant does not form the closed conformation when GTP is present using analytical centrifugation (Iismaa *et al.* 2000). This is consistent with the results from the native PAGE analysis carried out here. Taken together, this suggests that the conformational change induced by GTP is important for TG2 release.

4.2.7. Is thioredoxin-1 secreted via the same pathway as TG2 and facilitating TG2 export?

Extracellular TG2 is likely to adopt the open conformation due to Ca^{2+} binding as the concentration of Ca^{2+} is higher extracellularly and nucleotide concentration low, in parts due to active hydrolysis by ectonucleotidases. However, extracellular TG2 has been found to be predominantly in an inactive state. This is due to rapid oxidation resulting in disulphide bond formation at two vicinal cysteine residues (Stamnaes *et al.* 2010). A disulphide bond forms initially between C^{230} and C^{370}, which can convert into a disulphide bond between C^{370} and C^{371} (Fig. 4.9). Thioredoxin-1 has been suggested to reactivate oxidized enzyme by reducing the disulphide bond between C^{370} and ^{C371} (Jin *et al.* 2011). Hence, the question arises whether thioredoxin-1 interacts with TG2 intracellularly and is either co-secreted with TG2 or even mechanistically linked into the export process.

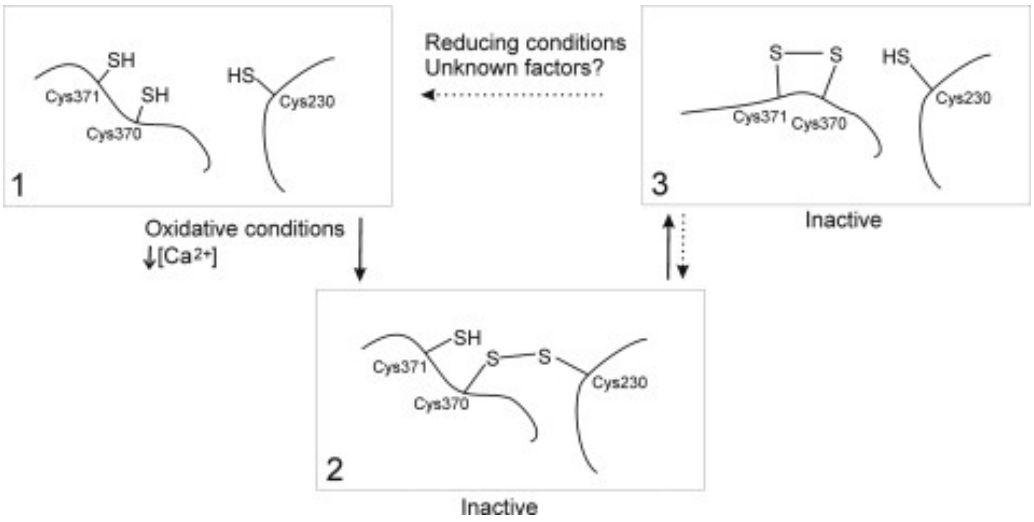

Fig. 4.9 Schematic of the oxidation of TG2 leading to its inactivation. The 'unknown factors' acting on inactive TG2, reducing the disulphide bond (shown in step 3) is likely to be thioredoxin-1 (Stamnaes *et al.* 2010) as subsequently demonstrated (Jin *et al.* 2011).

4.2.8. P2X7R activation leads to thioredoxin-1 secretion

As thioredoxin-1 is an unconventionally secreted protein with an important role in activating TG2 extracellularly, the potential for it to be secreted through the same pathway as TG2 was investigated initially. HEK293 P2X7R cells were stimulated with 0.1mM BzATP and conditioned media collected after 10 minutes of stimulation and a further 30 minute chase period in the absence of BzATP. Western blotting was performed and membranes were probed for thioredoxin-1. Thioredoxin-1 was found to be secreted in response to activation of the P2X7R, either in the absence of TG2 expression (Fig. 4.10 A) or in the presence of TG2 following transient transfection (Fig. 4.10 B). This shows that thioredoxin-1 export can be triggered through activation of P2X7R, and that this occurs independent of TG2.

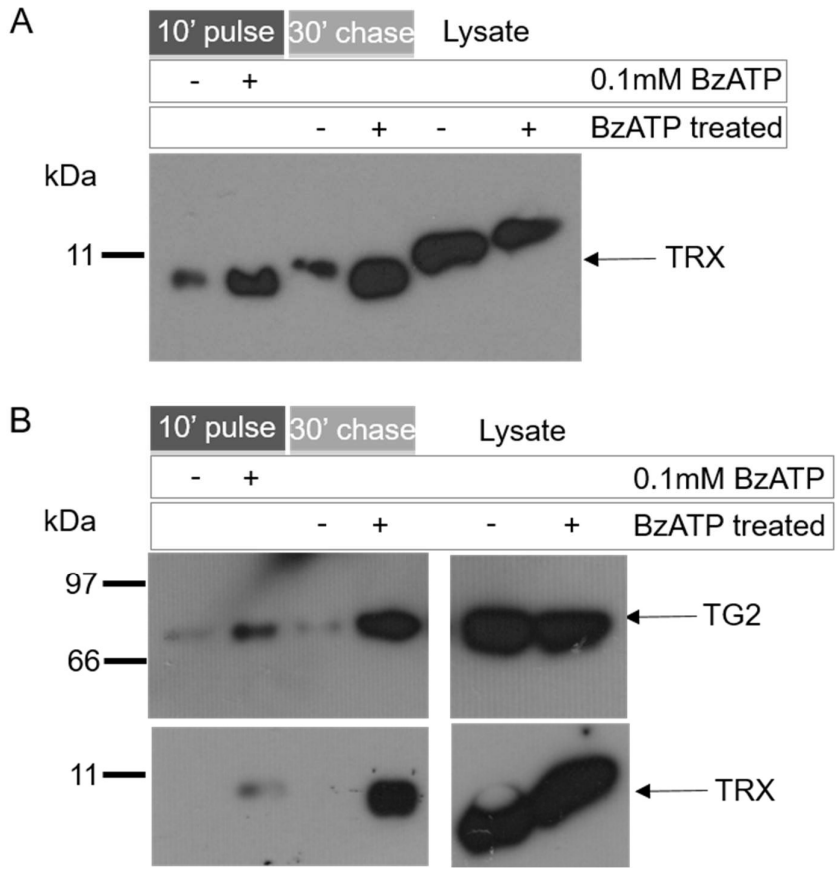

Fig. 4.10 Thioredoxin-1 release in response to P2X7R activation in the presence and absence of TG2 expression. A) HEK293 P2X7R cells were treated with 0.1mM BzATP or vehicle control in OptiMEM for 10 minutes. The conditioned media were collected and cells were further incubated for 30 minutes in OptiMEM without BzATP. Conditioned media were collected and cells lysed to allow assessment of TG2 expression levels. 400µl of concentrated conditioned media or 10µg total protein from lysate Were applied for each sample on a 16% tricine SDS-PAGE gel under reducing conditions. Samples were then subjected to Western blotting for thioredoxin-1 (TRX) (FL-105, 1µg/ml). Result shown is representative of 3 independent experiments. B) Experiments were conducted as in A, except that cells were transiently transfected with TG2 expression construct 48 hours prior to experiment. Western blotting for TG2 was performed by loading 150µl of concentrated conditioned media or 10µg total protein from cell lysate on a 4-20% SDS-PAGE gel under reducing conditions. Western blotting for TG2 (CUB7402, 200ng/ml) was performed. Analysis of samples for thioredoxin-1 was carried out as in A. Result shown is representative of 3 independent experiments.

4.2.9. Thioredoxin-1 secretion does not require P2X7R ion channel activity

To further investigate whether thioredoxin-1 is secreted by the same process as TG2, involving the same state of receptor activation (likely to be membrane pore formation), the involvement of the P2X7R ion channel or a membrane pore formed by pannexin-1 were investigated. In the presence of the pannexin-1 inhibitor, trovafloxacin, as described previously, thioredoxin-1 is still released from cells (Fig. 4.11 A). This suggests that pannexin-1 is not involved in thioredoxin-1 release, as I have already shown for TG2 release in HEK293 cells expressing P2X7R in the previous chapter.

Calmidazolium has previously been demonstrated to act as a P2X7R ion channel blocker, without affecting P2X7R membrane pore formation (Virginio *et al.* 1997). In the presence of calmidazolium, thioredoxin-1 release was unaffected (Fig. 4.11 B). We have previously shown that calmidazolium at this concentration blocks the increase in intracellular Ca^{2+} normally occurring upon P2X7R activation (Adamczyk 2013; Adamczyk *et al.* 2015). This shows that thioredoxin-1 release does not require ion channel activity which is in line with our findings for TG2 secretion. These results therefore suggest that the pathway for thioredoxin-1 release by P2X7R activation may be the same as that for TG2.

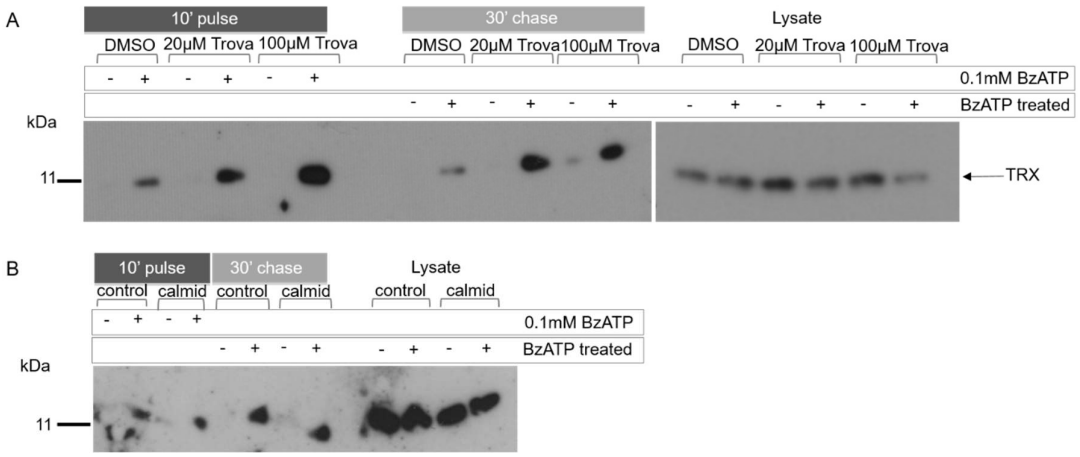

Fig. 4.11 Thioredoxin-1 release in the presence of pannexin-1 inhibitor or P2X7R ion channel blocker. Thioredoxin-1 release was investigated as in fig. 4.10, except that in A) cells were pre-treated with 20μM or 100μM trovafloxacin (trova, pannexin-1 inhibitor) for 30 minutes and trova was present at all times during the experiment. Result shown is representative of three independent experiments. B) Thioredoxin-1 release was investigated as before, but for this experiment cells were pre-treated with 1μM calmidazolium chloride for 10 minutes and calmidazolium was present at all times during the experiment. Result shown is representative of two independent experiments.

4.2.10. Is TG2 secretion prevented by thioredoxin-1 inhibition?

As thioredoxin-1 may be secreted via the same pathway as TG2, it is possible that it has a functional role in TG2 secretion. To assess whether TG2 secretion requires thioredoxin-1 activity, its secretion in the presence of two thioredoxin-1 inhibitors was assessed. Firstly, DNCB (1-Chloro-2,4-dinitrobenzene) is an intracellularly acting irreversible inhibitor of thioredoxin reductase (TRXR) (Arner *et al.* 1995; Rothmeier *et al.* 2015). TRXR catalyses reduction of oxidised thioredoxin-1 by NADPH, forming the SH_2 form of thioredoxin-1, which can act as a protein disulphide reductase. DNCB acts through inactivating the selenocysteine of TRXR with high specificity, when low concentrations of DNCB were used (low μM) (Fig. 4.12) (Arner *et al.* 1995). Secondly, PX12 is a specific, extracellularly acting thioredoxin-1 inhibitor, which binds irreversibly to thioredoxin-1 and inactivates it by oxidising vicinal thiols in thioredoxin-1 and competing with binding to TRXR (Kirkpatrick *et al.* 1998; Rothmeier *et al.* 2015) (Fig. 4.12).

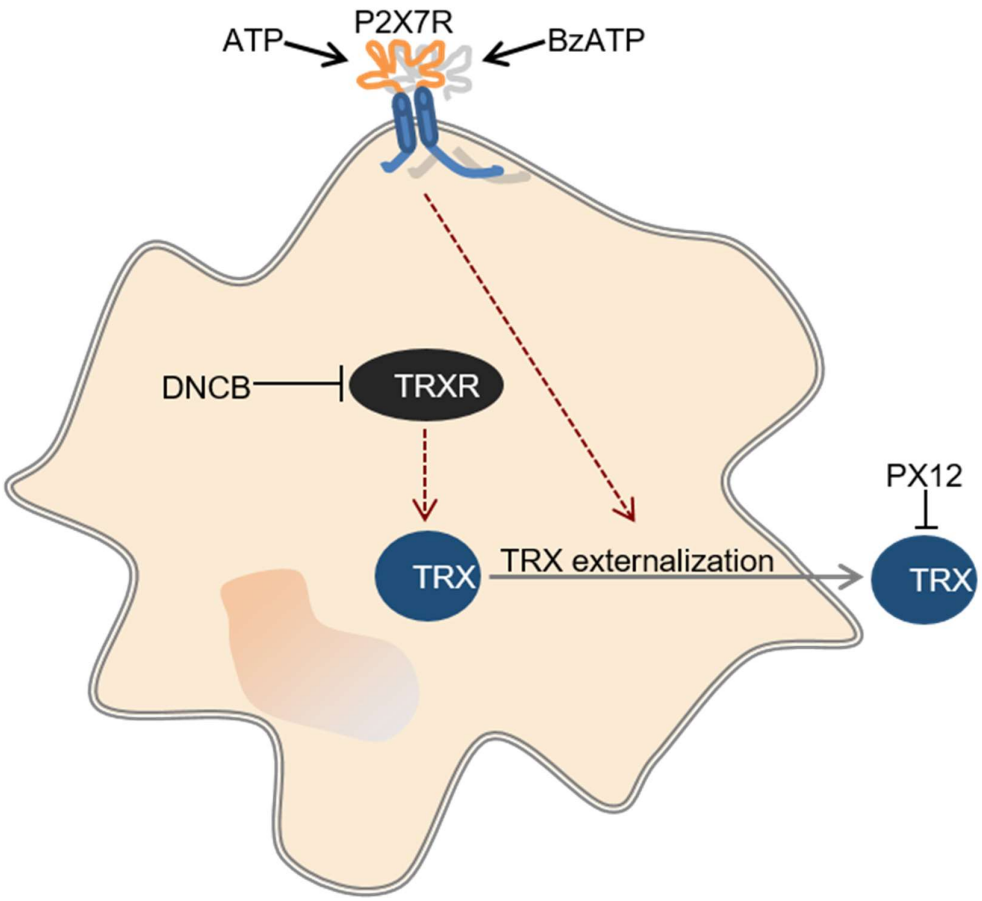

Fig. 4.12 Inhibition of thioredoxin-1 by DNCB and PX12. DNCB is capable of penetrating cells and inhibits TRXR, preventing activation of thioredoxin-1 (TRX). PX12 directly inhibits thioredoxin-1, and is not thought to be cell permeable.

TG2 and thioredoxin-1 release were investigated in the presence of these two thioredoxin-1 inhibitors. Inhibitor concentrations were chosen based upon those previously reported to specifically inhibit thioredoxin-1 activity (Rothmeier *et al.* 2015). When DNCB was present only during the pre-incubation period, there was no apparent inhibition of TG2 secretion (Fig. 4.13 A). Therefore, the experiment was repeated but with DNCB present at all times during the experiment (Fig. 4.13 B). Given that thioredoxin plays a critical role in maintaining the redox potential within the cytoplasm of the cell the concern was that extended inhibitor treatment could lead to cell death. Therefore, I decided to investigate caspase-3 activation. Caspase-3 activation requires processing, which results in 17 and 19kDa products and this can indicate that the cells are undergoing apoptosis. Cells treated with DNCB throughout the experiment were not found to have caspase-3 activation, either when analysed at

the end of the experiment (Fig. 4.13 B), indicating that the treatment is not causing cell death. Although some variation in TG2 secretion was seen between experiments, there was no clear dose-dependent reduction and it was apparent that DNCB does not appear to completely or effectively inhibit TG2 secretion. PX12 present at all times during the experiment, did not have any inhibitory effect on TG2 secretion. Unexpectedly, neither of these inhibitors were found to prevent thioredoxin-1 secretion, suggesting that its release was not dependent on its activity (Fig. 4.13 C).

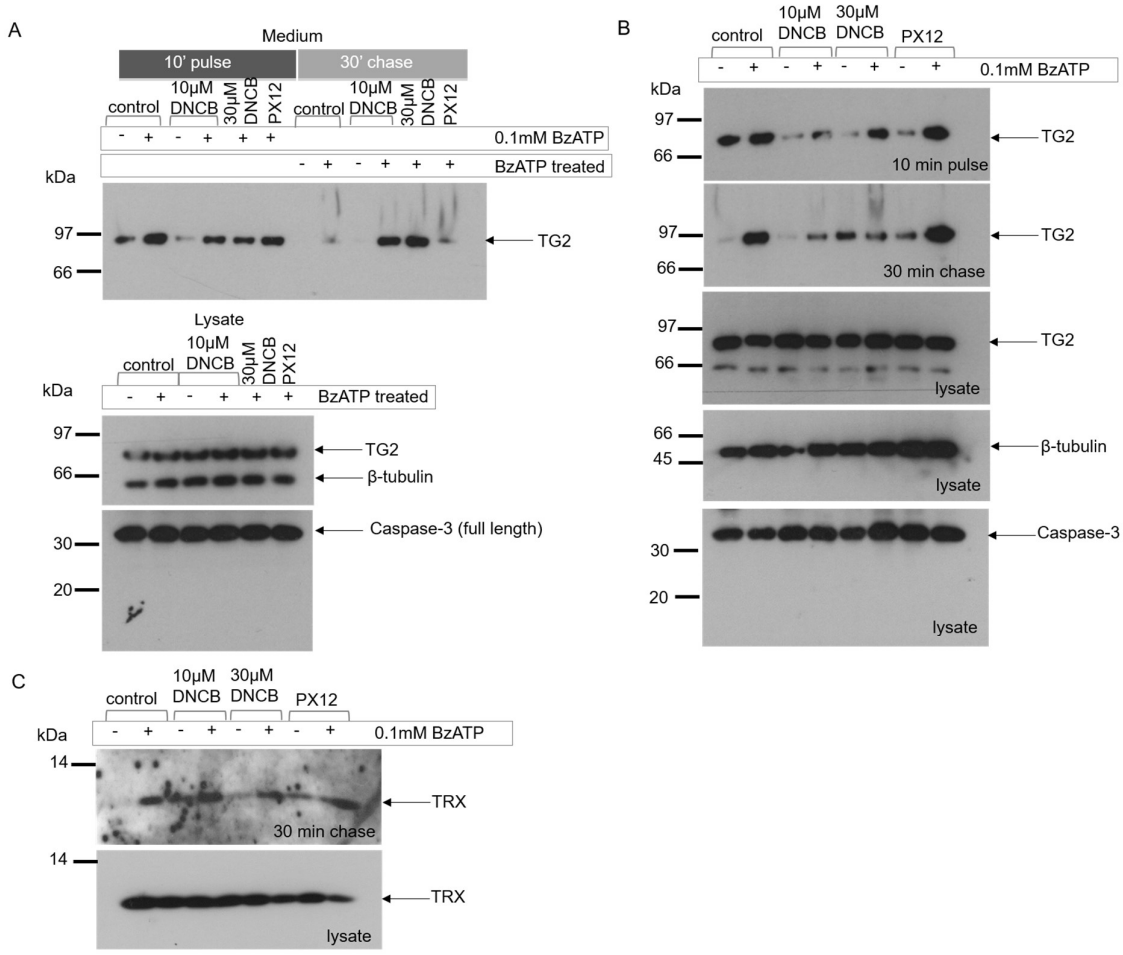

Fig. 4.13 TG2 secretion in the presence of thioredoxin-1 inhibitors. TG2 and thioredoxin-1 secretion experiments were performed as described in fig. 4.10 B, except that in A) cells were pre-treated with 10μM or 30μM DNCB or 50μM PX12 for 30 minutes, where indicated. 400μl of concentrated conditioned medium or 10μg total protein from lysate was applied for each sample on a 4-20% tris-glycine SDS-PAGE gel under reducing conditions. Samples were then subjected to Western blotting and membranes probed for TG2 (CUB7402, 200ng/ml), β-tubulin (TUB2.1, 2.6μg/ml), and caspase-3 (9662, 0.04μg/ml). Result is representative of two independent experiments. B) Experiment was performed as in A, except that inhibitors were present at the same concentrations for both the pre-treatment indicated as well as during the 10 minute pulse and 30 minute chase periods. Result is representative of two independent experiments. C) Experiment was performed as in A, with Western blotting performed for TRX (FL-105, 1μg/ml). Result is representative of two independent experiments.

4.3. Discussion

To assess whether GTP binding, hydrolysis or a conformational change in TG2 is required for TG2 secretion, mutations of residues involved in GTP binding were introduced into TG2. These TG2 variants were expressed in HEK293 cells expressing P2X7R and their secretion in response to P2X7R activation by BzATP was assessed (by Western blotting). The variants were also recombinantly produced in *E. Coli* in mg quantities, allowing biochemical analysis of the effect of the mutations on protein folding, TG2 activity, and interaction GTP. Wild type TG2 was confirmed to be secreted by P2X7R activation in HEK293 cells. Wild type TG2, expected to be GTP-bound intracellularly, is capable of GTP hydrolysis. Conformational changes in TG2, associated with GTP binding or hydrolysis, or the energy released from GTP hydrolysis could play a role in the protein export process.

TG2 $K^{173}N$ was found to be released from HEK293 cells on P2X7R activation to a similar level to wild type TG2. This variant is known to have a similar level of activity to wild type TG2 (Datta *et al.* 2007) and the inhibition of activity by GTP is also not thought to be significantly different to wild type TG2 (Iismaa *et al.* 2000; Datta *et al.* 2007). In my experiments, the activity of this mutant was confirmed to be moderately increased or similar to wild-type TG2 in transamidation and isopeptidase assays, respectively, confirming protein functionality. Native PAGE analysis of TG2 $K^{173}N$ in the absence and presence of GTP showed the shift of conformation in response to GTP. This indicates that this conservative amino acid substitution does not significantly affect the interaction with GTP, possibly also explaining why the release from HEK293 cells is unaffected. It has, however, been shown previously that TG2 $K^{173}N$ has a significantly reduced capacity to hydrolyse GTP (Datta *et al.* 2007). As this TG2 mutant is still secreted from HEK293 cells, this suggests that GTP hydrolysis may not be important for TG2 secretion.

TG2 $K^{173}L$ gave reduced P2X7R-mediated release in comparison to wild type TG2 in our HEK cell model. This is in line with the prior observation that TG2 $K^{173}L$ was not secreted by chondrocytes (without stimulation) (Johnson and Terkeltaub 2005). TG2 $K^{173}L$ has a similar level of transamidation activity to wild type TG2, in agreement with data published regarding this mutant (Johnson and Terkeltaub 2005). Likewise, my data showed that the apparent affinity for GTP regulation of TG2 $K^{173}L$ is

comparable to wild type TG2. However, this data is in contradiction to published data, which suggests that the inhibition of transamidation activity by GTP is reduced in this mutant (A 6-fold increase in IC_{50} in comparison to wild-type TG2, fig 4.6) (Iismaa *et al.* 2000). TG2 $K^{173}L$ showed a shift in conformation in response to GTP in the native PAGE analysis, however, there appears to be a reduction in the proportion of the enzyme that shifts in comparison to wild type TG2. This could suggest that GTP binding affinity is reduced in this mutant, which is supported by published work (Iismaa *et al.* 2000), but is not consistent with my own work from the isopeptidase assay. Alternatively, the enzyme may exist in a conformation that can rapidly bind GTP and one with low affinity for GTP. My data would be consistent with such an interpretation and a shift in the prevalence of the respective conformations with TG2 $K^{173}L$ towards the conformation that is not or only weakly interacting with GTP could explain my results (Fig. 4.14). These data, alongside the TG2 $K^{173}N$ data, further indicate that GTP binding or the conformational change induced by GTP binding play a role in TG2 secretion, as the TG2 $K^{173}L$ mutant shows reduced, but not completely abolished, release by cells.

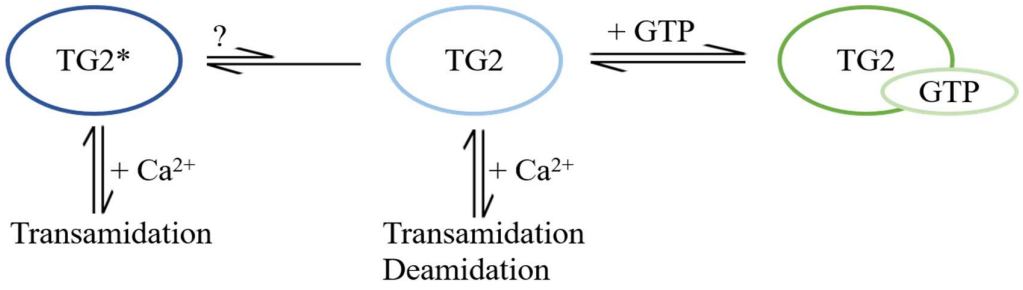

Fig. 4.14 Schematic for proposed model of TG2 $K^{173}L$ conformational states. In contrast to wild-type TG2, TG2 $K^{173}L$ adopts preferentially a state (TG2*) that is not capable of binding GTP or convert directly into the 'open conformation' that is necessary for binding of a crosslinked substrate and TG2 $K^{173}L$ therefore lacks isopeptidase activity.

To investigate this further, the TG2 $K^{173}N/F^{174}D$ mutant was generated and was demonstrated to have negligible release in response to P2X7R activation in comparison to wild type TG2. This mutant has a significantly shifted GTP inhibition curve in comparison to wild type TG2, requiring a high concentration of GTP for inhibition (K_D >0.6mM for K173N/F174D, approx. 20µM for wild type TG2, fig 4.6). Enzymatic activity of TG2 $K^{173}N/F^{174}D$ is substantially reduced in comparison to wild

type TG2. Although no structural differences were seen using circular dichroism spectroscopy (personal communication with Shannon Turberville), which confirms folding of the protein, this indicates that minor conformational changes in the respective loop are deleterious for enzyme function. Furthermore, the conformational change in response to GTP cannot be shown in native PAGE with this mutant suggesting that no stable GTP-bound species is formed. These data, alongside the TG2 $K^{173}N$ and TG2 $K^{173}L$ data strongly suggest that the conformational change associated with GTP-binding is required for TG2 secretion.

Finally, a mutation ($R^{580}A$) previously suggested to prevent GTP binding but located within a different part of the protein (β barrel 2) was introduced into TG2 (Begg *et al.* 2006b; Datta *et al.* 2007). TG2 $R^{580}A$ had significantly reduced activity in comparison to wild type TG2, which was also found *in vitro* by another group (Ruan *et al.* 2008). However, it has also been suggested that this mutation results in increased TG2 activity compared to wild-type TG2 when expressed in cells, possibly due to activity regulation being uncoupled from GTP inhibition and consequently sensitive to small changes in intracellular Ca^{2+} (Begg *et al.* 2006b; Ruan *et al.* 2008). It has also been shown that this mutation prevents any inhibition by GTP (Datta *et al.* 2007), whichI was also able to similarly demonstrate here. Native PAGE showed that TG2 $R^{580}A$ does not show a shift in conformation in the presence of GTP. It has been suggested that $R^{580}A$ mutation could destabilise the compact conformation (Begg *et al.* 2006a), resulting in the open conformation being more likely to be present. Importantly, TG2 $R^{580}A$ is not released by HEK293 cells on P2X7R activation, confirming that the conformational change in TG2 associated with GTP-binding is required for TG2 secretion.

The two TG2 mutants that were both not released in response to P2X7R activation, $K^{173}N/F^{174}D$ and $R^{580}A$, both show reduced TG activity. Previous experiments in our lab using the catalytically inactive active site mutant TG2 $C^{277}S$ have demonstrated that TG2 activity is not required for TG2 release (Adamczyk 2013; Adamczyk *et al.* 2015). This indicates that the lack of release of these mutants is unlikely to be due to the reduced activity of TG2 *per se*, and should therefore be as a result of altered interactions with GTP.

Taken together, the results with these TG2 mutants suggest that GTP hydrolysis is likely not essential for TG2 secretion, due to the fact that variants with mutations at K^{173}, previously shown to have reduced GTP hydrolysis can be released by cells. However, these results also suggest that GTP binding may play a role in TG2 secretion, as mutations resulting in decrease of GTP binding affinity also result in reduced TG2 release. TG2 $R^{580}A$ and $K^{173}N/F^{174}D$ were both not released on P2X7R activation, and both do not show a conformational change in the presence of GTP. This suggests that this conformational change is required for TG2 secretion. This is consistent with prior work, demonstrating that the $Y^{274}A$ mutation, which affects a peptide bond near to the active site thereby affecting the conformation of the enzyme in this region shows greatly reduced secretion (Balklava *et al.* 2002).

To further investigate whether regulation of TG2 activity is linked to the export process, the release of thioredoxin-1 by the same mechanism of release as TG2 was examined. In parallel with our work in HEK cells (Adamczyk *et al.* 2015), It has been demonstrated that thioredoxin-1 can be released upon P2X7R activation by mouse macrophages (Rothmeier *et al.* 2015) lending further insight into the potential importance of this unconventional protein export pathway in the context of inflammation. The work performed here extends these findings and shows that although being a regulator of TG2 activity, thioredoxin-1 release can occur independently of TG2 expression, therefore an interaction between TG2 and thioredoxin-1 is not required for thioredoxin-1 secretion to occur.

To assess whether the pathway for thioredoxin-1 release is the same pathway as that for TG2 export, I employed inhibitors of specific functions of the P2X7R. Using an inhibitor of pannexin-1, a possible pore-forming component linked to P2X7R activation, I did not see a reduction in thioredoxin-1 secretion. However, as already discussed in the previous chapter, this inhibitor also did not affect TG2 secretion or membrane pore formation per se in HEK293 cells, and hence this result was expected. I also did not see a reduction in thioredoxin-1 release when cells were treated with calmidazolium, a blocker of the P2X7R ion channel (Virginio *et al.* 1997). This is also in agreement with our TG2 secretion data. Preliminary experiments using HEK293 cells expressing the P2X7R, $A^{348}T$, that displays enhanced pore formation, suggest that there is increased release of thioredoxin-1 by these cells in comparison to cells

expressing wild type P2X7R, as with TG2. Taken together, these results show that thioredoxin and TG2 export is linked to P2X7R and suggest that thioredoxin-1 and TG2 may be secreted via the same pathway. Published data also suggests that thioredoxin-1 is secreted in free-protein form and not in microvesicles (Rothmeier *et al.* 2015), as we have also shown for TG2 (Adamczyk 2013; Adamczyk *et al.* 2015), again suggesting that both proteins could be secreted by the same pathway. This is an important finding because thioredoxin-1 plays a role in the activation of TG2 extracellularly. The release of both TG2 and thioredoxin-1 by the same pathway would give an increased activity of TG2 extracellularly, in a localised manner, consistent with these proteins playing a role in immune functions and associated inflammatory responses (Arner and Holmgren 2000; Iismaa *et al.* 2009).

To investigate whether thioredoxin-1 activity is required for TG2 secretion, thioredoxin-1 inhibitors, DNCB and PX12, were used. It has previously been shown that both of these inhibitors can prevent thioredoxin-1 secretion, despite having different mechanisms of thioredoxin-1 inhibition (Rothmeier *et al.* 2015). DNCB is capable of entering the cell and preventing thioredoxin-1 activation by thioredoxin-1 reductase (Arner *et al.* 1995; Rothmeier *et al.* 2015). PX12 on the other hand, should not be capable of entering the cell, and the thioredoxin-1 inhibition will therefore occur extracellularly (Rothmeier *et al.* 2015). Treatment of cells with either of these inhibitors did not result in blocking of TG2 export. However, I could also not verify blocking of secretion of thioredoxin itself that was previously reported for mouse macrophages (Rothmeier *et al.* 2015). The reason for this remains unclear but may relate to different cell types being used.

Chapter 5

5. Do primary human macrophages release TG2 in response to P2X7R stimulation?

5.1. Introduction

All of the previous work in this thesis was performed in HEK293 cells as a 'clean' system, lacking endogenous P2 receptor or TG expression. To confirm that the mechanism outlined in these cells was relevant in a more physiological system, I decided to use primary human macrophages. TG2 appears to have important roles in immunity, and has been shown to be expressed and active in macrophages (Hodrea *et al.* 2010). In macrophages, TG2 is present extracellularly at the surface of the cell, where it may have a role in inflammatory disease, for example in coeliac disease (Hodrea *et al.* 2010). Cell surface TG2 may be involved in the generation of the immunogenic peptides. Furthermore, TG2 in macrophages has also been shown to be involved in cell migration, through an interaction with syndecan-4, and apoptotic cell clearance, through an interaction with CD44 (Nadella *et al.* 2015). In support of this, cells from $TG2^{-/-}$ mice still perform apoptosis, but there is decreased clearance of these cells, due to reduced phagocytosis by macrophages (Szondy *et al.* 2003). These functions of TG2 highlight an important role for extracellular TG2 in inflammatory processes, indicating that TG2 secretion from immune cells, such as macrophages, is required for proper resolution of inflammation.

P2X7R is widely expressed, with some of the highest levels of expression being on haematopoietic cells (Idzko *et al.* 2014). Macrophages have been shown to express the highest levels of P2X7R, followed by dendritic cells, monocytes, natural killer cells, B lymphocytes, T lymphocytes and erythrocytes (Gu *et al.* 2000). Macrophages also express other purinergic receptors, including P2Y receptors, P2X1, P2X4 and P2X5 (Idzko *et al.* 2014). Purinergic receptors can be activated during the immune response due to the release of nucleotides from many different cell types (Idzko *et al.* 2014). This release can occur due to cell death, for example necrosis (where the intracellular components of damaged cells are released into the extracellular environment) (Hotchkiss *et al.* 2009) or apoptosis (Chekeni *et al.* 2010), through activation of inflammatory cells (Eltzschig *et al.* 2006; Chekeni *et al.* 2010) or mechanical damage, such as shear stress (Wan *et al.* 2008). When inflammatory cells, for example neutrophils, are activated, ATP can be secreted through a pathway involving either

connexins (Eltzschig *et al.* 2006) or pannexins (Chekeni *et al.* 2010). This extracellular ATP can then activate purinergic receptors, one effect of which is to attract phagocytic cells to sites of tissue damage (McDonald *et al.* 2010).

The P2X7R has been shown to be important for the immune response and is involved in several steps of the process, including active cytokine production through activation of the NALP3 inflammasome following NF-κB activation (Ferrari *et al.* 1997), leading to transcription of cytokine genes (Mariathasan *et al.* 2006). In macrophages, the pathway for IL-1β secretion has been well characterised, and has been shown to involve activation of both TLR and P2X7R (Netea *et al.* 2009). The NALP3 inflammasome includes the adaptor protein, ASC, which is required for procaspase-1 conversion to caspase-1 (Mariathasan *et al.* 2004). The activation of caspase-1 is required for processing and secretion of cytokines, such as conversion of pro-IL-1β to IL-1β which can then be secreted from the cell in microvesicles (Pizzirani *et al.* 2007; Netea *et al.* 2009). It is therefore possible that components of this pathway are also required for TG2 secretion in macrophages.

P2X7R activation in macrophages is also known to regulate secretion of other mediators including IL-18 (Mariathasan *et al.* 2004), IL-6 (Solini *et al.* 1999), MMP9 (Gu and Wiley 2006) and proteases including caspase-1 (Laliberte *et al.* 1999) and cathepsins B, K, L and S (Lopez-Castejon *et al.* 2010). Deficiency in P2X7R activation can result in reduced elimination of intracellular pathogens e.g. *mycobacterium tuberculosis*, or reduced clearance of infected cells (Idzko *et al.* 2014), demonstrating a role in immune defence.

To investigate whether TG2 secretion occurs through a pathway involving P2X7R in a more physiologically relevant system than HEK293 cells, primary human monocytes were isolated from human peripheral blood and differentiated to M1 macrophages for use in TG2 secretion experiments. As discussed above, these cells are known to express high levels of P2X7R and have also been demonstrated to express TG2 and to translocate it to the cell surface, and are therefore a good system to use as they are expected to secrete TG2 to a sufficient level to allow detection by Western blotting.

Aims of this chapter:

1. To establish whether human M1 macrophages respond to BzATP by secreting TG2, in a P2X7R dependent manner.
2. To assess the involvement of caspase-1 in TG2 secretion by M1 macrophages.
3. To investigate potential differences in mechanistic aspects of TG2 secretion between M1 macrophages and HEK293 cells.

5.2. Results

5.2.1. Characterisation of the cells extracted from human peripheral blood

Monocytes were isolated from human peripheral blood, and cultured for 7 to 10 days in the presence of 20ng/ml GM-CSF. This protocol has been shown in our lab to result in monocyte differentiation to M1 macrophages (Jegundo dos Reis 2017) as evidenced by induction of expression of iNOS. The isolation protocol used, separation of cells by centrifugation through Ficoll of specific density, should result in purification of mainly monocytes but I cannot exclude co-purification of some platelets and other blood cells. Initially, the cells grow in suspension, but over 7-10 days in the presence of 20ng/ml GM-CSF a proportion of the monocytes become adherent and spread on the flask surface, as they differentiate into M1 macrophages (Fig. 5.1 A). Replacement of the media removes any non-adherent cells, including any that were not monocytes, leaving the adherent M1 macrophages on the surface of the flask for use in experiments. The adherent cells were then transferred into 24-well plates and allowed to settle for 24 hours, before use in P2X7R stimulation experiments. Initially, the expression of both P2X7R and TG2 was investigated in these M1 macrophages, and both proteins were found to be present as determined by Western blotting (Fig. 5.1 B and C). Membrane shown in B was probed for TG2, followed by P2X7R. As P2X7R was found at a lower molecular weight than expected, Western blotting was performed again using the same samples, first probed for P2X7R, demonstrating that the main band present was the ~66kDa band, and the 80kDa band was largely absent. Some differences in expression levels between individuals were noted, in line with previous reports (Hodrea *et al.* 2010; Jegundo dos Reis 2017). The majority of P2X7R detected in M1 macrophage cell extracts was found at approximately 66kDa, rather than the expected ~80kDa, demonstrated in Fig. 5.1 C, likely to be due to changes in glycosylation of the receptor.

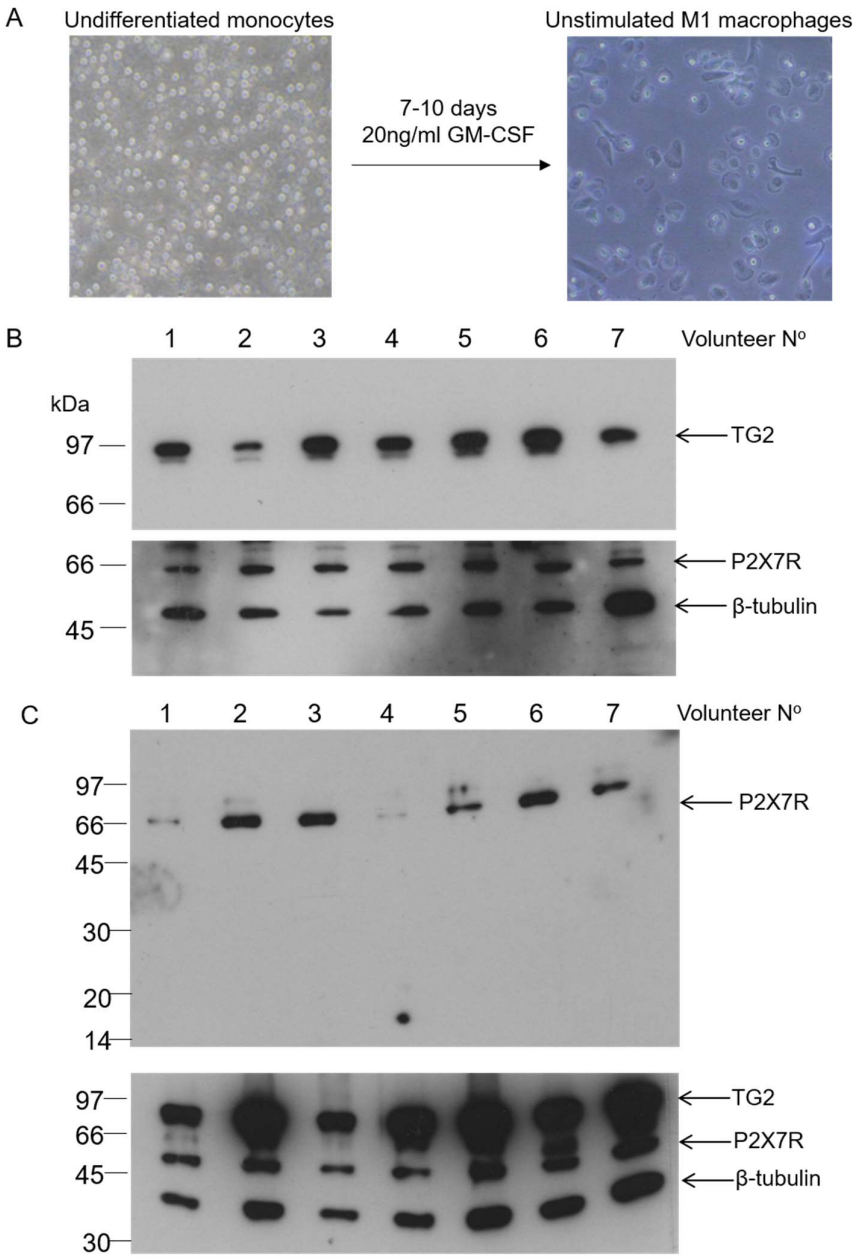

Fig. 5.1 Characterisation of M1 macrophages generated from human peripheral blood mononuclear cells. A) Phase contrast images (10x magnification) of cells extracted from human peripheral blood using centrifugation through Ficoll Paque, day 0 (left) and after 7 days of culture with 20ng/ml GM-CSF (right), where M1 macrophages have adhered to the surface of the flask (Day 7). Images shown are representative of cells appearance in all experiments. B and C) Western blotting performed using 10µg total cell protein isolated from M1 macrophages of 7 blood donors and run on a 4-20% SDS PAGE gel under reducing conditions and blotted for TG2 (CUB7402, 200ng/ml), P2X7R (Sc-25698, 2µg/ml) and β-tubulin (TUB2.1, 2.6µg/ml). Result shown for 7 individuals, out of a total 16 used, is representative for the cohort.

5.2.2. P2X7R regulates TG2 secretion by M1 macrophages

To assess TG2 secretion, macrophages were stimulated for 10 minutes with 0.1mM BzATP or control medium, followed by a 30 minute chase period in the absence of BzATP. This demonstrated that TG2 secretion occurs on P2X7R stimulation in M1 macrophages during the 10 minute pulse of BzATP (Fig. 5.2). In contrast to what occurs in HEK293 cells, release does not continue during the 30 minute chase period. Furthermore, the released form of TG2 is a 66kDa processed form, TG2', whereas the 78kDa full-length form of TG2 is present in the cell lysate (Fig. 5.2). To confirm that this release was specific to P2X7R activation and not due to non-specific release of the contents of damaged or necrotic cells, the Western blot was probed for proteins that are exclusively intracellular – β-tubulin and IκBα. Both of these proteins were detected in the cell lysate, but were absent from the conditioned media samples. This indicates that the TG2 release seen in these cells is specific release triggered by P2X7R activation and not non-specific release of cell contents due to damage. Note, stimulation of receptor with saturating ligand concentrations leads to release of the 78kDa form of TG2 suggesting that the activation state of the receptor has an impact on TG2 processing.

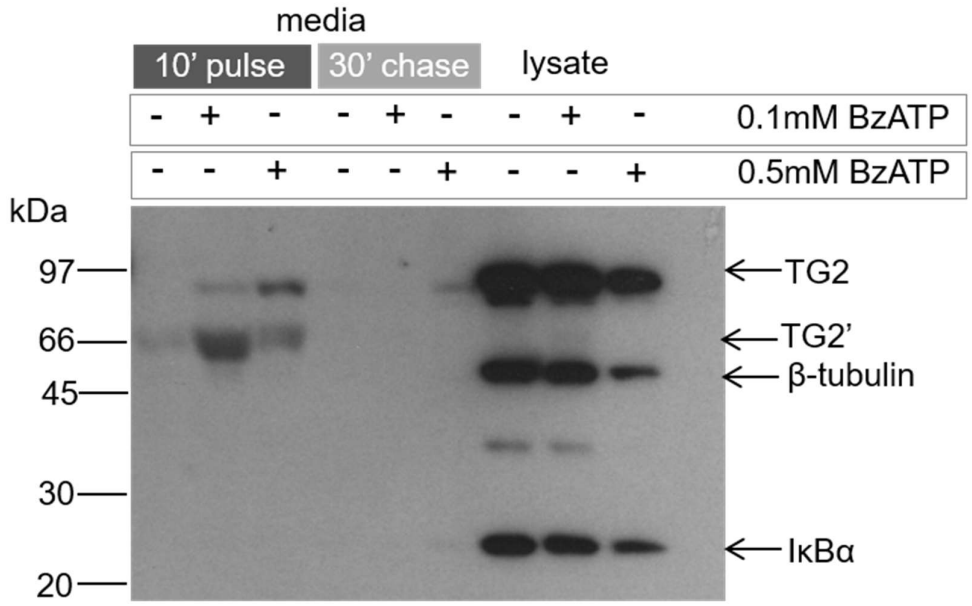

Fig. 5.2 TG2 release occurs on P2X7R activation. M1 macrophages (VOL006), generated as described in fig. 5.1, were stimulated using 0.1mM or 0.5mM BzATP in OptiMem or OptiMem only for 10 minutes (pulse), then fresh OptiMem without BzATP was added for a further 30 minutes (chase). 500µl media was run on a 4-20% SDS PAGE gel under reducing conditions, and Western blotting performed for TG2 (CUB7402, 200ng/ml), β-tubulin (TUB2.1, 2.6µg/ml), and IκBα (1µg/ml). Experiment shown is representative of three independent experiments for this volunteer.

To account for any potential differences between individuals, monocytes were isolated from a second individual and TG2 release assessed (Fig. 5.3 A). This individual also responded to 0.1mM BzATP by secreting TG2 in the 10 minute pulse period, and again had an absence of release during the 30 minute chase period. TG2 from this individual was also detected as the processed, 66kDa form in the media and full-length 78kDa TG2 in the lysate. This indicates that the processing observed in fig. 5.2 was not specific to a particular individual or due to any sample handling issues. To further confirm that this 66kDa band is TG2, a second antibody to TG2 which recognises an epitope in the *N*-terminal β-sheet domain (A034, Zedira) was used to probe a medium sample from BzATP stimulated cells (Fig. 5.3 B) (Note, CUB7402 recognises an epitope in the core domain (Lai *et al.* 2007)). This antibody was also capable of detecting the 66kDa band, confirming that this band is a processed version of TG2 and not an off-target interaction of the CUB7402 antibody. Due to M1 macrophages expressing several P2 receptors, which would be capable of responding to BzATP, the

experiment was also performed in the presence of 2.5mM $CaCl_2$, which is known to specifically inhibit P2X7R (Virginio *et al.* 1997) (Fig. 5.3 C). In these conditions, TG2 was no longer detectable in the media samples. This further supports that the TG2 release is due to P2X7R activation and not non-P2X7R related effects of BzATP.

Pre-treatment of cells with apyrase breaks down endogenous ATP (and other nucleotides) from the extracellular environment, enabling us to block any baseline signalling and meaning that any TG2 secretion observed is due to the BzATP treatment only. However, after pre-treatment with apyrase, TG2 secretion was reduced compared to no pre-treatment (performed in parallel) and the full-length form of TG2 is present in the 10 minute pulse, BzATP treated conditioned media and both 30 minute chase media samples, with a small increase in TG2 secretion in response to BzATP activation during the 10 minute pulse (Fig. 5.3 D). This full-length TG2 release may be due to some cell death, possibly due to the apyrase pre-treatment. However, it is also possible that other P2 receptors play a role in this, for example P2Y6 (Campwala *et al.* 2014). While this is a potentially important observation, it is not the focus here and was not investigated further at this point. Finally, thioredoxin-1 secretion in M1 macrophages was assessed. Thioredoxin-1 appears to be released in response to BzATP stimulation (Fig. 5.3 E). This confirms that thioredoxin-1 secretion occurs in parallel with TG2 secretion on P2X7R activation in M1 macrophages as well as in HEK293 cells, as shown in chapter 4.

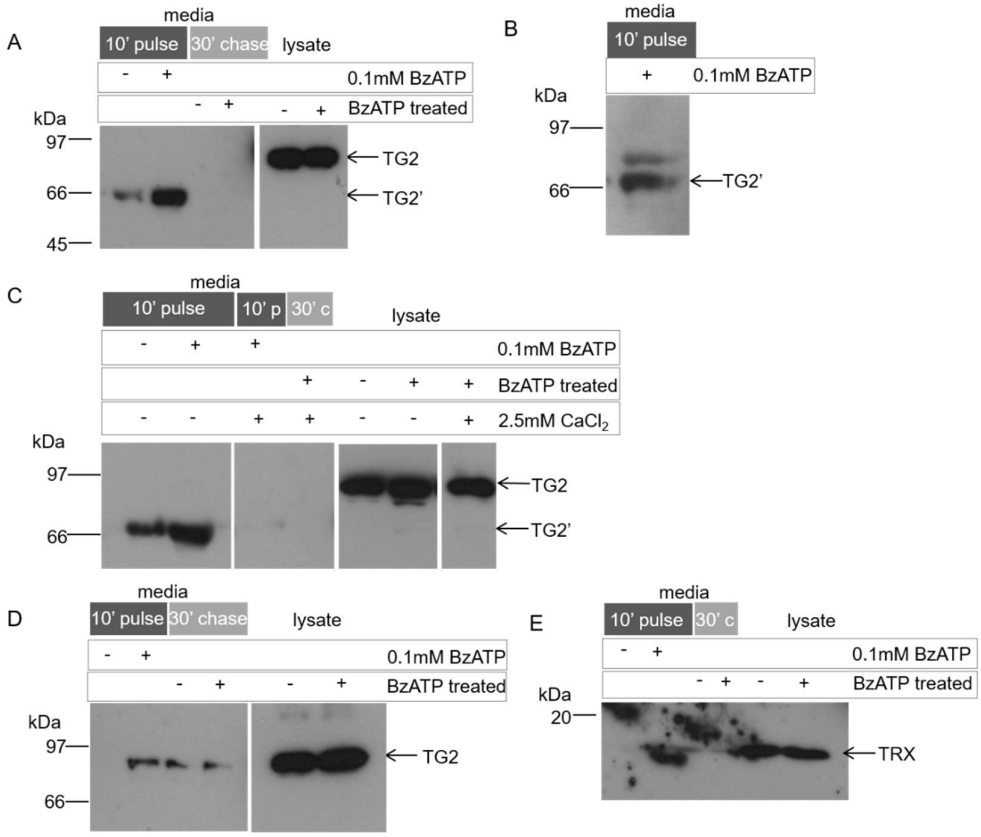

Fig. 5.3 TG2 and TRX secretion occur in response to BzATP stimulation in M1 macrophages. P2X7R stimulation experiments and Western blotting were performed as described in fig. 5.2. In A) macrophages from a second individual (VOL002) were used and Western blot probed for TG2 (CUB7402, 200ng/ml), representative of three independent experiments for this individual. B) Conditioned medium from M1 macrophages (VOL006) stimulated for 10 minutes with 0.1mM BzATP analysed by Western blotting using an anti TG2 β-sheet domain antibody (A034, 200ng/ml), representative of two individual experiments probed with this antibody. C) M1 macrophages (VOL005) were pre-treated for 10 minutes with 2.5mM $CaCl_2$ and 2.5mM $CaCl_2$ was present at all times during the P2X7R activation experiment (experiment was performed as described in fig. 5.2), representative of two independent experiments. TG2 secretion in the absence of high Ca^{2+} was confirmed in parallel. D) Macrophages (VOL002) were pre-treated for 15 minutes with 1U/ml apyrase, then apyrase was removed and absent during the 10 minute pulse and 30 minute chase periods of the experiment, experiment performed as described in Fig. 5.2. Experiment was performed once. E) Western blot shown in A was probed for thioredoxin-1 (FL-105, 1µg/ml) (VOL002).

5.2.3. Role of caspase-1 in processing and release of TG2

In macrophages, P2X7R activation results in caspase-1 activation, which could be responsible for TG2 processing. The caspase-1 inhibitor ac-YVAD-cmk (a chloromethyl ketone peptide based on the target sequence of IL-1β) was applied to the

cells at the same time as BzATP, inhibiting any secreted caspase-1 present in the media and preventing its processing of proteins in the media. I used 100μM of the chloromethyl ketone as this dose was shown to be effective in previous studies (Kelk *et al.* 2003). In the presence of ac-YVAD-cmk, the processed but not the full-length form of TG2 was still present in the media (Fig. 5.4 A). To confirm that caspase-1 was not responsible for TG2 processing, recombinant TG2 was incubated with recombinant caspase-1. I observed some TG2 complexes, possibly due to either auto-crosslinking of TG2 or aggregation of the protein due to purification. Incubation of recombinant caspase-1 with TG2 did not result in processing of TG2 to give the 66kDa form (Fig. 5.4 B), indicating that caspase-1 is unlikely to be processing TG2 in the conditioned media of M1 macrophages. This suggests that either TG2 processing in the media is performed by a different protease, or TG2 processing occurs prior to its release.

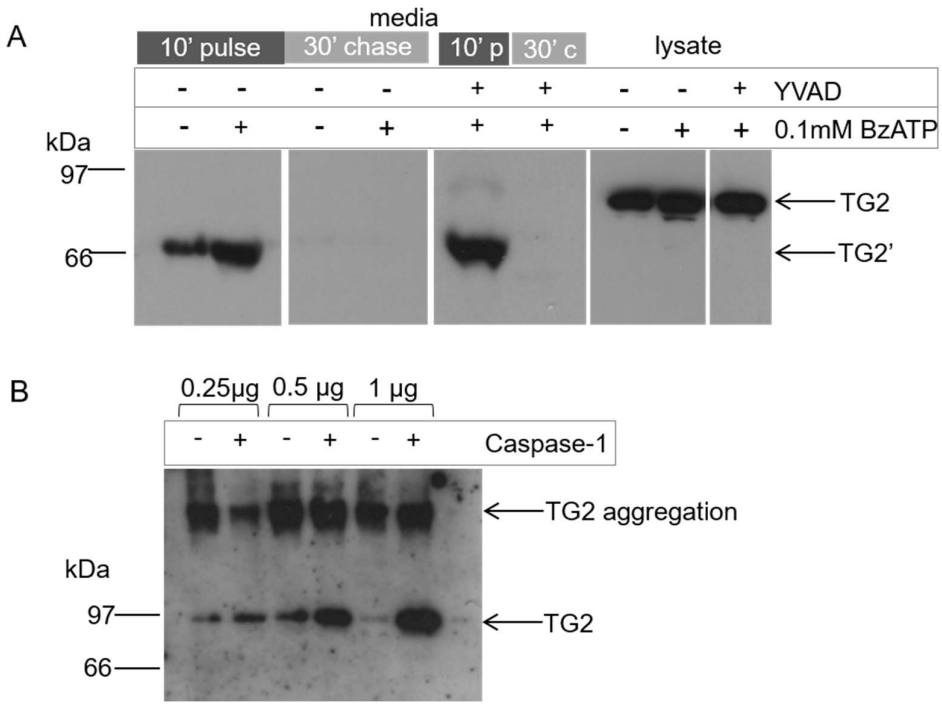

Fig. 5.4 Caspase-1 does not process TG2 in the media of M1 macrophages. A) Experiment was performed as in fig. 5.2, except that 100µM ac-YVAD-cmk was included in the media during P2X7R stimulation (10 minute pulse) and during the 30 minute chase period, where indicated (cells from VOL005), representative of three independent experiments. B) The indicated amounts of recombinant TG2 were incubated for 3 hours with recombinant caspase-1 (1 unit/reaction) or H_2O control in caspase-1 activity buffer, at 25ºC. This was then run on a 4-20% SDS PAGE gel under reducing conditions and probed for TG2 (CUB7402, 200ng/µl). Experiment performed once.

As caspase-1 is required for the secretion of IL-1β in response to P2X7R activation (Netea *et al.* 2009), I investigated whether it was also required for TG2 secretion. Cells were pre-incubated with ac-YVAD-cmk for 10 minutes and the inhibitor was also present at all times during the experiment. Note, this inhibitor is cell permeable. Surprisingly, under these conditions, TG2 release was completely blocked (Fig. 5.5 A). In contrast, the presence of ac-YVAD-cmk during pulse and chase only, with no pre-incubation, does not prevent TG2 secretion (Fig. 5.5 B, also shown in fig. 5.4 A). The reproducibility of the inhibition of TG2 secretion by 10 minutes of pre-treatment with caspase-1 inhibitor was confirmed; however, pre-incubating the cells for 30 minutes with ac-YVAD-cmk, only partially inhibits TG2 secretion. This suggests that 30 minutes of incubation with ac-YVAD-cmk is too long, potentially resulting in

clearance of the inhibitor from the relevant cellular compartment. Importantly, under all conditions only processed, but not full-length TG2 was observed, again confirming that TG2 processing is not caspase-1 dependent; however, this indicates that caspase-1 activity is required for TG2 secretion.

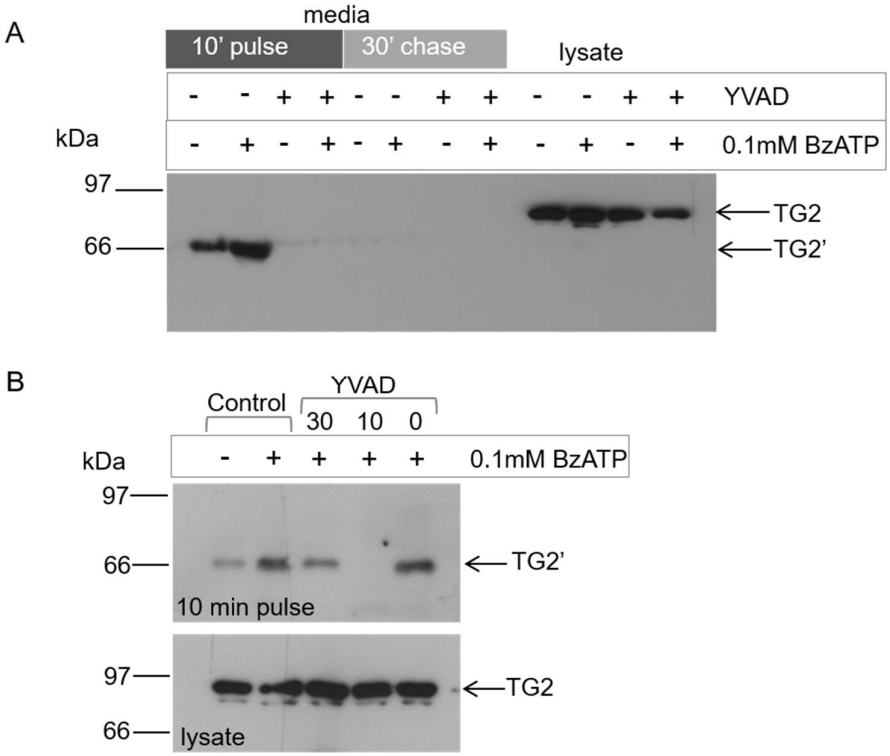

Fig. 5.5 TG2 secretion is dependent on caspase-1 activity. TG2 secretion experiments were performed as described in fig. 5.2, except that in A) cells were pre-incubated with 100µM ac-YVAD-cmk for 10 minutes, and 100µM ac-YVAD-cmk was present at all times during the subsequent P2X7R stimulation experiment (Cells from VOL005), representative of three independent experiments. In B) cells were pre-treated with 100µM ac-YVAD-cmk for either 10 or 30 minutes prior to P2X7R stimulation and also at all times during the experiment, or was present during the pulse and chase periods of the experiment only (0 minutes pre-incubation) (Cells from VOL001), representative of three independent experiments.

5.2.4. Can TG2 processing be blocked with selected protease inhibitors?

As TG2 processing was found to be independent of caspase-1 activity, the involvement of other proteases was investigated. Initially, using general inhibitors of classes of proteases, instead of ones specific to one particular protease, to narrow the field of possible candidate proteases for involvement in TG2 processing. Metalloproteases were inhibited using 5mM EDTA, cathepsins (cysteine proteases) were inhibited using

100µM E64 and serine proteases were inhibited using 10µg/ml aprotinin. Cathepsins were specifically targeted because it has been shown that cathepsins B, L, K and S are secreted in response to P2X7R activation (Lopez-Castejon *et al.* 2010), and the respective inhibitors were chosen because of their low toxicity and therefore compatibility with use in cell culture. DMSO is commonly used as a carrier for organic compounds. An initial experiment with a 0.1% DMSO control showed that DMSO itself interfered with TG2 secretion (Fig. 5.6 A). The P2X7R inhibitor, A740003, pitstop-2 (an endocytosis inhibitor) and E64 were all reconstituted in DMSO and therefore their effect on TG2 secretion could not be reliably assessed. The endocytosis inhibitor was used here as TG2 is able to bind to the surface of the cell, and has been demonstrated to undergo endocytosis (Zemskov *et al.* 2007). It is possible that this occurs only to full-length TG2, preventing detection of its accumulation outside the cell.

To ensure that this effect of the carrier was not due to the specific brand or type of DMSO used i.e. due to a contamination in the reagent, two different brands of cell culture grade DMSO were tested for interference with TG2 secretion. This experiment was also performed on cells from a different individual to that used in fig. 5.6 A, to account for the possibility of any individual-specific effects of DMSO (Fig. 5.6 B). Therefore, it was not possible to use any inhibitor that could only be solubilised in DMSO, as effects of the inhibitor could not be distinguished from effects of DMSO. Hence, the P2X7R inhibitor, A740003, could not be used as it is not sufficiently soluble in H_2O. This inhibitor was substituted for 2.5mM $CaCl_2$ treatment (Fig. 5.6 C), which is capable of preventing P2X7R activation (Adamczyk *et al.* 2015). In the presence of this high calcium concentration, TG2 was not secreted. It was also not possible to use Pitstop-2, as this also required solubilisation in DMSO, so the role of endocytosis was not further investigated. EDTA, E64 and aprotinin were soluble in H_2O, and were found to be unable to inhibit TG2 processing (Fig. 5.6 C), suggesting that metalloproteases, select cysteine proteases and serine proteases were unlikely to be involved in TG2 processing in the media of M1 macrophages.

To investigate further whether TG2 processing occurs in the media of M1 macrophages, conditioned medium from M1 macrophages was incubated with recombinant TG2. Unexpectedly, processing of the recombinant TG2 was not seen

(Fig. 5.6 D). To exclude that freezing of the medium leads to loss of the processing activity a wide panel of inhibitors was tested in combination with freshly collected medium and recombinant TG2 (Fig. 5.6 E), however as TG2 processing was not seen, the effects of these inhibitors could not be assessed. Taken together, this suggests that TG2 processing occurs prior to its secretion into the media, and may occur intracellularly or in a specific compartment. As no processing of TG2 in cell lysate is seen (Fig. 5.6 B), this suggests that processing is directly linked to externalisation.

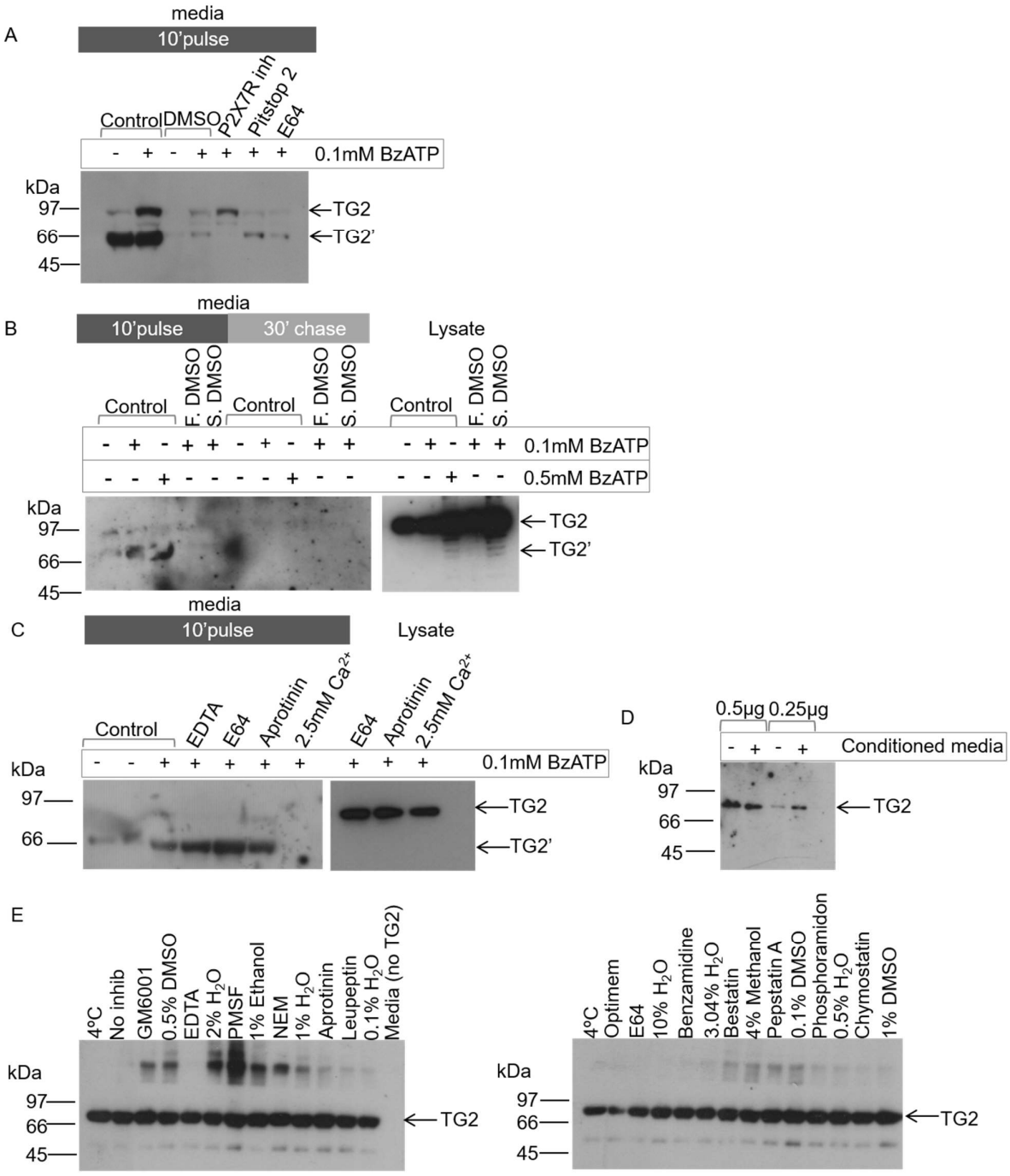

Fig. 5.6 TG2 processing is not inhibited by a range of protease inhibitors. TG2 secretion experiments were performed as described in fig. 5.2, except that in A) cells were pre-treated with 0.1% DMSO (vehicle control), 5µM P2X7R inhibitor, 20µM pitstop 2 and 100µM E64 for 10 minutes (all in DMSO) and inhibitors were present at all times during the experiment (cells from VOL003). Media were analysed for TG2 by Western blotting. Experiment performed once. B) cells were pre-treated for 10 minutes with 0.1% DMSO, either Fisher (F. DMSO) or Sigma (S. DMSO), cell

culture grade, as indicated and DMSO was present at all times during the experiment (cells from VOL016). Representative of two independent experiments. C) Cells were pre-treated with 5mM EDTA, 100µM E64 or 10µg/ml aprotinin (all made up in H2O) for 10 minutes, and inhibitors were present at all times during the experiment (cells from VOL002). Experiment performed once, except 2.5mM $CaCl_2$ condition, which is representative of two independent experiments. D) control medium (fresh OptiMem(-)) or conditioned medium (+) from M1 macrophages following BzATP stimulation (10 min pulse) were incubated with the indicated amounts of recombinant TG2 for 18 hours at 25ºC and the sample run on a 4-20% SDS PAGE gel under reducing conditions and Western blotting performed for TG2 (medium collected from VOL006 cells). Note, processed form of TG2 present in conditioned medium is of too low concentration relative to recombinant enzyme to be detected. Experiment was performed once. E) Experiment was performed as in D (using medium from VOL006 cells), except that the indicated inhibitors were present during the incubation of conditioned media with recombinant TG2, at the following concentrations: 50µM GM6001, 5mM EDTA, 1mM PMSF, 1mM NEM, 10µg/ml aprotinin, 100µM E64, 10mM benzamidine, 40µM bestatin, 10µg/ml leupeptin, 1µM pepstatin A, 5µM phosphoramidon, 100µM chymostatin. Medium was also incubated at 4ºC to prevent proteolysis. Experiment was performed once.

5.2.5. Identifying the cleavage site in TG2

Identifying the position of processing in TG2 is important as it determines the function of the protein, in terms of activity, regulation of activity and protein interactions. It may also provide information regarding candidate proteases involved in cleavage. It is likely that approximately 12kDa of either the *N*-terminal β-sheet domain or of the *C*-terminal β-barrel 2 domain is removed. Therefore, Western blots were probed using two different monoclonal antibodies, one with an epitope in the *N*-terminal β-sheet domain (A034) and the other recognising an epitope in the *C*-terminal β-barrel (A037, Zedira) (Fig. 5.7 A). The antibody previously used (CUB7402, Thermo scientific) is directed against an epitope within the core domain of TG2. Both *N*-terminal β-sheet domain and the *C*-terminal β-barrel domain antibodies were capable of recognising the processed form of TG2 (Fig. 5.7 B), however, this could be due to the position of the epitopes in this domain, as in both cases they are closer to the core domain than the *N*- or *C*-terminus of the protein, meaning that the processing could occur closer to the *N*- or *C*-terminus than the antibody epitope. Based on size, it is also possible that both ends of TG2 are modified. To further investigate this, the processed form of TG2 was isolated from the medium by immunoprecipitation, using the anti-TG2 CUB7402 antibody, to allow for tandem mass-spectrometry analysis (Fig. 5.7 C). Interestingly, both the intact and processed form were recovered from both the medium and cell

lysates. Unfortunately, even though a very faint band was visible on the Coomassie blue stained gel, the amount of TG2 recovered by immunoprecipitation was insufficient to obtain a match of sufficient quality to deduce any information using ms/ms. However, if the yield can be improved for the IP, this approach is likely to yield further insight.

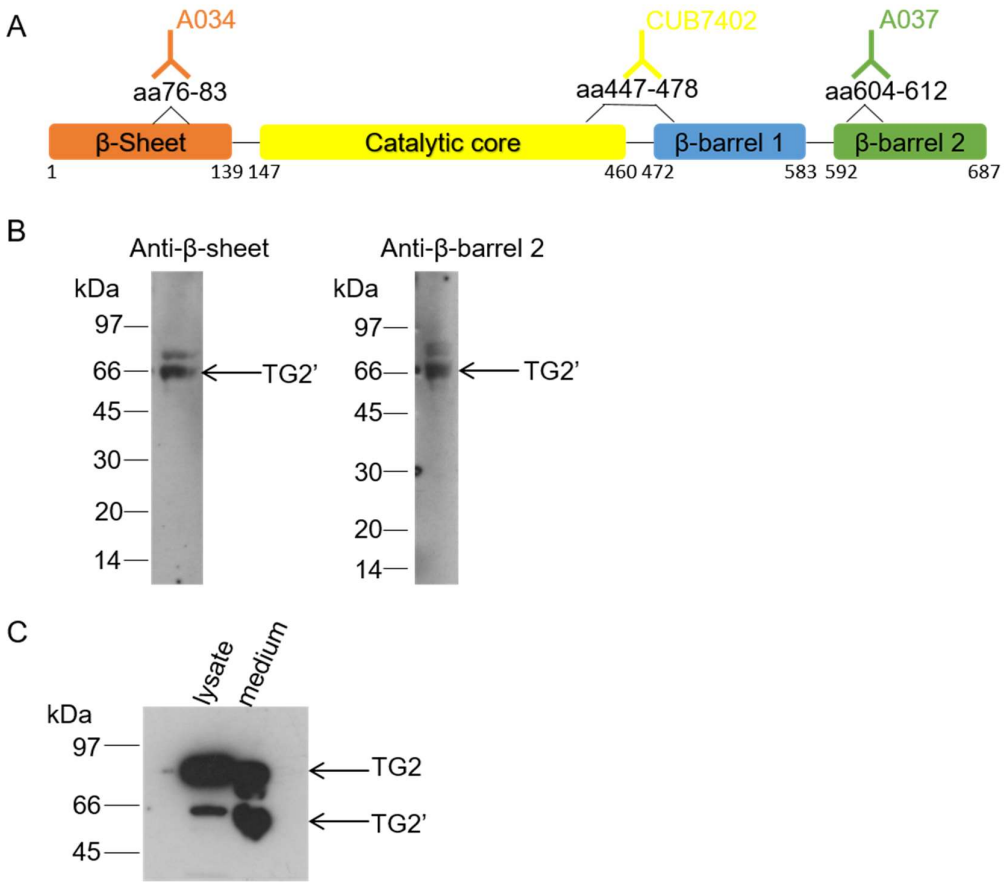

Fig. 5.7 Identifying the processed form of TG2. A) Diagram depicting the epitopes for the anti-β-sheet antibody (A034), anti-β-barrel 2 antibody (A037) and antibody to the core domain (CUB7402). B) Cell experiment was performed as described in fig. 5.2, using cells from VOL006, and two samples of BzATP treated 10 minute pulse samples were run on a 4-20% SDS PAGE gel under reducing conditions and Western blotting performed for TG2, then probed using either the anti-β-sheet antibody (A034, 200ng/ml) or anti-β-barrel antibody (A037, 200ng/ml). C) TG2 was extracted from 5ml conditioned medium (10 minute pulse sample) or 850µg total cell protein and immunoprecipitated using 1µg CUB7402 antibody. 10µl of each sample was then run on a 4-20% SDS PAGE gel and Western blotting performed using anti-TG2 antibody (CUB7402, 200ng/ml) to confirm the presence of the correct TG2 band for mass-spectrometry analysis (from VOL006 experiment). Experiment is representative of using these antibodies to probe two different blots from independent experiments.

5.2.6. TG2 binds to the cell surface of M1 macrophages

It is known that TG2 is capable of binding to the surface of many cell types, therefore I investigated whether cell surface binding occurred in M1 macrophages, and whether this was affected by P2X7R activation. This was important as 'secretion' based on measurement of the component in the medium alone could provide and incorrect impression if a component is largely cell surface bound, and hence this constitutes an overwhelming proportion of the extracellular fraction. Cells that had not been stimulated with BzATP were used as a mock-cell surface extraction control (following every step of the cell surface protein extraction and isolation protocol except addition of the NHS-Biotin cross-linker) to confirm that no proteins that were not modified by the cross-linker were isolated on the streptavidin matrix. This resulted in a very low background and therefore confirmed specificity (Fig. 5.8 A). I was able to detect only full-length TG2 on the cell surface, and there was not a large increase in cell-surface associated TG2 after P2X7R activation (Fig. 5.8 A). This indicates that TG2 secretion on P2X7R activation results in the majority of released TG2 being present in the soluble fraction. In the presence of EDTA, which inhibits TG2 cross-linking activity as well as metalloproteases, there was no change in the amount of TG2 on the cell surface, indicating that the cell surface binding is not cross linking dependent and it is not removed from the surface of the cell by metalloproteases (Fig. 5.8 A), in line with my previous findings showing that EDTA does not prevent TG2 processing (Fig. 5.6 C). I also investigated whether there were differences in the amount of TG2 on the cell surface after the 10 minute pulse and after a 10 minute pulse followed by a 30 minute chase period (Fig. 5.8 B). TG2 binding to the surface of the cell during the 30 minute chase period could account for the lack of soluble TG2 in the respective media. However, no differences in the amount of TG2 associated with the cell surface were seen after the 30 minute chase period when compared to a cell surface protein isolate after the 10 minute pulse period, indicating that the cell surface pool of TG2 changes little over the experiment, although my experiment would not detect dynamic changes as a consequence of parallel secretion and endocytosis. HEK293 cells were also stimulated, then the cell surface protein isolated either after the 10 minute pulse with P2X7R agonist only or after the 10 minute pulse followed by the 30 minute chase (Fig. 5.8 C). No TG2 was found to be associated with the cell surface in any conditions, indicating that TG2 is unable to bind to the surface of HEK293 cells.

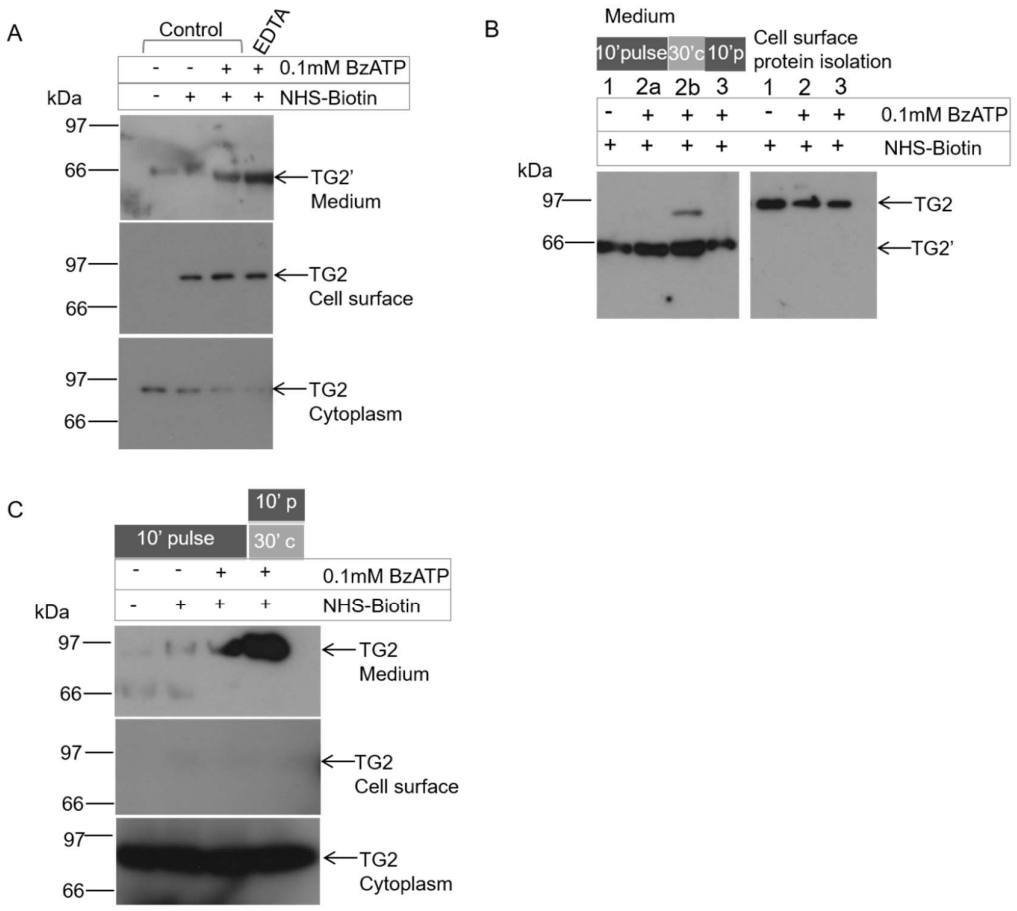

Fig. 5.8 TG2 is associated with the surface of M1 macrophages. Cell experiments were performed as described in fig 5.2, except that in A) cells from VOL002 were pre-incubated for 10 minutes with 5mM EDTA where indicated, and EDTA was present at all times during the experiment. Following stimulation with 0.1mM BzATP (10 minute pulse only), cell surface proteins were biotin labelled and subsequently isolated using a streptavidin column, using the Pierce cell surface protein extraction kit. 15µl cell surface protein isolate and 15µl of the total cell protein (flow through from the streptavidin column) were run on a 4-20% SDS PAGE gel under reducing conditions, then Western blotting was performed for TG2 (CUB7402, 200ng/ml). Experiment was performed once. B) Cell experiments and cell surface protein extraction was performed as in A, also using cells from VOL002, but without an EDTA treatment group. Where indicated, cells were either treated with BzATP for 10 minutes, then cell surface protein extracted, or both the 10 minute pulse and 30 minute chase were performed, then cell surface proteins were extracted. Representative of two independent experiments C) Experiment was performed as described in B, except HEK293 cells stably expressing wild type P2X7R and transiently transfected to express TG2 were used. Representative of two independent experiments.

5.3. Discussion

To demonstrate that the recently discovered process of TG2 secretion by activation of the P2X7R is applicable in a more physiologically relevant cell system than the HEK293 cell model stably transfected to express P2X7R used previously, human M1 macrophages were used. These cells were derived from monocytes extracted from human peripheral blood, through treatment with 20ng/ml GM-CSF. Another PhD project in this lab has demonstrated that this treatment, over 7-10 days results in differentiation of monocytes to M1 macrophages (Jegundo dos Reis 2017). These cells are, however, not fully activated M1 macrophages, as they have not been exposed to the necessary stimulus e.g. LPS or cytokines. Monocytes and macrophages have been shown to express high levels of P2X7R (Gu *et al.* 2000), and results in our lab suggest that M1 macrophages also express a high level of TG2 (Jegundo dos Reis 2017). It has been shown that monocytes express a low level of TG2, and that levels of TG2 rise as cells differentiate (Murtaugh *et al.* 1984). It has also been demonstrated that macrophages have a pool of extracellular TG2 that localizes to the surface of the cell, and that the cell surface TG2 is active (Toth *et al.* 2009; Hodrea *et al.* 2010). Here, Western blotting of cell lysates demonstrated expression of both TG2 and P2X7R, however, the P2X7R appeared at a lower molecular weight than expected. This is consistent with results previously seen in our lab in the THP-1 cell line (Adamczyk 2013), suggesting that this species of the P2X7R is present in monocytes/macrophages generally and may be the predominant version of the receptor in this cell lineage. Treatment of mouse and rat P2X7R with PNGase F has been shown to decrease observed molecular weight from ~75 and ~78kDa respectively to 68kDa (Young *et al.* 2007), suggesting that the ~65kDa form of the receptor observed here lacks glycosylation. The calculated mass of the 595 amino acid full-length receptor is 69kDa. It has been suggested that the 65kDa form is a naïve version of the receptor, which can be present both intracellularly and on the cell surface (Feng *et al.* 2005). The mature, fully glycosylated ~80kDa form of the receptor is mainly found on the surface of the cell, not intracellularly (Feng *et al.* 2005). The band for the larger form of the receptor may be missing from the Western blots here due to the difference in relative abundance of the two forms, whereby the ~65kDa form of the receptor is present in much greater levels than the ~80kDa form in whole cell lysate, meaning that the ~80kDa form was not detected. However, given that P2X7R has at least 10

splice variants (for humans), and that P2X7R variant B expression is widespread (Cheewatrakoolpong *et al.* 2005), it is possible that the detected ~65kDa form is a splice variant rather than the full length receptor.

Here I show that by stimulating the P2X7R with 0.1mM BzATP in primary M1 macrophages, I was able to stimulate the release of TG2. This indicates that the process elucidated using the HEK293 cell model is likely to be relevant more generally in different types of cells, however, there were clearly some differences in the process given the appearance of TG2 at approximately ~66kDa (TG2') instead of the expected ~78kDa band in the media of the macrophages, which will be discussed later in this section. I was able to demonstrate that this release is specific to P2X7R activation and drives externalisation of select proteins (TG2 and thioredoxin-1), and not general leakage of the contents of the cell as intracellular proteins such as β-tubulin and IκBα were absent from media samples containing TG2. Using cells from several different volunteers, I have consistently seen release of TG2' in response to 0.1mM BzATP, indicating that both the involvement of P2X7R and the processing of TG2 were part of a mechanism to the population as a whole and not specific to one individual. To further confirm that the 66kDa band seen in Western blotting was TG2 and not a result of non-specific binding of the antibody used, Western blots were probed with several different monoclonal antibodies targeting different epitopes of TG. This confirmed that the observed 66kDa band is TG2. As discussed previously in chapter 4, in HEK293 cells thioredoxin-1 secretion is likely to occur through the same pathway as TG2 secretion. I therefore assessed whether thioredoxin-1 is secreted on P2X7R activation in M1 macrophages, and found that thioredoxin-1 is also secreted by these cells on P2X7R activation. This suggests that the pathway of secretion being shared for TG2 and thioredoxin-1 is a feature common to different cell types and therefore may be physiologically important. As extracellular TG2 is required for essential macrophage functions such as clearance of apoptotic cells (Szondy *et al.* 2003; Toth *et al.* 2009), these findings start to elucidate a critical mechanism linking cell damage to an appropriate innate immune response.

In HEK293 cells, stimulation of the P2X7R with 0.5mM BzATP results in a biphasic receptor response, characterised by distinct patterns of 'pore' activity. This suggests that further dilation of the P2X7R pore occurs at high agonist concentrations or that a

second, unrelated mechanism is involved, absent when 0.1mM BzATP is applied (Adamczyk 2013). It is well established that prolonged stimulation of receptor with saturating agonist concentrations can result in cell death (Mackenzie *et al.* 2005). This suggests that TG2 release could be affected when different concentrations of agonist are applied. In M1 macrophages, 0.5mM BzATP does not appear to further enhance TG2 secretion, and may actually result in cell death or general leakage of the contents of the cell. This is thought to be the case due to the presence of full-length TG2 in the media in addition to processed TG2', suggesting that an alternative mechanism is active under those conditions that is not seen at lower agonist concentrations. In HEK293 cells, TG2 secretion can be first detected 5 to 10 minutes following stimulation with BzATP, and there is then continued secretion of TG2 during at least a 30 minute period, in the absence of BzATP. M1 macrophages, however, secrete TG2 during the 10 minute pulse with BzATP but secretion does not continue during the 30 minute chase period. This indicates a very tightly regulated secretion of TG2, requiring the presence of the P2X7R stimulus, but also likely a mechanism that terminates secretion as soon as the stimulus is gone (e.g. when ATP released from damaged cells is degraded by ATPases).

The process of TG2 secretion was inhibited by the presence of 2.5mM $CaCl_2$ in the medium, indicating that this is a P2X7R specific effect, as high levels of Ca^{2+} in the medium have been shown to inhibit P2X7R (Surprenant *et al.* 1996; Adamczyk *et al.* 2015). The P2X7R-specific inhibitor, A740003, appeared to block TG2 secretion, however, the vehicle control (0.1% DMSO) also substantially inhibited TG2 secretion. This occurred with different DMSO reagents, indicating that the effect is not due to a specific type or contamination of the DMSO, and is a DMSO specific effect. I have not been able to demonstrate, at this point, whether the inhibitory effect of DMSO applies also when other functions of the P2X7R are investigated, or whether this effect is specific to TG2 secretion. DMSO has been shown to have a variety of effects on macrophages, at different concentrations. For example, 1% DMSO was found to significantly increase levels of cell death in monocyte cultures (Elisia *et al.* 2016), however, this is a higher level of DMSO than used here (0.1%). The same study does not indicate that there is any effect on cell death of 0.1% DMSO, however, levels as low as 0.08% appear to affect macrophage polarization without affecting cell viability (Elisia *et al.* 2016). This suggests a general effect of DMSO on macrophages, even at

low concentrations (less than 0.5%) usually considered 'safe' for cell culture and where possible, the use of DMSO should therefore be avoided. This apparent sensitivity to DMSO prevents the use of many inhibitors which are not soluble in aqueous solutions, including the P2X7R inhibitor A740003.

Cells have been shown to secrete low levels of ATP into the culture media, including in response to mechanical stimuli (Corriden and Insel 2010). It has been suggested that changing the culture media can result in ATP release from cells (Corriden and Insel 2010), which could activate other purinergic receptors present. I therefore treated cells with apyrase to remove endogenous ATP, prior to BzATP treatment. Removal of endogenous extracellular ATP prevented TG2 secretion in response to P2X7R activation by BzATP and appears to prevent TG2 processing, demonstrated by the presence of low levels of full-length TG2 in the media. This suggests that ATP plays a role in TG2 secretion in M1 macrophages, possibly through activation of a P2Y receptor, which could activate downstream processes required for TG2 processing and secretion. It is also possible that ATP has a role in the polarisation of the macrophages, for example, it has been shown that inhibition of P2Y11 activity affects the ability of cells to polarise to M1 macrophages (Sakaki *et al.* 2013). Therefore, removing ATP may have diverse effects on the macrophages, thereby affecting TG2 secretion. However, given that this is a fast event (15 min) it is likely that the effect of apyrase in this system is a critical observation, which could also relate to the mediators generated by apyrase, including ADP, a potent P2Y6 agonist (Communi *et al.* 1996), or adenosine which activates adenosine receptors (Fredholm *et al.* 2001).

P2X7R activation also results in the activation and secretion of caspase-1 (Laliberte *et al.* 1999), which is required for the intracellular processing and secretion of IL-1β (Mariathasan *et al.* 2006). It was therefore essential to investigate the role of caspase-1 in TG2 processing and secretion. When cells were pre-incubated for a short period of time (10 minutes) with an irreversible cell-permeable caspase-1 inhibitor (ac-YVAD-cmk), TG2 secretion was prevented, suggesting that the activity of caspase-1 is required for TG2 secretion from M1 macrophages. The HEK293 cell model used previously lacks expression of NALP3 inflammasome components, including caspase-1 (Kawana *et al.* 2013), and TG2 secretion can still occur. This highlights the difference between the processes in HEK293 cells and macrophages, and the

importance of investigating the pathway in primary cells. However, it also highlights that caspase-1 is not an essential component for TG2 secretion *per se*. It is therefore possible that the secretion of TG2 by M1 macrophages requires its processing either directly by caspase-1 or by a protease downstream of caspase-1 activation. Alternatively, there may be cross-talk between inflammasome assembly and the mechanism involved in TG2 externalisation. Interestingly, addition of the caspase-1 inhibitor during and following stimulation was ineffective, making it unlikely that externalised caspase-1 is involved.

Exclusively full-length TG2 was detected in the lysate of M1 macrophages, indicating that the shortened version of TG2 is not a splice variant found in these cells, and therefore must in fact be a processed form. This processing could occur either intracellularly, prior to TG2 secretion and be part of this secretion process, or extracellularly after secretion has occurred. Processed TG2 was not detected in the cell lysate, indicating that the processing occurs very quickly after P2X7R stimulation. This also suggests that part of the mechanism of TG2 secretion is its processing, either in response to P2X7R activation or through stimulation of another purinergic receptor (hence the lack of release of processed TG2 when cells were pre-treated with apyrase). However, ATP break-down products could also negatively regulate the process and effectively constitute the negative feedback mechanism. As mentioned previously, caspase-1 is both activated and secreted as a result of P2X7R activation (Laliberte *et al.* 1999), and could therefore be responsible for TG2 processing either inside or outside of the cell. As discussed above, it is conceivable that caspase-1 processes TG2 intracellularly, as its inhibition inside the cell appears to prevent TG2 secretion, and this in turn could be due to a lack of processing. The processing of TG2 does not appear to be performed by caspase-1 extracellularly, as ac-YVAD-cmk present at the time of P2X7R stimulation does not prevent TG2 secretion or processing. Incubation of recombinant TG2 with recombinant caspase-1 suggests that caspase-1 is not directly involved in TG2 processing, as the processed form of TG2 was not generated. However, I was not able to independently verify the activity of the commercially obtained caspase-1. Nevertheless, this suggests that if caspase-1 has a role in TG2 processing, it is likely to be through the activation of another protease.

Cathepsins B, K, L and S, and other proteases such as MMP9 are also secreted in response to P2X7R activation (Gu and Wiley 2006; Lopez-Castejon *et al.* 2010), therefore a panel of protease inhibitors were tested for their effect on TG2 processing. Neither E64 nor EDTA were effective in blocking TG2 processing, even with pre-incubation of cells with these inhibitors. Furthermore, recombinant TG2 was incubated with conditioned medium from BzATP treated macrophages and no TG2 processing was seen. As there was no processing even in the absence of any protease inhibitor, these results suggest that the protease responsible for cleaving TG2 is not secreted into the conditioned media, and therefore possibly being cell-surface associated or intracellular. I cannot conclusively rule out the involvement of ADAMs as EDTA may not block their activity effectively. The nature of the protease involved is therefore unknown, and it was not possible to test the effect of many inhibitors to different classes of proteases due to their requirement for organic solvent for solubility or their toxicity for cells.

It will be important to identify the cleavage site in TG2, as dependent on where processing occurs this may affect TG2 activity. Identifying the cleavage site may also provide an indication as to which class of proteases may be involved. As the majority of other transglutaminases are activated by proteolytic processing, notably in the hinge region between core domain and β-barrel domains, it is possible that the processed form of TG2 is still active. Splice variants lacking parts of the *C*-terminus have been found to have reduced ability to bind GTP, therefore showing reduced sensitivity to allosteric regulation of transglutaminase activity (Monsonego *et al.* 1997; Citron *et al.* 2001; Lai *et al.* 2007). A 55kDa form of TG2 has also been identified, which is proteolytically processed and active (Fraij 2011). In this truncated form of TG2, the processing occurs towards the *C*-terminus of the protein, again possibly removing some of the residues required for GTP binding and therefore preventing allosteric regulation of transglutaminase activity (Fraij 2011). In this chapter, data presented shows that at least part of both the *N*- and *C*-terminal domain, respectively, were present for antibodies to each of these domains to detect the presence of TG2 in Western blotting. The epitopes for both of these antibodies were closer to the core domain than the *N*- or *C*-terminus of TG2, respectively, therefore it remains unclear which part of the protein is missing. To enable analysis of the processed TG2 by mass spectrometry, TG2 was isolated from the conditioned media by immunoprecipitation

and run on an SDS PAGE gel. This approach would allow comparison of a peptide map of the full-length and shortened TG2, to assess which part of the protein is retained, and as a consequence what is likely to be missing. Although TG2 was detected in the immunoprecipitated sample in Western blotting, the amounts of protein obtained were insufficient for successful mass spectrometry analysis. As it is essential to know which part of TG2 is missing, an improved method for increasing the amount of TG2 recovered from the conditioned media will be developed, to allow mass spectrometry to be performed.

I also investigated cell surface association of TG2 as this pool of TG2 may be relevant to macrophage function (Szondy *et al.* 2003; Toth *et al.* 2009). TG2 was found to be cell surface associated, under control conditions (without P2X7R activation), and the TG2 that was present was full-length. I found that there was no substantial increase in TG2, after P2X7R activation, suggesting that TG2 secreted through this pathway does not become cell-surface associated, consistent with the finding that the cell surface associated TG2 again was full-length only. A binding site for fibronectin within the *N*-terminal β-sandwich domain of TG2 may be required for cell surface association (Gaudry *et al.* 1999; Stamnaes *et al.* 2016). Hence, if the processing occurs in the *N*-terminal domain of TG2, the lack of cell surface association of the 66kDa form could be explained by loss of the fibronectin binding site. The lack of change in surface levels of TG2 during the 10 minute stimulation with P2X7R agonist also suggests that the cleaved TG2 is unlikely to be due to cell surface TG2 being processed, and thereby releasing it from the surface of the cell, but that the processed TG2 is more likely to be secreted directly into the soluble fraction and is unlikely to bind to the cell surface. The amount of TG2 at the cell surface following a 10 minute pulse and 30 minute chase period was also investigated, to assess whether the apparent lack of TG2 in the media of the 30 minute chase was due to an accumulation at the cell surface. Again, the levels of TG2 found at the cell surface were unchanged in comparison to control, indicating that TG2 released through the activation of the P2X7R pathway is unlikely to become cell surface associated. However, it is possible that under specific conditions secretion and processing may be de-coupled, perhaps indicated by results from apyrase treatment, and this may lead to secretion of the full-length enzyme that binds to the cell surface. In HEK293 cells, TG2 was not detected at the surface. This is likely to be due to the lack of expression of a suitable interaction partner such as

fibronectin or GPR56, the cell surface receptor for TG2, in HEK293 cells (Adamczyk *et al.* 2015). This notion again being in line with the idea that TG2 secretion and cell surface association are independent and consecutive events.

Macrophages were also treated with EDTA and the cell surface TG2 assessed. EDTA will have several functions, in this context. Firstly, EDTA will prevent TG2 activation by chelating the calcium present in the medium. As EDTA had no effect on the cell surface levels of TG2, this indicates that TG2 cross linking activity is not required for cell surface association. Secondly, the EDTA will also inhibit MMPs present in the conditioned medium. If MMPs were responsible for cleaving TG2 to remove it from the surface of the cell, inhibiting them with EDTA would cause accumulation of TG2 at the cell membrane, which is not seen. EDTA also did not prevent the cleavage of TG2 present in the medium, indicating that MMPs were unlikely to be responsible for the processing of TG2, although cell surface associated ADAMs may be less sensitive to inhibition by EDTA.

Taken together, the data presented in this chapter indicates that the proposed pathway for TG2 secretion elucidated using HEK293 cells is, with some modifications, conserved in primary macrophages and therefore likely to be physiologically relevant. A working model outlined in Fig. 5.9 summarises the state-of-play with regards to various hypotheses in light of my data. P2X7R activation and activation of another P2 receptor result in caspase-1 activation and processing of TG2 by an unknown protease, followed by its secretion into the soluble fraction. Although the involvement of P2X7R in TG2 secretion is shared between HEK293 cells and M1 macrophages, there were some differences in the process of TG2 secretion between these cell types. These differences include the apparent involvement of another purinergic receptor in M1 macrophages, the difference in kinetics of the TG2 release (highlighted by the lack of TG2 secretion in the 30 minute chase period in M1 macrophages, whereas release occurs predominantly during this period in HEK293 cells) and also the processing of TG2 in M1 macrophages but not in HEK293 cells. Collectively, this data indicates that ATP release from damaged/dying cells is likely to be capable of inducing TG2 secretion from M1 macrophages through activation of P2X7R, allowing an appropriate immune response.

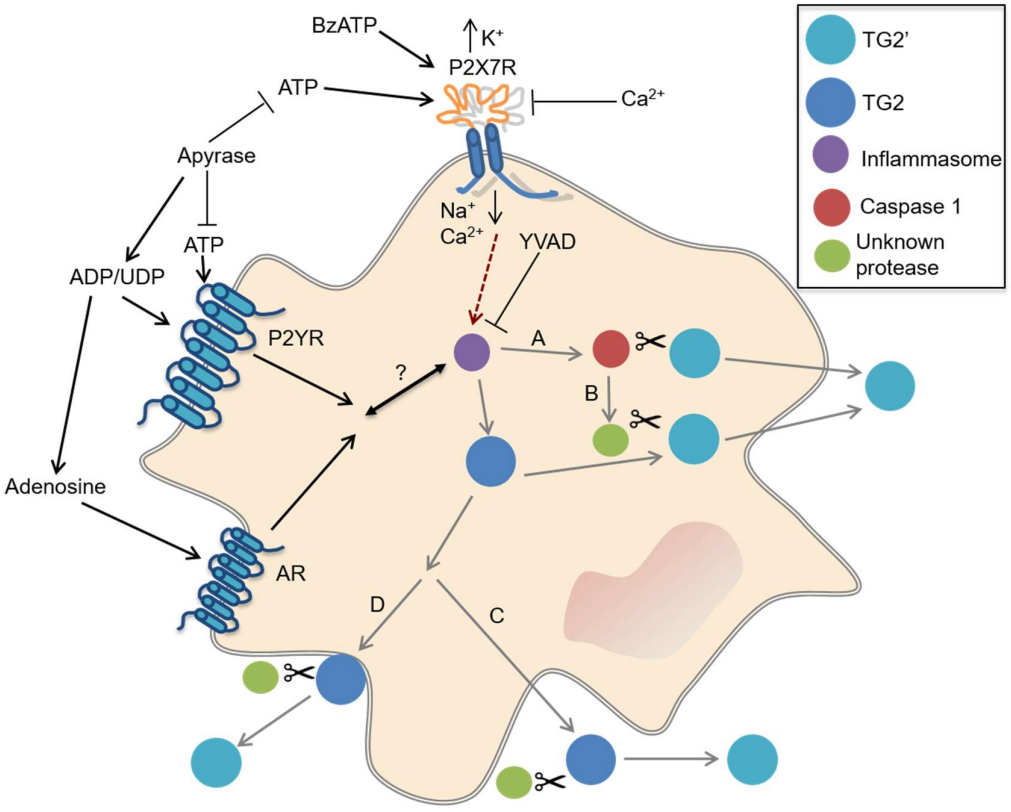

Fig. 5.9 Summary diagram of possible mechanisms involved in processing and secretion of TG2 investigated in this chapter. Several different proteins were investigated for their involvement in TG2 release in this chapter. Different inhibitors were applied at different times to reveal where and how the respective targets may be involved in TG2 processing and secretion in M1 macrophages. Common to all pathways investigated, I found the BzATP activation of P2X7R resulted in TG2 secretion, inhibited by 2.5mM $CaCl_2$. This process involves endogenous ATP but likely also other nucleotides or derivatives thereof, possibly through activation of a P2Y receptor, inhibited when ATP is removed by apyrase prior to BzATP stimulation or activated by a breakdown product, such as ADP, UDP or adenosine. The exact contribution of this other receptor predicted to be involved is unknown. P2X7R activation leads to caspase-1 activation, shown to be important in this context through intracellular caspase-1 blocking using ac-YVAD-cmk. A) Caspase-1 itself could process TG2 inside the cell, resulting in secretion of TG2', however recombinant caspase-1 was unable to cleave TG2. It is therefore more likely that there is some cross-talk between inflammasome assembly or caspase-1 activation and TG2 release. Therefore, the hypothesis shown in B) is more likely to be the process by which caspase-1 is involved in TG2 secretion. In this hypothesis, downstream of caspase-1 another protease could be activated, processing TG2 inside the cell resulting in secretion of TG2'. C) Full-length TG2 could be secreted into the soluble fraction, with unknown steps occurring between caspase-1 activation and TG2 secretion, with TG2 then being processed extracellularly by an unknown protease. Cleavage of TG2 would have to occur very quickly in this scenario, due to the absence of large amounts of full-length TG2 in the conditioned medium. Several protease inhibitors did not prevent TG2

processing in the medium, suggesting that this is unlikely to be the location of TG2 processing. D) Full-length TG2 is secreted in a manner that results in its attachment to the cell membrane, where it is then processed by an unknown protease, releasing TG2' into the media. As the pool of cell-surface associated TG2 was unchanged on P2X7R activation, this seems unlikely as some accumulation would be expected prior to the processing occurring.

Chapter 6

6. The impact of sequence polymorphisms in P2X7R on TG2 secretion

6.1. Introduction

The human P2X7R has been found to be highly polymorphic, with 32 currently known common non-synonymous single nucleotide polymorphisms (Fuller *et al.* 2009). The 1000 human genome project identified over 35000 SNPs in P2RX7, as listed in the Ensembl database (Auton *et al.* 2015). Polymorphisms in the coding sequence have been found to be associated with specific populations, with some present in people with Caucasian European ancestry but absent from some Asian populations (Fuller *et al.* 2009). This indicates that there has been selective pressure for certain variants of the P2X7R across different populations due to different environmental or disease factors, for example the presence or prevalence of different bacteria. Functional polymorphisms in the P2X7R have been linked to various diseases, indicating the importance of the role of P2X7R in immunity and pain perception. For example, a loss of function polymorphism was found to reduce the effectiveness of macrophages against *Mycobacterium tuberculosis* (Fernando *et al.* 2007). Polymorphisms discussed in this section are indicated on fig. 6.1, demonstrating the position of these mutations in relation to P2X7R transmembrane structure.

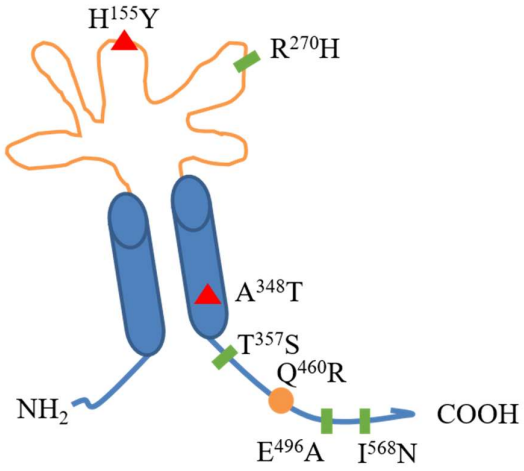

Fig. 6.1 Schematic showing positions of P2X7R polymorphisms discussed in this chapter. P2X7R polymorphisms are indicated at their approximate positions, relative to the transmembrane structure of the receptor. Amino acid changes resulting in gain of function are indicated as red triangles, those with unknown or neutral effects are shown as orange circles and those resulting in loss of function are indicated as green rectangles.

A number of P2X7R polymorphisms have been identified which result in increased activity of the receptor, for example $H^{155}Y$ is a polymorphism causing increases in both Ca^{2+} and ethidium uptake by the cell, indicating that it affects both ion channels and membrane pore formation (Portales-Cervantes *et al.* 2012). It has been suggested that the increased function observed with this receptor is due to either increased total protein expression (Ursu *et al.* 2014) or increased presence on the cell surface (Bradley *et al.* 2011), rather than direct effects on the activity of P2X7R. $H^{155}Y$ has been linked to increased post-mastectomy pain and pain in osteoarthritis (Sorge *et al.* 2012) and is also a risk factor in febrile seizures, where seizures occur without an underlying health condition (Emsley *et al.* 2014). There are also P2X7R mutations which result in increased receptor function due to direct effects on the receptor, for example the $A^{348}T$ mutation discussed in chapter 3 results in a hyperactive receptor due to modulation of channel opening as the residue is located in the second transmembrane domain, and forms part of the channel (Stokes *et al.* 2010). Substitution of A^{348} with amino acids with the smallest side chains (For example $A^{348}G$) results in increased currents, and amino acids with the largest side chains (For example $A^{348}F$) result in decreased currents (Bradley *et al.* 2011). This suggests that the residue present here directly affects the properties of the P2X7R channel. The $A^{348}T$ mutation has been found to be linked with anxiety disorder (Erhardt *et al.* 2007) and post-menopausal osteoporosis (Jorgensen *et al.* 2012), as well as reducing the effects of *Toxoplasma gondii* infection in a foetus (Jamieson *et al.* 2010).

There are also several known polymorphisms that result in decreased receptor function. $R^{270}H$ reduces ethidium uptake, indicating that it causes reduced membrane pore formation by the P2X7R (Stokes *et al.* 2010). This residue is located in the extracellular domain in a region that undergoes a conformational change during activation, meaning that the respective amino acid change potentially interferes with this conformational change, resulting in reduced activity (Caseley *et al.* 2014). The $R^{270}H$ mutation has been linked to decreased pain in both mastectomy patients and in osteoarthritis (Sorge *et al.* 2012). The $E^{496}A$ amino acid exchange in the *C*-terminus also results in reduced ethidium uptake but importantly has similar ion channel properties to wild-type P2X7R, suggesting a role in membrane pore formation only (Cabrini *et al.* 2005). However, other data suggest that this mutation affects both ion channel formation and membrane pore formation (Roger *et al.* 2010). It has also been

suggested that this polymorphism reduces IL-18 release (Sluyter *et al.* 2004). As this receptor appears to have normal surface expression, the effects of the mutation are likely to be protein structure related, rather than due to expression level differences (Gu *et al.* 2001). In contrast, the $I^{568}N$ mutation, which also reduces Ca^{2+} influx and dye uptake, results in decreased surface expression (Wiley *et al.* 2003). This decrease is likely to be due to the presence of the mutation in the 551-581 region, known to be important for membrane trafficking of the receptor (Smart *et al.* 2003).

The $Q^{460}R$ mutation occurs in the *C*-terminus of the P2X7R and appears to have a minimal effect on P2X7R functionality (Roger *et al.* 2010). Several different groups have studied the effect of this mutation on P2X7R, some finding that there was no effect (Cabrini *et al.* 2005; Roger *et al.* 2010), another found slight hyperactivity (Denlinger *et al.* 2006) and another a small reduction in membrane pore formation (Stokes *et al.* 2010). Despite an apparent lack of effect on P2X7R, $Q^{460}R$ has been linked to mood disorders such as bipolar disorder (Barden *et al.* 2006) and major depressive disorder (Lucae *et al.* 2006). This suggests that there should be an effect of this mutation on the function of P2X7R, however, it has also been found to be co-inherited with mutations increasing receptor function, $A^{348}T$ and $H^{155}Y$, as well as with $R^{270}H$, which reduces receptor function (Stokes *et al.* 2010). It is therefore possible that the causes of these mood disorders are related to these linked mutations with clear functional effects on the P2X7R, rather than $Q^{460}R$ itself. Both, $H^{155}Y$ and $Q^{460}R$, have been linked to patients more likely to experience severe sepsis following surgical trauma (Geistlinger *et al.* 2012). $A^{348}T$ and $Q^{460}R$ have been linked to increased bone mineral density and decreased vertebral fracture post-menopausally, where osteoporosis incidence rises (Jorgensen *et al.* 2012). In both of these cases, it could again be due to the linked inheritance that $Q^{460}R$ has been identified as contributing to these diseases alongside other polymorphisms. It is also possible that a combination of SNPs in *trans* produces functionally very different receptors from those formed by a single allele, i.e. a homotrimeric receptor.

Analysis of the various known polymorphisms in P2X7R demonstrates that there can be a variety of reasons why a mutation affects receptor activity. These can be direct, through affecting agonist affinity or channel opening, or indirect, by affecting total protein or cell surface expression, as outlined above. Added to these different factors

affecting P2X7R functionality is the complexity of co-inheritance of certain polymorphisms, for example $Q^{460}R$ being co-inherited with a variety of other mutations (Stokes *et al.* 2010). There is also linkage disequilibrium between $E^{496}A$ and $H^{155}Y$, a mutation that decreases activity and a mutation which increases activity respectively (Fuller *et al.* 2009), suggesting that mutations that may have unfavourable effects on the P2X7R function may be inherited alongside mutations that could counteract the negative effects.

A study assessing the possible co-inheritance of P2X7R mutations found a haplotype block, where 4 mutations were more likely to occur together – $A^{348}T$, $T^{357}S$, $Q^{460}R$ and $E^{496}A$ (Fuller *et al.* 2009). This study found that 5 common haplotypes of P2X7R were present in the Caucasian population (study of over 3000 individuals). This includes the wild-type P2X7R (P2X7-1), which occurs at the highest frequency (34% of the population tested, table 7.1), a haplotype containing only the $A^{348}T$ mutation (P2X7-2) and a haplotype containing only $T^{357}S$, a loss of function polymorphism (P2X7-5). P2X7-3 contains both the $A^{348}T$ and $E^{496}A$ polymorphisms, which results in decreased function of the receptor. Finally, P2X7-4 contains both $Q^{460}R$ and $A^{348}T$, which results in increased activity of the receptor.

Table 7.1 Population frequencies of five P2X7R variants. Data reproduced from (Fuller *et al.* 2009).

	Polymorphisms	Receptor function	Population frequency
P2X7-1	Wild-type	Wild-type	0.342
P2X7-2	$A^{348}T$	Increased	0.232
P2X7-3	$A^{348}T$, $E^{496}A$	Decreased	0.175
P2X7-4	$A^{348}T$, $Q^{460}R$	Increased	0.169
P2X7-5	$T^{357}S$	Decreased	0.082

As the human P2X7R is known to be highly polymorphic, variations in the receptor could impact on TG2 secretion, particularly those that impact on receptor pore functionality. Therefore, the aims of this chapter are:

1. Investigate whether the release of TG2 is different in different individuals, e.g. do some individuals show increased or decreased TG2 secretion?

2. Sequence genomic DNA to identify variations in the P2X7R of individuals and correlate the TG2 secretion findings with sequencing data, to assess how mutations affect TG2 secretion.

6.2. Results

6.2.1. Expression levels of P2X7R and TG2

Firstly, it was necessary to establish whether there were significant differences in P2X7R or TG2 expression, which may affect levels of TG2 secreted by cells. Monocytes were isolated from human peripheral blood and differentiated into M1 macrophages, as in chapter 5, using GM-CSF. By performing Western blotting using equivalent amounts of total cell protein, I found that in the volunteers used here there were no large differences in TG2 or P2X7R expression; that would explain overt changes in TG2 secretion, as shown in chapter 5 (Fig. 6.2). There were small differences in expression levels of both TG2 and P2X7R but these were not considered to be significant enough (such as almost complete absence of TG2 or P2X7R expression) to substantially alter TG2 secretion, although I have only analysed total P2X7R and not cell surface-associated P2X7R.

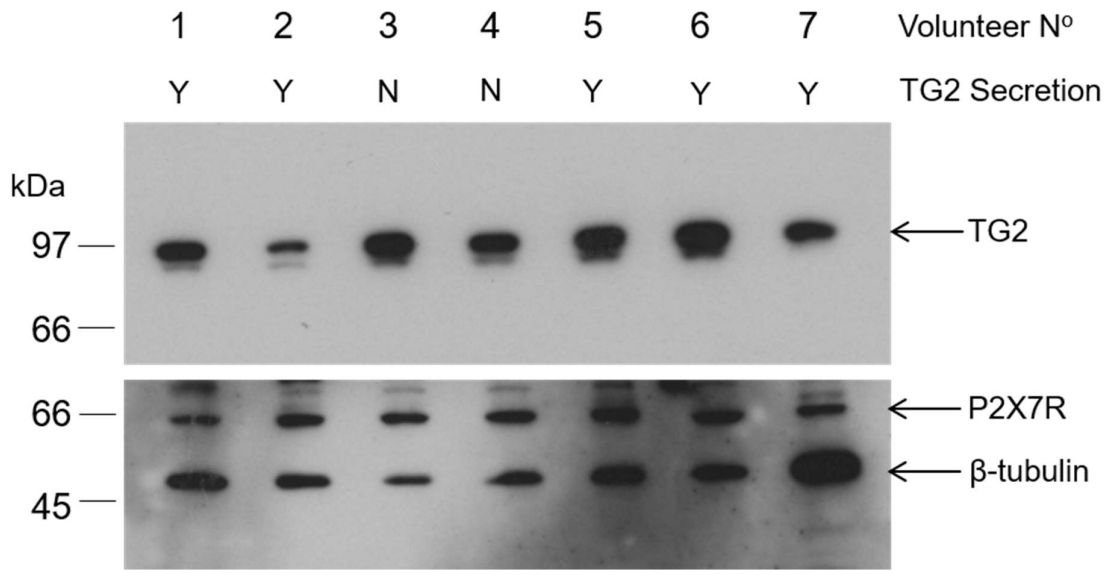

Fig. 6.2 Expression of P2X7R and TG2 in all volunteers. Monocytes were isolated from human peripheral blood using centrifugation through Ficoll Paque, then cultured for 7 days with 20ng/ml GM-CSF. Cells were lysed and Western blotting performed using 10µg total cell protein run on a 4-20% SDS PAGE gel under reducing conditions and blotted for TG2 (CUB7402, 200ng/ml), P2X7R (Sc-25698, 2µg/ml) and β-tubulin (TUB2.1, 2.6µg/ml). Blot shown is of 7 volunteers, representative of all 16 volunteers tested. P2X7R was activated using 0.1mM BzATP and media were analysed for TG2 using Western blotting. Result indicates whether an agonist-specific response was detectable, given as yes/no (Y/N). Expression levels showed no correlation with functional response.

6.2.2. Do different individuals respond differently to P2X7R activation?

As all individuals expressed both P2X7R and TG2, any differences in TG2 secretion after P2X7R activation were not due to a lack of expression of either protein. Fig. 6.3 A illustrates and example where TG2 release did occur in response to P2X7R activation using 0.1mM BzATP, which was observed for 11 of the 16 individuals tested. The 66kDa, processed form of TG2, was the form detected in the medium for all individuals, as described in the previous chapter. When M1 macrophages from an individual who secretes TG2 in response to 0.1mM BzATP were treated with 0.5mM BzATP (saturating agonist), some individuals secreted modestly increased amounts of TG2 (Fig. 6.3 B), whereas others secreted modestly decreased amounts (Fig. 6.3 C). Notably, in both Fig. 6.3 B and C, treatment of cells with 0.5mM BzATP resulted in the release of full-length TG2, which is possibly due to non-specific leakage of a proportion of the content of the cells due to cell necrosis. Finally, there was also one individual where TG2 release only occurred at 0.5mM BzATP, with 0.1mM BzATP apparently being insufficient to induce TG2 secretion (Fig. 6.3 D). In this individual 0.5mM BzATP stimulation induced exclusively the processed form of TG2 suggesting that this individual harbours a receptor with reduced agonist sensitivity. However, cells from this individual have only been tested once, therefore to confirm that there are individuals who require higher agonist concentrations and to rule out experimental issues, this experiment will need repeating. In all cases, TG2 release occurred during the initial 10 minute BzATP application, and did not continue during the 30 minute chase period in the absence of BzATP.

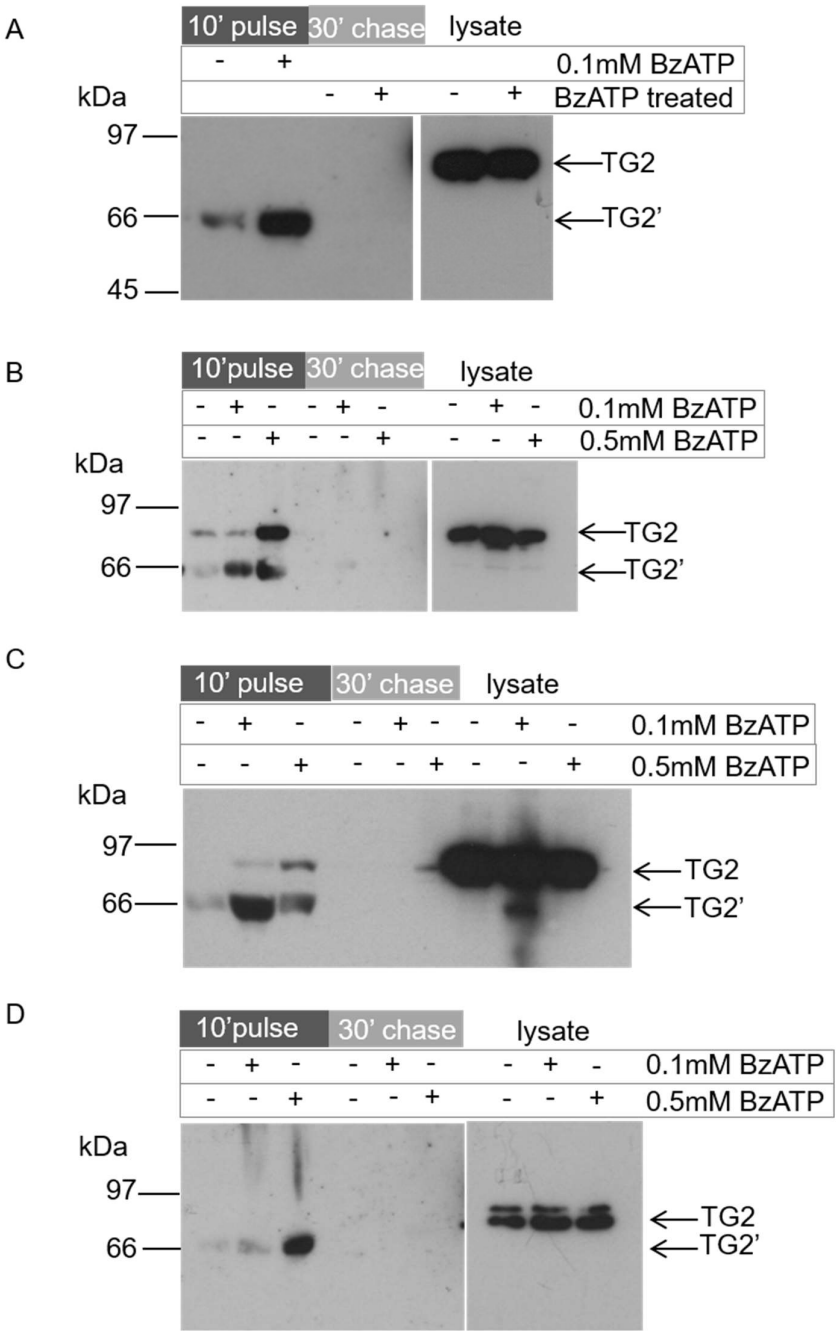

Fig. 6.3 Pattern of TG2 secretion in response to BzATP mediated activation of P2X7R in various individuals. A (VOL002, representative of three independent experiments), B (VOL014, experiment performed once), C (VOL006, representative of three independent experiments) and D (VOL008) (experiment performed once) M1 macrophages, generated as described in fig. 6.1, were stimulated using 0.1mM or 0.5mM BzATP in OptiMem or with OptiMem control alone for 10 minutes (pulse), then fresh OptiMem without BzATP was added for a further 30 minutes (chase).

Cells were lysed after stimulation and 500µl media or 10µl lysate were run on a 4-20% SDS PAGE gel under reducing conditions, and Western blotting performed for TG2 (CUB7402, 200ng/ml).

Although in many individuals TG2 release was observed in response to BzATP treatment, there were also individuals identified who did not release TG2 in response to either 0.1mM or 0.5mM BzATP (Fig. 6.4 A and B). This was five of the 16 (~31%) individuals tested. This suggests that while the majority of the population are capable of secreting TG2 in response to P2X7R activation, about 1/3 do not appear to do so. Despite lacking secretion of the processed form of TG2, the full length form of TG2 was still observed in the conditioned media after application of 0.5mM BzATP. This substantiates that the full-length enzyme is released in a different way than the processed enzyme, as discussed previously. Fig. 6.4 B shows an individual where a low level of TG2 secretion occurs at baseline, but does not increase in response to BzATP application. In these individuals, as seen for 'responders' (individuals who secrete TG2 in response to BzATP), there is no TG2 detected in the conditioned media during the 30 minute chase period. This indicates that the lack of TG2 secretion is not due to a delayed response. As the differences in TG2 secretion may relate to polymorphisms in P2X7R, DNA was extracted and sequencing performed in an attempt to identify the underlying mechanistic explanation.

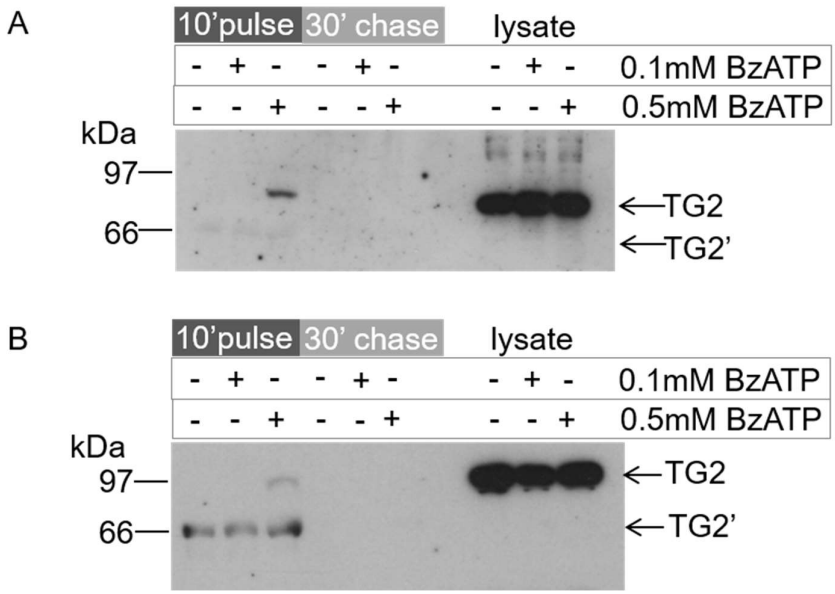

Fig. 6.4 Lack of response to BzATP treatment of M1 macrophages isolated from some individuals. A (VOL013, representative of two independent experiments) and B (VOL004, representative of two independent experiments) M1 macrophages, generated as described in fig. 6.1, were stimulated using 0.1mM or 0.5mM BzATP in OptiMem or OptiMem control for 10 minutes (pulse), then fresh OptiMem without BzATP added for a further 30 minutes (chase). Cells were lysed after stimulation and 500µl media or 10µl lysate were run on a 4-20% SDS PAGE gel under reducing conditions, and Western blotting performed for TG2 (CUB7402, 200ng/ml).

6.2.3. Identifying mutations in P2X7R affecting TG2 secretion

To investigate the potential involvement of P2X7R polymorphisms in differences in TG2 secretion, genomic DNA was extracted from whole blood and PCR performed to amplify individual exons (Fig. 6.5). The PCR product was run on a gel and the band of the appropriate length extracted. The resulting DNA was used for sequencing. So far, only four of the volunteers used have been sequenced fully, and hence only these can be used to allow assessment of the contribution of their mutations to TG2 release. The mutations found in these individuals are summarised in table 6.2.

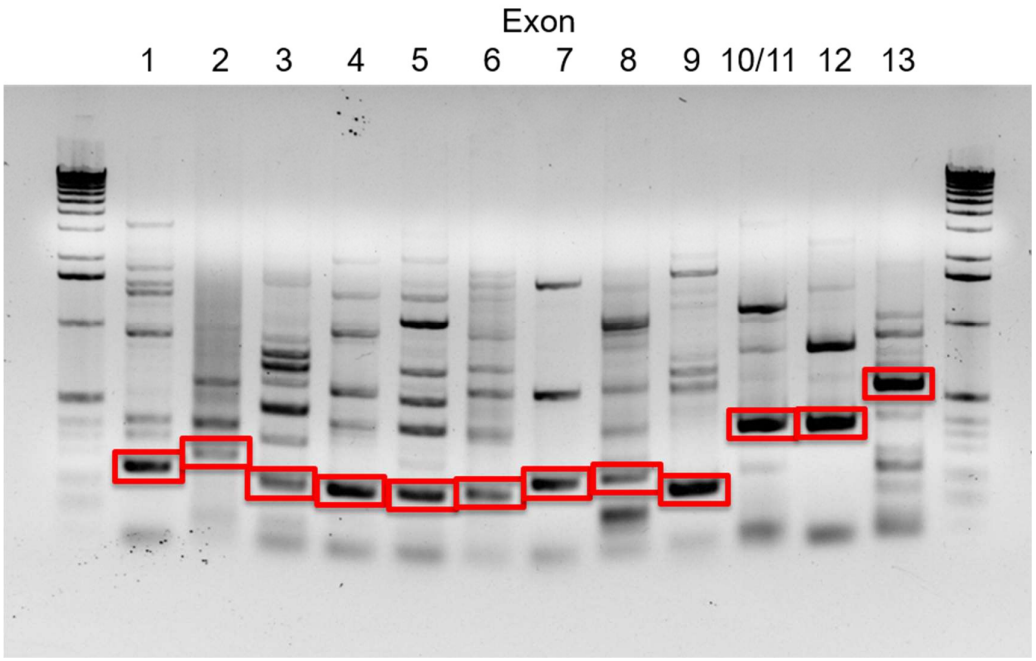

Fig. 6.5 PCR products of P2X7R exon amplification of VOL004 DNA. After PCR was performed to amplify individual P2X7R exons, a 1% agarose gel was run to allow extraction of the band of the desired size, ringed in red. Intense bands were gel extracted and DNA sequenced, less intense bands (for example, as seen here in exon 2) were used for a second round of PCR, then sequenced.

Table 6.2 Mutations present in fully sequenced individuals.

	TG2 secretion	V76A	H155Y	R270H	A348T	Q460R	E496A
VOL001	Y						
VOL004	N						
VOL006	Y						
VOL013	N						

No mutation
Heterozygous mutation
Homozygous mutation

Volunteer 004 and 013 were both found to lack secretion of TG2 in response to P2X7R activation. Both of these individuals have the $R^{270}H$ mutation, which is absent from the two fully sequenced volunteers who do release TG2 in response to P2X7R activation. None of the other SNPs identified were shared by these 2 individuals who fail to secrete TG2. However, $R^{270}H$ has been found in homozygote form in an individual who does secrete TG2 (Table 6.3 summarises all of the mutations found so far). VOL013 also contains the $A^{348}T$ mutation, also present in VOL006, who does secrete TG2, and $Q^{460}R$, which has also been identified in another individual who secretes TG2. VOL004 also has the $V^{76}A$ and $E^{496}A$ mutations, present in both of the fully sequenced responders and $H^{155}Y$, present in one of the other fully sequenced responders. These findings highlight the complexity of the polymorphisms of the P2X7R, where combinations of mutations may affect the functionality differently than an individual mutation, or the effect of mutations may be effectively cancelled out by the presence of another mutation. It is also important to highlight that these mutations were frequently heterozygous, indicating that the expressed receptors may not carry these mutations, or the mutation may be present in only some of the expressed receptors.

A summary of all of the mutations found so far is presented in table 6.3. Additional mutations were found, other than the ones present in the four individuals summarised above, in the other volunteers, however, due to a lack of sequence data for much of the P2X7R gene, it is not possible to meaningfully discuss these mutations in the context of TG2 secretion at this point. It appears that there are certain mutations that are likely to be present at a high frequency within the population. In particular, both $A^{348}T$ and $E^{496}A$ were found in 50% of the sequenced volunteers, suggesting that they are highly prevalent. They were also present with a high frequency in individuals who secrete TG2 on P2X7R activation, however, as the contribution of other mutations in combination with these has not been assessed, the direct involvement of these mutations cannot be confirmed or ruled out. On the other hand, several mutations appear to be rare, for example, the $T^{357}S$, which has so far only been identified in one individual who was capable of releasing TG2 in response to BzATP (at 0.5mM). The $S^{274}N$ mutation was also only identified in one individual, despite 13 of the 16 volunteers' DNA for the relevant exon having been sequenced. The individual carrying this mutation was incapable of secreting TG2 in response to BzATP treatment. Further

sequence analysis is required to establish the effect of these mutations on TG2 secretion. However, given that non-responders were relatively common, the underlying reason is unlikely to be rare SNPs.

Table 6.3 Summary of all mutations found so far in sequencing analysis. **Sample size refers to the number of volunteers for whom the relevant exon, in which that mutation would be found, has been sequenced. Number of affected individuals indicates the number of volunteers found to carry the indicated mutation. 'Responders' were those who release TG2 on P2X7R activation, and 'non-responders' were those who do not. *indicates that one of the individuals was the volunteer found to secreted TG2 only at 0.5mM BzATP.**

Mutation	Sample size	Nº affected individuals	Responders	Non-responders	ExAC frequency non-Finnish Caucasian
$V^{76}A$	5	3	2	1	0.068
$H^{155}Y$	5	2	1	1	0.39
$K^{160}N$	5	1	1	0	N/A
$R^{270}H$	13	5	1	4	0.26
$S^{274}N$	13	1	0	1	N/A
$G^{345}S$	8	1	1	0	N/A
$A^{348}T$	16	8	6*	2	0.39
$T^{357}S$	16	1	1*	0	0.077
$Q^{460}R$	16	2	1	1	0.17
$E^{496}A$	16	8	6	2	0.18

6.3. Discussion

The work presented in this chapter demonstrates that intrinsic differences exist with regards to TG2 secretion in different individuals. Approximately 69% of the individuals tested were capable of secreting TG2 in response to treatment with BzATP, with one of these individuals requiring 0.5mM BzATP for secretion to occur. The remaining 31% of individuals tested were unable to secrete TG2 in response to BzATP. This is consistent with previous data, which suggest that mutations causing loss of function in P2X7R are present in approximately 35% of the Caucasian population (Stokes *et al.* 2010). As the human P2X7R is known to be highly polymorphic, it was likely that this difference in TG2 secretion was due to specific mutations in P2X7R.

Genomic DNA sequence analysis identified changes that translated into amino acid sequence changes in every tested individual. The $V^{76}A$ mutation occurs in the extracellular domain of the receptor and has been linked to increased responses by the P2X7R, increasing both calcium uptake and ethidium uptake (Oyanguren-Desez *et al.* 2011), related to ion channel and membrane pore formation respectively. This mutation has been demonstrated to increase the effect of another common gain-of-function polymorphism, $H^{155}Y$, when expressed in the same receptor (Oyanguren-Desez *et al.* 2011). VOL006, who is a responder in terms of TG2 secretion and for whom complete P2X7R sequencing has been performed, is heterozygous for both $V^{76}A$ and $H^{155}Y$, as well as another polymorphism $A^{348}T$ that causes receptor hyperactivity. This individual is also heterozygous for $E^{496}A$, a mutation which has been identified to decrease receptor responses by 50% where it is heterozygous (Gu *et al.* 2001), as seen here in VOL006. The presence of this latter mutation could therefore downregulate the P2X7R response, returning it to a 'normal' level, effectively cancelling out some of the increased activity due to the other mutations. However, as absolute quantitation of TG2 secretion proved difficult, it remains unknown whether the TG2 secretion in this individual is increased in comparison to other individuals.

Similarly to VOL006, the non-responder VOL004 is also heterozygous for $V^{76}A$, $H^{155}Y$ and $E^{496}A$. In addition to these mutations, VOL004 has an $R^{270}H$ mutation, a loss of function polymorphism (Stokes *et al.* 2010). Therefore, in this case, the presence of both $E^{496}A$ and $R^{270}H$ loss of function polymorphisms is likely to be the cause of the lack of TG2 secretion, counteracting the effect of gain of function

polymorphisms, $V^{76}A$ and $H^{155}Y$. It has been shown previously that mutating $H^{155}Y$ and $H^{270}R$ back to their original amino acids in a variant also carrying $A^{348}T$ reduces the gain of function effect by 37%, suggesting that the $A^{348}T$ accounts for the majority of the hyperactivity seen in variants carrying this mutation (64% of the hyperactivity) (Stokes *et al.* 2010). This indicates that VOL004 is lacking the most important gain of function mutation, possibly explaining why VOL004 has a lack of TG2 secretion phenotype, despite containing two gain of function SNPs.

VOL013 is also heterozygous for $R^{270}H$, alongside $Q^{460}R$, which appears to have no substantial effects on P2X7R function (Roger *et al.* 2010). $Q^{460}R$ has been proposed to cause an increased response in P2X7R activity, although this is suggested to be due to its co-inheritance with the $A^{348}T$ mutation, known to cause gain of function in P2X7R (Stokes *et al.* 2010). VOL013 is homozygous for $A^{348}T$, suggesting that in this case the two mutations were co-inherited on one of the alleles, as has previously been predicted to be likely (Stokes *et al.* 2010). Despite the presence of the gain of function mutation, $A^{348}T$, VOL013 does not secrete TG2 in response to BzATP treatment, suggesting that the loss of function $R^{270}H$ mutation has a dominant effect.

VOL001 is homozygous for the $E^{496}A$ mutation, of which homozygosity has been shown to cause almost complete loss of P2X7R activity (Gu *et al.* 2001). Despite this, VOL001 was still capable of releasing TG2, possibly due to the presence of the $V^{76}A$ mutation on one allele, partially rescuing P2X7R function. This individual may show decreased TG2 secretion in comparison to what would be expected for a wild-type receptor, but due to the lack of an assay capable of quantifying the amount of TG2 in the media it was not possible to measure this. A commercial ELISA assay that was tried was shown to lack the necessary sensitivity. To enable more in-depth analysis of the effects of these mutations on TG2 secretion, an assay needs to be established allowing TG2 quantification and therefore comparison between individuals.

In all individuals, including those that were not fully sequenced, $E^{496}A$ and $A^{348}T$ were the most commonly occurring P2X7R polymorphisms. In general, these were more likely to be found in individuals who secreted TG2 in response to BzATP stimulation. For $A^{348}T$, this is as would be expected, given that it is a gain of function polymorphism (Stokes *et al.* 2010). As discussed previously, the $E^{469}A$ mutation reduces P2X7R function, and would therefore be expected to be found more commonly in non-

responders (Gu *et al.* 2001). However, linkage disequilibrium has been found between $E^{496}A$ and $H^{155}Y$ (Stokes *et al.* 2010), a mutation causing hyperactive function of the P2X7R (Portales-Cervantes *et al.* 2012). $H^{155}Y$ was also found in 2 of 5 individuals, and is possibly responsible for secretion occurring where the $E^{496}A$ mutation is also present. The $R^{270}H$ mutation was also found in a large number of sequenced individuals, with all but one being unable to secrete TG2. This is consistent with prior observations that $R^{270}H$ leads to reduction in ethidium uptake (Stokes *et al.* 2010), therefore being associated with reduced P2X7R pore formation, and consequently resulting in a decrease in TG2 secretion.

Some SNPs occur much less frequently, for example, $S^{274}N$ was identified in only one of 13 sequenced individuals. This mutation does not appear to have been previously reported in the literature, therefore the exact effects of this mutation on receptor function are unknown. The one individual identified as having this mutation did not secrete TG2 in response to BzATP stimulation suggesting that it may reduce receptor function. It is also possible that this individual has other mutations in P2X7R that lead to the reduction in function. The $G^{345}S$ mutation was also only identified in one individual out of 8 sequenced, however in this case the one individual was able to secrete TG2 in response to BzATP treatment. The $G^{345}S$ mutation to my knowledge is not specifically discussed in the literature, however a $G^{345}Y$ exchange has been introduced into the P2X7R by site-directed mutagenesis and overexpressed in microglia (Monif *et al.* 2009). In these cells, this mutation was found to prevent P2X7R membrane pore activity, without affecting the ion channel (Monif *et al.* 2009). This suggests that this residue is important for P2X7R pore formation. However, the specific effect of $G^{345}S$ substitution is unknown.

Due to the fact that each individual carries multiple heterozygous mutations, and possible cumulative effects of mutations on the same allele, it is difficult to assess the effects of each mutation, and the combination of mutations, on TG2 secretion. It will therefore be interesting to express combinations of these mutations in P2X7R in HEK293 cells, both in *cis* and in *trans*, to allow a more in depth analysis of their effects. However, as this encompasses a significant effort in experimentation, a first step should include the expansion of the current data set to more clearly identify the potential polymorphisms involved and therefore relevant to subseqently

systematically investigate. It is also important to note that the expression levels of each of the alleles are unknown, and could differ either due to regulation at the DNA or RNA level, leading to favoured expression of one allele, or at the protein level in terms of targeting the protein for degradation or lack of expression at the surface of the cell due to the presence of an unfavourable polymorphism. It is therefore not possible to know which receptor subunit is actually present at the cell surface, and in which combination and therefore to what extent the identified mutations were affecting TG2 secretion.

Chapter 7

7. General Discussion

In this thesis I have presented work which furthers our understanding of the mechanism of TG2 secretion in the context of inflammation. Our group has previously demonstrated that rapid TG2 secretion can be induced by P2X7R activation, in a manner independent of P2X7R ion channel function (Adamczyk 2013; Adamczyk *et al.* 2015). Here, I have demonstrated that this process relies on membrane-pore formation by the receptor, and ruled out any involvement of pannexin-1. P2X7R is activated by ATP (Burnstock 2007), which can be released by damaged cells (Lazarowski *et al.* 2003). This may occur in OA due to excessive mechanical stress experienced by joint tissues. Extracellular TG2 may then induce chondrocyte hypertrophy and tissue mineralisation (Aeschlimann *et al.* 1993; Aeschlimann *et al.* 1996; Johnson and Terkeltaub 2005), contributing to the pathology of OA. This presents the P2X7R as a possible target for pharmacological modulation to alter TG2 secretion and thereby alter the disease process. It is also possible that P2X7R polymorphisms could contribute to either disease susceptibility or disease severity and population screening for such polymorphisms could therefore aid in assessing disease risk in general or risk for progressive disease. Due to the involvement of TG2 in the generation of immunogenic neo-epitopes in RA, coeliac disease and possibly also OA, P2X7R modulation in any of these diseases may reduce disease burden or alleviate progressive autoimmunity by reduction of extracellular TG2 activity.

I investigated the role of TG2 activity regulation in its secretion. I found that the ability of TG2 to bind to GTP is essential for its secretion upon P2X7R activation. GTP binding may be required due to the conformation adopted by TG2 when this occurs (a compact, 'closed' conformation) (Pinkas *et al.* 2007). Although counterintuitive, this finding is supported by previous studies demonstrating that secretion of a TG2 GTP binding mutant is reduced (Johnson and Terkeltaub 2005). However, it is also possible that energy generated from hydrolysis of GTP is required in the export process. I have also demonstrated that in human cells the TG2-activating protein thioredoxin-1 is secreted through activation of P2X7R, as has also been demonstrated by Rothmeier *et al.* for mouse bone marrow cells (Rothmeier *et al.* 2015). However, my data suggest that thioredoxin-1 activity is not required for TG2 export per se. These findings demonstrate that the TG2 secreted through the P2X7R pathway is highly likely to be

active extracellularly, and due to a possible co-secretion with thioredoxin-1, this activity may be persistent in the context of inflammation and possibly drive disease processes.

Here, I have been able to translate these mechanistic findings from a HEK293 cell model to M1 macrophages derived from human peripheral blood monocytes, a physiologically relevant context as both P2X7R and TG2 are expressed in these cells and are of functional significance in innate immunity. The primary cells showed some differences in TG2 secretion when compared to the HEK293 model, likely to be due to expression of a wider panel of receptors capable of responding to ATP or ATP-derived products, as well as expression of components of the NLRP3 inflammasome pathway. Firstly, the secreted form of TG2 is a processed version, running at ~66kDa in SDS PAGE, instead of the expected 78kDa full-length form. It has been shown that the autoantibodies generated in Coeliac disease are unable to recognise cell surface associated TG2 and only recognise soluble TG2 (Iversen *et al.* 2013). As I observed that cell-surface associated TG2 is full-length, whereas the form in the soluble fraction is a 66kDa processed form, it is possible that the autoantibodies are specific to epitopes only exposed on this processed form. Therefore, the disease-generating form of TG2 may in fact be the 66kDa processed form of TG2 detected in conditioned media in my experiments. Secondly, in M1 macrophages, there also appears to be a role for caspase-1 in the secretion of TG2, which was unexpected as HEK293 cells do not express caspase-1 and were still capable of TG2 secretion. This suggests that caspase-1 involvement is not essential to the process, but is involved in some way. Caspase-1 may activate the protease involved in TG2 processing, or of another yet to be identified pathway contributing to TG2 secretion.

7.1 TG2 secretion involving vesicles

P2X7R activation has been shown to result in microvesicle shedding by cells (Pizzirani *et al.* 2007; Adamczyk *et al.* 2015). Previous work in our lab has shown that TG2 is absent from such microvesicles and is only present in the soluble protein fraction (Adamczyk *et al.* 2015). However, other studies have found that TG2 is released in microvesicles from cancer cells, in response to serum starvation (Antonyak *et al.* 2011). TG2 has also been suggested to be constitutively released in microvesicles from mouse vascular smooth muscle cells, in a manner dependent on TG2 activity

(van den Akker *et al.* 2012). We have demonstrated that regulated TG2 secretion as a result of P2X7R activation does not require enzymatic activity, as the $C^{277}S$ active site mutant is still externalised (Adamczyk *et al.* 2015). TG2 has been shown to localise to the surface of microvesicles after externalisation and to associate with fibronectin (Antonyak *et al.* 2011). Therefore, it is possible that TG2 is binding to the surface of the microvesicle after externalisation, and is not being secreted as the cargo of the microvesicles. Furher work is needed to clarify the relationship between membrane topology and TG2. The mechanism discovered by us results in large increases in extracellular TG2 on a very short time scale (10 minutes), in a regulated manner. This does not necessarily explain all of the previous findings and it is therefore possible that TG2 can be secreted through different mechanisms – one for constitutive release and another for acute release in specific situations (i.e. where extracellular ATP is elevated), requiring regulated TG2 secretion. This would allow rapid rises in the levels of extracellular TG2 during the inflammatory response, for example.

TG2 has also been proposed to be associated with recycling endosomes, through identification of TG2 in vesicles expressing Rab11 (a recycling endosome marker) (Zemskov *et al.* 2011). This process has been shown to require an interaction with phosphoinositides, as mutation of a binding motif in TG2, thought to be important for this interaction, reduced the level of TG2 at the cell surface (Zemskov *et al.* 2011). Preventing the fusion of endosomes with the plasma membrane also reduced the rate of TG2 secretion (Zemskov *et al.* 2011). The binding site for phosphoinositides in TG2 is located in the β-barrel 2 domain of TG2. However, absence of this domain has been shown to have no effect on TG2 secretion by another group (Chou *et al.* 2011), contradicting the data suggesting the phosphoinositide interaction is required for secretion. It is unclear whether these differences relate to the fact that different biological systems or cell types were employed and reflect true differences between different types of cells or whether technical limitations of the experimental approach lead to these contradictory conclusions. It is important to note that TG2 has also been shown to be actively endocytosed via LRP1 and transferrin receptor {Zemskov, 2007, Cell-surface transglutaminase undergoes internalization and lysosomal degradation: an essential role for LRP1} and hence retrograde transport from the surface would explain its presence in the endosome pathway.

7.2 The role of fibronectin or heparan sulphate binding in TG2 secretion

Several groups have assessed the impact of fibronectin binding on TG2 secretion. The N-terminal β-sandwich domain of TG2 was shown to be crucial for the interaction of TG2 with fibronectin, and absence of this domain prevented cell-surface association of TG2, potentially suggesting that export was also prevented (Gaudry *et al.* 1999){Cardoso, 2017, Dissecting the interaction between transglutaminase 2 and fibronectin}. Chou *et al.* demonstrated that this effect was related to deletion of aa88-106 in the β-sandwich domain. Addition of this motif to the core domain of TG2 (a construct lacking the β-sheet and both β-barrel domains) restored its externalisation (Chou *et al.* 2011). This suggested that fibronectin binding is involved in TG2 secretion, and that TG2 could be co-secreted with fibronectin. However, fibronectin knockout did not prevent TG2 secretion, suggesting it is a different effect of this domain rather than direct fibronectin binding that influences TG2 secretion (Chou *et al.* 2011). Introduction of either $D^{94}A$ or $D^{97}A$ mutations in this domain are proposed to disrupt the 3D structure of the loop formed by the fibronectin binding domain {Hang, 2005, Identification of a novel recognition sequence for fibronectin within the NH2-terminal beta-sandwich domain of tissue transglutaminase}. Either of these mutations alone was shown to reduce TG2 secretion by 50% and both together completely prevented secretion (Chou *et al.* 2011). Due to the position of these mutations, it is possible that the effect seen of mutations in this region on TG2 secretion are due to the conformational changes they induce, rather than fibronectin binding directly. As fibronectin is a conventionally secreted protein, it is highly unlikely that TG2 and fibronectin would be present in the same place inside the cell, due to the difference in secretory pathways. It is therefore more likely that the 'secretion' being measured is in fact binding of TG2 to fibronectin extracellularly, at the surface of the cell, after externalisation of both proteins via independent pathways.

TG2 has also been demonstrated to be capable of binding to heparan sulphates, in a GTP dependent manner, where GTP bound TG2 has a higher affinity for heparan sulphate than 'open' conformation TG2 {Lortat-Jacob, 2012, Transglutaminase-2 Interaction with Heparin: Identification of a heparin binding site that regulates cell adhesion to fibronectin-transglutaminase-2 matrix}. This could be consistent with my finding that GTP-binding of TG2 is required for its secretion and hence may be of

significance functionally. In syndecans-1 to -4, the proteoglycan makes up the protein core, with heparan sulphate side chains. Activation of MMPs results in proteolytic processing of syndecan, releasing the heparan sulphate-rich ectodomain into the extracellular environment (Brule *et al.* 2006), specifically syndecan-4 is cleaved by MMP2 or MMP9 (Chou *et al.* 2011). However, although termed 'secretion' in the literature, this is more likely to reflect release of TG2 from the cell surface which has previously been secreted by a different mechanism. General inhibition of MMPs resulted in reduced levels of TG2 in the extracellular matrix, suggesting that TG2 can be released through this mechanism (Wang *et al.* 2012). Inhibition of MMP2 and MMP9 specifically also reduced the amount of TG2 in the extracellular matrix, indicating that this is specifically due to binding to heparan sulphate side chains of syndecan-4 (Wang *et al.* 2012). The syndecan-4 knockout has also been linked to a reduced amount of extracellular TG2 in mouse models of chronic kidney disease. However, extracellular TG2 levels were similar in wild-type and syndecan-4 knockout healthy mice (Scarpellini *et al.* 2009). As TG2 is likely to interact with heparan sulphate extracellularly, at the cell surface, it is possible that this mechanism relates to release of TG2 from the cell surface after its secretion, rather than being the direct mechanism through which TG2 is secreted. Based on my experimental observations, I have proposed that cell-surface associated TG2 and TG2 found in the soluble fraction are secreted via different mechanisms. Therefore, syndecan binding may be part of the mechanism by which TG2 is externalised and then remains on the cell surface (although it can then be released by proteolysis), rather than the process of regulated protein export *per se*.

7.3 TG2 secretion in the context of unconventional secretion of other proteins

Conventional protein secretion occurs through targeting of a protein to the ER/Golgi pathway and then to the surface of the cell, due to the presence of an *N*-terminal or internal signal peptide (Nickel and Rabouille 2008). There are also proteins that are not secreted through this pathway; instead they can be secreted through a pathway involving the ER, but then being transported directly to the surface of the cell, bypassing the Golgi apparatus, or through one of several entirely ER/Golgi independent processes (Nickel and Rabouille 2008). TG2 is likely to be secreted

through a pathway independent of the ER/Golgi due to the absence of a signal peptide and a lack of glycosylation, expected if this pathway were the route for its secretion (Aeschlimann and Paulsson 1994).

There are several pathways for unconventional protein secretion, including i) a pathway involving secretory lysosomes, ii) the formation of multivesicular bodies, where ultimately endosomes containing vesicles fuse with the plasma membrane and release the vesicles to the extracellular environment, iii) proteins secreted by microvesicle shedding from the plasma membrane or iv) proteins secreted through selective transporters or intrinsic ability for formation of pores in the plasma membrane. These pathways have diverse activating signals, with P2X7R activation resulting in both microvesicle shedding and membrane pore formation (Virginio *et al.* 1999b; North 2002). This likens TG2 secretion most closely to either a pathway similar to that for IL-1β secretion or FGF2 secretion.

In immune cells, P2X7R activation results in assembly of the inflammasome and processing of pro-caspase-1 to active caspase-1 {Netea, 2009, Differential requirement for the activation of the inflammasome for processing and release of IL-1beta in monocytes and macrophages}. Caspase-1 is essential for the secretion of active IL-1β as the enzyme which processes pro-IL-1β, but has also been implicated in downstream steps in the secretion of IL-1β in microvesicles {Netea, 2009, Differential requirement for the activation of the inflammasome for processing and release of IL-1beta in monocytes and macrophages}{Pizzirani, 2007, Stimulation of P2 receptors causes release of IL-1beta-loaded microvesicles from human dendritic cells}. I have investigated aspects of this pathway in M1 macrophages, and demonstrated that inhibition of caspase-1 intracellularly prevents TG2 secretion. I was, however, unable to demonstrate a role for caspase-1 in the processing of TG2 itself. As HEK293 cells do not express caspase-1 and were capable of secreting TG2 on P2X7R activation, this suggests that caspase-1 can be involved in TG2 secretion, but is not essential. The involvement of caspase-1 may be in activation of another protease that process TG2 or in activation of another pathway which alters the kinetics of TG2 secretion, and hence, thereby having an indirect effect on TG2 secretion. This may explain the differences seen between TG2 secretion in HEK293 cells and primary human M1 macrophages.

Several studies have likened TG2 secretion to the process by which FGF2 is secreted, namely through a 'molecular trap' mechanism (Chou *et al.* 2011; Zemskov *et al.* 2011). Both TG2 and FGF2 secretion have been proposed to require an interaction with heparan sulphates (Zehe *et al.* 2006; Chou *et al.* 2011). FGF2 secretion involves formation of a membrane pore, through oligomerisation of FGF2 monomers (Muller *et al.* 2015). This process requires a component of the Na/K-ATPase, ATP1A1, which recruits FGF2 to the plasma membrane, allowing it to interact with $PI(4,5)P_2$, which aids oligomerisation and becomes part of the pore (Muller *et al.* 2015; Zacherl *et al.* 2015). This pore may then either disassemble outside the cell or allow passage of FGF2 monomers (La Venuta *et al.* 2015). Inhibition of the ATPase was demonstrated to reduce TG2 secretion, however blocking FGF2 secretion with sodium chlorate, failed to prevent TG2 secretion (Zemskov *et al.* 2011). As an unknown pore is involved in TG2 secretion, it is possible that components of this pathway are also involved in TG2 secretion and may therefore be worth further investigation.

Gasdermin D has been demonstrated to form a plasma membrane channel, in a process called pyroptosis (Shi *et al.* 2015). This is a form of cell death similar to necrosis, where there is pore formation and disruption of the plasma membrane and cell swelling (Shi *et al.* 2015). This results in leakage of the cell contents, releasing intracellular bacteria for killing by neutrophils (Miao *et al.* 2010). Active caspase-4/-5 (human), -11 (mouse) or -1 are capable of cleaving gasdermin D, to produce two fragments (Shi *et al.* 2015). The *N*-terminal fragment has been shown to be important for secretion of IL-1β and induction of pyroptosis (Shi *et al.* 2014) and the *C*-terminus was found to be released into the culture medium (He *et al.* 2015). The *N*-terminus has been demonstrated to be capable of forming ring-like structures in the cell membrane, functioning as large diameter pores (Aglietti *et al.* 2016). As the pore formed by gasdermin D is non-selective and large enough to allow secretion of cytokines such as IL-1β, it disrupts cell (membrane) integrity (Chen *et al.* 2016). Activation of gasdermin D may result in cross-talk from the caspase-4 mediated pyroptosis pathway to the NLRP3 inflammasome pathway, activating caspase-1, suggesting that activation of this inflammasome is downstream of gasdermin D, rather than upstream (Kayagaki *et al.* 2015). The ionophore, nigericin, is capable of activating NLRP3 and allowing recruitment of gasdermin D to this inflammasome (He *et al.* 2015). This suggests that conditions induced by P2X7R activation may conceivably also activate gasdermin D,

supported by evidence that mature IL-1β is secreted when gasdermin D is activated (He *et al.* 2015). I have demonstrated that TG2 secretion occurs in the absence of leakage of intracellular proteins (β-tubulin and IκBα), suggesting that a non-selective pore, such as that formed by gasdermin D is unlikely to be involved in this process. Nevertheless, it will be necessary to further investigate whether my conditions induce cleavage of gasdermin D, before it can be completely ruled out that the pyroptosis pathway is responsible for the observed secretion of TG2.

7.4 Limitations

As is expected with a project of this nature, there are several limitations in how these experiments were performed. Firstly, it would be preferable to measure TG2 secretion by ELISA or another quantitative assay, rather than relying on Western blotting and densitometry. However, in the case of TG2, there is not a sufficiently sensitive ELISA for detection in the conditioned medium from a relatively small number of cells as used here. Densitometry is usually performed by normalising data to a loading control, for example β-tubulin, the levels of which do not change within cells, however, as there is a lack of a secreted loading control, it was not possible to adjust for this. In the absence of another method of quantification densitometry was therefore used, however it would be useful in future to develop a more reliable method of quantification. ELISA would also allow direct comparison of TG2 secretion between all individuals tested, which could aid in also identifying whether TG2 secretion is enhanced in certain individuals, as well as being able to identify non-responders.

Secondly, it is important to note that the washes in between the 10 minute pulse and 30 minute chase could result in the release of ATP by the cells, which could drive the continued TG2 secretion seen in the HEK293 cells. However, as this continued secretion was not seen after agonist removal and the same wash steps in the human macrophages, it suggests that the continued secretion may in fact be occurring in the absence of agonist in HEK293 cells. It is possible that this is not a physiologically relevant observation, and these cells may lack some components of a pathway capable of quickly switching off P2X7R activation in the absence of agonist, as the 'switching off' of this mechanism appears to occur very quickly in the primary human macrophages.

The requirement for the use of an antibody directed to the intracellular *C*-terminus of P2X7R for immunostaining presents some problems with regards to ensuring surface expression. Permeabilising the cells means that cytoplasmic receptor was also stained, however, as demonstrated in chapter 3, alternative antibodies were explored and were not specific enough for use in immunostaining. This issue was addressed by measurement of total protein levels, to ensure a similar expression level, and immunostaining demonstrated membrane staining of both P2X7R variants. Use of functional assays, calcium flux and YO PRO-1 uptake, also demonstrate that P2X7R is surface expressed.

Finally, the use of 2.5mM $CaCl_2$ as a P2X7R inhibitor was not ideal, as it has the potential to affect other receptors. This was used as A740003 lacks inhibitory effects on other P2 receptors, but has poor solubility in H_2O, needing to be reconstituted in DMSO. As DMSO had profound effects on TG2 secretion, as discussed in chapter 5, it was therefore not possible to use this inhibitor. Other commercially available P2X7R inhibitors also have poor solubility in water, making them unsuitable for this application.

7.5 Future Objectives

In order to provide more evidence that TG2 secretion requires larger membrane pore formation than was shown in chapter 3, it would be necessary to first identify the pore forming component. As evidence suggests that this is a pore formed by the P2X7R itself, a high-resolution microscopy technique could be applied to capture images of P2X7R forming larger membrane pores to establish how this might occur. Alternatively, other components required for larger membrane pore formation could be identified through investigation of proteins capable of interacting with P2X7R, identifying possible candidates. Following identification of this larger membrane pore, it would be possible to apply inhibitors of this component and assess the effect on TG2 secretion.

It is also important to assess the activity of the processed form of secreted TG2 seen in macrophages, to assess which functions of TG2 are intact and to establish the exact nature of the processing, as was begun in this thesis. Further work is also required to connect specific P2X7R polymorphisms to enhanced or decreased TG2 secretion.

Sequencing information gathered so far will advise us as to combinations of P2X7R polymorphisms present in the human population. Variants can then be generated and expressed in HEK293 cells to perform functional studies to assess how these combinations affect P2X7R functions. Analysis of sequencing data from patients e.g. osteoarthritis patients of coeliac disease patients may further identify common polymorphisms in these groups which could result in increased TG2 secretion and therefore impact disease risk. It could also identify polymorphisms present at a lower frequency in these populations, suggesting possible protective functions. This information could eventually be used for screening for disease susceptibility and potential patient stratification. This could then advise further treatment options, possibly using P2X7R antagonists in patients where they are most likely to be effective.

To complete work performed regarding TG2 GTP binding mutants, the hydrolysis of these mutants needs to be assessed to confirm that any changes in TG2 secretion are related to conformational change, as current data indicates, rather than a requirement for hydrolysis. This work is being performed as part of another sutdents' PhD within the group. It will also be interesting to assess the structure of the $K^{173}L$ TG2 in the presence and absence of GTP to confirm the hypothesis that this mutant forms an alternative structure, as demonstrated in fig 4.14.

I am continuing this work with a one year post-doc project, aiming to investigate the effect of P2X7R polymorphisms on TG2 secretion (in healthy volunteers) and whether specific P2X7R polymorphisms are present in coeliac disease patients. In parallel with this I will also investigate further the mechanistic process by which TG2 is externalised. The specific objectives are as follows:

1. To investigate the role of P2X7R polymorphisms in altered TG2 secretion further, through recruiting more volunteers allowing us to better correlate TG2 secretion to receptor polymorphisms.
2. To investigate the role of P2X7R mediated TG2 secretion in the context of antigen presentation in coeliac disease.
3. Understanding the details of the mechanism of TG2 secretion by further investigating the involvement of caspase-1 and to assess whether P2X7R

activation alone can induce cleavage of gasdermin D, and begin the process of pyroptosis.

4. Investigate the nature of and proteolytic enzyme responsible for TG2 processing in M1 macrophages.

Adamczyk, M. (2013). Biomarkers for arthritis: Regulation of extracellular transglutaminase activity by non-conventional export. Thesis PhD, Cardiff University.

Adamczyk, M., Griffiths, R., Dewitt, S., Knauper, V. and Aeschlimann, D. (2015). P2X7 receptor activation regulates rapid unconventional export of transglutaminase-2. *J Cell Sci* **128:**4615-4628.

Adamczyk, M., Heil, A. and Aeschlimann, D. (2013). Real-time fluorescence assay for monitoring transglutaminase activity. *BMG Labtech Application Note* **234**.

Adinolfi, E., Cirillo, M., Woltersdorf, R., Falzoni, S., Chiozzi, P., Pellegatti, P., Callegari, M. G. *et al.* (2010). Trophic activity of a naturally occurring truncated isoform of the P2X7 receptor. *Faseb j* **24:**3393-3404.

Adriouch, S., Dox, C., Welge, V., Seman, M., Koch-Nolte, F. and Haag, F. (2002). Cutting edge: a natural P451L mutation in the cytoplasmic domain impairs the function of the mouse P2X7 receptor. *J Immunol* **169:**4108-4112.

Aeschlimann, D., Mosher, D. and Paulsson, M. (1996). Tissue transglutaminase and factor XIII in cartilage and bone remodeling. *Semin Thromb Hemost* **22:**437-443.

Aeschlimann, D. and Paulsson, M. (1991). Cross-linking of laminin-nidogen complexes by tissue transglutaminase. A novel mechanism for basement membrane stabilization. *J Biol Chem* **266:**15308-15317.

Aeschlimann, D. and Paulsson, M. (1994). Transglutaminases: protein cross-linking enzymes in tissues and body fluids. *Thromb Haemost* **71:**402-415.

Aeschlimann, D. and Thomazy, V. (2000). Protein crosslinking in assembly and remodelling of extracellular matrices: the role of transglutaminases. *Connect Tissue Res* **41:**1-27.

Aeschlimann, D., Wetterwald, A., Fleisch, H. and Paulsson, M. (1993). Expression of tissue transglutaminase in skeletal tissues correlates with events of terminal differentiation of chondrocytes. *J Cell Biol* **120:**1461-1470.

Aglietti, R. A., Estevez, A., Gupta, A., Ramirez, M. G., Liu, P. S., Kayagaki, N., Ciferri, C. *et al.* (2016). GsdmD p30 elicited by caspase-11 during pyroptosis forms pores in membranes. *Proc Natl Acad Sci U S A* **113:**7858-7863.

Ahvazi, B., Boeshans, K. M., Idler, W., Baxa, U. and Steinert, P. M. (2003). Roles of calcium ions in the activation and activity of the transglutaminase 3 enzyme. *J Biol Chem* **278:**23834-23841.

Ai, L., Skehan, R. R., Saydi, J., Lin, T. and Brown, K. D. (2012). Ataxia-Telangiectasia, Mutated (ATM)/Nuclear Factor kappa light chain enhancer of activated B cells (NFkappaB) signaling controls basal and DNA damage-induced transglutaminase 2 expression. *J Biol Chem* **287:**18330-18341.

Akimov, S. S. and Belkin, A. M. (2001). Cell surface tissue transglutaminase is involved in adhesion and migration of monocytic cells on fibronectin. *Blood* **98:**1567-1576.

Akimov, S. S., Krylov, D., Fleischman, L. F. and Belkin, A. M. (2000). Tissue transglutaminase is an integrin-binding adhesion coreceptor for fibronectin. *J Cell Biol* **148:**825-838.

Al-Shukaili, A., Al-Kaabi, J. and Hassan, B. (2008). A comparative study of interleukin-1beta production and p2x7 expression after ATP stimulation by peripheral blood mononuclear cells isolated from rheumatoid arthritis patients and normal healthy controls. *Inflammation* **31:**84-90.

Alberto, A. V., Faria, R. X., Couto, C. G., Ferreira, L. G., Souza, C. A., Teixeira, P. C., Froes, M. M. *et al.* (2013). Is pannexin the pore associated with the P2X7 receptor? *Naunyn Schmiedebergs Arch Pharmacol* **386:**775-787.

Almami, I., Dickenson, J. M., Hargreaves, A. J. and Bonner, P. L. (2014). Modulation of transglutaminase 2 activity in H9c2 cells by PKC and PKA signalling: a role for transglutaminase 2 in cytoprotection. *Br J Pharmacol* **171:**3946-3960.

Alonso-Torre, S. R. and Trautmann, A. (1993). Calcium responses elicited by nucleotides in macrophages. Interaction between two receptor subtypes. *J Biol Chem* **268:**18640-18647.

Al-Shukaili, A., Al-Kaabi, J., Hassan, B., Al-Araimi, T., Al-Tobi, M., Al-Kindi, M., Al-Maniri, A. *et al.* (2011). P2X7 receptor gene polymorphism analysis in rheumatoid arthritis. *International Journal of Immunogenetics* **38:**389-396.

Andrei, C., Dazzi, C., Lotti, L., Torrisi, M. R., Chimini, G. and Rubartelli, A. (1999). The secretory route of the leaderless protein interleukin 1beta involves exocytosis of endolysosome-related vesicles. *Mol Biol Cell* **10:**1463-1475.

Antonyak, M. A., Jansen, J. M., Miller, A. M., Ly, T. K., Endo, M. and Cerione, R. A. (2006). Two isoforms of tissue transglutaminase mediate opposing cellular fates. *Proc Natl Acad Sci U S A* **103:**18609-18614.

Antonyak, M. A., Li, B., Boroughs, L. K., Johnson, J. L., Druso, J. E., Bryant, K. L., Holowka, D. A. *et al.* (2011). Cancer cell-derived microvesicles induce transformation by transferring tissue transglutaminase and fibronectin to recipient cells. *Proc Natl Acad Sci U S A* **108:**4852-4857.

Anwar, R. and Miloszewski, K. J. (1999). Factor XIII deficiency. *Br J Haematol* **107:**468-484.

Arend, W. P., Malyak, M., Smith, M. F., Jr., Whisenand, T. D., Slack, J. L., Sims, J. E., Giri, J. G. *et al.* (1994). Binding of IL-1 alpha, IL-1 beta, and IL-1 receptor antagonist by soluble IL-1 receptors and levels of soluble IL-1 receptors in synovial fluids. *J Immunol* **153:**4766-4774.

Arner, E. S., Bjornstedt, M. and Holmgren, A. (1995). 1-Chloro-2,4-dinitrobenzene is an irreversible inhibitor of human thioredoxin reductase. Loss of thioredoxin disulfide reductase activity is accompanied by a large increase in NADPH oxidase activity. *J Biol Chem* **270:**3479-3482.

Arner, E. S. and Holmgren, A. (2000). Physiological functions of thioredoxin and thioredoxin reductase. *Eur J Biochem* **267:**6102-6109.

Aschrafi, A., Sadtler, S., Niculescu, C., Rettinger, J. and Schmalzing, G. (2004). Trimeric architecture of homomeric P2X2 and heteromeric P2X1+2 receptor subtypes. *J Mol Biol* **342:**333-343.

Attur, M., Statnikov, A., Samuels, J., Li, Z., Alekseyenko, A. V., Greenberg, J. D., Krasnokutsky, S. *et al.* (2015). Plasma levels of interleukin-1 receptor antagonist (IL1Ra) predict radiographic progression of symptomatic knee osteoarthritis. *Osteoarthritis Cartilage* **23:**1915-1924.

Auton, A., Brooks, L. D., Durbin, R. M., Garrison, E. P., Kang, H. M., Korbel, J. O., Marchini, J. L. *et al.* (2015). A global reference for human genetic variation. *Nature* **526:**68-74.

Baek, K. J., Das, T., Gray, C., Antar, S., Murugesan, G. and Im, M. J. (1993). Evidence that the Gh protein is a signal mediator from alpha 1-adrenoceptor to a phospholipase C. I. Identification of alpha 1-adrenoceptor-coupled Gh family and purification of Gh7 from bovine heart. *J Biol Chem* **268:**27390-27397.

Baek, K. J., Kang, S., Damron, D. and Im, M. (2001). Phospholipase Cdelta1 is a guanine nucleotide exchanging factor for transglutaminase II (Galpha h) and promotes alpha 1B-adrenoreceptor-mediated GTP binding and intracellular calcium release. *J Biol Chem* **276:**5591-5597.

Balajthy, Z., Csomos, K., Vamosi, G., Szanto, A., Lanotte, M. and Fesus, L. (2006). Tissue-transglutaminase contributes to neutrophil granulocyte differentiation and functions. *Blood* **108:**2045-2054.

Balklava, Z., Verderio, E., Collighan, R., Gross, S., Adams, J. and Griffin, M. (2002). Analysis of tissue transglutaminase function in the migration of Swiss 3T3 fibroblasts: the active-state conformation of the enzyme does not affect cell motility but is important for its secretion. *J Biol Chem* **277:**16567-16575.

Bao, L., Sachs, F. and Dahl, G. (2004). Connexins are mechanosensitive. *Am J Physiol Cell Physiol* **287:**C1389-1395.

Barbour, K. E., Helmick, C. G., Boring, M. and Brady, T. J. (2017). Vital Signs: Prevalence of Doctor-Diagnosed Arthritis and Arthritis-Attributable Activity Limitation. *MMWR* **66:**246-253.

Barden, N., Harvey, M., Gagne, B., Shink, E., Tremblay, M., Raymond, C., Labbe, M. *et al.* (2006). Analysis of single nucleotide polymorphisms in genes in the chromosome 12Q24.31 region points to P2RX7 as a susceptibility gene to bipolar affective disorder. *Am J Med Genet B Neuropsychiatr Genet* **141b:**374-382.

Bay-Jensen, A. C., Reker, D., Kjelgaard-Petersen, C. F., Mobasheri, A., Karsdal, M. A., Ladel, C., Henrotin, Y. *et al.* (2016). Osteoarthritis year in review 2015: soluble biomarkers and the BIPED criteria. *Osteoarthritis Cartilage* **24:**9-20.

Bayardo, M., Punzi, F., Bondar, C., Chopita, N. and Chirdo, F. (2012). Transglutaminase 2 expression is enhanced synergistically by interferon-γ and tumour necrosis factor-α in human small intestine. *Clin Exp Immunol* **168:**95-104.

Begg, G. E., Carrington, L., Stokes, P. H., Matthews, J. M., Wouters, M. A., Husain, A., Lorand, L. *et al.* (2006a). Mechanism of allosteric regulation of transglutaminase 2 by GTP.*Proc Natl Acad Sci U S A*. Vol. 103. pp. 19683-19688.

Begg, G. E., Holman, S. R., Stokes, P. H., Matthews, J. M., Graham, R. M. and Iismaa, S. E. (2006b). Mutation of a Critical Arginine in the GTP-binding Site of Transglutaminase 2 Disinhibits Intracellular Cross-linking Activity. *J Biol Chem* **281:**12603-12609.

Beninati, S. and Piacentini, M. (2004). The transglutaminase family: an overview: minireview article. *Amino Acids* **26:**367-372.

Bertini, R., Howard, O. M., Dong, H. F., Oppenheim, J. J., Bizzarri, C., Sergi, R., Caselli, G. *et al.* (1999). Thioredoxin, a redox enzyme released in infection and inflammation, is a unique chemoattractant for neutrophils, monocytes, and T cells. *J Exp Med* **189:**1783-1789.

Bodin, P. and Burnstock, G. (1998). Increased release of ATP from endothelial cells during acute inflammation. *Inflamm Res* **47:**351-354.

Bradley, H. J., Baldwin, J. M., Goli, G. R., Johnson, B., Zou, J., Sivaprasadarao, A., Baldwin, S. A. *et al.* (2011). Residues 155 and 348 contribute to the determination of P2X7 receptor function via distinct mechanisms revealed by single-nucleotide polymorphisms. *J Biol Chem* **286:**8176-8187.

Brederson, J. D. and Jarvis, M. F. (2008). Homomeric and heteromeric P2X3 receptors in peripheral sensory neurons. *Curr Opin Investig Drugs* **9:**716-725.

Browne, L. E., Compan, V., Bragg, L. and North, R. A. (2013). P2X7 receptor channels allow direct permeation of nanometer-sized dyes. *J Neurosci* **33:**3557-3566.

Brule, S., Charnaux, N., Sutton, A., Ledoux, D., Chaigneau, T., Saffar, L. and Gattegno, L. (2006). The shedding of syndecan-4 and syndecan-1 from HeLa cells and human primary macrophages is accelerated by SDF-1/CXCL12 and mediated by the matrix metalloproteinase-9. *Glycobiology* **16:**488-501.

Bruzzone, R., Barbe, M. T., Jakob, N. J. and Monyer, H. (2005). Pharmacological properties of homomeric and heteromeric pannexin hemichannels expressed in Xenopus oocytes. *J Neurochem* **92:**1033-1043.

Bruzzone, R. and Dermietzel, R. (2006). Structure and function of gap junctions in the developing brain. *Cell Tissue Res* **326:**239-248.

Burnstock, G. (2007). Purine and pyrimidine receptors. *Cell Mol Life Sci* **64:**1471-1483.

Burnstock, G. and Kennedy, C. (1985). Is There a Basis for Distinguishing Two Types of P2-Purinoceptor? *Gen Pharmacol* **16:**433-440.

Cabrini, G., Falzoni, S., Forchap, S. L., Pellegatti, P., Balboni, A., Agostini, P., Cuneo, A. *et al.* (2005). A His-155 to Tyr polymorphism confers gain-of-function to the human P2X7 receptor of human leukemic lymphocytes. *J Immunol* **175:**82-89.

Campwala, H., Sexton, D. W., Crossman, D. C. and Fountain, S. J. (2014). P2Y(6) receptor inhibition perturbs CCL2-evoked signalling in human monocytic and peripheral blood mononuclear cells. *J Cell Sci* **127:**4964-4973.

Candi, E., Oddi, S., Paradisi, A., Terrinoni, A., Ranalli, M., Teofoli, P., Citro, G. *et al.* (2002). Expression of transglutaminase 5 in normal and pathologic human epidermis. *J Invest Dermatol* **119:**670-677.

Cao, Q., Zhong, X. Z., Zou, Y., Murrell-Lagnado, R., Zhu, M. X. and Dong, X. P. (2015). Calcium release through P2X4 activates calmodulin to promote endolysosomal membrane fusion. *J Cell Biol* **209:**879-894.

Caseley, E. A., Muench, S. P., Roger, S., Mao, H. J., Baldwin, S. A. and Jiang, L. H. (2014). Non-synonymous single nucleotide polymorphisms in the P2X receptor genes: association with diseases, impact on receptor functions and potential use as diagnosis biomarkers. *Int J Mol Sci* **15:**13344-13371.

Cassidy, A. J., van Steensel, M. A., Steijlen, P. M., van Geel, M., van der Velden, J., Morley, S. M., Terrinoni, A. *et al.* (2005). A homozygous missense mutation in TGM5 abolishes epidermal transglutaminase 5 activity and causes acral peeling skin syndrome. *Am J Hum Genet* **77:**909-917.

Cauwels, A., Rogge, E., Vandendriessche, B., Shiva, S. and Brouckaert, P. (2014). Extracellular ATP drives systemic inflammation, tissue damage and mortality. *Cell Death Dis* **5:**e1102.

Cerio, R., Griffiths, C. E. M., Cooper, K. D., Nickoloff, B. J. and Headington, J. T. (1989). Characterization of factor-XIIIA positive dermal dendritic cells in normal and inflamed skin. *British Journal of Dermatology* **121:**421-431.

Cesaro, A., Brest, P., Hofman, V., Hebuterne, X., Wildman, S., Ferrua, B., Marchetti, S. *et al.* (2010). Amplification loop of the inflammatory process is induced by P2X7R activation in intestinal epithelial cells in response to neutrophil transepithelial migration. *Am J Physiol Gastrointest Liver Physiol* **299:**G32-42.

Cheewatrakoolpong, B., Gilchrest, H., Anthes, J. C. and Greenfeder, S. (2005). Identification and characterization of splice variants of the human P2X7 ATP channel. *Biochem Biophys Res Commun* **332:**17-27.

Chekeni, F. B., Elliott, M. R., Sandilos, J. K., Walk, S. F., Kinchen, J. M., Lazarowski, E. R., Armstrong, A. J. *et al.* (2010). Pannexin 1 channels mediate 'find-me' signal release and membrane permeability during apoptosis. *Nature* **467:**863-867.

Chen, C.-C., Akopian, A. N., Sivilottit, L., Colquhoun, D., Burnstock, G. and Wood, J. N. (1995). A P2X purinoceptor expressed by a subset of sensory neurons. *Nature* **377:**428-431.

Chen, X., He, W., Hu, L., Li, J., Fang, Y., Wang, X., Xu, X. *et al.* (2016). Pyroptosis is driven by non-selective gasdermin-D pore and its morphology is different from MLKL channel-mediated necroptosis. *Cell Res* **26:**1007-1020.

Cheng, T., Hitomi, K., van Vlijmen-Willems, I. M., de Jongh, G. J., Yamamoto, K., Nishi, K., Watts, C. *et al.* (2006). Cystatin M/E is a high affinity inhibitor of cathepsin V and cathepsin L by a reactive site that is distinct from the legumain-binding site. A novel clue for the role of cystatin M/E in epidermal cornification. *J Biol Chem* **281:**15893-15899.

Chessell, I. P., Hatcher, J. P., Bountra, C., Michel, A. D., Hughes, J. P., Green, P., Egerton, J. *et al.* (2005). Disruption of the P2X7 purinoceptor gene abolishes chronic inflammatory and neuropathic pain. *Pain* **114:**386-396.

Chou, C. Y., Streets, A. J., Watson, P. F., Huang, L., Verderio, E. A. and Johnson, T. S. (2011). A crucial sequence for transglutaminase type 2 extracellular trafficking in renal tubular epithelial cells lies in its N-terminal beta-sandwich domain. *J Biol Chem* **286:**27825-27835.

Christgau, S., Garnero, P., Fledelius, C., Moniz, C., Ensig, M., Gineyts, E., Rosenquist, C. *et al.* (2001). Collagen type II C-telopeptide fragments as an index of cartilage degradation. *Bone* **29:**209-215.

Citron, B. A., SantaCruz, K. S., Davies, P. J. and Festoff, B. W. (2001). Intron-exon swapping of transglutaminase mRNA and neuronal Tau aggregation in Alzheimer's disease. *J Biol Chem* **276:**3295-3301.

Clifford, E. E., Parker, K., Humphreys, B. D., Kertesy, S. B. and Dubyak, G. R. (1998). The P2X1 Receptor, an Adenosine Triphosphate–Gated Cation Channel, Is Expressed in Human Platelets but not in Human Blood Leukocytes. *Blood* **91:**3172-3181.

Cockayne, D. A., Hamilton, S. G., Zhu, Q. M., Dunn, P. M., Zhong, Y., Novakovic, S., Malmberg, A. B. *et al.* (2000). Urinary bladder hyporeflexia and reduced pain-related behaviour in P2X3-deficient mice. *Nature* **407:**1011-1015.

Coddou, C., Yan, Z., Obsil, T., Huidobro-Toro, J. P., Stojilkovic, S. S. and Sibley, D. R. (2011). Activation and Regulation of Purinergic P2X Receptor Channels. *Pharm Rev* **63:**641-683.

Communi, D., Parmentier, M. and Boeynaems, J. M. (1996). Cloning, functional expression and tissue distribution of the human P2Y6 receptor. *Biochem Biophys Res Commun* **222:**303-308.

Compan, V., Ulmann, L., Stelmashenko, O., Chemin, J., Chaumont, S. and Rassendren, F. (2012). P2X2 and P2X5 Subunits Define a New Heteromeric Receptor with P2X7-Like Properties. *J Neurosci* **32:**4282-4296.

Connon, C. J., Young, R. D. and Kidd, E. J. (2003). P2X(7) receptors are redistributed on human monocytes after pore formation in response to prolonged agonist exposure. *Pharmacology* **67:**163-168.

Corriden, R. and Insel, P. A. (2010). Basal release of ATP: an autocrine-paracrine mechanism for cell regulation. *Sci Signal* **3:**re1.

Costa-Junior, H. M., Sarmento Vieira, F. and Coutinho-Silva, R. (2011). C terminus of the P2X7 receptor: treasure hunting. *Purinergic Signal* **7:**7-19.

Coutinho-Silva, R. and Persechini, P. M. (1997). P2Z purinoceptor-associated pores induced by extracellular ATP in macrophages and J774 cells. *Am J Physiol* **273:**C1793-1800.

Cowen, D. S., Lazarus, H. M., Shurin, S. B., Stoll, S. E. and Dubyak, G. R. (1989). Extracellular adenosine triphosphate activates calcium mobilization in human phagocytic leukocytes and neutrophil/monocyte progenitor cells. *J Clin Invest* **83:**1651-1660.

Curtis, C. G., Stenberg, P., Brown, K. L., Baron, A., Chen, K., Gray, A., Simpson, I. *et al.* (1974). Kinetics of transamidating enzymes - production of thiol in reactions of thiol esters with fibrinoligase. *Biochemistry* **13:**3257-3262.

Datta, S., Antonyak, M. A. and Cerione, R. A. (2007). GTP-binding-defective forms of tissue transglutaminase trigger cell death. *Biochemistry* **46:**14819-14829.

Davis, C. J., Taishi, P., Honn, K. A., Koberstein, J. N. and Krueger, J. M. (2016). P2X7 receptors in body temperature, locomotor activity, and brain mRNA and lncRNA responses to sleep deprivation. *Am J Physiol Regul Integr Comp Physiol* **311:**R1004-r1012.

de Baaij, J. H. F., Kompatscher, A., Viering, D., Bos, C., Bindels, R. J. M. and Hoenderop, J. G. J. (2016). P2X6 Knockout Mice Exhibit Normal Electrolyte Homeostasis. *PLoS One* **11**.

De Laurenzi, V. and Melino, G. (2001). Gene disruption of tissue transglutaminase. *Mol Cell Biol* **21:**148-155.

Dean, M. D. (2013). Genetic disruption of the copulatory plug in mice leads to severely reduced fertility. *PLoS Genet* **9:**e1003185.

Deasey, S., Grichenko, O., Du, S. and Nurminskaya, M. (2012). Characterization of the Transglutaminase Gene Family in Zebrafish and in vivo Analysis of Transglutaminase-Dependent Bone Mineralization. *Amino Acids* **42:**1065-1075.

Dell'Antonio, G., Quattrini, A., Cin, E. D., Fulgenzi, A. and Ferrero, M. E. (2002). Relief of inflammatory pain in rats by local use of the selective P2X7 ATP receptor inhibitor, oxidized ATP. *Arthritis Rheum* **46:**3378-3385.

Denlinger, L. C., Coursin, D. B., Schell, K., Angelini, G., Green, D. N., Guadarrama, A. G., Halsey, J. *et al.* (2006). Human P2X7 pore function predicts allele linkage disequilibrium. *Clin Chem* **52:**995-1004.

Denlinger, L. C., Fisette, P. L., Sommer, J. A., Watters, J. J., Prabhu, U., Dubyak, G. R., Proctor, R. A. *et al.* (2001). Cutting edge: the nucleotide receptor P2X7 contains multiple protein- and lipid-interaction motifs including a potential binding site for bacterial lipopolysaccharide. *J Immunol* **167:**1871-1876.

Di Virgilio, F., Chiozzi, P., Ferrari, D., Falzoni, S., Sanz, J. M., Morelli, A., Torboli, M. *et al.* (2001). Nucleotide receptors: an emerging family of regulatory molecules in blood cells. *Blood* **97:**587-600.

Diaz-Hernandez, J. I., Gomez-Villafuertes, R., Leon-Otegui, M., Hontecillas-Prieto, L., Del Puerto, A., Trejo, J. L., Lucas, J. J. *et al.* (2012). In vivo P2X7 inhibition reduces amyloid plaques in Alzheimer's disease through GSK3beta and secretases. *Neurobiol Aging* **33:**1816-1828.

Diaz-Hernandez, M., Cox, J. A., Migita, K., Haines, W., Egan, T. M. and Voigt, M. M. (2002). Cloning and characterization of two novel zebrafish P2X receptor subunits. *Biochem Biophys Res Commun* **295:**849-853.

Diaz-Hernandez, M., Diez-Zaera, M., Sanchez-Nogueiro, J., Gomez-Villafuertes, R., Canals, J. M., Alberch, J., Miras-Portugal, M. T. *et al.* (2009). Altered P2X7-receptor level and function in mouse models of Huntington's disease and therapeutic efficacy of antagonist administration. *Faseb j* **23:**1893-1906.

Dieterich, W., Ehnis, T., Bauer, M., Donner, P., Volta, U., Riecken, E. O. and Schuppan, D. (1997). Identification of tissue transglutaminase as the autoantigen of celiac disease. *Nat Med* **3:**797-801.

Ding, S. and Sachs, F. (1999). Single channel properties of P2X2 purinoceptors. *J Gen Physiol* **113:**695-720.

Eckert, R. L., Kaartinen, M. T., Nurminskaya, M., Belkin, A. M., Colak, G., Johnson, G. V. W. and Mehta, K. (2014). Transglutaminase Regulation of Cell Function.*Physiol Rev*. Vol. 94. pp. 383-417.

Egberts, F., Heinrich, M., Jensen, J. M., Winoto-Morbach, S., Pfeiffer, S., Wickel, M., Schunck, M. *et al.* (2004). Cathepsin D is involved in the regulation of transglutaminase 1 and epidermal differentiation. *J Cell Sci* **117:**2295-2307.

Eickhorst, A. N., Berson, A., Cockayne, D., Lester, H. A. and Khakh, B. S. (2002). Control of P2X2 Channel Permeability by the Cytosolic Domain. *J Gen Physiol* **120:**119-131.

Eklund, H., Cambillau, C., Sjoberg, B. M., Holmgren, A., Jornvall, H., Hoog, J. O. and Branden, C. I. (1984). Conformational and functional similarities between glutaredoxin and thioredoxins. *Embo j* **3:**1443-1449.

Elisia, I., Nakamura, H., Lam, V., Hofs, E., Cederberg, R., Cait, J., Hughes, M. R. *et al.* (2016). DMSO Represses Inflammatory Cytokine Production from Human Blood Cells and Reduces Autoimmune Arthritis. *PLoS One* **11:**e0152538.

Eltzschig, H. K., Eckle, T., Mager, A., Kuper, N., Karcher, C., Weissmuller, T., Boengler, K. *et al.* (2006). ATP release from activated neutrophils occurs via connexin 43 and modulates adenosine-dependent endothelial cell function. *Circ Res* **99:**1100-1108.

Eltzschig, H. K., Sitkovsky, M. V. and Robson, S. C. (2012). Purinergic Signaling during Inflammation. *N Engl J Med* **367:**2322-2333.

Emsley, H. C., Appleton, R. E., Whitmore, C. L., Jury, F., Lamb, J. A., Martin, J. E., Ollier, W. E. *et al.* (2014). Variations in inflammation-related genes may be associated with childhood febrile seizure susceptibility. *Seizure* **23:**457-461.

Erhardt, A., Lucae, S., Unschuld, P. G., Ising, M., Kern, N., Salyakina, D., Lieb, R. *et al.* (2007). Association of polymorphisms in P2RX7 and CaMKKb with anxiety disorders. *J Affect Disord* **101:**159-168.

Evangelou, E., Kerkhof, H. J., Styrkarsdottir, U., Ntzani, E. E., Bos, S. D., Esko, T., Evans, D. S. *et al.* (2014). A meta-analysis of genome-wide association studies identifies novel variants associated with osteoarthritis of the hip. *Ann Rheum Dis* **73:**2130-2136.

Evans, R. J., Lewis, C., Virginio, C., Lundstrom, K., Buell, G., Surprenant, A. and North, R. A. (1996). Ionic permeability of, and divalent cation effects on, two ATP-gated cation channels (P2X receptors) expressed in mammalian cells. *J Physiol* **497 (Pt 2):**413-422.

Fang, J., Chen, X., Zhang, L., Chen, J., Liang, Y., Li, X., Xiang, J. *et al.* (2013). P2X7R suppression promotes glioma growth through epidermal growth factor receptor signal pathway. *Int J Biochem Cell Biol* **45:**1109-1120.

Feng, J. F., Readon, M., Yadav, S. P. and Im, M. J. (1999). Calreticulin down-regulates both GTP binding and transglutaminase activities of transglutaminase II. *Biochemistry* **38:**10743-10749.

Feng, J. F., Rhee, S. G. and Im, M. J. (1996). Evidence that phospholipase delta1 is the effector in the Gh (transglutaminase II)-mediated signaling. *J Biol Chem* **271:**16451-16454.

Feng, Y. H., Wang, L., Wang, Q., Li, X., Zeng, R. and Gorodeski, G. I. (2005). ATP stimulates GRK-3 phosphorylation and beta-arrestin-2-dependent internalization of P2X7 receptor. *Am J Physiol Cell Physiol* **288:**C1342-1356.

Fernando, S. L., Saunders, B. M., Sluyter, R., Skarratt, K. K., Goldberg, H., Marks, G. B., Wiley, J. S. *et al.* (2007). A polymorphism in the P2X7 gene increases susceptibility to extrapulmonary tuberculosis. *Am J Respir Crit Care Med* **175:**360-366.

Ferrari, D., Wesselborg, S., Bauer, M. K. and Schulze-Osthoff, K. (1997). Extracellular ATP activates transcription factor NF-kappaB through the P2Z purinoreceptor by selectively targeting NF-kappaB p65. *J Cell Biol* **139:**1635-1643.

Fesus, L., Horvath, A. and Harsfalvi, J. (1983). Interaction between tissue transglutaminase and phospholipid vesicles. *FEBS Lett* **155:**1-5.

Findlay, D. M. and Atkins, G. J. (2014). Osteoblast-chondrocyte interactions in osteoarthritis. *Curr Osteoporos Rep* **12:**127-134.

Finger, T. E., Danilova, V., Barrows, J., Bartel, D. L., Vigers, A. J., Stone, L., Hellekant, G. *et al.* (2005). ATP signaling is crucial for communication from taste buds to gustatory nerves. *Science* **310:**1495-1499.

Fitz, J. G. (2007). Regulation of cellular ATP release. *Trans Am Clin Climatol Assoc* **118:**199-208.

Folk, J. E., Cole, P. W. and Mullooly, J. P. (1968). Mechanim of action of guinea pig liver transglutaminase. V. The hydrolysis reaction. *J Biol Chem* **243:**418-427.

Fraij, B. M. (2011). "Activation of tissue tranglutsaminase by removal of carboxyl-terminal peptides". *J Cell Biochem* **112:**3469-3481.

Fredholm, B. B., Irenius, E., Kull, B. and Schulte, G. (2001). Comparison of the potency of adenosine as an agonist at human adenosine receptors expressed in Chinese hamster ovary cells. *Biochem Pharmacol* **61:**443-448.

Fuller, S. J., Stokes, L., Skarratt, K. K., Gu, B. J. and Wiley, J. S. (2009). Genetics of the P2X7 receptor and human disease.*Purinergic Signal*. Vol. 5. pp. 257-262.

Gabel, C. A. (2007). P2 purinergic receptor modulation of cytokine production. *Purinergic Signal* **3:**27-38.

Garcia-Guzman, M., Soto, F., Laube, B. and Stuhmer, W. (1996). Molecular cloning and functional expression of a novel rat heart P2X purinoceptor. *FEBS Lett* **388:**123-127.

García-Huerta, P., Díaz-Hernandez, M., Delicado, E. G., Pimentel-Santillana, M., Miras-Portugal, M. T. and Gómez-Villafuertes, R. (2012). The Specificity Protein Factor Sp1 Mediates Transcriptional Regulation of P2X7 Receptors in the Nervous System*. *J Biol Chem* **287:**44628-44644.

Garnero, P., Piperno, M., Gineyts, E., Christgau, S., Delmas, P. D. and Vignon, E. (2001). Cross sectional evaluation of biochemical markers of bone, cartilage, and synovial tissue metabolism in patients with knee osteoarthritis: relations with disease activity and joint damage. *Ann Rheum Dis* **60:**619-626.

Gaudry, C. A., Verderio, E., Aeschlimann, D., Cox, A., Smith, C. and Griffin, M. (1999). Cell Surface Localization of Tissue Transglutaminase Is Dependent on a Fibronectin-binding Site in Its N-terminal β-Sandwich Domain. *J Biol Chem* **274:**30707-30714.

Gee, H. Y., Noh, S. H., Tang, B. L., Kim, K. H. and Lee, M. G. (2011). Rescue of DeltaF508-CFTR trafficking via a GRASP-dependent unconventional secretion pathway. *Cell* **146:**746-760.

Geistlinger, J., Du, W., Groll, J., Liu, F., Hoegel, J., Foehr, K. J., Pasquarelli, A. *et al.* (2012). P2RX7 genotype association in severe sepsis identified by a novel Multi-Individual Array for rapid screening and replication of risk SNPs. *Clin Chim Acta* **413:**39-47.

Genetos, D. C., Geist, D. J., Liu, D., Donahue, H. J. and Duncan, R. L. (2005). Fluid shear-induced ATP secretion mediates prostaglandin release in MC3T3-E1 osteoblasts. *J Bone Miner Res* **20:**41-49.

Germaschewski, F. M., Matheny, C. J., Larkin, J., Liu, F., Thomas, L. R., Saunders, J. S., Sully, K. *et al.* (2014). Quantitation OF ARGS aggrecan fragments in synovial fluid, serum and urine from osteoarthritis patients. *Osteoarthritis Cartilage* **22:**690-697.

Goldring, M. B. (2000). The role of the chondrocyte in osteoarthritis. *Arthritis Rheum* **43:**1916-1926.

Goldring, M. B. and Goldring, S. R. (2007). Osteoarthritis. *J Cell Physiol* **213:**626-634.

Goldring, M. B. and Marcu, K. B. (2009). Cartilage homeostasis in health and rheumatic diseases. *Arthritis Res Ther* **11:**224.

Gomez-Villafuertes, R., Garcia-Huerta, P., Diaz-Hernandez, J. I. and Miras-Portugal, M. T. (2015). PI3K/Akt signaling pathway triggers P2X7 receptor expression as a pro-survival factor of neuroblastoma cells under limiting growth conditions. *Sci Rep* **5:**18417.

Grenard, P., Bates, M. K. and Aeschlimann, D. (2001). Evolution of transglutaminase genes: identification of a transglutaminase gene cluster on human chromosome 15q15. Structure of the gene encoding transglutaminase X and a novel gene family member, transglutaminase Z. *J Biol Chem* **276:**33066-33078.

Gu, B. J. and Wiley, J. S. (2006). Rapid ATP-induced release of matrix metalloproteinase 9 is mediated by the P2X7 receptor. *Blood* **107:**4946-4953.

Gu, B. J., Zhang, W., Worthington, R. A., Sluyter, R., Dao-Ung, P., Petrou, S., Barden, J. A. *et al.* (2001). A Glu-496 to Ala polymorphism leads to loss of function of the human P2X7 receptor. *J Biol Chem* **276:**11135-11142.

Gu, B. J., Zhang, W. Y., Bendall, L. J., Chessell, I. P., Buell, G. N. and Wiley, J. S. (2000). Expression of P2X(7) purinoceptors on human lymphocytes and monocytes:

evidence for nonfunctional P2X(7) receptors. *Am J Physiol Cell Physiol* **279:**C1189-1197.

Guan, W. J., Wang, J. L., Liu, Y. T., Ma, Y. T., Zhou, Y., Jiang, H., Shen, L. *et al.* (2013). Spinocerebellar ataxia type 35 (SCA35)-associated transglutaminase 6 mutants sensitize cells to apoptosis. *Biochem Biophys Res Commun* **430:**780-786.

Gudipaty, L., Humphreys, B. D., Buell, G. and Dubyak, G. R. (2001). Regulation of P2X(7) nucleotide receptor function in human monocytes by extracellular ions and receptor density. *Am J Physiol Cell Physiol* **280:**C943-953.

Hadjivassiliou, M., Aeschlimann, P., Sanders, D. S., Maki, M., Kaukinen, K., Grunewald, R. A., Bandmann, O. *et al.* (2013). Transglutaminase 6 antibodies in the diagnosis of gluten ataxia. *Neurology* **80:**1740-1745.

Hadjivassiliou, M., Aeschlimann, P., Strigun, A., Sanders, D. S., Woodroofe, N. and Aeschlimann, D. (2008). Autoantibodies in gluten ataxia recognize a novel neuronal transglutaminase. *Ann Neurol* **64:**332-343.

Hanley, P. J., Musset, B., Renigunta, V., Limberg, S. H., Dalpke, A. H., Sus, R., Heeg, K. M. *et al.* (2004). Extracellular ATP induces oscillations of intracellular Ca2+ and membrane potential and promotes transcription of IL-6 in macrophages. *Proc Natl Acad Sci U S A* **101:**9479-9484.

Hattori, M. and Gouaux, E. (2012). Molecular mechanism of ATP binding and ion channel activation in P2X receptors. *Nature* **485:**207-212.

Haywood, L., McWilliams, D. F., Pearson, C. I., Gill, S. E., Ganesan, A., Wilson, D. and Walsh, D. A. (2003). Inflammation and angiogenesis in osteoarthritis. *Arthritis Rheum* **48:**2173-2177.

He, W. T., Wan, H., Hu, L., Chen, P., Wang, X., Huang, Z., Yang, Z. H. *et al.* (2015). Gasdermin D is an executor of pyroptosis and required for interleukin-1beta secretion. *Cell Res* **25:**1285-1298.

Henriksson, P., Becker, S., Lynch, G. and McDonagh, J. (1985). Identification of intracellular factor XIII in human monocytes and macrophages. *J Clin Invest* **76:**528-534.

Hettasch, J. M. and Greenberg, C. S. (1994). Analysis of the catalytic activity of human factor XIIIa by site-directed mutagenesis. *J Biol Chem* **269:**28309-28313.

Hodrea, J., Demeny, M. A., Majai, G., Sarang, Z., Korponay-Szabo, I. R. and Fesus, L. (2010). Transglutaminase 2 is expressed and active on the surface of human monocyte-derived dendritic cells and macrophages. *Immunol Lett* **130:**74-81.

Hoffman, R. L., Duff, S. and Qadir, N. (2005). Ion channel assay development using invitrogen's FRET-based voltage sensor probes. BMG application note 123.

Holmgren, A. (1995). Thioredoxin structure and mechanism: conformational changes on oxidation of the active-site sulfhydryls to a disulfide. *Structure* **3:**239-243.

Honore, P., Donnelly-Roberts, D., Namovic, M. T., Hsieh, G., Zhu, C. Z., Mikusa, J. P., Hernandez, G. *et al.* (2006). A-740003 [N-(1-{[(cyanoimino)(5-quinolinylamino) methyl]amino}-2,2-dimethylpropyl)-2-(3,4-dimethoxyphenyl)acetamide], a novel and selective P2X7 receptor antagonist, dose-dependently reduces neuropathic pain in the rat. *J Pharmacol Exp Ther* **319:**1376-1385.

Hotchkiss, R. S., Strasser, A., McDunn, J. E. and Swanson, P. E. (2009). Cell death. *N Engl J Med* **361:**1570-1583.

Huang, L., Haylor, J. L., Hau, Z., Jones, R. A., Vickers, M. E., Wagner, B., Griffin, M. *et al.* (2009). Transglutaminase inhibition ameliorates experimental diabetic nephropathy. *Kidney Int* **76:**383-394.

Huang, S. W., Walker, C., Pennock, J., Else, K., Muller, W., Daniels, M. J., Pellegrini, C. *et al.* (2016). P2X7 receptor-dependent tuning of gut epithelial responses to infection. *Immunol Cell Biol* **95:**178-188.

Huebner, J. L., Johnson, K. A., Kraus, V. B. and Terkeltaub, R. A. (2009). Transglutaminase 2 is a Marker of Chondrocyte Hypertrophy and Osteoarthritis Severity in the Hartley Guinea Pig Model of Knee OA. *Osteoarthritis Cartilage* **17:**1056-1064.

Hunter, D. J., Nevitt, M., Losina, E. and Kraus, V. (2014). Biomarkers for osteoarthritis: Current position and steps towards further validation. *Best Pract Res Clin Rheumatol* **28:**61-71.

Idzko, M., Ferrari, D. and Eltzschig, H. K. (2014). Nucleotide signalling during inflammation. *Nature* **509:**310-317.

Iglesias, R., Locovei, S., Roque, A., Alberto, A. P., Dahl, G., Spray, D. C. and Scemes, E. (2008). P2X7 receptor-Pannexin1 complex: pharmacology and signaling. *Am J Physiol Cell Physiol* **295:**C752-760.

Iismaa, S. E., Mearns, B. M., Lorand, L. and Graham, R. M. (2009). Transglutaminases and disease: lessons from genetically engineered mouse models and inherited disorders. *Physiol Rev* **89:**991-1023.

Iismaa, S. E., Wu, M. J., Nanda, N., Church, W. B. and Graham, R. M. (2000). GTP binding and signaling by Gh/transglutaminase II involves distinct residues in a unique GTP-binding pocket. *J Biol Chem* **275:**18259-18265.

Iversen, R., Di Niro, R., Stamnaes, J., Lundin, K. E., Wilson, P. C. and Sollid, L. M. (2013). Transglutaminase 2-specific autoantibodies in celiac disease target clustered, N-terminal epitopes not displayed on the surface of cells. *J Immunol* **190:**5981-5991.

Jamieson, S. E., Peixoto-Rangel, A. L., Hargrave, A. C., de Roubaix, L. A., Mui, E. J., Boulter, N. R., Miller, E. N. *et al.* (2010). Evidence for associations between the purinergic receptor P2X7 (P2RX7) and toxoplasmosis. *Genes Immun* **11:**374-383.

Jang, T. H., Lee, D. S., Choi, K., Jeong, E. M., Kim, I. G., Kim, Y. W., Chun, J. N. *et al.* (2014). Crystal structure of transglutaminase 2 with GTP complex and amino acid sequence evidence of evolution of GTP binding site. *PLoS One* **9:**e107005.

Jegundo dos Reis, A. M. (2017). autoantibodies that drive extraintestinal manifestations of gluten related disorders are developed in the gut. Thesis PhD, Cardiff University.

Jensik, P. J., Holbird, D., Collard, M. W. and Cox, T. C. (2001). Cloning and characterization of a functional P2X receptor from larval bullfrog skin. *Am J Physiol Cell Physiol* **281:**C954-962.

Jiang, L.-H. (2017). P2X receptor-mediated ATP purinergic signaling in health and disease. *Cell Health and Cytoskeleton* **Volume 4:**83-101.

Jiang, L. H., Baldwin, J. M., Roger, S. and Baldwin, S. A. (2013). Insights into the Molecular Mechanisms Underlying Mammalian P2X7 Receptor Functions and Contributions in Diseases, Revealed by Structural Modeling and Single Nucleotide Polymorphisms. *Front Pharmacol* **4:**55.

Jiang, W. G., Ablin, R., Douglas-Jones, A. and Mansel, R. E. (2003). Expression of transglutaminases in human breast cancer and their possible clinical significance. *Oncol Rep* **10:**2039-2044.

Jiang, W. G. and Ablin, R. J. (2011). Prostate transglutaminase: a unique transglutaminase and its role in prostate cancer. *Biomark Med* **5:**285-291.

Jin, X., Stamnaes, J., Klock, C., DiRaimondo, T. R., Sollid, L. M. and Khosla, C. (2011). Activation of extracellular transglutaminase 2 by thioredoxin. *J Biol Chem* **286:**37866-37873.

Johnson, K. A. and Terkeltaub, R. A. (2005). External GTP-bound transglutaminase 2 is a molecular switch for chondrocyte hypertrophic differentiation and calcification. *J Biol Chem* **280:**15004-15012.

Johnson, K. A., van Etten, D., Nanda, N., Graham, R. M. and Terkeltaub, R. A. (2003a). Distinct transglutaminase 2-independent and transglutaminase 2-dependent pathways mediate articular chondrocyte hypertrophy. *J Biol Chem* **278:**18824-18832.

Johnson, T. S., El-Koraie, A. F., Skill, N. J., Baddour, N. M., El Nahas, A. M., Njloma, M., Adam, A. G. *et al.* (2003b). Tissue transglutaminase and the progression of human renal scarring. *J Am Soc Nephrol* **14:**2052-2062.

Jorgensen, N. R., Husted, L. B., Skarratt, K. K., Stokes, L., Tofteng, C. L., Kvist, T., Jensen, J. E. *et al.* (2012). Single-nucleotide polymorphisms in the P2X7 receptor gene are associated with post-menopausal bone loss and vertebral fractures. *Eur J Hum Genet* **20:**675-681.

Kang, S. K., Kim, D. K., Damron, D. S., Baek, K. J. and Im, M. J. (2002). Modulation of intracellular Ca(2+) via alpha(1B)-adrenoreceptor signaling molecules, G alpha(h) (transglutaminase II) and phospholipase C-delta 1. *Biochem Biophys Res Commun* **293:**383-390.

Karasawa, A. and Kawate, T. (2016). Structural basis for subtype-specific inhibition of the P2X7 receptor. *eLife* **5**.

Kastbom, A., Strandberg, G., Lindroos, A. and Skogh, T. (2004). Anti-CCP antibody test predicts the disease course during 3 years in early rheumatoid arthritis (the Swedish TIRA project). *Ann Rheum Dis* **63:**1085-1089.

Kawana, N., Yamamoto, Y., Ishida, T., Saito, Y., Konno, H., Arima, K. and Satoh, J.-i. (2013). Reactive astrocytes and perivascular macrophages express NLRP3

inflammasome in active demyelinating lesions of multiple sclerosis

and necrotic lesions of neuromyelitis optica and cerebral infarction. *Clinical and Experimental Neuroimmunology* **4:**296-304.

Kawate, T., Michel, J. C., Birdsong, W. T. and Gouaux, E. (2009). Crystal structure of the ATP-gated P2X4 ion channel in the closed state. *Nature* **460:**592-598.

Kayagaki, N., Stowe, I. B., Lee, B. L., O'Rourke, K., Anderson, K., Warming, S., Cuellar, T. *et al.* (2015). Caspase-11 cleaves gasdermin D for non-canonical inflammasome signalling. *Nature* **526:**666-671.

Kelk, P., Johansson, A., Claesson, R., Hanstrom, L. and Kalfas, S. (2003). Caspase 1 involvement in human monocyte lysis induced by Actinobacillus actinomycetemcomitans leukotoxin. *Infect Immun* **71:**4448-4455.

Khakh, B. S. (2001). Molecular Physiology of P2X receptors and ATP signaling at synapses. **2:**165-174.

Khakh, B. S., Bao, X. R., Labarca, C. and Lester, H. A. (1999). Neuronal P2X transmitter-gated cation channels change their ion selectivity in seconds. *Nat Neurosci* **2:**322-330.

Khakh, B. S., Gittermann, D., Cockayne, D. A. and Jones, A. (2003). ATP modulation of excitatory synapses onto interneurons. *J Neurosci* **23:**7426-7437.

Kiesselbach, T. H. and Wagner, R. H. (1972). Demonstration of factor XIII in human megakaryocytes by a fluorescent antibody technique. *Ann N Y Acad Sci* **202:**318-328.

Kim, H., Walsh, M. C., Takegahara, N., Middleton, S. A., Shin, H. I., Kim, J. and Choi, Y. (2017). The purinergic receptor P2X5 regulates inflammasome activity and hyper-multinucleation of murine osteoclasts. *Sci Rep* **7**.

Kim, H. C., Lewis, M. S., Gorman, J. J., Park, S. C., Girard, J. E., Folk, J. E. and Chung, S. I. (1990). Protransglutaminase E from guinea pig skin. Isolation and partial characterization. *J Biol Chem* **265:**21971-21978.

Kim, J., Noh, S. H., Piao, H., Kim, D. H., Kim, K., Cha, J. S., Chung, W. Y. *et al.* (2016). Monomerization and ER Relocalization of GRASP Is a Requisite for Unconventional Secretion of CFTR. *Traffic* **17:**733-753.

King, B. F., Townsend-Nicholson, A., Wildman, S. S., Thomas, T., Spyer, K. M. and Burnstock, G. (2000). Coexpression of rat P2X2 and P2X6 subunits in Xenopus oocytes. *J Neurosci* **20:**4871-4877.

Kiraly, R., Csosz, E., Kurtan, T., Antus, S., Szigeti, K., Simon-Vecsei, Z., Korponay-Szabo, I. R. *et al.* (2009). Functional significance of five noncanonical Ca2+-binding sites of human transglutaminase 2 characterized by site-directed mutagenesis. *Febs j* **276:**7083-7096.

Kirkpatrick, D. L., Kuperus, M., Dowdeswell, M., Potier, N., Donald, L. J., Kunkel, M., Berggren, M. *et al.* (1998). Mechanisms of inhibition of the thioredoxin growth factor system by antitumor 2-imidazolyl disulfides. *Biochem Pharmacol* **55:**987-994.

Knapp, T., Zlokarnik, G., Negulescu, P., Tsien, R. Y., Rink, T. and Corporation, A. B. (2001). Photon reducing agents for use in fluorescence assays. *US patent* **US 6221612 B1**.

Knight, M. M., McGlashan, S. R., Garcia, M., Jensen, C. G. and Poole, C. A. (2009). Articular chondrocytes express connexin 43 hemichannels and P2 receptors - a putative mechanoreceptor complex involving the primary cilium? *J Anat* **214:**275-283.

Kobayashi, K., Takahashi, E., Miyagawa, Y., Yamanaka, H. and Noguchi, K. (2011). Induction of the P2X7 receptor in spinal microglia in a neuropathic pain model. *Neurosci Lett* **504:**57-61.

Koolpe, M., Pearson, D. and Benton, H. P. (1999). Expression of both P1 and P2 purine receptor genes by human articular chondrocytes and profile of ligand-mediated prostaglandin E2 release. *Arthritis Rheum* **42:**258-267.

Kotnis, S., Bingham, B., Vasilyev, D. V., Miller, S. W., Bai, Y., Yeola, S., Chanda, P. K. *et al.* (2010). Genetic and Functional Analysis of Human P2X5 Reveals a Distinct Pattern of Exon 10 Polymorphism with Predominant Expression of the Nonfunctional Receptor Isoform. *Mol Pharm* **77:**953-960.

Kronlage, M., Song, J., Sorokin, L., Isfort, K., Schwerdtle, T., Leipziger, J., Robaye, B. *et al.* (2010). Autocrine purinergic receptor signaling is essential for macrophage chemotaxis. *Sci Signal* **3:**ra55.

Kuncio, G. S., Tsyganskaya, M., Zhu, J., Liu, S. L., Nagy, L., Thomazy, V., Davies, P. J. *et al.* (1998). TNF-alpha modulates expression of the tissue transglutaminase gene in liver cells. *Am J Physiol* **274:**G240-245.

Kuramoto, N., Takizawa, T., Matsuki, M., Morioka, H., Robinson, J. M. and Yamanishi, K. (2002). Development of ichthyosiform skin compensates for defective permeability barrier function in mice lacking transglutaminase 1. *J Clin Invest* **109:**243-250.

La Venuta, G., Zeitler, M., Steringer, J. P., Muller, H. M. and Nickel, W. (2015). The Startling Properties of Fibroblast Growth Factor 2: How to Exit Mammalian Cells without a Signal Peptide at Hand. *J Biol Chem* **290:**27015-27020.

Labrousse, V. F., Costes, L., Aubert, A., Darnaudéry, M., Ferreira, G., Amédée, T. and Layé, S. (2009). Impaired Interleukin-1β and c-Fos Expression in the Hippocampus Is Associated with a Spatial Memory Deficit in P2X7 Receptor-Deficient Mice. *PLoS ONE* **4**.

Lai, T. S., Liu, Y., Li, W. and Greenberg, C. S. (2007). Identification of two GTP-independent alternatively spliced forms of tissue transglutaminase in human leukocytes, vascular smooth muscle, and endothelial cells. *Faseb j* **21:**4131-4143.

Laliberte, R. E., Eggler, J. and Gabel, C. A. (1999). ATP treatment of human monocytes promotes caspase-1 maturation and externalization. *J Biol Chem* **274:**36944-36951.

Lalo, U., Pankratov, Y., Wichert, S. P., Rossner, M. J., North, R. A., Kirchhoff, F. and Verkhratsky, A. (2008). P2X1 and P2X5 subunits form the functional P2X receptor in mouse cortical astrocytes. *J Neurosci* **28:**5473-5480.

Lalo, U., Roberts, J. A. and Evans, R. J. (2011). Identification of Human P2X1 Receptor-interacting Proteins Reveals a Role of the Cytoskeleton in Receptor Regulation. *J Biol Chem* **286:**30591-30599.

Lane, N. E., Brandt, K., Hawker, G., Peeva, E., Schreyer, E., Tsuji, W. and Hochberg, M. C. (2011). OARSI-FDA initiative: defining the disease state of osteoarthritis. *Osteoarthritis Cartilage* **19:**478-482.

Larsson, S., Englund, M., Struglics, A. and Lohmander, L. S. (2015). Interleukin-6 and tumor necrosis factor alpha in synovial fluid are associated with progression of radiographic knee osteoarthritis in subjects with previous meniscectomy. *Osteoarthritis Cartilage* **23:**1906-1914.

Lauer, P., Metzner, H. J., Zettlmeissl, G., Li, M., Smith, A. G., Lathe, R. and Dickneite, G. (2002). Targeted inactivation of the mouse locus encoding coagulation factor XIII-A: hemostatic abnormalities in mutant mice and characterization of the coagulation deficit. *Thromb Haemost* **88:**967-974.

Lazarowski, E. R., Boucher, R. C. and Harden, T. K. (2003). Mechanisms of release of nucleotides and integration of their action as P2X- and P2Y-receptor activating molecules. *Mol Pharmacol* **64:**785-795.

Le, K. T., Babinski, K. and Seguela, P. (1998). Central P2X4 and P2X6 channel subunits coassemble into a novel heteromeric ATP receptor. *J Neurosci* **18:**7152-7159.

Lecut, C., Frederix, K., Johnson, D. M., Deroanne, C., Thiry, M., Faccinetto, C., Maree, R. *et al.* (2009). P2X1 ion channels promote neutrophil chemotaxis through Rho kinase activation. *J Immunol* **183:**2801-2809.

Lee, K. H., Lee, N., Lim, S., Jung, H., Ko, Y. G., Park, H. Y., Jang, Y. *et al.* (2003). Calreticulin inhibits the MEK1,2-ERK1,2 pathway in alpha 1-adrenergic receptor/Gh-stimulated hypertrophy of neonatal rat cardiomyocytes. *J Steroid Biochem Mol Biol* **84:**101-107.

Lees, M. P., Fuller, S. J., McLeod, R., Boulter, N. R., Miller, C. M., Zakrzewski, A. M., Mui, E. J. *et al.* (2010). P2X7 receptor-mediated killing of an intracellular parasite, Toxoplasma gondii, by human and murine macrophages. *J Immunol* **184:**7040-7046.

Lenertz, L. Y., Wang, Z., Guadarrama, A., Hill, L. M., Gavala, M. L. and Bertics, P. J. (2010). Mutation of putative N-linked glycosylation sites on the human nucleotide receptor P2X7 reveals a key residue important for receptor function. *Biochemistry* **49:**4611-4619.

Lindblad, S. and Hedfors, E. (1987). Arthroscopic and immunohistologic characterization of knee joint synovitis in osteoarthritis. *Arthritis Rheum* **30:**1081-1088.

Liu, S., Cerione, R. A. and Clardy, J. (2002). Structural basis for the guanine nucleotide-binding activity of tissue transglutaminase and its regulation of transamidation activity. *Proc Natl Acad Sci U S A* **99:**2743-2747.

Locovei, S., Scemes, E., Qiu, F., Spray, D. C. and Dahl, G. (2007). Pannexin1 is part of the pore forming unit of the P2X7 receptor death complex. *FEBS Lett* **581:**483-488.

Loeser, R. F., Goldring, S. R., Scanzello, C. R. and Goldring, M. B. (2012). Osteoarthritis: A Disease of the Joint as an Organ. *Arthritis Rheum* **64:**1697-1707.

Long, F. and Ornitz, D. M. (2013). Development of the Endochondral Skeleton.*Cold Spring Harb Perspect Biol*. Vol. 5.

Lopez-Castejon, G., Theaker, J., Pelegrin, P., Clifton, A. D., Braddock, M. and Surprenant, A. (2010). P2X(7) receptor-mediated release of cathepsins from macrophages is a cytokine-independent mechanism potentially involved in joint diseases. *J Immunol* **185:**2611-2619.

Lorand, L. (2001). Factor XIII: structure, activation, and interactions with fibrinogen and fibrin. *Ann N Y Acad Sci* **936:**291-311.

Lorand, L. and Graham, R. M. (2003). Transglutaminases: crosslinking enzymes with pleiotropic functions. *Nat Rev Mol Cell Biol* **4:**140-156.

Lorand, L., Lockridge, O. M., Campbell, L. K., Myhrman, R. and Bruner-Lorand, J. (1971). Transamidating enzymes. II. A continuous fluorescent method suited for automating measurements of factor XIII in plasma. *Anal Biochem* **44:**221-231.

Lortat-Jacob, H., Burhan, I., Scarpellini, A., Thomas, A., Imberty, A., Vivès, R. R., Johnson, T. *et al.* (2012). Transglutaminase-2 Interaction with Heparin: Identification of a heparin binding site that regulates cell adhesion to fibronectin-transglutaminase-2 matrix. *J Biol Chem* **287:**18005-18017.

Lotz, M., Martel-Pelletier, J., Christiansen, C., Brandi, M. L., Bruyere, O., Chapurlat, R., Collette, J. *et al.* (2013). Value of biomarkers in osteoarthritis: current status and perspectives. *Ann Rheum Dis* **72:**1756-1763.

Loughlin, J. (2015). Genetic contribution to osteoarthritis development: current state of evidence. *Curr Opin Rheumatol* **27:**284-288.

Lucae, S., Salyakina, D., Barden, N., Harvey, M., Gagne, B., Labbe, M., Binder, E. B. *et al.* (2006). P2RX7, a gene coding for a purinergic ligand-gated ion channel, is associated with major depressive disorder. *Hum Mol Genet* **15:**2438-2445.

Lê, K.-T., Paquet, M., Nouel, D., Babinski, K. and Séguéla, P. (1997). Primary structure and expression of a naturally truncated human P2X ATP receptor subunit from brain and immune system. *FEBS Letters* **418:**195-199.

Mackenzie, A. B., Young, M. T., Adinolfi, E. and Surprenant, A. (2005). Pseudoapoptosis induced by brief activation of ATP-gated P2X7 receptors. *J Biol Chem* **280:**33968-33976.

Makarova, K. S., Aravind, L. and Koonin, E. V. (1999). A superfamily of archaeal, bacterial, and eukaryotic proteins homologous to animal transglutaminases. *Protein Sci* **8:**1714-1719.

Mansoor, S. E., Lu, W., Oosterheert, W., Shekhar, M., Tajkhorshid, E. and Gouaux, E. (2016). X-ray structures define human P2X3 receptor gating cycle and antagonist action. *Nature* **538:**66-71.

Mariathasan, S., Newton, K., Monack, D. M., Vucic, D., French, D. M., Lee, W. P., Roose-Girma, M. *et al.* (2004). Differential activation of the inflammasome by caspase-1 adaptors ASC and Ipaf. *Nature* **430:**213-218.

Mariathasan, S., Weiss, D. S., Newton, K., McBride, J., O'Rourke, K., Roose-Girma, M., Lee, W. P. *et al.* (2006). Cryopyrin activates the inflammasome in response to toxins and ATP. *Nature* **440:**228-232.

Marques-da-Silva, C., Chaves, M., Castro, N., Coutinho-Silva, R. and Guimaraes, M. (2011). Colchicine inhibits cationic dye uptake induced by ATP in P2X2 and P2X7 receptor-expressing cells: implications for its therapeutic action. **163:**912-926.

Matic, I., Sacchi, A., Rinaldi, A., Melino, G., Khosla, C., Falasca, L. and Piacentini, M. (2010). Characterization of transglutaminase type II role in dendritic cell differentiation and function. *J Leukoc Biol* **88:**181-188.

McDonald, B., Pittman, K., Menezes, G. B., Hirota, S. A., Slaba, I., Waterhouse, C. C., Beck, P. L. *et al.* (2010). Intravascular danger signals guide neutrophils to sites of sterile inflammation. *Science* **330:**362-366.

McLarnon, J. G. (2005). Purinergic mediated changes in Ca2+ mobilization and functional responses in microglia: effects of low levels of ATP. *J Neurosci Res* **81:**349-356.

Miao, E. A., Leaf, I. A., Treuting, P. M., Mao, D. P., Dors, M., Sarkar, A., Warren, S. E. *et al.* (2010). Caspase-1-induced pyroptosis is an innate immune effector mechanism against intracellular bacteria. *Nat Immunol* **11:**1136-1142.

Milakovic, T., Tucholski, J., McCoy, E. and Johnson, G. V. (2004). Intracellular localization and activity state of tissue transglutaminase differentially impacts cell death. *J Biol Chem* **279:**8715-8722.

Millward-Sadler, S. J., Wright, M. O., Flatman, P. W. and Salter, D. M. (2004). ATP in the mechanotransduction pathway of normal human chondrocytes. *Biorheology* **41:**567-575.

Monif, M., Reid, C. A., Powell, K. L., Smart, M. L. and Williams, D. A. (2009). The P2X7 receptor drives microglial activation and proliferation: a trophic role for P2X7R pore. *J Neurosci* **29:**3781-3791.

Monsonego, A., Shani, Y., Friedmann, I., Paas, Y., Eizenberg, O. and Schwartz, M. (1997). Expression of GTP-dependent and GTP-independent tissue-type transglutaminase in cytokine-treated rat brain astrocytes. *J Biol Chem* **272:**3724-3732.

Moos, V., Fickert, S., Muller, B., Weber, U. and Sieper, J. (1999). Immunohistological analysis of cytokine expression in human osteoarthritic and healthy cartilage. *J Rheumatol* **26:**870-879.

Morelli, A., Chiozzi, P., Chiesa, A., Ferrari, D., Sanz, J. M., Falzoni, S., Pinton, P. *et al.* (2003). Extracellular ATP causes ROCK I-dependent bleb formation in P2X7-transfected HEK293 cells. *Mol Biol Cell* **14:**2655-2664.

Muller, H. M., Steringer, J. P., Wegehingel, S., Bleicken, S., Munster, M., Dimou, E., Unger, S. *et al.* (2015). Formation of disulfide bridges drives oligomerization, membrane pore formation, and translocation of fibroblast growth factor 2 to cell surfaces. *J Biol Chem* **290:**8925-8937.

Mulryan, K., Gitterman, D. P., Lewis, C. J., Vial, C., Leckie, B. J., Cobb, A. L., Brown, J. E. *et al.* (2000). Reduced vas deferens contraction and male infertility in mice lacking P2X1 receptors. *Nature* **403:**86-89.

Murtaugh, M. P., Arend, W. P. and Davies, P. J. A. (1984). Induction of tissue transglutaminase in human peripheral blood monocytes. *J Exp Med* **159:**114-125.

Murtaugh, M. P., Mehta, K., Johnson, J., Myers, M., Juliano, R. L. and Davies, P. J. (1983). Induction of tissue transglutaminase in mouse peritoneal macrophages. *J Biol Chem* **258:**11074-11081.

Murthy, S. N., Lomasney, J. W., Mak, E. C. and Lorand, L. (1999). Interactions of G(h)/transglutaminase with phospholipase Cdelta1 and with GTP. *Proc Natl Acad Sci U S A* **96:**11815-11819.

Nadella, V., Wang, Z., Johnson, T. S., Griffin, M. and Devitt, A. (2015). Transglutaminase 2 interacts with syndecan-4 and CD44 at the surface of human macrophages to promote removal of apoptotic cells. *Biochim Biophys Acta* **1853:**201-212.

Nakano, Y., Al-Jallad, H. F., Mousa, A. and Kaartinen, M. T. (2007). Expression and localization of plasma transglutaminase factor XIIIA in bone. *J Histochem Cytochem* **55:**675-685.

Nakaoka, H., Perez, D. M., Baek, K. J., Das, T., Husain, A., Misono, K., Im, M. J. *et al.* (1994). Gh: a GTP-binding protein with transglutaminase activity and receptor signaling function. *Science* **264:**1593-1596.

Nemes, Z., Marekov, L. N., Fesus, L. and Steinert, P. M. (1999). A novel function for transglutaminase 1: attachment of long-chain omega-hydroxyceramides to involucrin by ester bond formation. *Proc Natl Acad Sci U S A* **96:**8402-8407.

Netea, M. G., Nold-Petry, C. A., Nold, M. F., Joosten, L. A., Opitz, B., van der Meer, J. H., van de Veerdonk, F. L. *et al.* (2009). Differential requirement for the activation of the inflammasome for processing and release of IL-1beta in monocytes and macrophages. *Blood* **113:**2324-2335.

Newton, J. L., Harney, S. M., Wordsworth, B. P. and Brown, M. A. (2004). A review of the MHC genetics of rheumatoid arthritis. *Genes Immun* **5:**151-157.

NICE. (2014). Osteoarthritis: Care and management in adults.

Nicke, A., Bäumert, H. G., Rettinger, J., Eichele, A., Lambrecht, G., Mutschler, E. and Schmalzing, G. (1998). P2X1 and P2X3 receptors form stable trimers: a novel structural motif of ligand-gated ion channels. *EMBO* **17:**2971-3216.

Nicke, A., Kerschensteiner, D. and Soto, F. (2005). Biochemical and functional evidence for heteromeric assembly of P2X1 and P2X4 subunits. *J Neurochem* **92:**925-933.

Nickel, W. and Rabouille, C. (2008). Mechanisms of regulated unconventional protein secretion. *Nature Reviews Molecular Cell Biology* **10:**148-155.

Noronha-Matos, J. B., Coimbra, J., Sá-e-Sousa, A., Rocha, R., Marinhas, J., Freitas, R., Guerra-Gomes, S. *et al.* (2014). P2X7-induced zeiosis promotes osteogenic differentiation and mineralization of postmenopausal bone marrow-derived mesenchymal stem cells. *FASEB j* **28:**5208-5222.

North, R. A. (2002). Molecular physiology of P2X receptors. *Physiol Rev* **82:**1013-1067.

Nunes, I., Gleizes, P. E., Metz, C. N. and Rifkin, D. B. (1997). Latent transforming growth factor-beta binding protein domains involved in activation and transglutaminase-dependent cross-linking of latent transforming growth factor-beta. *J Cell Biol* **136:**1151-1163.

Nurminskaya, M. V. and Belkin, A. M. (2012). Cellular Functions of Tissue Transglutaminase. *Int Rev Cell Mol Biol* **294:**1-97.

Nurminskaya, M. V., Recheis, B., Nimpf, J., Magee, C. and Linsenmayer, T. F. (2002). Transglutaminase factor XIIIA in the cartilage of developing avian long bones. *Dev Dyn* **223:**24-32.

Ohtsubo, K. and Marth, J. D. (2006). Glycosylation in cellular mechanisms of health and disease. *Cell* **126:**855-867.

Orlandi, A., Oliva, F., Taurisano, G., Candi, E., Di Lascio, A., Melino, G., Spagnoli, L. G. *et al.* (2009). Transglutaminase-2 differently regulates cartilage destruction and osteophyte formation in a surgical model of osteoarthritis. *Amino Acids* **36:**755-763.

Otsuki, S., Taniguchi, N., Grogan, S. P., D'Lima, D., Kinoshita, M. and Lotz, M. (2008). Expression of novel extracellular sulfatases Sulf-1 and Sulf-2 in normal and osteoarthritic articular cartilage. *Arthritis Res Ther* **10:**R61.

Oury, C., Toth-Zsamboki, E., Van Geet, C., Thys, C., Wei, L., Nilius, B., Vermylen, J. *et al.* (2000). A natural dominant negative P2X1 receptor due to deletion of a single amino acid residue. *J Biol Chem* **275:**22611-22614.

Oyanguren-Desez, O., Rodriguez-Antiguedad, A., Villoslada, P., Domercq, M., Alberdi, E. and Matute, C. (2011). Gain-of-function of P2X7 receptor gene variants in multiple sclerosis. *Cell Calcium* **50:**468-472.

Park, E. S., Won, J. H., Han, K. J., Suh, P. G., Ryu, S. H., Lee, H. S., Yun, H. Y. *et al.* (1998). Phospholipase C-delta1 and oxytocin receptor signalling: evidence of its role as an effector. *Biochem J* **331 (Pt 1):**283-289.

Parvathenani, L. K., Tertyshnikova, S., Greco, C. R., Roberts, S. B., Robertson, B. and Posmantur, R. (2003). P2X7 mediates superoxide production in primary microglia and is up-regulated in a transgenic mouse model of Alzheimer's disease. *J Biol Chem* **278:**13309-13317.

Pedersen, L. C., Yee, V. C., Bishop, P. D., Le Trong, I., Teller, D. C. and Stenkamp, R. E. (1994). Transglutaminase factor XIII uses proteinase-like catalytic triad to crosslink macromolecules. *Protein Sci* **3:**1131-1135.

Pelegrin, P. and Surprenant, A. (2006). Pannexin-1 mediates large pore formation and interleukin-1? release by the ATP-gated P2X7 receptor. *EMBO J* **25:**5071-5082.

Petersson, I. F. and Jacobsson, L. T. (2002). Osteoarthritis of the peripheral joints. *Best Pract Res Clin Rheumatol* **16:**741-760.

Pietroni, V., Di Giorgi, S., Paradisi, A., Ahvazi, B., Candi, E. and Melino, G. (2008). Inactive and highly active, proteolytically processed transglutaminase-5 in epithelial cells. *J Invest Dermatol* **128:**2760-2766.

Pinkas, D. M., Strop, P., Brunger, A. T. and Khosla, C. (2007). Transglutaminase 2 undergoes a large conformational change upon activation. *PLoS Biol* **5:**e327.

Pizzirani, C., Ferrari, D., Chiozzi, P., Adinolfi, E., Sandona, D., Savaglio, E. and Di Virgilio, F. (2007). Stimulation of P2 receptors causes release of IL-1beta-loaded microvesicles from human dendritic cells. *Blood* **109:**3856-3864.

Poon, I. K., Chiu, Y. H., Armstrong, A. J., Kinchen, J. M., Juncadella, I. J., Bayliss, D. A. and Ravichandran, K. S. (2014). Unexpected link between an antibiotic, pannexin channels and apoptosis. *Nature* **507:**329-334.

Portales-Cervantes, L., Nino-Moreno, P., Salgado-Bustamante, M., Garcia-Hernandez, M. H., Baranda-Candido, L., Reynaga-Hernandez, E., Barajas-Lopez, C. *et al.* (2012). The His155Tyr (489C>T) single nucleotide polymorphism of P2RX7 gene confers an enhanced function of P2X7 receptor in immune cells from patients with rheumatoid arthritis. *Cell Immunol* **276:**168-175.

Qu, Y., Misaghi, S., Newton, K., Gilmour, L. L., Louie, S., Cupp, J. E., Dubyak, G. R. *et al.* (2011). Pannexin-1 is required for ATP release during apoptosis but not for inflammasome activation. *J Immunol* **186:**6553-6561.

Raghunath, M., Hopfner, B., Aeschlimann, D., Luthi, U., Meuli, M., Altermatt, S., Gobet, R. *et al.* (1996). Cross-linking of the dermo-epidermal junction of skin regenerating from keratinocyte autografts. Anchoring fibrils are a target for tissue transglutaminase. *J Clin Invest* **98:**1174-1184.

Ren, J., Bian, X., DeVries, M., Schnegelsberg, B., Cockayne, D. A., Ford, A. P. and Galligan, J. J. (2003). P2X2 subunits contribute to fast synaptic excitation in myenteric neurons of the mouse small intestine. *J Physiol* **552:**809-821.

Ritter, S. J. and Davies, P. J. (1998). Identification of a transforming growth factor-beta1/bone morphogenetic protein 4 (TGF-beta1/BMP4) response element within the mouse tissue transglutaminase gene promoter. *J Biol Chem* **273:**12798-12806.

Roger, S., Mei, Z. Z., Baldwin, J. M., Dong, L., Bradley, H., Baldwin, S. A., Surprenant, A. *et al.* (2010). Single nucleotide polymorphisms that were identified in affective mood disorders affect ATP-activated P2X7 receptor functions. *J Psychiatr Res* **44:**347-355.

Rothmeier, A. S., Marchese, P., Petrich, B. G., Furlan-Freguia, C., Ginsberg, M. H., Ruggeri, Z. M. and Ruf, W. (2015). Caspase-1-mediated pathway promotes generation of thromboinflammatory microparticles. *J Clin Invest* **125:**1471-1484.

Ruan, Q., Tucholski, J., Gundemir, S. and Johnson Voll, G. V. (2008). The Differential Effects of R580A Mutation on Transamidation and GTP Binding Activity of Rat and Human Type 2 Transglutaminase. *Int J Clin Exp Med* **1:**248-259.

Rubartelli, A., Bajetto, A., Allavena, G., Wollman, E. and Sitia, R. (1992). Secretion of thioredoxin by normal and neoplastic cells through a leaderless secretory pathway. *J Biol Chem* **267:**24161-24164.

Ruppelt, A., Ma, W., Borchardt, K., Silberberg, S. D. and Soto, F. (2001). Genomic structure, developmental distribution and functional properties of the chicken P2X5 receptor. *Journal of Neurochemistry* **77:**1256-1265.

Ryten, M., Koshi, R., Knight, G. E., Turmaine, M., Dunn, P., Cockayne, D. A., Ford, A. P. *et al.* (2007). Abnormalities in neuromuscular junction structure and skeletal muscle function in mice lacking the P2X2 nucleotide receptor. *Neuroscience* **148:**700-711.

Sakaki, H., Tsukimoto, M., Harada, H., Moriyama, Y. and Kojima, S. (2013). Autocrine regulation of macrophage activation via exocytosis of ATP and activation of P2Y11 receptor. *PLoS One* **8:**e59778.

Sanz, J. M., Falzoni, S., Rizzo, R., Cipollone, F., Zuliani, G. and Di Virgilio, F. (2014). Possible protective role of the 489C>T P2X7R polymorphism in Alzheimer's disease. *Exp Gerontol* **60:**117-119.

Scarpellini, A., Germack, R., Lortat-Jacob, H., Muramatsu, T., Billett, E., Johnson, T. and Verderio, E. A. M. (2009). Heparan Sulfate Proteoglycans Are Receptors for the Cell-surface Trafficking and Biological Activity of Transglutaminase-2. *J Biol Chem* **284:**18411-18423.

Schafer, T., Zentgraf, H., Zehe, C., Brugger, B., Bernhagen, J. and Nickel, W. (2004). Unconventional secretion of fibroblast growth factor 2 is mediated by direct translocation across the plasma membrane of mammalian cells. *J Biol Chem* **279:**6244-6251.

Seiving, B., Ohlsson, K., Linder, C. and Stenberg, P. (1991). Transglutaminase differentiation during maturation of human blood monocytes to macrophages. *Eur J Haematol* **46:**263-271.

Shi, J., Zhao, Y., Wang, K., Shi, X., Wang, Y., Huang, H., Zhuang, Y. *et al.* (2015). Cleavage of GSDMD by inflammatory caspases determines pyroptotic cell death. *Nature* **526:**660-665.

Shi, J., Zhao, Y., Wang, Y., Gao, W., Ding, J., Li, P., Hu, L. *et al.* (2014). Inflammatory caspases are innate immune receptors for intracellular LPS. *Nature* **514:**187-192.

Shimizu, I., Iida, T., Guan, Y., Zhao, C., Raja, S. N., Jarvis, M. F., Cockayne, D. A. *et al.* (2005). Enhanced thermal avoidance in mice lacking the ATP receptor P2X3. *Pain* **116:**96-108.

Skovbjerg, H., Koch, C., Anthonsen, D. and Sjostrom, H. (2004). Deamidation and cross-linking of gliadin peptides by transglutaminases and the relation to celiac disease. *Biochim Biophys Acta* **1690:**220-230.

Sluyter, R., Dalitz, J. G. and Wiley, J. S. (2004). P2X7 receptor polymorphism impairs extracellular adenosine 5'-triphosphate-induced interleukin-18 release from human monocytes. *Genes Immun* **5:**588-591.

Smart, M. L., Gu, B., Panchal, R. G., Wiley, J., Cromer, B., Williams, D. A. and Petrou, S. (2003). P2X7 receptor cell surface expression and cytolytic pore formation are regulated by a distal C-terminal region. *J Biol Chem* **278:**8853-8860.

Sokolova, E., Skorinkin, A., Moiseev, I., Agrachev, A., Nistri, A. and Giniatullin, R. (2006). Experimental and modeling studies of desensitization of P2X3 receptors. *Mol Pharmacol* **70:**373-382.

Solini, A., Chiozzi, P., Morelli, A., Fellin, R. and Di Virgilio, F. (1999). Human primary fibroblasts in vitro express a purinergic P2X7 receptor coupled to ion fluxes, microvesicle formation and IL-6 release. *J Cell Sci* **112 (Pt 3):**297-305.

Sorge, R. E., Trang, T., Dorfman, R., Smith, S. B., Beggs, S., Ritchie, J., Austin, J. S. *et al.* (2012). Genetically determined P2X7 receptor pore formation regulates variability in chronic pain sensitivity. *Nat Med* **18:**595-599.

Soto, F., Garcia-Guzman, M., Gomez-Hernandez, J. M., Hollmann, M., Karschin, C. and Stuhmer, W. (1996). P2X4: an ATP-activated ionotropic receptor cloned from rat brain. *Proc Natl Acad Sci U S A* **93:**3684-3688.

Souri, M., Koseki-Kuno, S., Takeda, N., Yamakawa, M., Takeishi, Y., Degen, J. L. and Ichinose, A. (2008). Male-specific cardiac pathologies in mice lacking either the A or B subunit of factor XIII. *Thromb Haemost* **99:**401-408.

Stamnaes, J., Cardoso, I., Iversen, R. and Sollid, L. M. (2016). Transglutaminase 2 strongly binds to an extracellular matrix component other than fibronectin via its second C-terminal beta-barrel domain. *Febs j* **283:**3994-4010.

Stamnaes, J., Pinkas, D. M., Fleckenstein, B., Khosla, C. and Sollid, L. M. (2010). Redox Regulation of Transglutaminase 2 Activity*. *J Biol Chem* **285:**25402-25409.

Steinert, P. M., Chung, S. I. and Kim, S. Y. (1996). Inactive zymogen and highly active proteolytically processed membrane-bound forms of the transglutaminase 1 enzyme in human epidermal keratinocytes. *Biochem Biophys Res Commun* **221:**101-106.

Stephens, P., Grenard, P., Aeschlimann, P., Langley, M., Blain, E., Errington, R., Kipling, D. *et al.* (2004). Crosslinking and G-protein functions of transglutaminase 2 contribute differentially to fibroblast wound healing responses. *J Cell Sci* **117:**3389-3403.

Steringer, J. P., Bleicken, S., Andreas, H., Zacherl, S., Laussmann, M., Temmerman, K., Contreras, F. X. *et al.* (2012). Phosphatidylinositol 4,5-bisphosphate (PI(4,5)P2)-dependent oligomerization of fibroblast growth factor 2 (FGF2) triggers the formation of a lipidic membrane pore implicated in unconventional secretion. *J Biol Chem* **287:**27659-27669.

Steringer, J. P., Muller, H. M. and Nickel, W. (2015). Unconventional secretion of fibroblast growth factor 2--a novel type of protein translocation across membranes? *J Mol Biol* **427:**1202-1210.

Stokes, L., Fuller, S. J., Sluyter, R., Skarratt, K. K., Gu, B. J. and Wiley, J. S. (2010). Two haplotypes of the P2X(7) receptor containing the Ala-348 to Thr polymorphism exhibit a gain-of-function effect and enhanced interleukin-1beta secretion. *Faseb j* **24:**2916-2927.

Styrkarsdottir, U., Thorleifsson, G., Helgadottir, H. T., Bomer, N., Metrustry, S., Bierma-Zeinstra, S., Strijbosch, A. M. *et al.* (2014). Severe osteoarthritis of the hand associates with common variants within the ALDH1A2 gene and with rare variants at 1p31. *Nature Genetics* **46:**498-502.

Suadicani, S. O., Brosnan, C. F. and Scemes, E. (2006). P2X7 Receptors Mediate ATP Release and Amplification of Astrocytic Intercellular Ca2+ Signaling. *The Journal of Neuroscience* **26:**1378-1385.

Summey, B. T., Jr., Graff, R. D., Lai, T. S., Greenberg, C. S. and Lee, G. M. (2002). Tissue transglutaminase localization and activity regulation in the extracellular matrix of articular cartilage. *J Orthop Res* **20:**76-82.

Sun, C., Chu, J., Singh, S. and Salter, R. D. (2010). Identification and characterization of a novel variant of the human P2X(7) receptor resulting in gain of function. *Purinergic Signal* **6:**31-45.

Sun, C., Heid, M. E., Keyel, P. A. and Salter, R. D. (2013). The second transmembrane domain of P2X7 contributes to dilated pore formation. *PLoS One* **8:**e61886.

Surprenant, A. and North, R. A. (2009). Signaling at purinergic P2X receptors. *Annu Rev Physiol* **71:**333-359.

Surprenant, A., Rassendren, F., Kawashima, E., North, R. A. and Buell, G. (1996). The cytolytic P2Z receptor for extracellular ATP identified as a P2X receptor (P2X7). *Science* **272:**735-738.

Suto, N., Ikura, K. and Sasaki, R. (1993). Expression induced by interleukin-6 of tissue-type transglutaminase in human hepatoblastoma HepG2 cells. *J Biol Chem* **268:**7469-7473.

Symmons, D. P. M., Arthritis and Rheumatism Council Epidemiology Research Unit, U. o. M., Manchester, UK, Arthritis and Rheumatism Council Epidemiology Research Unit, S. B., University of Manchester, Oxford Road, Manchester M13 9PT, UK, Bankhead, C. R., Arthritis and Rheumatism Council Epidemiology Research Unit, U. o. M., Manchester, UK, Harrison, B. J., Arthritis and Rheumatism Council Epidemiology Research Unit, U. o. M., Manchester, UK *et al.* (2016). Blood transfusion, smoking, and obesity as risk factors for the development of rheumatoid arthritis. Results from a primary care-based incident case-control study in Norfolk, England. *Arthritis & Rheumatology* **40:**1955-1961.

Szondy, Z., Sarang, Z., Molnár, P., Németh, T., Piacentini, M., Mastroberardino, P. G., Falasca, L. *et al.* (2003). Transglutaminase 2-/- mice reveal a phagocytosis-associated crosstalk between macrophages and apoptotic cells. *Proc Natl Acad Sci U S A* **100:**7812-7817.

Tarantino, U., Ferlosio, A., Arcuri, G., Spagnoli, L. G. and Orlandi, A. (2013). Transglutaminase 2 as a biomarker of osteoarthritis: an update. *Amino Acids* **44:**199-207.

Tarcsa, E., Marekov, L. N., Andreoli, J., Idler, W. W., Candi, E., Chung, S. I. and Steinert, P. M. (1997). The fate of trichohyalin. Sequential post-translational modifications by peptidyl-arginine deiminase and transglutaminases. *J Biol Chem* **272:**27893-27901.

Tatsukawa, H., Fukaya, Y., Frampton, G., Martinez-Fuentes, A., Suzuki, K., Kuo, T. F., Nagatsuma, K. *et al.* (2009). Role of transglutaminase 2 in liver injury via cross-linking and silencing of transcription factor Sp1. *Gastroenterology* **136:**1783-1795.e1710.

Tee, A. E., Marshall, G. M., Liu, P. Y., Xu, N., Haber, M., Norris, M. D., Iismaa, S. E. *et al.* (2010). Opposing effects of two tissue transglutaminase protein isoforms in neuroblastoma cell differentiation. *J Biol Chem* **285:**3561-3567.

Telci, D., Wang, Z., Li, X., Verderio, E. A., Humphries, M. J., Baccarini, M., Basaga, H. *et al.* (2008). Fibronectin-tissue transglutaminase matrix rescues RGD-impaired cell adhesion through syndecan-4 and beta1 integrin co-signaling. *J Biol Chem* **283:**20937-20947.

Tetlow, L. C., Adlam, D. J. and Woolley, D. E. (2001). Matrix metalloproteinase and proinflammatory cytokine production by chondrocytes of human osteoarthritic cartilage: associations with degenerative changes. *Arthritis Rheum* **44:**585-594.

Thomas, H., Beck, K., Adamczyk, M., Aeschlimann, P., Langley, M., Oita, R. C., Thiebach, L. *et al.* (2013). Transglutaminase 6: a protein associated with central nervous system development and motor function. *Amino Acids* **44:**161-177.

Thomazy, V. and Fesus, L. (1989). Differential expression of tissue transglutaminase in human cells. An immunohistochemical study. *Cell Tissue Res* **255:**215-224.

Torres, G. E., Egan, T. M. and Voigt, M. M. (1998). N-Linked glycosylation is essential for the functional expression of the recombinant P2X2 receptor. *Biochemistry* **37:**14845-14851.

Torres, G. E., Egan, T. M. and Voigt, M. M. (1999). Hetero-oligomeric Assembly of P2X Receptor Subunits. *J Biol Chem* **274:**6653-6659.

Toth, B., Garabuczi, E., Sarang, Z., Vereb, G., Vamosi, G., Aeschlimann, D., Blasko, B. *et al.* (2009). Transglutaminase 2 is needed for the formation of an efficient phagocyte portal in macrophages engulfing apoptotic cells. *J Immunol* **182:**2084-2092.

Tsuda, M., Tozaki-Saitoh, H. and Inoue, K. (2012). Purinergic system, microglia and neuropathic pain. *Curr Opin Pharmacol* **12:**74-79.

Turner, P. M. and Lorand, L. (1989). Complexation of fibronectin with tissue transglutaminase. *Biochemistry* **28:**628-635.

Ulmann, L., Hatcher, J. P., Hughes, J. P., Chaumont, S., Green, P. J., Conquet, F., Buell, G. N. *et al.* (2008). Up-regulation of P2X4 receptors in spinal microglia after peripheral nerve injury mediates BDNF release and neuropathic pain. *J Neurosci* **28:**11263-11268.

Ursu, D., Ebert, P., Langron, E., Ruble, C., Munsie, L., Zou, W., Fijal, B. *et al.* (2014). Gain and loss of function of P2X7 receptors: mechanisms, pharmacology and relevance to diabetic neuropathic pain. *Mol Pain* **10:**37.

van den Akker, J., van Weert, A., Afink, G., Bakker, E. N., van der Pol, E., Boing, A. N., Nieuwland, R. *et al.* (2012). Transglutaminase 2 is secreted from smooth muscle cells by transamidation-dependent microparticle formation. *Amino Acids* **42:**961-973.

van Kuijk, A. W., Reinders-Blankert, P., Smeets, T. J., Dijkmans, B. A. and Tak, P. P. (2006). Detailed analysis of the cell infiltrate and the expression of mediators of synovial inflammation and joint destruction in the synovium of patients with psoriatic arthritis: implications for treatment. *Ann Rheum Dis* **65:**1551-1557.

Verma, P. and Dalal, K. (2013). Serum cartilage oligomeric matrix protein (COMP) in knee osteoarthritis: a novel diagnostic and prognostic biomarker. *J Orthop Res* **31:**999-1006.

Vezza, R., Habib, A. and FitzGerald, G. A. (1999). Differential signaling by the thromboxane receptor isoforms via the novel GTP-binding protein, Gh. *J Biol Chem* **274:**12774-12779.

Vial, C. and Evans, R. J. (2005). Disruption of lipid rafts inhibits P2X1 receptor-mediated currents and arterial vasoconstriction. *J Biol Chem* **280:**30705-30711.

Virginio, C., Church, D., North, R. A. and Surprenant, A. (1997). Effects of divalent cations, protons and calmidazolium at the rat P2X7 receptor. *Neuropharmacology* **36:**1285-1294.

Virginio, C., MacKenzie, A., North, R. A. and Surprenant, A. (1999a). Kinetics of cell lysis, dye uptake and permeability changes in cells expressing the rat P2X7 receptor. *The Journal of Physiology* **519:**335-346.

Virginio, C., MacKenzie, A., Rassendren, F. A., North, R. A. and Surprenant, A. (1999b). Pore dilation of neuronal P2X receptor channels. *Nature Neuroscience* **2:**315-321.

Wan, J., Ristenpart, W. D. and Stone, H. A. (2008). Dynamics of shear-induced ATP release from red blood cells. *Proc Natl Acad Sci U S A* **105:**16432-16437.

Wang, H., Wang, Q., Yang, M., Yang, L., Wang, W., Ding, H., Zhang, D. *et al.* (2017). Histomorphology and Innate Immunity during the Progression of Osteoarthritis: Does Synovitis Affect Cartilage Degradation? *J Cell Physiol* **9999:**1-17.

Wang, M. and Kaufman, R. J. (2016). Protein misfolding in the endoplasmic reticulum as a conduit to human disease. *Nature* **529:**326-335.

Wang, X., Matteson, J., An, Y., Moyer, B., Yoo, J. S., Bannykh, S., Wilson, I. A. *et al.* (2004). COPII-dependent export of cystic fibrosis transmembrane conductance regulator from the ER uses a di-acidic exit code. *J Cell Biol* **167:**65-74.

Wang, Z., Collighan, R. J., Pytel, K., Rathbone, D. L., Li, X. and Griffin, M. (2012). Characterization of heparin-binding site of tissue transglutaminase: its importance in cell surface targeting, matrix deposition, and cell signaling. *J Biol Chem* **287:**13063-13083.

Wiley, J. S., Dao-Ung, L.-P., Li, C., Shemon, A. N., Gu, B. J., Smart, M. L., Fuller, S. J. *et al.* (2003). An Ile-568 to Asn Polymorphism Prevents Normal Trafficking and Function of the Human P2X7 Receptor. **278:**17108-17113.

Wiley, J. S., Sluyter, R., Gu, B. J., Stokes, L. and Fuller, S. J. (2011). The human P2X7 receptor and its role in innate immunity. *Tissue Antigens* **78:**321-332.

Xu, L., Begum, S., Hearn, J. D. and Hynes, R. O. (2006). GPR56, an atypical G protein-coupled receptor, binds tissue transglutaminase, TG2, and inhibits melanoma tumor growth and metastasis. *Proc Natl Acad Sci U S A* **103:**9023-9028.

Yamamoto, K., Sokabe, T., Matsumoto, T., Yoshimura, K., Shibata, M., Ohura, N., Fukuda, T. *et al.* (2005). Impaired flow-dependent control of vascular tone and remodeling in P2X4-deficient mice. *Nature Medicine* **12:**133-137.

Yan, Z., Khadra, A., Li, S., Tomic, M., Sherman, A. and Stojilkovic, S. S. (2010). Experimental characterization and mathematical modeling of P2X7 receptor channel gating. *J Neurosci* **30:**14213-14224.

Yi, S. J., Groffen, J. and Heisterkamp, N. (2009). Transglutaminase 2 regulates the GTPase-activating activity of Bcr. *J Biol Chem* **284:**35645-35651.

Young, M. T., Pelegrin, P. and Surprenant, A. (2007). Amino acid residues in the P2X7 receptor that mediate differential sensitivity to ATP and BzATP. *Mol Pharmacol* **71:**92-100.

Yuan, G. H., Masuko-Hongo, K., Kato, T. and Nishioka, K. (2003). Immunologic intervention in the pathogenesis of osteoarthritis. *Arthritis Rheum* **48:**602-611.

Zacherl, S., La Venuta, G., Muller, H. M., Wegehingel, S., Dimou, E., Sehr, P., Lewis, J. D. *et al.* (2015). A direct role for ATP1A1 in unconventional secretion of fibroblast growth factor 2. *J Biol Chem* **290:**3654-3665.

Zehe, C., Engling, A., Wegehingel, S., Schäfer, T. and Nickel, W. (2006). Cell-surface heparan sulfate proteoglycans are essential components of the unconventional export machinery of FGF-2.*Proc Natl Acad Sci U S A*. Vol. 103. pp. 15479-15484.

Zemskov, E. A., Mikhailenko, I., Hsia, R. C., Zaritskaya, L. and Belkin, A. M. (2011). Unconventional secretion of tissue transglutaminase involves phospholipid-dependent delivery into recycling endosomes. *PLoS One* **6:**e19414.

Zemskov, E. A., Mikhailenko, I., Strickland, D. K. and Belkin, A. M. (2007). Cell-surface transglutaminase undergoes internalization and lysosomal degradation: an essential role for LRP1. *J Cell Sci* **120:**3188-3199.

Zhu, L., Kahwash, S. B. and Chang, L. S. (1998). Developmental expression of mouse erythrocyte protein 4.2 mRNA: evidence for specific expression in erythroid cells. *Blood* **91:**695-705.

Supplement 1

```
<< A348T_clone...                GG CCACT GTGTT CATCG ACTTC CTCAT CGACA CTTAC
gi|568815586:1... TGCAT TCTCC CCAGG CCGCT GTGTT CATCG ACTTC CTCAT CGACA CTTAC
                  |52526|52531|52536|52541|52546|52551|52556|52561|52566|
Contig1           ----- ----- ---GG CCACT GTGTT CATCG ACTTC CTCAT CGACA CTTAC


<< A348T_clone... TCCAG TAACT GCTGT CGCTC CCATA TTTAT CCCTG GTGCA AGTGC TGTCA
gi|568815586:1... TCCAG TAACT GCTGT CGCTC CCATA TTTAT CCCTG GTGCA AGTGC TGTCA
                  |52576|52581|52586|52591|52596|52601|52606|52611|52616|
Contig1           TCCAG TAACT GCTGT CGCTC CCATA TTTAT CCCTG GTGCA AGTGC TGTCA


<< A348T_clone... GCCCT GTGTG GTCAA CGAAT ACTAC TACAG GAAGA AGTGC GAGTC CATTG
gi|568815586:1... GCCCT GTGTG GTCAA CGAAT ACTAC TACAG GAAGA AGTGC GAGTC CATTG
                  |52626|52631|52636|52641|52646|52651|52656|52661|52666|
Contig1           GCCCT GTGTG GTCAA CGAAT ACTAC TACAG GAAGA AGTGC GAGTC CATTG


<< A348T_clone... TGGAG CCAAA GCCG
gi|568815586:1... TGGAG CCAAA GCCG
                  |52676|52681|52686
Contig1           TGGAG CCAAA GCCG
```

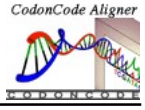


```
P45IL_clone2-P2X7Rfor3_002_A08                                    AGA CCTGC
<< P45IL_clone2-PCR3.1-BGHrev_008_D08                             AGA CCTGC
gi|568815586:121124758-121194610_5 (... GTTTG GAAAC TTGCT TTTTC AGAGA CCTGC
                                       |59526|59531|59536|59541|59546|59551
Contig2                                ----- ----- ----- ----- --AGA CCTGC


P45IL_clone2-P2X7Rfor3_002_A08          GATGG ACTTC ACAGA TTTGT CCAGG CTGCC
<< P45IL_clone2-PCR3.1-BGHrev_008_D08   GATGG ACTTC ACAGA TTTGT CCAGG CTGCC
gi|568815586:121124758-121194610_5 (... GATGG ACTTC ACAGA TTTGT CCAGG CTGCC
                                       |59556|59561|59566|59571|59576|59581
Contig2                                GATGG ACTTC ACAGA TTTGT CCAGG CTGCC


P45IL_clone2-P2X7Rfor3_002_A08          CCTGG CCCTC CATGA CACAC CCCTG ATTCC
<< P45IL_clone2-PCR3.1-BGHrev_008_D08   CCTGG CCCTC CATGA CACAC CCCTG ATTCC
gi|568815586:121124758-121194610_5 (... CCTGG CCCTC CATGA CACAC CCCCG ATTCC
                                       |59586|59591|59596|59601|59606|59611
Contig2                                CCTGG CCCTC CATGA CACAC CCCTG ATTCC


P45IL_clone2-P2X7Rfor3_002_A08          TGGAC AACCA GAGGA GATAC AGCTG CTTAG
<< P45IL_clone2-PCR3.1-BGHrev_008_D08   TGGAC AACCA GAGGA GATAC AGCTG CTTAG
gi|568815586:121124758-121194610_5 (... TGGAC AACCA GAGGA GATAC AGCTG CTTAG
                                       |59616|59621|59626|59631|59636|59641
Contig2                                TGGAC AACCA GAGGA GATAC AGCTG CTTAG


P45IL_clone2-P2X7Rfor3_002_A08          AAAGG AGGCG ACTCC TAGAT C
<< P45IL_clone2-PCR3.1-BGHrev_008_D08   AAAGG AGGCG ACTCC TAGAT C
gi|568815586:121124758-121194610_5 (... AAAGG AGGCG ACTCC TAGAT C
                                       |59646|59651|59656|59661|59666
Contig2                                AAAGG AGGCG ACTCC TAGAT C
```

Supplement 2

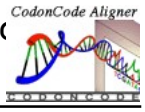


```
<< hTG2 pcDNA3.txt          CTGCC CAAAA TTCCA AGGTA TGTTC TTGAT GAACT TGGCC
<< K-L-Clone1-Up102_010_E06 CTGCC CAAAA TTCCA AGGTA TGTTC TTGAT GAATA AGGCC
K-L-Clone1-Down103_011_F07  CTGCC CAAAA TTCCA AGGTA TGTTC TTGAT GAATA AGGCC
                            |6020  |6025  |6030  |6035  |6040  |6045  |6050  |6055
Contig1                     CTGCC CAAAA TTCCA AGGTA TGTTC TTGAT GAATA AGGCC


<< hTG2 pcDNA3.txt          GAGCC CTGGT AGATA AAGCC CTGCT GGGTG AGGAC ATACT
<< K-L-Clone1-Up102_010_E06 GAGCC CTGGT AGATA AAGCC CTGCT GGGTG AGGAC ATACT
K-L-Clone1-Down103_011_F07  GAGCC CTGGT AGATA AAGCC CTGCT GGGTG AGGAC ATACT
                            |6060  |6065  |6070  |6075  |6080  |6085  |6090  |6095
Contig1                     GAGCC CTGGT AGATA AAGCC CTGCT GGGTG AGGAC ATACT


<< hTG2 pcDNA3.txt          CCTGC CGCTC -CTCT --TCC GAGTC CAGGT ACACA GCATC
<< K-L-Clone1-Up102_010_E06 CCTGC CGCTC TCTCC GATCC ATAAC ATGCT A-ACA GT
K-L-Clone1-Down103_011_F07  CCTGC CGCTC -CTCT --TCC GAGTC CAGGT ACACA GCATC
                            |6100  |6105  |6110  |6115  |6120  |6125  |6130  |6135
Contig1                     CCTGC CGCTC -CTCT --TCC GAGTC CAGGT ACACA GCATC


<< hTG2 pcDNA3.txt          CGCTG GGCAC CAGGC GTTGA AGAGC AAAAT GAAGT GGCCC
K-L-Clone1-Down103_011_F07  CGCTG GGCAC CAGGC GTTGA AGAGC AAAAT GAAGT GGCCC
                            |6140  |6145  |6150  |6155  |6160  |6165  |6170  |6175
Contig1                     CGCTG GGCAC CAGGC GTTGA AGAGC AAAAT GAAGT GGCCC


<< hTG2 pcDNA3.txt          AGCAC AAAGC TGGAT CCCTG GTAGC CAGTG GAGGC C
K-L-Clone1-Down103_011_F07  AGCAC AAAGC TGGAT CCCTG GTAGC CAGTG GAGGC C
                            |6180  |6185  |6190  |6195  |6200  |6205  |6210  |6215
Contig1                     AGCAC AAAGC TGGAT CCCTG GTAGC CAGTG GAGGC C
```

```
<< hTG2 pcDNA3.txt_1          AAACT GCCCA AAATT CCAAG GTATG TTCTT GATGA ACTTG
<< KF-ND-Clone1-Up102_014_G06 AAACT GCCCA AAATT CCAAG GTATG TTCTT GATGT CATTG
KF-ND-Clone1-Down103_015_H07  AAACT GCCCA AAATT CCAAG GTATG TTCTT GATGT CATTG
                              |6016 |6021 |6026 |6031 |6036 |6041 |6046 |6051
Contig1                       AAACT GCCCA AAATT CCAAG GTATG TTCTT GATGT CATTG

<< hTG2 pcDNA3.txt_1          GCCGA GCCCT GGTAG ATAAA GCCCT GCTGG GTGAG GACAT
<< KF-ND-Clone1-Up102_014_G06 GCCGA GCCCT GGTAG ATAAA GCCCT GCTGG GTGAG GACAT
KF-ND-Clone1-Down103_015_H07  GCCGA GCCCT GGTAG ATAAA GCCCT GCTGG GTGAG GACAT
                              |6056 |6061 |6066 |6071 |6076 |6081 |6086 |6091
Contig1                       GCCGA GCCCT GGTAG ATAAA GCCCT GCTGG GTGAG GACAT

<< hTG2 pcDNA3.txt_1          ACTCC TGCCG CTCCT CTTCC GAGTC CAGGT ACACA GCATC
<< KF-ND-Clone1-Up102_014_G06 ACTCC TGCCG CTCCT CT-CC GATTA TACAG CGAAA GTTCG
KF-ND-Clone1-Down103_015_H07  ACTCC TGCCG CTCCT CTTCC GAGTC CAGGT ACACA GCATC
                              |6096 |6101 |6106 |6111 |6116 |6121 |6126 |6131
Contig1                       ACTCC TGCCG CTCCT CTTCC GAGTC CAGGT ACACA GCATC

<< hTG2 pcDNA3.txt_1          CGCTG GGCAC CAGGC GTTGA AGAGC AAAAT GAAGT GGCCC
KF-ND-Clone1-Down103_015_H07  CGCTG GGCAC CAGGC GTTGA AGAGC AAAAT GAAGT GGCCC
                              |6136 |6141 |6146 |6151 |6156 |6161 |6166 |6171
Contig1                       CGCTG GGCAC CAGGC GTTGA AGAGC AAAAT GAAGT GGCCC

<< hTG2 pcDNA3.txt_1          AGCAC AAAGC TGGAT CCCTG GTAGC CAGTG GAGGC CTCCA
KF-ND-Clone1-Down103_015_H07  AGCAC AAAGC TGGAT CCCTG GTAGC CAGTG GAGGC CTCCA
                              |6176 |6181 |6186 |6191 |6196 |6201 |6206 |6211
Contig1                       AGCAC AAAGC TGGAT CCCTG GTAGC CAGTG GAGGC CTCCA
```

Supplement 3

blue = exon sequence
yellow = primer sequence

Exon 1, 244bp amplicon

```
ttactgggag ggggcttgct gtgg ccctgt caggaagagt agagc tctgg                    121
tccagctccg cgcagggagg gaggctgtca ccatgccggc ctgctgcagc tgcagtgatg           181
ttttccagta tgagacgaac aaagtcactc ggatccagag catgaattat ggcaccatta           241
agtggttctt ccacgtgatc atcttttcct acgtttggta agtgggatct ggggaggacc           301
cagatctctg cagtggc cga cagcacagaa agccccag cg ggcagcttca ggtgcacatt
```

Exon 2, 290bp amplicon

```
                                                        ctg catcctc         21901
caacgcctgc atcc caaccc gctgtgctat gcctcccgtt gatgctttcc catgtctgcc          21961
atttagcttt gctctggtga gtgacaagct gtaccagcgg aaagagcctg tcatcagttc           22021
tgtgcacacc aaggtgaagg ggatagcaga ggtgaaagag gagatcgtgg agaatggagt           22081
gaagaagttg gtgcacagtg tctttgacac cgcagactac accttccctt tgcaggtgag           22141
cacctcgtag cattctccca gg ctcgtcgc tggtcaccgt cgc cagggcc tagctccctt         22201
```

Exon 3, 231bp amplicon

```
ttagaaaagt ggagaggttc gcccagcaag c tggattatt ataattaagt agttctcttt         23221
tcaaaggcct tgcatttttct tagcctctcc ttctccacag gggaactctt tcttcgtgat          23281
gacaaacttt ctcaaaacag aaggccaaga gcagcggttg tgtcccgagg taaggagggg           23341
acctggagtg gtgggtcagg tcttaagagt tcctgggggа ggtgcaagtc ggaagaagca          23401
g aaatgcgga
```

Exon 4, 212bp amplicon

```
                                                attctggt gg atatcgaatc       28021
acttctccac g tcttagtaa cacacgtcac ttactcccca ctctgtcatc cttctatctg           28081
cagtatccca cccgcaggac gctctgttcc tctgaccgag gttgtaaaaa gggatggatg           28141
gacccgcaga gcaaaggtac cttctgtttc ttttcccgag accctagggg tggatg gtct           28201
ggcatcttgg tgacatttg t gatgcccagg tcaggtcttc
```

Exon 5, 206bp amplicon

```
   gttgagttaa tgatgtccct cctggagaac gtcctctc cg cagttctttc acatctgtgg        29581
ttctacgatg ctttgacccc tataggaatt cagaccggaa ggtgtgtagt gtatgaaggg           29641
aaccagaaga cctgtgaagt ctctgcctgg tgccccatcg aggcagtgga agaggccccc           29701
cggtgagtcg catggggaga cagacacagt ggccctcagc ggc gaccaga tgaggccttg          29761
ccga ggctgc ttgggccttc
```

Exon 6, 218bp amplicon

```
ga ccaagcca agaaaccaga
agcctctggt cccactggcc catgggctcc ctcggttcccccgtcacta atggccattt            32521
tgcatgtctc tctcccaggc ctgctctctt gaacagtgcc gaaaacttca ctgtgctcat           32581
caagaacaat atcgacttcc ccggccacaa ctacaccacg taagtgccca ggctgc ctgg          32641
ctgtcttagt tatctactgc tgagtaataa attatcccaa acctcagaag cctgaaacaa
```

Exon 7, 248bp amplicon

```
                                              ctggctcact cctgggaaag          33181
aga cagatct gttttcaatc gagatg tttg tttgtttgtt tgcttttaat tatgcacagg          33241
agaaacatcc tgccaggttt aaacatcact tgtaccttcc acaagactca gaatccacag           33301
tgtcccattt tccgactagg agacatcttc cgagaaacag gcgataattt ttcagatgtg           33361
gcaattcagg ttggtggtgc tttgtacact gggatgtggg gctgtgt gtc tagggatgga           33421
ggatgtcaaa c agccaagag gccgggccac
```

Exon 8, 256bp amplicon

```
                                        tggctatgc a gggagatgtc tggcggttgc    34621
gtaactcaca cccagcagcc atagagactg tcccttgttg atccttcagg gcggaataat           34681
gggcattgag atctactggg actgcaacct agaccgttgg ttccatcact gccgtcccaa           34741
atacagtttc cgtcgccttg acgacaagac caccaacgtg tccttgtacc ctggctacaa           34801
cttcaggtaa ctccaaggcc caggtcaaac tcac ccagtg gctgaatcgc attcc cagga          34861
actggtgaga ctaattttgg tttccaaggc
```

Exon 9, 204bp amplicon

```
tcaaaaaaaa aaaaaaaaaa acccaaaac c cagcactttc aaagggatct                      42541
tacaaataca gatccttttc ttcctacaga tacgccaagt actacaagga aaacaatgtt            42601
gagaaacgga ctctgataaa agtcttcggg atccgttttg acatcctggt ttttggcacc            42661
gtaagtctcg tttcccagct ccgggcaccg gcatcctat g actgtgtcct aattactgct           42721
gtg gggcctc catggaggga
```

Exon 10 & 11, 401bp amplicon

```
                              gaaccaacaa tt gcacgttg aagcaaaaga              44281
gcg ttgctct gaatttcacc tgagtaaact ctcccactct gtttttaggg aggaaaattt            44341
gacattatcc agctggttgt gtacatcggc tcaaccctct cctacttcgg tctggtaaga             44401
gattctcttt tccatgcttt aggaaaatgg tttggagaag gaagtgacta acgcagcgct             44461
tgtctgcatt ctccccaggc cgctgtgttc atcgacttcc tcatcgacac ttactccagt             44521
aactgctgtc gctcccatat ttatccctgg tgcaagtgct gtcagccctg tgtggtcaac             44581
gaatactact acaggaagaa gtgcgagtcc attgtggagc caaagccggt gaggccgctg             44641
t gttcacagg acaccaagac atg gagagat tccatgaaat cactcagaaa tgcacgaaaa           44701
ttaggcccaa
```

Exon 12, 395bp amplicon

```
           gagtttt gag ccagcttgtt caatagtcta tc atttggca aataggaatt          47461
acagttgcct ttagataggc aattcttgat aattctgtac aaaaatgggt aaactttcaa          47521
accatctttt cctagacatt aaagtatgtg tcctttgtgg atgaatccca cattaggatg          47581
gtgaaccagc agctactagg gagaagtctg caagatgtca agggccaaga agtcccagta          47641
agttaaatca ttttgtcttt ttttttttt taagaaaatt tactgttaaa tataaacaca            47701
tctagaaact tgtacaaatc aaaactgatg gattttaaca aagtaaacat actcatataa          47761
ccggcactca gattaaacaa ttgaaaatta ctagcaggag tccctttttat gc ccccctcc        47821
aatcactacc
```

Exon 13, 564bp amplicon

```
                                                          ataagttaat        51421
aaaattaaag aaccta gaac ctgagggctt gtcatgg cta ataggtttgg aaacttgctt         51481
tttcagagac ctgcgatgga cttcacagat ttgtccaggc tgcccctggc cctccatgac           51541
acacccccga ttcctggaca accagaggag atacagctgc ttagaaagga ggcgactcct          51601
agatccaggg atagccccgt ctggtgccag tgtggaagct gcctcccatc tcaactccct           51661
gagagccaca ggtgcctgga ggagctgtgc tgccggaaaa agccgggggc ctgcatcacc           51721
acctcagagc tgttcaggaa gctggtcctg tccagacacg tcctgcagtt cctcctgctc           51781
taccaggagc ccttgctggc gctggatgtg gattccacca acagccggct gcggcactgt           51841
gcctacaggt gctacgccac ctggcgcttc ggctcccagg acatggctga ctttgccatc           51901
ctgcccagct gctgccgctg gaggatccgg aaagagtttc cgaagagtga agggcagtac           51961
agtggcttca agagtcctta ctgaagccag gcaccgtggc tcacgtctgt aatcccagcg           52021
ctttgggagg ccgaggcagg cagatcacct gaggtcggga
```

Supplement 1 – Sequence alignment of P2X7R primers used for sequencing

Supplement 4

© 2015. Published by The Company of Biologists Ltd | Journal of Cell Science (2015) 128, 4615-4628 doi:10.1242/jcs.175968

RESEARCH ARTICLE

P2X7 receptor activation regulates rapid unconventional export of transglutaminase-2

Magdalena Adamczyk*, Rhiannon Griffiths, Sharon Dewitt, Vera Knäuper and Daniel Aeschlimann*

ABSTRACT

Transglutaminases (denoted TG or TGM) are externalized from cells via an unknown unconventional secretory pathway. Here, we show for the first time that purinergic signaling regulates active secretion of TG2 (also known as TGM2), an enzyme with a pivotal role in stabilizing extracellular matrices and modulating cell–matrix interactions in tissue repair. Extracellular ATP promotes TG2 secretion by macrophages, and this can be blocked by a selective antagonist against the purinergic receptor P2X7 (P2X7R, also known as P2RX7). Introduction of functional P2X7R into HEK293 cells is sufficient to confer rapid, regulated TG2 export. By employing pharmacological agents, TG2 release could be separated from P2X7R-mediated microvesicle shedding. Neither Ca^{2+} signaling alone nor membrane depolarization triggered TG2 secretion, which occurred only upon receptor membrane pore formation and without pannexin channel involvement. A gain-of-function mutation in P2X7R associated with autoimmune disease caused enhanced TG2 externalization from cells, and this correlated with increased pore activity. These results provide a mechanistic explanation for a link between active TG2 secretion and inflammatory responses, and aberrant enhanced TG2 activity in certain autoimmune conditions.

KEY WORDS: Transglutaminase, Extracellular matrix stabilization, Purinergic signaling, P2X7 receptor, Unconventional protein secretion, Innate immunity

INTRODUCTION

Unconventional export of cytoplasmic proteins [i.e. the processes by which proteins that do not follow the classical endoplasmic reticulum (ER)-to-Golgi secretory pathway are secreted by cells] is being studied extensively because many molecules that fall into this category constitute potent biological signals with key roles in developmental or inflammatory processes. Such proteins lack posttranslational modifications that occur during ER-to-Golgi protein maturation but might be subject to *N*-terminal processing and acetylation or acylation (Muesch et al., 1990; Stegmayer et al., 2005). Several fundamentally different mechanisms appear to support unconventional protein secretion, including self-sustained or transporter-facilitated direct membrane translocation at the plasma membrane, or release in specialized vesicles, the biogenesis of which is distinct from vesicles coated with coat protein complex II (Nickel and Rabouille, 2009; Rabouille et al., 2012). Neither export through the compartment for unconventional protein secretion (CUPS) and multivesicular body pathway nor direct microvesicle shedding at the plasma membrane requires membrane translocation of the cargo, and release is thought to occur by vesicle lysis in the extracellular environment.

Transglutaminases (denoted TG or TGM) are a family of structurally similar enzymes that posttranslationally modify proteins through transamidation, deamidation or esterification of glutaminyl residues (Aeschlimann and Thomazy, 2000). Several of these enzymes have well-established functions in stabilizing extracellular protein assemblies, including TG2 (wound healing), TG4 (semen coagulation) and factor XIII (blood coagulation) (Aeschlimann and Paulsson, 1994; Lorand and Graham, 2003). More recently, TG3 and TG6 have been implicated in extracelluar functions (Zone et al., 2011; Thomas et al., 2013). Despite it being 20 years since we first postulated export of TGs through an unconventional secretory pathway (Aeschlimann and Paulsson, 1994), the underlying process remains elusive. This has gained much attention recently because although matrix stabilization by TG2 is required for an effective tissue repair response, aberrant TG2 action has a central role in the pathogenesis of inflammatory diseases and autoimmunity, most noteably celiac disease (Aeschlimann and Thomazy, 2000; Iismaa et al., 2009). Externalization from cells appears to control TG2 function because Ca^{2+} binding serves as a molecular 'switch' for its activation, facilitating transition into a conformation that enables catalysis (Pinkas et al., 2007). Early studies pointed to passive release of TG2 through cell damage (Upchurch et al., 1987; Siegel et al., 2008). More recently, several alternative mechanisms for constitutive release of TG2 have been proposed, including microvesicle shedding (Antonyak et al., 2011; van den Akker et al., 2011) and perinuclear import into Rab11-positive recycling endosomes (Zemskov et al., 2011). However, the proposed mechanisms implicated different domains of TG2 (Chou et al., 2011; Zemskov et al., 2011). Furthermore, constitutive export is difficult to reconcile with the lack of a correlation between TG2 synthesis level and extracellular activity, and the fact that export appears to be cell-type- or differentiation-stage-specific, as exemplified in endochondral bone formation (Aeschlimann et al., 1995). Such sudden, context-dependent externalization of TG2 indicates that its export is regulated by an unidentified signaling event.

One emerging pathway for non-classically secreted proteins including interleukin (IL)-1β involves activation of the purinergic receptor P2X7 (P2X7R, also known as P2RX7), leading to formation of an inflammasome in a NALP3-dependent manner (Dubyak, 2012; Strowig et al., 2012). Inflammasome assembly drives caspase-1 autoprocessing, maturation of IL-1β by caspase-1 cleavage and ultimately IL-1β release (Mariathasan et al., 2006).

Matrix Biology & Tissue Repair Research Unit and Arthritis Research UK Biomechanics and Bioengineering Center of Excellence, College of Biomedical and Life Sciences, Cardiff University, Cardiff CF14 4XY, UK.

*Authors for correspondence (AdamczykM@Cardiff.ac.uk; AeschlimannDP@Cardiff.ac.uk)

Received 18 June 2015; Accepted 29 October 2015

Journal of Cell Science (2015) 128, 4615-4628 doi:10.1242/jcs.175968

Activated macrophages derived from P2X7R$^{-/-}$ mice are unable to secrete the mature form of IL-1 family cytokines, including IL-1β and IL-18 (Solle et al., 2001; Pelegrin et al., 2008) and hence, these animals show reduced severity in models of acute inflammatory joint or lung disease (Labasi et al., 2002; Lucattelli et al., 2011; Bartlett et al., 2014).

P2X7R is a member of the P2X family of nucleotide-gated ion channels that is activated by high concentrations of extracellular ATP. Besides K^+ efflux that triggers inflammasome assembly, the ion channel also supports Ca^{2+} and Na^+ influx, leading to membrane depolarization and activation of intracellular signaling cascades (Coddou et al., 2011; Bartlett et al., 2014). The P2X4R (also known as P2RX4) crystal structure confirmed that assembly of three subunits, each harboring two transmembrane domains, forms the functional P2X receptor (Kawate et al., 2009). The large extracellular domain has ATP- and metal-ion-binding sites that regulate receptor activation state. Channel opening is associated with conformational changes that reposition the transmembrane segments whereby different states of dilation might be adopted (Hattori and Gouaux, 2012; Jiang et al., 2013). The feature that distinguishes P2X7R from the other P2X family members is a long C-terminal tail (Surprenant et al., 1996; Rassendren et al., 1997) that has been implicated in the process of 'membrane pore' formation, which enables plasma membrane permeability to larger organic cations (Virginio et al., 1999; Browne et al., 2013).

High extracellular ATP is a consequence of cell damage, and enforced by ATP release from activated innate immune cells. This acts as a danger signal amplification system that spreads the alarm within the local milieu. However, ATP is not only released upon tissue or cell injury, or stress, but can also be secreted through membrane channels or secretory vesicles (Garcia and Knight, 2010; Sorge et al., 2012; Burnstock, 2015). Given that TG2 is abundantly secreted in the context of inflammation but that extracellular TG2 also has formative roles in tissue development and homeostasis, we hypothesized that its export might be associated with P2X7R signaling. Here, we show for the first time that rapid TG2 export is regulated by P2X7R-mediated membrane pore formation.

RESULTS

Macrophages secrete TG2 in a P2X7R-dependent manner

The THP-1 monocyte or macrophage cell model was chosen to investigate TG2 export as these cells have been reported to be competent in P2X7R-mediated IL-1β secretion (Mackenzie et al., 2001). We confirmed initially that activation of inflammasome formation by priming cells with lipopolysaccharide (LPS) for Toll-like receptor (TLR) signaling combined with subsequent stimulation with ATP induces IL-1β secretion into the cell supernatant, as determined by capture ELISA (Fig. S1A). TG2 is expressed in differentiated macrophages but not in monocyte precursors (Mehta and Lopez-Berestein, 1986). Therefore, THP-1 cells were treated with the phorbol ester TPA to induce differentiation (Fig. S1B), and TG2 upregulation was confirmed by western blotting of cell lysates (Fig. 1A). We then used the ATP analogue BzATP for P2X7R activation as it shows a high degree of selectivity for P2X7R and does not activate P2Y family ATP-sensing receptors (Coddou et al., 2011). Differentiated cells were stimulated with BzATP for 10 min, and culture supernatants were collected at the end of agonist treatment (pulse) and after a further

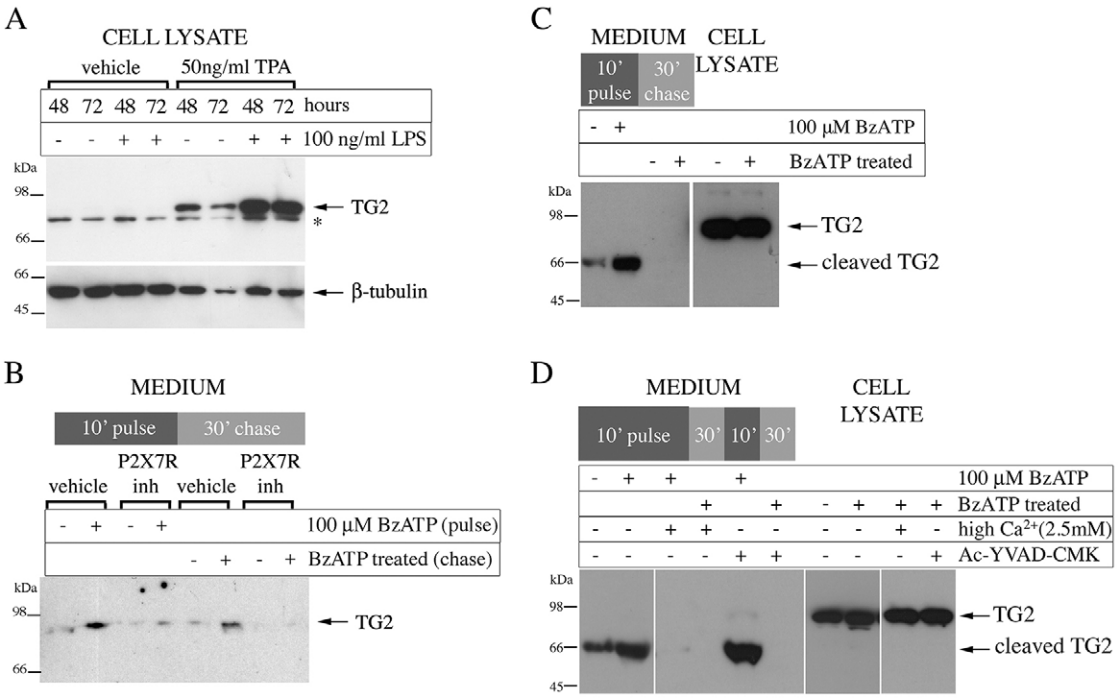

Fig. 1. P2X7R inhibition blocks TG2 secretion by macrophages. (A) Differentiated monocytes express TG2. THP-1 cells were differentiated for the indicated time with TPA and stimulated with LPS as indicated. Cell extracts were analyzed by western blotting for TG2 or β-tubulin as a loading control (*, non-specific reactivity). (B) TG2 export requires P2X7R activity. Differentiated THP-1 cells were pre-treated with vehicle or 5 μM P2X7R inhibitor A740003 for 10 min, then stimulated as indicated with BzATP for 10 min with or without inhibitor (inh, pulse). Cells were chased for 30 min in P2X7R agonist and antagonist-free medium. Collected medium from the pulse and chase (200 μl) were rendered cell-free by centrifugation, and analyzed for TG2 by western blotting. (C,D) P2X7R activation triggers TG2 secretion in macrophages derived from peripheral blood mononuclear cells. Macrophages were stimulated with BzATP and chased as in B, and collected medium from the of pulse and chase were analyzed for TG2 by western blotting alongside the cell lysates (C). The presence of 100 μM Ac-YVAD-CMK did not prevent externalization or cleavage of TG2, indicating a caspase-1-independent process (D).

Journal of Cell Science (2015) 128, 4615-4628 doi:10.1242/jcs.175968

30 min in the absence of agonist (chase) to capture immediate and potentially delayed TG2 secretion. BzATP stimulation induced a substantial increase in TG2 secretion as determined by western blotting of cell-free supernatant (Fig. 1B). TG2 export was blocked by the P2X7R antagonist A740003 (Fig. 1B), which inhibits IL-1β secretion in differentiated monocytes (Honore et al., 2006). To substantiate this finding, we analyzed TG2 secretion in response to P2X7R activation in primary human M1 macrophages. BzATP triggered rapid TG2 secretion, contributing to soluble (Fig. 1C) and cell-surface-associated enzyme (Fig. S1C), whereby the soluble enzyme was undergoing processing generating a ∼66 kDa species. Processing did not involve inflammasome-associated caspase-1 nor cell surface MT1-MMP (also known as MMP14) cleavage (Belkin et al., 2001) as it occurred in the presence of *N*-acetyl-YVAD-chloromethyl ketone (Ac-YVAD-CMK) and EDTA, respectively (Fig. 1D; Fig. S1C). Collectively, these data show that P2X7R regulates not only 1L-1β but also TG2 secretion in macrophages.

Expression of P2X7R confers agonist-inducible, rapid TG2 secretion to HEK293 cells

To investigate whether P2X7R alone was sufficient or other inflammasome pathway components are required for TG2 export, we established HEK293 cells stably expressing wild-type (hereafter P2X7R cells) or tagged human P2X7R. This cell model was selected as it lacks endogenous expression of P2X receptor family members (Mackenzie et al., 2005) and secretes mature IL-1β in response to agonist when co-transfected with P2X7R and pro-caspase-1 (Gudipaty et al., 2003). P2X7R expression was confirmed by western blotting of cell extracts, whereby for tagged P2X7R a single band reactive to antibodies against the P2X7R and the V5 tag was detected (Fig. S2A). Immunocytochemistry confirmed membrane localization of the receptor in P2X7R cells and its absence in parental cells (Fig. S2B). In order to assess P2X7R functionality, changes in the intracellular free Ca^{2+} concentration in response to BzATP were investigated using Fluo-4-AM. Only P2X7R cells, and not parental cells, responded to this agonist (Fig. S2C). A dose–response analysis for BzATP stimulation of P2X7R cells using Ca^{2+} signaling as a readout derived an apparent K_D of ∼75 μM (Fig. S2D). This is in line with literature data ranging from 40–100 μM depending on extracellular Ca^{2+} concentration (Rassendren et al., 1997). Therefore, stimulation with 100 μM BzATP produced a P2X7R-specific and, in terms of ligand occupancy, relevant response for further investigation of downstream events.

We then investigated whether P2X7R activation induces TG2 secretion. TG2-transfected P2X7R cells were treated with agonist for 5, 10 or 30 min, followed by a 30-min chase period after agonist wash out. Supernatants of both fractions were analyzed for TG2 by western blotting. Within 10 min of BzATP application, pulse fractions revealed substantial TG2 secretion in agonist-treated but not vehicle-treated cells (Fig. 2A). No TG2 export was seen after 5 min indicating that kinetics were considerably slower than Ca^{2+} signaling. Interestingly, elevated TG2 levels in the chase fraction were observed in cells that were exposed to BzATP for 5 min (Fig. 2A) or even 1 min (data not shown), indicating that P2X7R activation, and not subsequent events occurring upon prolonged agonist exposure, triggers TG2 export. As TG2 levels in the chase fraction were independent of the agonist exposure time (Fig. 2A), it appears that, once initiated, the TG2 export mechanism is active over an extended time period and leads to gradual extracellular TG2 accumulation at a constant rate. Note, the amount of secreted TG2 is small compared to the total and, hence, export does not deplete cellular TG2 over the time period investigated (Fig. 2D, cell lysate). To further demonstrate that this cell response required P2X7R activity, we employed the competitive P2X7R inhibitor A740003. At 5 μM, it completely blocks a rise in the intracellular Ca^{2+} concentration ($[Ca^{2+}]_i$) in response to BzATP (Fig. 2B, top panel), and this is reversible upon inhibitor wash out (Fig. 2B, bottom panel). BzATP stimulation of cells in the presence of this inhibitor was unable to trigger TG2 secretion (Fig. 2C), demonstrating that active secretion of TG2 is a P2X7R-regulated process.

P2X7R-mediated TG2 export is not linked to loss of cell membrane integrity or apoptosis

Shedding of membrane-bound particles containing TG2 together with the lipid raft protein flotillin-2 has been reported (Antonyak et al., 2011). Hence, we investigated whether P2X7R-mediated TG2 secretion correlated with flotillin-2 release. Western blot analysis of cell lysates confirmed that flotillin-2 and TG2 were expressed at comparable levels in P2X7R and parental cells (Fig. 2D, cell lysate). Only P2X7R cells responded to BzATP stimulation with release of flotillin-2 into the cell supernatant, indicating P2X7R-dependent vesicle shedding (Fig. 2D, medium). Similar to TG2, flotillin-2 was present in the pulse fraction and accumulated in the chase fraction, potentially indicating co-release. To further analyze secreted material and exclude protein release through passive cell lysis we investigated externalization of the cytosolic proteins IκBα, GAPDH and β-tubulin, as well as of HMGB-1 which is secreted non-classically via the exosome pathway (Lu et al., 2012). We were unable to detect any of these proteins in the cell supernatant after P2X7R activation (Fig. 2E and data not shown). However, given that prolonged stimulation of P2X7R can lead to cell death (Mackenzie et al., 2005), and this crucially affects the conclusions, we designed experiments to more selectively investigate loss of membrane integrity and apoptosis, respectively. First, release of cytosolic lactate dehydrogenase (LDH) was quantified after stimulation of either P2X7R or parental cells with BzATP for 10 min. No P2X7R-induced release of LDH was seen (Fig. S3A). Second, BzATP-treated P2X7R cells were chased for various times up to 22 h and assessed for caspase-3 activation by western blotting. Activated caspase-3 could not be detected at any time (Fig. S3B) whereas within 6 h of TNFα stimulation caspase-3 cleavage was evident as reported (Arlt et al., 2003). These data show that TG2 externalization is not related to cell damage or death but is a selective process, possibly linked to P2X7R-dependent membrane changes. This is consistent with activation of P2X7R triggering rapid alterations in membrane topology without causing cell death in a manner that completely reverses as $[Ca^{2+}]_i$ falls, unless receptor stimulation is sustained for long time periods (Mackenzie et al., 2005).

TG2 localizes to membrane subdomains upon cell stimulation with P2X7R agonist

In P2X7R-expressing cells, the prolonged increase in $[Ca^{2+}]_i$ upon BzATP application was followed within 30 s by extensive cell blebbing as visualized by real-time microscopy (Fig. 3A, arrows). The term ‘blebbing’ is used here to describe formation of plasma membrane projections due to Rho-dependent actin reorganization that follow P2X7R activation (MacKenzie et al., 2001; Pfeiffer et al., 2004). This response is P2X specific. Stimulation of the parental cells, which express P2Y receptors, with ATP induced smaller transient oscillations in $[Ca^{2+}]_i$ but no apparent morphological changes (Fig. 3A). This led us to speculate that TG2 externalization might be linked to membrane bleb formation,

Journal of Cell Science (2015) 128, 4615-4628 doi:10.1242/jcs.175968

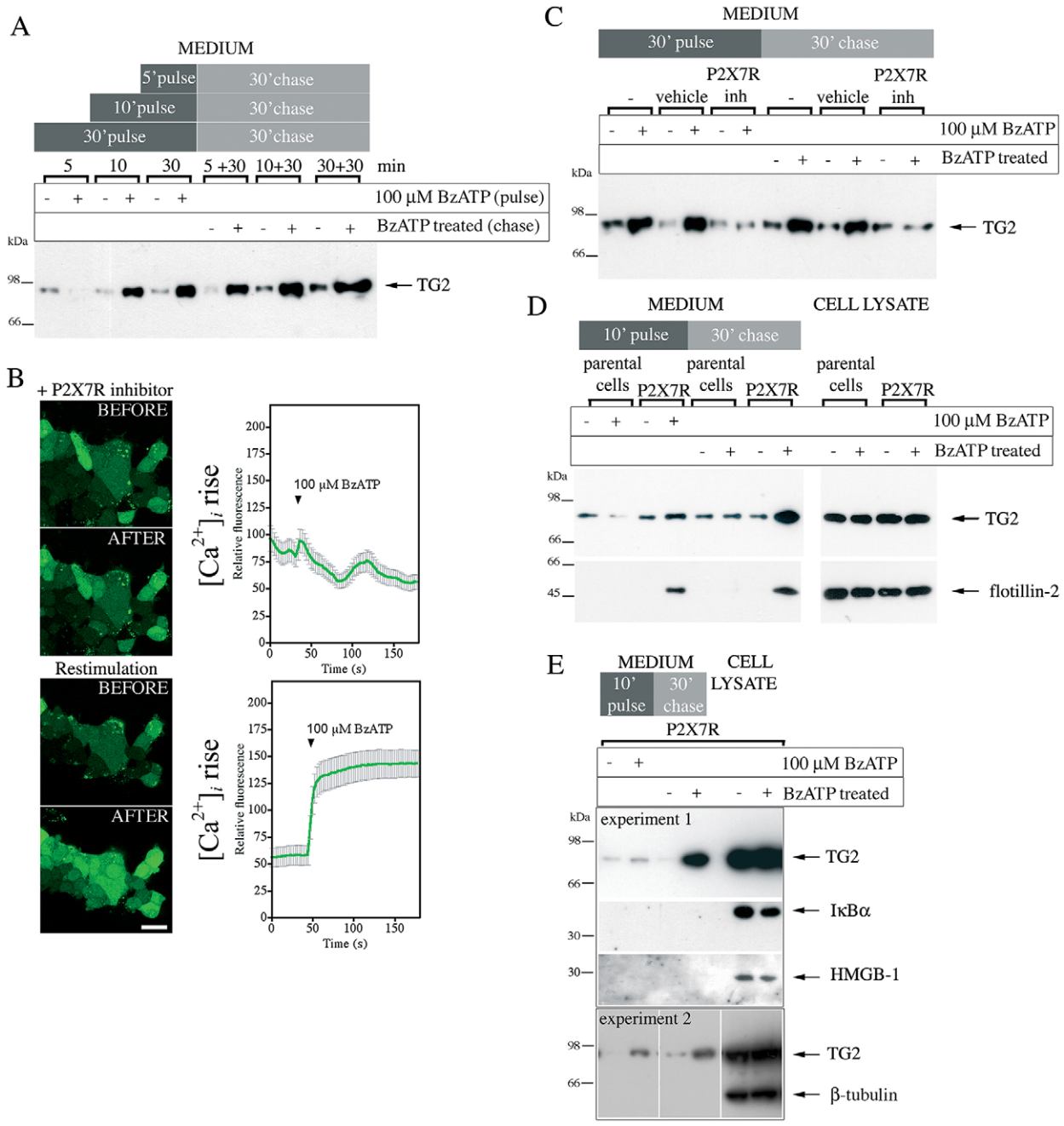

Fig. 2. P2X7R activation mediates TG2 externalization. (A) Analysis of TG2 secretion in HEK293 P2X7R cells. TG2-transfected cells were stimulated with BzATP or vehicle for indicated time (pulse), then incubated for 30 min in agonist-free medium (chase). TG2 secretion into cell-free supernatants was assessed by western blotting. (B) Inhibitor A740003 reversibly blocks P2X7R activation. P2X7R cells were incubated with Fluo-4-AM and 5 µM P2X7R inhibitor for 20 min prior to BzATP stimulation in the presence of inhibitor (top), washed with inhibitor-free medium for 5 min, and then re-stimulated with BzATP (bottom). The fluorescence (λ_{ex}, 488 nm; λ_{em}, 500–535 nm) change in individual cells was monitored by confocal microscopy (mean±s.e.m., *n*=30) (right). Optical sections of the same field before and 180 s after BzATP addition are shown (left). Scale bar: 25 µm. (C) P2X7R inhibitor (inh) blocks TG2 secretion. TG2-transfected P2X7R cells were pre-treated with P2X7R inhibitor or vehicle for 10 min before BzATP stimulation as indicated. TG2 release into medium was assessed as in A. (D,E) Cells release membrane-bound particles upon P2X7R activation. TG2 transfected P2X7R or parental cells were BzATP stimulated for 10 min, and chased in agonist-free medium. Conditioned media and cell lysate were analyzed by western blotting for TG2 and the microvesicle marker flotillin-2 (D) or, as a control, β-tubulin, IκBα and HMGB-1 (E).

and we used GFP-tagged TG2 to monitor its redistribution in live cells. We confirmed that P2X7R activation triggered externalization of tagged TG2 similar to wild-type TG2 (Fig. 3B). Analysis by confocal microscopy revealed a clear ubiquitous cytoplasmic distribution for TG2–GFP (Fig. 3C). Upon P2X7R activation, TG2–GFP was rapidly translocated into membrane blebs, and freely re-localized to sites where new membrane protrusions formed (Fig. 3C, arrow). However, despite abundant bleb formation, careful reconstruction from image sequences revealed that these large membrane protrusions remained continuous with the plasma membrane and were eventually retracted by cells. We obtained similar results for N- and C-terminally tagged TG2 indicating that

Journal of Cell Science (2015) 128, 4615-4628 doi:10.1242/jcs.175968

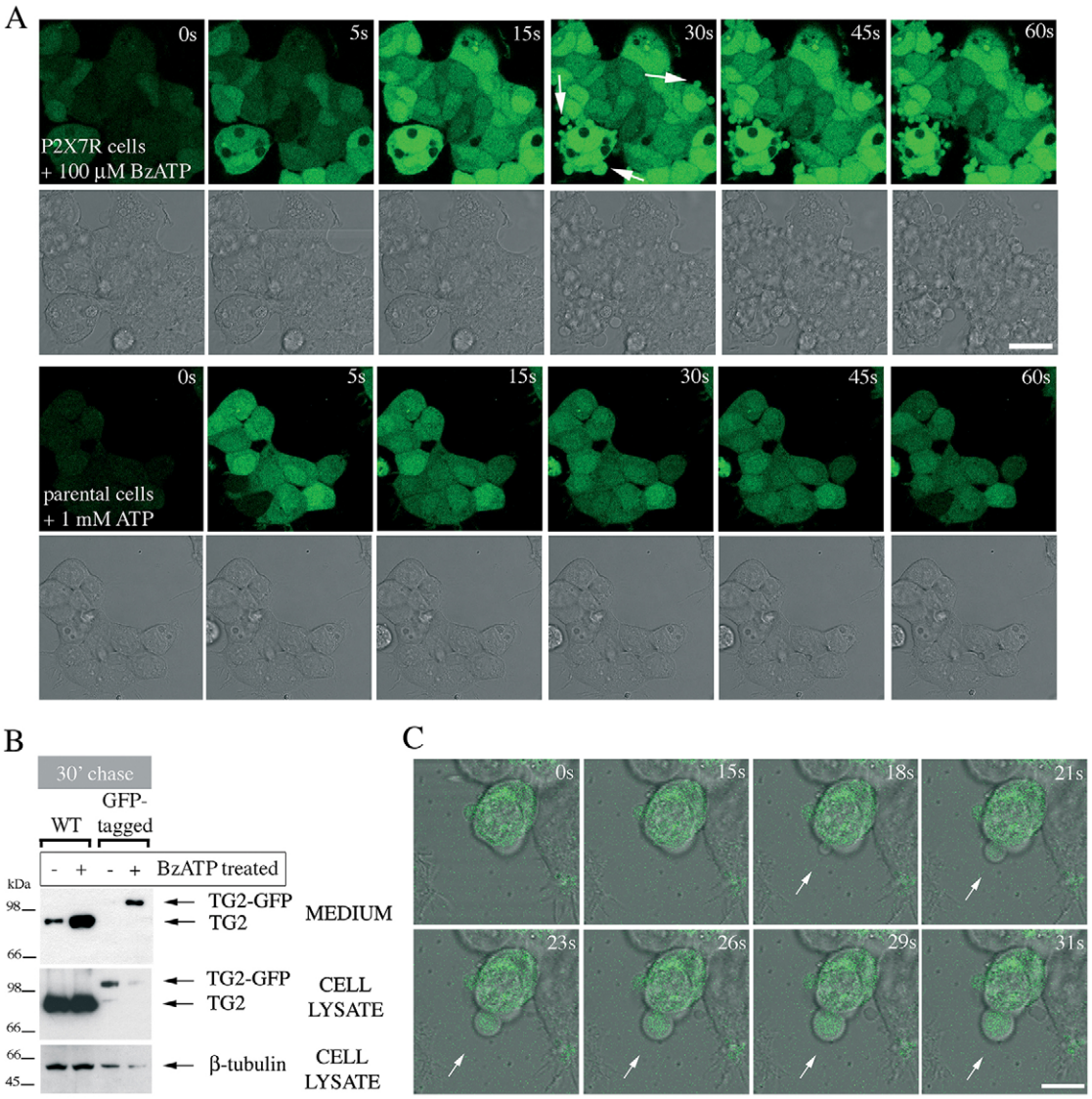

Fig. 3. Membrane blebs induced by P2X7R activation contain TG2. (A) P2X7R signaling induces rapid membrane blebbing. Fluo-4-AM-loaded P2X7R cells were stimulated with BzATP while acquiring fluorescence and phase-contrast images by real-time microscopy to visualize morphological changes and Ca^{2+} signaling simultaneously (top). Membrane blebs are indicated by arrows. ATP stimulation of parental cells induces oscillating Ca^{2+} signals but no overt morphological changes (bottom). Scale bar: 25 µm. (B,C) TG2 redistributes into membrane blebs. To confirm export of tagged TG2, TG2- (wild-type, WT) or TG2–GFP-expressing P2X7R cells were stimulated with 100 µM BzATP for 10 min, chased for 30 min in agonist-free medium, followed by analysis of conditioned media and cell extracts for TG2 by western blotting (B). To localize GFP-tagged TG2 during BzATP stimulation, real-time confocal microscopy was employed. Genesis of a membrane bleb is depicted (arrows), with an optical section of GFP fluorescence overlaid onto phase-contrast images to correlate morphological changes with changes in TG2 distribution (C). Scale bar: 10 µm.

the position of the tag did not substantially alter protein localization. Although we were unable to directly visualize TG2 release, a noticeable reduction in fluorescence upon P2X7R activation indicated that the intracellular pool of TG2 was rapidly diminished, consistent with its relocation into the medium (Fig. 3B).

P2X7R-agonist-induced TG2 secretion is independent of microvesicle shedding

As small vesicles might be released by cells that are beyond the resolution of conventional confocal microscopy, we used light scattering combined with particle tracking to further analyze cell-free supernatants for nanoparticles. A robust increase in particle shedding by P2X7R cells upon BzATP treatment was observed during stimulation and in the subsequent chase period (Fig. 4A). Most of the secreted particles had diameters of 81–262 nm (Fig. 4B) in line with more variably sized microvesicles, rather than exosomes that originate from multivesicular bodies, which are size-constrained and typically <90 nm (Cococci et al., 2009). TG2 expression modestly increased the proportion of larger particles (Fig. 4B) but did not substantially alter total particle release (Fig. 4A). To understand whether TG2 localizes in microvesicles, freshly harvested conditioned medium was subjected to differential centrifugation and resulting pellets and supernatant were analyzed by western blotting (Fig. 4C). TG2 mainly localized to the 100,000 ***g*** supernatant fraction containing soluble proteins (S5), with some TG2 found in very large aggregates or associated with organelles (P2) but not in the microvesicle fraction (P4). To substantiate this, microvesicles were separated using a sucrose density gradient

Journal of Cell Science (2015) 128, 4615-4628 doi:10.1242/jcs.175968

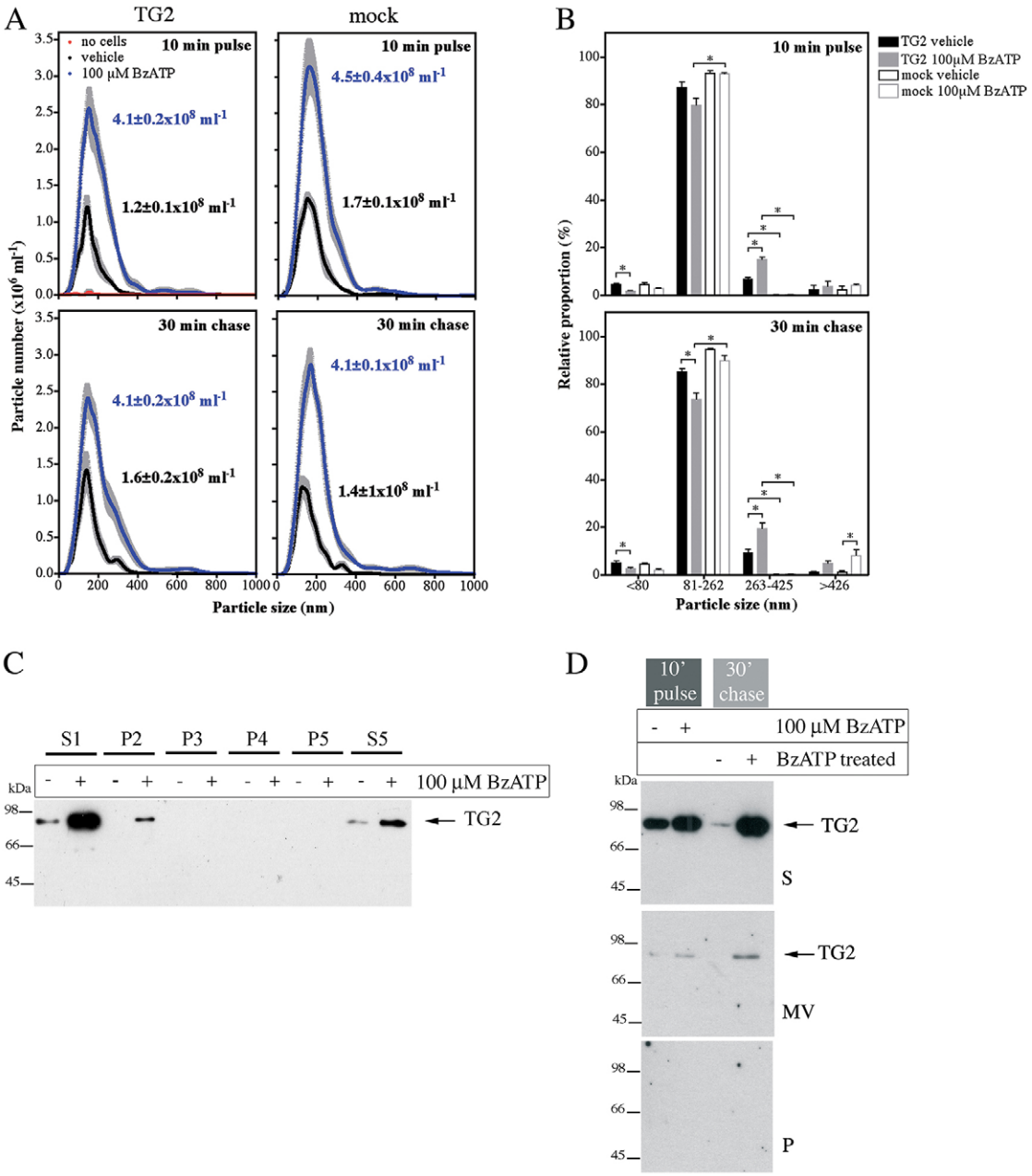

Fig. 4. P2X7R-mediated TG2 export is not due to microvesicle release. (A,B) Analysis of vesicle release by nanoparticle tracking. TG2- or mock-transfected P2X7R cells were stimulated with BzATP for 10 min, chased for 30 min in agonist-free medium, and conditioned media were analyzed for nanoparticles using light scattering in combination with particle tracking (Nanosight). Particle distribution and total particle concentration is shown (mean±s.e.m.; *n*=5) (A). Particles were broadly assigned to one of four fractions based on volume: representing exosomes (~60 nm; ≤80 nm diameter), microvesicles (~145 nm; 81–262 nm), larger vesicles (~335 nm; 263–425 nm) and aggregates or membrane blebs (≥426 nm) (B). (C,D) Analysis of isolated microvesicles for TG2. Cell-free medium (S1) from BzATP- or control-treated cells was subjected to differential centrifugation (P, pellet; S, supernatant): in C, 3000 ***g*** twice (P2, P3), 10,000 ***g*** (P4), and 100,000 ***g*** (P5, S5), and in D, 3000 ***g*** followed by separation of microvesicles (MV) on a sucrose cushion. Fractions were analyzed for TG2 by western blotting.

(Fig. 4D). Again, TG2 was predominantly in the soluble protein fraction. These data suggest that although P2X7R activation induces abundant microvesicle release by cells, secreted TG2 is not apparently associated with microvesicles but present as a free form.

Extracellular Ca^{2+} regulates TG2 externalization, but its secretion is independent of catalytic enzyme functions

TG2 secretion was effectively stimulated by P2X7R activation in medium that contains 0.9 mM Ca^{2+}, which is similar to the free ionized extracellular Ca^{2+} concentration estimated at 1.1–1.3 mM (Riccardi and Kemp, 2012), but surprisingly not in medium containing high Ca^{2+} (Figs 1D and 5A). BzATP treatment of cells in the absence of Ca^{2+} led to enhanced TG2 secretion during stimulation only (Fig. 5A), indicating that TG2 export was faster but not sustained. In contrast, flotillin-2 release occurring at 0.9 mM Ca^{2+} was greatly reduced when cells were stimulated with agonist at either 0 or 2.2 mM Ca^{2+} (Fig. 5A). This shows that TG2 and flotillin-2 secretion is differentially affected by the extracellular Ca^{2+} concentration ($[Ca^{2+}]_{ex}$) and hence, that the underlying mechanisms are distinct. As microvesicle shedding is a Ca^{2+}-dependent process,

Journal of Cell Science (2015) 128, 4615-4628 doi:10.1242/jcs.175968

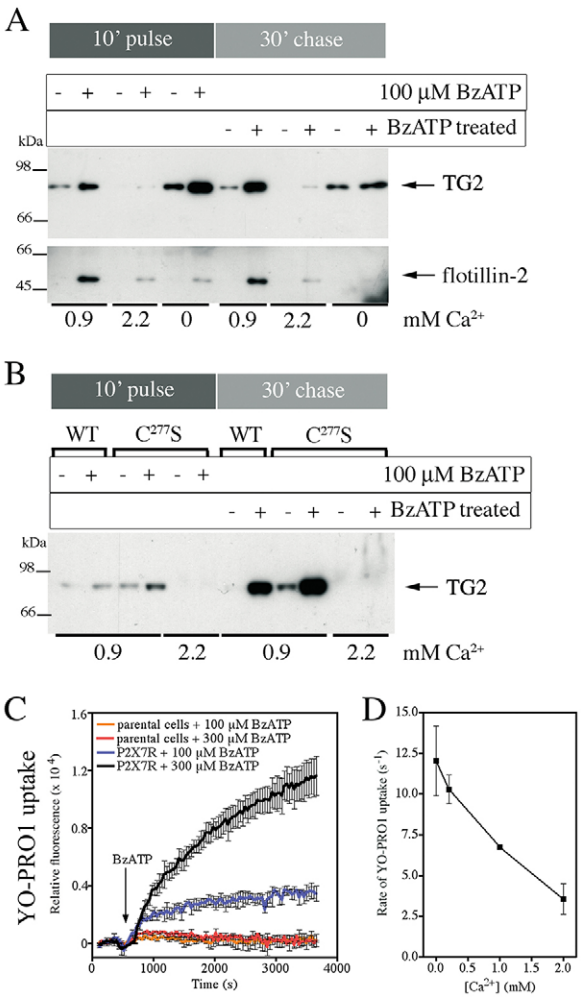

Fig. 5. Extracellular Ca^{2+} regulates TG2 secretion. (A) P2X7R-mediated TG2 export at different $[Ca^{2+}]_{ex}$. P2X7R cells expressing TG2 were stimulated with BzATP for 10 min in medium containing 0.9 or 2.2 mM Ca^{2+} or in Ca^{2+}-free medium, and chased for 30 min in respective media without BzATP. Conditioned media were analyzed by western blotting for TG2 and flotillin-2. (B) TG2 catalytic activity is not required for P2X7R-mediated export. P2X7R cells expressing TG2 or the TG2 C277S mutant were stimulated with BzATP in medium containing 0.9 or 2.2 mM Ca^{2+} and TG2 export was assessed as above. (C,D) $[Ca^{2+}]_{ex}$ regulates P2X7R activity. P2X7R or parental cells were stimulated with BzATP, as indicated, in PSS containing YO-PRO1 and different concentrations of Ca^{2+}. To determine YO-PRO1 uptake by cells after BzATP application, changes in well-specific fluorescence (λ_{ex}, 480-10 nm; λ_{em}, 520-10 nm) were monitored over time. A representative experiment of dye uptake in Ca^{2+}-free PSS is shown as mean±s.e.m. of two wells (C). In D, the initial rates of YO-PRO1 uptake at different $[Ca^{2+}]_{ex}$ in response to 300 µM BzATP are given (mean±s.e.m.; *n*=2).

TG2 release in Ca^{2+}-free medium supports a vesicle-independent mode of release, in line with previous data (Fig. 4).

To exclude Ca^{2+}-dependent loss of externalized TG2 due to cell surface retention through interaction with substrates or autocatalytic crosslinking, we compared secretion of wild-type TG2 with crosslinking-incompetent TG2 C277S (Stephens et al., 2004). BzATP stimulation of cells induced export of both TG2 and TG2 C277S at 0.9 mM Ca^{2+} but not at 2.2 mM (Fig. 5B). This indicates that the lack of TG2 secretion at high $[Ca^{2+}]_{ex}$ is not due to TG2 activity but might reflect differences in the P2X7R activation state. This is further supported by high $[Ca^{2+}]_{ex}$ also affecting flotillin-2 release (Fig. 5A). Besides cation transport, activation of P2X7R can lead to 'membrane pore' formation which manifests as apparent permeability of the plasma membrane to cationic molecules such as YO-PRO1 (Virginio et al., 1999; Pelegrín, 2011; Browne et al., 2013). Measurement of YO-PRO1 uptake confirmed that P2X7R cells, but not parental cells, form membrane pores upon BzATP treatment (Fig. 5C), and that the dye uptake rate is inversely correlated to $[Ca^{2+}]_{ex}$ (Fig. 5D). Ca^{2+}–nucleotide interactions could potentially limit the effective agonist concentration. However, the observed BzATP dose response is not consistent with this explanation (Fig. S3C). Therefore, in our experiments, Ca^{2+} likely acts as an allosteric regulator of P2X7R, either directly or indirectly inhibiting receptor activation as previously suggested (Yan et al., 2011). Taken together, this suggests that high $[Ca^{2+}]_{ex}$ is an important negative regulator of TG2 secretion, whereby Ca^{2+} ions appear to regulate P2X7R activation rather than influencing TG2 activity during export.

TG2 export is linked to P2X7R-mediated membrane pore formation

To assess the contribution of the initial ion flux on TG2 secretion, calmidazolium was employed. This compound is an inhibitor with broad selectivity for voltage-gated fast-acting Na^+/K^+ and L-type Ca^{2+} channels that also inhibits the initial ATP-evoked ion flux through P2X7R without affecting the downstream membrane pore formation (Virginio et al., 1997). Calmidazolium has an extracellular mode of action on P2X7R. BzATP-induced TG2 export in P2X7R cells was unaffected by the presence of calmidazolium but flotillin-2 secretion was blocked (Fig. 6A). The inhibitor had no effect on pore formation activity of P2X7R (Fig. 6B) but substantially reduced the rise in $[Ca^{2+}]_i$ mediated by P2X7R activation (Fig. 6C). This indicates that TG2 secretion is linked to P2X7R-dependent pore formation but not the initial ion flux and associated membrane depolarization.

Given that TG2 secretion was induced by P2X7R activation in Ca^{2+}-free medium but the kinetics of export were altered (Fig. 5A), we investigated whether Ca^{2+} release from intracellular stores plays a role. P2X7R cells were pre-loaded with the Ca^{2+} chelator BAPTA-AM to buffer free cytosolic Ca^{2+} prior to BzATP stimulation in Ca^{2+}-free medium. This reduced TG2 release to near baseline levels (Fig. S3D), confirming that Ca^{2+} signaling has a role in TG2 export as previously suggested (Zemskov et al., 2011). Conversely, cyclopiazonic acid (CPA) was applied to inhibit the SERCA Ca^{2+} transporter to trigger a rise in $[Ca^{2+}]_i$ in the absence of P2X7R activation. CPA addition alone was unable to induce TG2 secretion (Fig. S3D), despite inducing a peak $[Ca^{2+}]_i$ of the same magnitude as P2X7R activation when used at 20 µM (Fig. S3E). This indicates that a rise in $[Ca^{2+}]_i$ by itself is not sufficient to induce TG2 export.

TG2 secretion is pannexin independent but enhanced by activating mutations in P2X7R

P2X7R-mediated membrane pore formation has been proposed to relate to P2X7R channel dilation upon saturation of ATP-binding sites, possibly combined with acquisition of additional subunits (Browne et al., 2013) or alternatively, by coupling to another channel (i.e. pannexin-1) (Pelegrin and Surprenant, 2007; Gulbransen et al., 2012). We evaluated the latter by treating cells with pannexin inhibitors. Neither the peptidic competitor ^{10}Panx (Pelegrin and Surprenant, 2007) nor trovafloxacin (Poon et al., 2014) had any effect on BzATP-stimulated YO-PRO1 uptake (Fig. 7A) or TG2 export. We therefore sought to clarify whether the C-terminally truncated P2X7R splice variant B that lacks pore forming ability (Adinolfi et al., 2010) supports TG2 secretion.

Journal of Cell Science (2015) 128, 4615-4628 doi:10.1242/jcs.175968

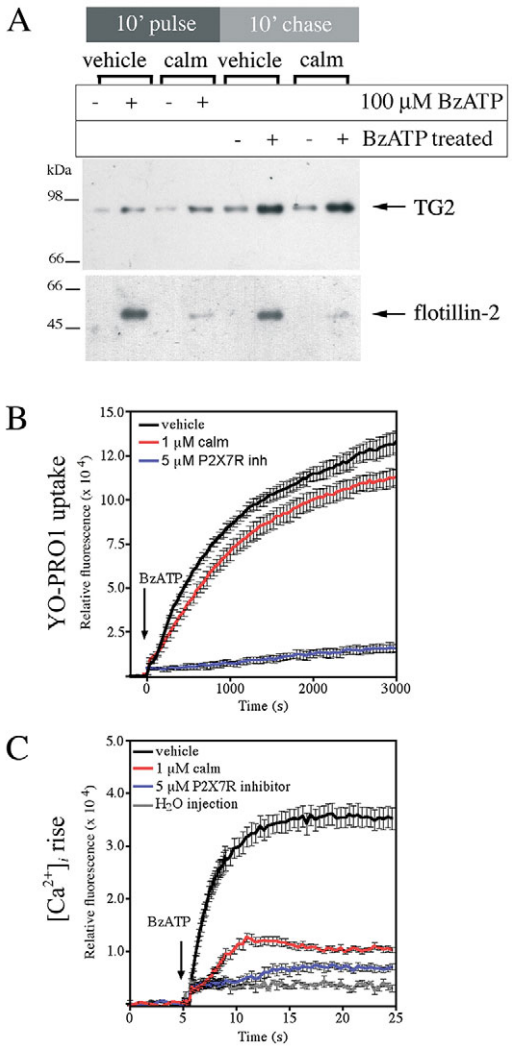

Fig. 6. TG2 export is independent of K^+ efflux and membrane depolarization. (A) Calmidazolium (calm) blocks flotillin-2 but not TG2 release. TG2-transfected P2X7R cells were pre-treated for 10 min and then stimulated with BzATP in medium containing 1 µM calmidazolium or vehicle. Cells were chased in agonist-free medium, and conditioned media analyzed by western blotting for TG2 and flotillin-2. (B) Calmidazolium does not affect P2X7R-dependent 'membrane pore' formation. P2X7R cells were pre-treated with calmidazolium, P2X7R inhibitor A740003 or vehicle for 10 min prior to stimulation with 100 µM BzATP in the presence of respective inhibitors or carrier in PSS containing YO-PRO1 and 0.9 mM Ca^{2+}. Dye uptake was monitored over time. Results are shown as mean±s.e.m. of two wells, and are representative of three independent experiments. (C) Calmidazolium ameliorates the large rise in $[Ca^{2+}]_i$. Fluo-4-AM-loaded P2X7R cells were pre-treated with calmidazolium, P2X7R inhibitor or vehicle for 20 min prior to stimulation with 100 µM BzATP in the presence of inhibitors or carrier. Fluorescence change (λ_{ex}, 485-12 nm; λ_{em}, 520-10 nm) relative to control in response to agonist treatment was monitored (mean±s.e.m. of eight replicate wells).

However, expression of this variant after site-specific stable integration or transient transfection was very low as determined by western blotting of cell lysates (Fig. 7B), and we were unable to confirm cell surface localization with antibodies against the P2X7R extracellular domain. Nevertheless, we attempted to confirm agonist-mediated membrane depolarization using the sensitive voltage-sensing FRET probes CC2-DMPE and $DiSBAC_2$ (Wolff et al., 2003). Only cells expressing wild-type P2X7R showed membrane channel activity (response ratio for P2X7R, 1.53±0.04 with BzATP, 2.17±0.12 with KCl, 1.07±0.06 with control solution; for P2X7R variant B, 1.10±0.03 with BzATP, 1.74±0.10 with KCl; mean±s.d., n=4), suggesting altered trafficking and degradation of the truncated receptor variant.

A mutation in mouse P2X7R renders it deficient in pore-forming activity (Sorge et al., 2012). As the affected sequence motif in the P2X7R C-terminal domain is conserved in humans, we generated cells expressing human P2X7R with the analogous mutation P451L (Fig. 7B,C). However, these cells formed membrane pores in response to BzATP as revealed by YO-PRO1 uptake (Fig. 7D). This led us to investigate the gain-of-function P2X7R variant, A348T, which confers increased risk for autoimmune disease in man (Stokes et al., 2010), to substantiate a link between pore formation and TG2 secretion. Cells expressing P2X7R A348T (Fig. 7B,C) had a substantially increased propensity to form membrane pores as evidenced by enhanced peak pore activity (Fig. 7D) and by pore formation at very low BzATP concentrations (Fig. 7E). This enhanced pore activity was reflected in a corresponding increase in TG2 export (Fig. 7F,G). Interestingly, we also observed BzATP-induced secretion of thioredoxin-1 (Fig. 7H), an enzyme that can re-activate oxidatively inactivated TG2. This not only indicates that membrane pore activity controls the rate of TG2 export but that it leads to co-secretion of TG2 with thioredoxin-1 (Fig. 8).

DISCUSSION

Here, we identify P2X7R as the central regulator of the pathway that enables active export of TG2 and its co-activator, thioredoxin-1. The action of both of these enzymes has been linked to specific immune responses (Iismaa et al., 2009; Jaeger et al., 2013), and this might therefore constitute a pathway for export of proteins relevant to innate immunity. Besides having roles in re-instating tissue integrity following injury or roles associated with infection control, TGs including TG2 have been implicated in immune regulation (Tóth et al., 2009; Loof et al., 2011). Here, we show that in monocytes and macrophages, purinergic signaling triggered rapid TG2 export in the absence of TLR engagement, and that this response was dependent on P2X7R but did not require caspase-1 activity. Likewise, introduction of P2X7R in HEK293 cells devoid of other inflammasome components (Lu et al., 2012) instated agonist-regulated rapid TG2 export. Taken together, the data demonstrate that P2X7R signaling alone is sufficient to trigger TG2 export, and involvement of an inflammasome-independent mechanism of export is further supported by the fact that externalized TG2 was not associated with vesicles or co-secreted with exosome-associated HMGB-1.

A redox-sensitive Cys switch promotes oxidative inactivation of TG2 (Stamnaes et al., 2010), a mechanism that is thought to contribute to rapid enzyme inactivation in the extracellular milieu (Jin et al., 2011) and thereby, to prevent aberrant crosslinking that might lead to fibrosis and potentially autoimmunity through neo-epitope formation (Aeschlimann and Thomazy, 2000; Iismaa et al., 2009). However, it has been shown that extracellular-matrix-associated TG2 can be reactivated by thioredoxin-1 released from activated monocytes during inflammation (Jin et al., 2011). Cell-surface-associated thioredoxin-1 plays a key role in innate immunity, particularly in mucosal epithelia where it activates β-defensin-1 (Jaeger et al., 2013). Interestingly, thioredoxin-1 is also an unconventionally secreted protein (Rubartelli et al., 1992), and our results show that it is in fact co-secreted with TG2. We speculate that thioredoxin-1 might not primarily act on pre-existing extracellular TG2 but could have a role as a chaperone during active TG2 export, enabling conversion of TG2 into its active

Journal of Cell Science (2015) 128, 4615-4628 doi:10.1242/jcs.175968

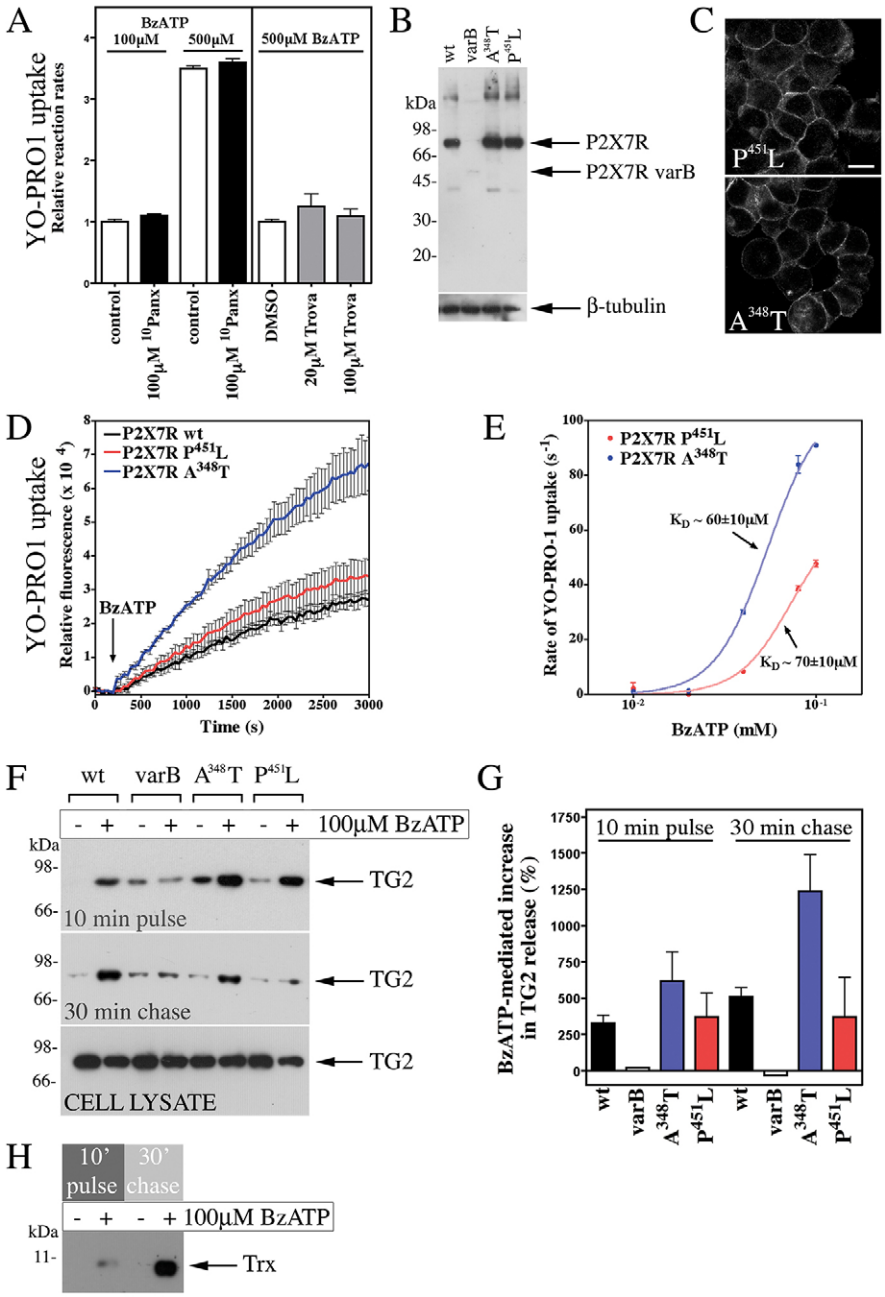

Fig. 7. P2X7R-mediated membrane pore formation is required for TG2 externalization. (A) P2X7R-mediated pore formation is pannexin independent. P2X7R cells were pre-treated with ^{10}Panx or trovafloxacin (Trova) as indicated, and then stimulated with BzATP in PSS with respective inhibitors, YO-PRO1 and 0.9 mM Ca^{2+}. Results are given as initial rates of dye uptake relative to control (mean±s.e.m.; *n*=3). Pannexin inhibitors did not affect dye uptake, neither at limiting nor saturating agonist concentration. (B,C) Characterization of expression of mutant P2X7Rs. Extracts of cells stably expressing wild-type (wt), A348T or P451L P2X7R, or the P2X7R variant B (varB) were analyzed by western blotting with antibodies against the P2X7R extracellular domain and β-tubulin, as a loading control (B). Membrane localization of receptor was confirmed by immunocytochemistry (C; compare to Fig. S2B). Images reflect an optical section acquired by confocal microscopy. Scale bar: 12.5 μm. (D,E) Pore formation is enhanced in cells expressing P2X7R A348T. YO-PRO1 uptake following stimulation of cells with 100 μM BzATP is shown as mean±s.e.m. (*n*=3) fluorescence (D). Comparison of initial rate of YO-PRO1 uptake for P2X7R-A348T- and P451L-expressing cells highlights increased pore activity for P2X7R A348T but unchanged ligand regulation (E). Results are mean±s.d. (*n*=2). (F–H) TG2 export correlates with receptor pore activity. TG2-transfected cells expressing P2X7R variants were stimulated with BzATP for 10 min, and chased in agonist-free medium. Conditioned media were analyzed by western blotting for TG2 (F), and results (mean±s.e.m., *n*=3) quantified by densitometry (G). Note, cell lysates confirm comparable TG2 expression levels in different cell lines (F). For thioredoxin-1 (Trx) detection, media (P2X7R cells) were analyzed by western blotting after separation in 16% SDS-PAGE Tricine gels (H).

conformation. Such a mechanism could explain why, in celiac disease, active TG2 accumulates in the intestinal mucosa (Korponay-Szabó et al., 2004).

Purinergic signaling fulfills the pre-requisites for a unifying pathway regulating TG export

As TG2, and also other TGs, can be externalized by a range of cells including myeloid, mesenchymal, endothelial and epithelial cells (Aeschlimann and Thomazy, 2000; Nurminskaya and Belkin, 2012), it is implausible that this involves multiple highly divergent mechanisms as proposed previously. P2X7R is not restricted to the hematopoietic lineage as originally thought but is also widely distributed among mesenchymal, endothelial and epithelial cells, and in the central and peripheral nervous system (Bartlett et al., 2014). Activation of P2X7R occurs not only in conjunction with injury, cell stress and inflammatory processes but has major independent roles in the musculoskeletal (Garcia and Knight, 2010) and nervous system (Burnstock, 2015), contexts within which TG2-mediated extracellular reactions are also prevalent (Aeschlimann et al., 1995; Iismaa et al., 2009; Thomas et al., 2013).

Unlike previous work, our data implicate a regulated pathway in TG2 export. This mechanism might be activated to a varying extent under different conditions. A key finding here is that Ca^{2+} levels present in many media formulations impair TG2 release. Our data with catalytically inactive TG2 C277S show that this is not related to the regulation of TG2 by Ca^{2+} but due to suppressed P2X7R functionality, in line with evidence suggesting that divalent cations, including Ca^{2+}, allosterically inhibit P2X7R (Yan et al., 2011). Therefore, the differences in extracellular Ca^{2+} or ATP concentrations might explain some contradictory findings in the literature. It is worth noting that modest shear stress during medium exchange or passaging can trigger cellular ATP release (Rumney

Journal of Cell Science (2015) 128, 4615-4628 doi:10.1242/jcs.175968

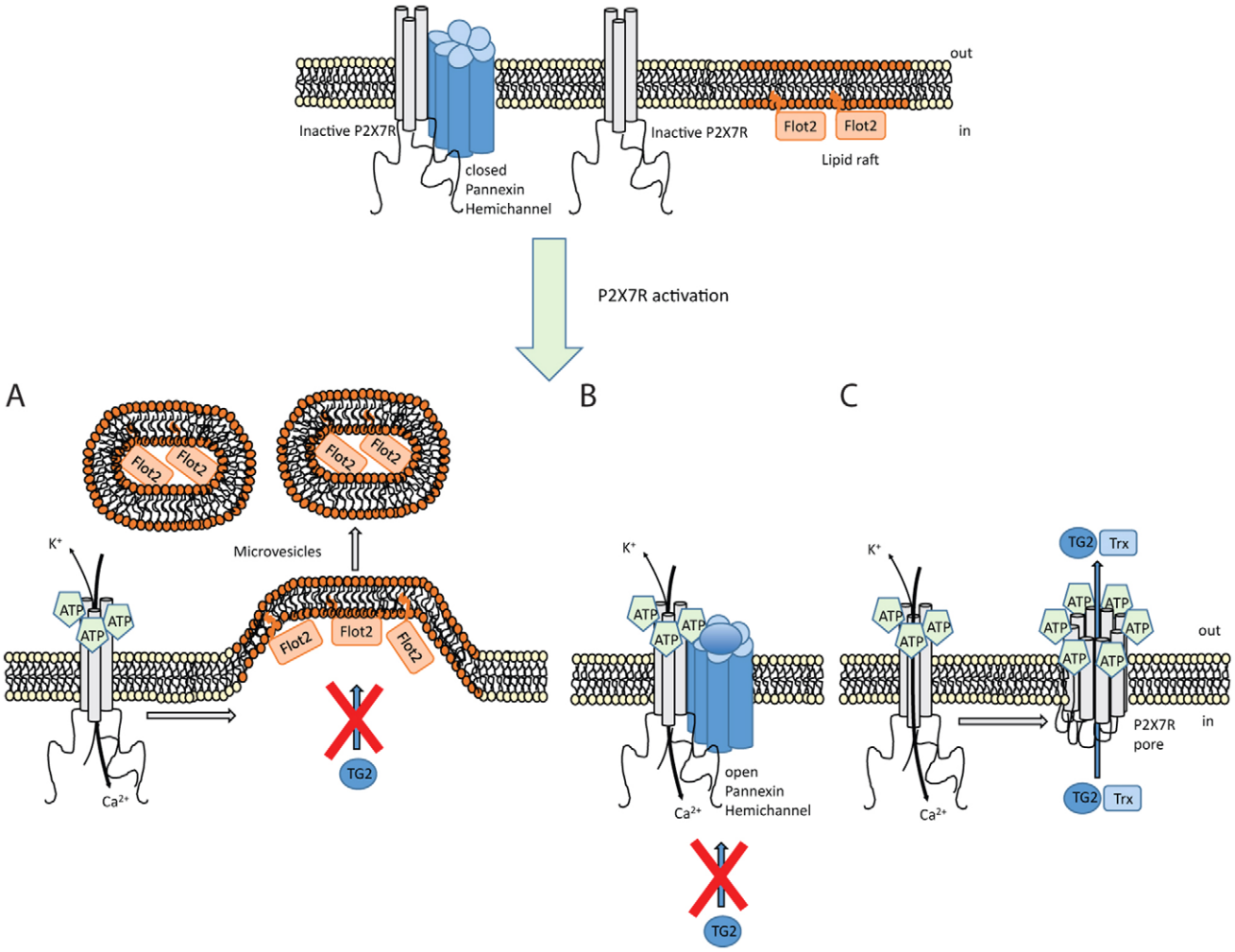

Fig. 8. Mechanism controlling TG2 export. Schematic showing different events occurring upon P2X7R activation by ATP. (A) Ion channel activity triggers intracellular signaling that results in actin reorganization and microvesicle shedding. However, these microvesicles do not contain TG2. (B) Coupling between P2X7R and pannexin-1 triggers hemichannel pore opening. TG2 secretion is unaffected by blocking pannexin-1 channels. (C) P2X7R itself can form a membrane pore through conformational changes and, possibly, receptor oligomerization in a process that involves the extended intracellular C-terminal sequence. TG2 secretion is associated with this membrane pore activity but independent of ion channel function, and occurs in conjunction with thioredoxin-1 (Trx) externalization. As thioredoxin can reactivate TG2 functionally blocked in an oxidized state, this might ensure that externalized TG2 has transamidation activity. Flot2, flotillin-2.

et al., 2012) and, consequently, P2X7R-mediated TG2 release at low (0–1 mM) but not high (≥2 mM) $[Ca^{2+}]_{ex}$. Hence, endogenous P2X7R activation might explain apparently ‘constitutive’ TG2 secretion.

Crucially, in our HEK293 model, TG2 is not retained at the cell surface or internalized, unless an appropriate cell surface receptor is introduced (Fig. S4). Hence, TG2 export can be directly assessed by quantification in the cell supernatant. Thus, our system is overcoming intrinsic difficulties that hampered progress in the analysis of TG2 export previously, including quantification of cell-surface-associated TG2 without disrupting cell integrity or endocytic TG2 uptake and retrograde transport. This, together with modulation of the different P2X7R activities with small molecules or by mutagenesis, provided strong evidence for a direct link between P2X7R signaling and TG2 export. Our data is not contradictory to passive TG2 release as a consequence of a substantial insult, including mechanical damage (Upchurch et al., 1987) or TLR engagement (Siegel et al., 2008), or to vesicle-associated TG2 release under circumstances such as serum-starvation-associated cell stress (Antonyak et al., 2011). Rather, it suggests that purinergic signaling links controlled TG2 export to specific extracellular functions. Furthermore, given that microvesicle-associated TG2 has been shown to colocalize with fibronectin (Antonyak et al., 2011), an extracellular enzyme localization is implied. Therefore, it is possible that TG2 preferentially binds to plasma membrane subdomains where specific types of microvesicle form (pericellular matrix reorganization), thereby explaining the apparent association, but that this occurs subsequent to membrane translocation.

Different activities of TG2 as well as sequence motifs for interaction with proteins and phospholipids have been implicated in the export process (Balklava et al., 2002; Scarpellini et al., 2009; Chou et al., 2011; Zemskov et al., 2011). Our data show that transamidation activity is dispensable for export and that tagging TG2 with GFP does not prevent export, thereby excluding a terminal targeting signal. Blocking TG2 interaction with classically secreted proteins such as fibronectin, syndecans and integrins might alter extracellular localization or endocytic uptake and trafficking of TG2 (Antonyak et al., 2011; Chou et al., 2011; Zemskov et al., 2011) but cannot explain how the implied membrane translocation occurs.

Journal of Cell Science (2015) 128, 4615-4628 doi:10.1242/jcs.175968

Mechanistically, TG2 export is linked to the secondary permeability pathway

Several lines of evidence show that TG2 export is linked to the 'membrane pore' activity associated with P2X7R activation (Fig. 8). Our data show that TG2 export is mechanistically separate from microvesicle shedding. In line with this, P2X7R induces bleb formation and microvesicle shedding through actin reorganization mediated by the MAPK p38 family and Rho activation, whereas YO-PRO1 uptake by cells is insensitive to cytochalasin-D (Pfeiffer et al., 2004). We further show that TG2 export is not induced by a $[Ca^{2+}]_i$ rise alone nor abrogated by pharmacological suppression of P2X7R ion channel function without affecting membrane pore formation. In contrast, introducing a mutation in P2X7R that enhanced pore activity resulted in accelerated TG2 export.

P2X7R is the only P2X receptor where membrane pore formation is consistently observed, and this activity is therefore a defining feature of it. Although mechanistically not fully understood, it requires the extended unique C-terminal intracellular tail (Smart et al., 2003; Sun et al., 2013). Recent data suggest that large cations can pass through the P2X7R channel itself, and that blocking the channel prevents dye uptake by cells (Browne et al., 2013). However, a larger channel diameter than expected from available structural data (Hattori and Gouaux, 2012) would be required to adequately explain permeation of some molecules, and a more substantial conformational change than predicted from existing structural data is indeed supported by a recent study (Allsopp and Evans, 2015). Interestingly, P2X7R also couples to effectors implicated in dye permeability, and a sustained $[Ca^{2+}]_i$ elevation by itself has been shown to trigger membrane pore opening (Bartlett et al., 2014). In our HEK293 model, calmidazolium attenuated Ca^{2+} influx but did not affect membrane pore activity suggesting that distinct permeation pathways are involved. Pannexin-1 is not involved, as shown with inhibitors, consistent with the data of others (Sun et al., 2013). Physiologically, the secondary permeability pathway might have a role in the release of secondary messengers, for example, glutamate release in P2X7R-expressing HEK293 cells has been reported (Cervetto et al., 2013). Given the delay between P2X7R-dependent Ca^{2+} signaling and detection of changes in extracellular TG2, we cannot exclude a role of a secondary messenger system. However, it is conceivable that this pathway constitutes a pore through which proteins can be trafficked through co-translocational unfolding (Rodriguez-Larrea and Bayley, 2014).

TG2 activation is biological context-dependent

Given its requirement for high extracellular ATP concentration, P2X7R will primarily be activated after injury, in the context of inflammation or in the tumor microenvironment. Enhanced TG2 expression by resident fibroblasts and infiltrating myeloid cells is an integral part of the tissue repair response and leads to accumulation of extracellular TG2. TG2 secretion is thought to bring about its activation through Ca^{2+}-induced conformational changes (Pinkas et al., 2007). However, it is possible that high extracellular nucleotide concentrations at sites of injury or inflammation not only activate P2X7R itself but also control TG2 activation as purine nucleotides are allosteric inhibitors, although the apparent binding affinity for ATP is low (~1 mM) compared to GTP (~3 µM) (Han et al., 2010; Thomas et al., 2013). Furthermore, a proposed heparan-sulfate-binding site is unique to the GTP-induced conformation (Lortat-Jacob et al., 2012) and such an interaction would stabilize this conformation and prevent Ca^{2+} binding. Therefore, it is worth noting that signaling functions for extracellular-nucleotide-bound enzyme have been postulated (Johnson and Terkeltaub, 2005; Tóth et al., 2009).

Implications for TG2-mediated disease processes

P2X7R is highly polymorphic, and it has become increasingly clear that some amino acid mutations predispose to disease (Bartlett et al., 2014). We have shown here that a polymorphism in the second transmembrane domain that is associated with autoimmune disease (Stokes et al., 2010) facilitates membrane pore formation leading to enhanced TG2 secretion. This opens the possibility that the threshold for activation of TG2 export differs between individuals depending on their *P2RX7* genotype, and this might constitute a risk factor for diseases where TG2-mediated reactions cause pathology. This extends to animal models of disease. Notably, in contrast to mouse strain 129, the C57BL/6 background widely used in genetic studies carries P2X7R P451L which lacks the capacity to form membrane pores (Sorge et al., 2012). Different mouse lines might therefore differ with regards to the capacity for active TG2 export.

In conclusion, we have demonstrated that TG2 export is regulated by purinergic signaling, and that P2X7R plays a central role in this process. Our findings provide an explanation for the link between high levels of extracellular TG2 activity and inflammatory responses, and thereby identify a new avenue to limit TG2 activity therapeutically in conditions where enzyme function directly drives pathogenic processes, including fibrotic disease and gluten-related disorders.

MATERIALS AND METHODS

Cell culture

THP-1 monocytic leukemia cells were grown in suspension in RPMI1640 medium containing 10% heat-inactivated fetal bovine serum (FBS), streptomycin and penicillin. Mononuclear cells were isolated from heparinized human blood (with informed consent of donors and approval of the Research Ethics Committees, REC10/MRE09/28) on Ficoll-Plaque PREMIUM (GE Healthcare), washed in PBS, and cultured for 7 days as THP-1 cells but with addition of 20 ng/ml human GM-CSF (Preprotech) to derive M1 macrophages. HEK293 flp-in cells (Invitrogen) were cultured in Dulbecco's modified Eagle's medium (DMEM) containing 10% FBS, the above antibiotics and 100 µg/ml zeocin (Invitrogen). Experiments were conducted without antibiotics.

Generation of stably transfected cell lines

P2X7R was amplified by PCR from image clone (ID:4298811) using the primers specified in Table S1 to generate wild-type, truncated and V5-tagged coding sequences, which were cloned into pcDNA5/V5-His/FRT vector (Invitrogen). Constructs for P2X7R mutants were generated by site-directed mutagenesis using the oligonucleotides given in Table S1. The coding sequence of all constructs was verified by sequencing. Cell lines were generated by co-transfection of P2X7R and recombinase (pOG44, Invitrogen) expression vectors into HEK293 flp-in cells using FuGENE 6 (Promega), followed by selection of stable transfectants with hygromycin B (100 µg/ml).

THP-1 cell differentiation and activation

Cells were differentiated with 0.05 µg/ml TPA, and for IL-1β upregulation, treated with 100 ng/ml LPS for 24 h. For activation, cells (1×10^6 cells/well) were suspended in PSS (10 mM Hepes-NaOH, pH 7.4, 147 mM NaCl, 2 mM KCl, 1 mM $MgCl_2$, the indicated $CaCl_2$ concentration and 12 mM glucose) and stimulated with ATP. Medium was carefully collected and rendered cell-free by centrifugation (1500 ***g***, 10 min). Cells were extracted on ice in 20 mM Hepes-NaOH, pH 7.4, 150 mM NaCl, 1 mM EGTA, 1% Triton X-100, 0.25% deoxycholate, 10% glycerol, 1 mM PMSF and 1 mM *N*-ethylmaleimide, and the extract was cleared by centrifugation (15,000 ***g***, 10 min, 4°C). IL-1β concentration in conditioned medium (100 µl) was determined by capture ELISA (Ready-SET-Go Set, eBioscience).

Immunocytochemistry

Cells grown on poly-L-lysine-coated coverslips were fixed with 2% paraformaldehyde in PBS for 10 min, and permeabilized in 0.1% Triton X-100 in PBS. After blocking of non-specific binding with 1% BSA in PBS,

Journal of Cell Science (2015) 128, 4615-4628 doi:10.1242/jcs.175968

P2X7R was detected with 2 µg/ml anti-P2X7R antibodies (sc-25698, Santa-Cruz Biotechnology) and Alexa-Fluor-488-conjugated secondary antibodies. Coverslips were mounted using Vectashield containing DAPI.

$[Ca^{2+}]_i$ measurements in individual cells

Fluo-4-AM (Invitrogen) Ca^{2+} indicator was prepared in DMSO containing 20% Pluronic F-127. Cells (7×10^4 cells/well) in poly-L-lysine-coated glass bottom dishes (50 mm; MatTek) were loaded for 20 min with 3 µM Fluo-4-AM in OptiMEM (Invitrogen). Medium was replaced with fresh OptiMEM, and cells were monitored by confocal microscopy during ATP or BzATP (Sigma) stimulation at 37°C and 5% CO_2. Real-time videos were acquired (2.62 s between frames, 63× objective) using sequential scanning. For experiments with P2X7R antagonist, cells were loaded with Fluo-4-AM in OptiMEM containing 5 µM A740003 (Tocris) prior to stimulation with agonist in A740003-containing OptiMEM. Images were analyzed using the LAS-AF software (Leica).

Analysis of TG2 externalization

Differentiated THP-1 cells (1×10^6 cells/well) and primary macrophages (1×10^5 cells/well, 24-well plates) were stimulated with P2X7R agonists in OptiMEM. HEK293 P2X7R or parental cells (1.5×10^5 cells/well, 24-well plates) were transfected with 0.5 µg expression construct for wild-type TG2 or TG2 C277S (Stephens et al., 2004), or GFP-tagged TG2 (Table S2) using FuGENE-6. After 48 h, cells were washed with pre-warmed and gassed OptiMEM, and stimulated with P2X7R agonist or CPA (Merck-Millipore) in OptiMEM (250 µl/well). For inhibitor studies, cells were treated with 5 µM A740003, 1 µM calmidazolium chloride (Merck-Millipore), 10 µM BAPTA-AM (Merck-Millipore) or vehicle for 10 min, and then stimulated with BzATP in the presence of the respective inhibitors as indicated. Caspase-1 inhibitor Ac-YVAD-CMK was prepared fresh in OptiMEM and diluted to a 100 µM final concentration in experiments. Cell supernatant (pulse fraction) was collected, and cells washed with and subsequently incubated in pre-warmed and gassed OptiMEM without agonist for 30 min (chase fraction). Conditioned medium from four wells (six wells for macrophages) were combined, and rendered cell-free by centrifugation (1500 ***g***, 10 min) for analysis. Cell surface protein labeling with Sulfo-NHS-SS-biotin and purification was carried out with the Pierce cell surface protein isolation kit.

Immunoblotting

Lyophilized (500 µl) or ethanol precipitated (1.3 ml, macrophages) conditioned media were reconstituted at 1/10th or 1/50th of the original volume in 12.5 mM Tris-HCl, pH 6.8, 4 M urea, 2% SDS, 20 mM EDTA, 2% β-mercaptoethanol and 15% glycerol. Protein concentrations of extracts were determined with a bicinchoninic acid protein assay. 20 µl reconstituted media or 10 µg cell extract together with Amersham LMW-SDS markers were separated on 4–20% SDS-PAGE Tris/glycine gels (Invitrogen) under reducing conditions, and transferred onto nitrocellulose membranes. For thioredoxin-1 detection, ethanol-precipitated (1:9, v/v) proteins (600 µl medium) were resuspended as above, and separated in 16% SDS-PAGE Tricine gels (Invitrogen) calibrated with Broad Range marker (11–190 kDa; NEB). Antibody labeling was performed as described previously (Aeschlimann et al., 1993) using the monoclonal antibodies CUB7402 against TG2 (0.2 µg/ml), TUB2.1 against β-tubulin (2.6 µg/ml), against flotillin-2 (0.5 µg/ml; 610383, BD-Biosciences), against HMGB-1 (0.73 µg/ml; ab184203, Abcam), against the V5tag (20 ng/ml) or the polyclonal anti-IκBα (1 µg/ml; sc-371, Santa Cruz Biotechnology), anti-caspase-3 (40 ng/ml; 9662, Cell Signaling), anti-P2X7R C-terminus (1 µg/ml) or anti-P2X7R extracellular domain (1.7 µg/ml; APR-008, Alomone Labs) antibodies. Anti-thioredoxin-1 antibodies (1:200; FL105, Santa Cruz Biotechnology) were used with 5% casein as blocking agent. Bound antibodies were detected with horseradish peroxidase (HRP)-conjugated secondary antibodies and Amersham ECL™ Plus/Prime. TG2 band intensity was quantified by densitometry using Image Lab 5.1 software (Bio-Rad).

Analysis of cell damage and apoptosis

To assess cell integrity, LDH release was measured using CytoTox-ONE™ HMI Assay (Promega). Cells (1.2×10^5 cells/well, 24-well plate) were treated with BzATP in 300 µl OptiMEM for 10 min (n=4), and cell-free conditioned media (100 µl) were analyzed for LDH. For estimation of total LDH, a replicate well set was subjected to cell lysis.

To assess whether treatment induced cell death, P2X7R cells were stimulated with BzATP and chased in OptiMEM as described above, and where indicated subsequently cultured in serum containing DMEM for up to 22 h. Cell extracts and particulate material recovered from conditioned media were analyzed for caspase-3 by immunoblotting.

Localization of GFP-tagged TG2 using confocal microscopy

P2X7R cells on poly-L-lysine-coated coverslips were transfected with constructs for expression of N- or C-terminally GFP-tagged TG2. After 24 h, the coverslip was mounted for microscopy into a customized holder using silicone grease. Cells were kept in OptiMEM at 37°C and 5% CO_2, and stimulated with a defined volume of agonist solution to obtain 1 mM ATP or 100 µM BzATP while monitoring GFP fluorescence and acquiring real-time movies.

Detection and isolation of microvesicles

TG2- or mock-transfected P2X7R cells were stimulated with 100 µM BzATP or vehicle. Freshly collected conditioned media were rendered cell-free by centrifugation (1500 ***g***, 10 min) and supernatants analyzed for microvesicles by particle tracking using the NanoSight LM12 system with a high-sensitivity camera (Webber and Clayton, 2013). Five 60-s videos per sample (1×10^8–5×10^8 particles/ml) were recorded at 25.6 frames/s (gain=250), and analyzed using the NTA2.3 software. Alternatively, freshly collected conditioned media were subjected to differential centrifugation at 4°C, with 1500 ***g*** for 10 min, followed by 3000 ***g*** for 20 min, and then either 10,000 ***g*** for 30 min and 100,000 ***g*** (SW32Ti, Beckman) for 1 h or subjected to density gradient centrifugation. Supernatant (1.0 ml) was carefully layered on a Tris-buffered sucrose-step gradient (0, 20% and 60%) and centrifuged at 100,000 ***g*** for 90 min. Fractions (~1 ml) constituting the top layer and 20%–60% interface (microvesicle fraction) as well as pellets were collected. Proteins were precipitated with 9 volumes of ethanol at 4°C, and analyzed using immunoblotting.

P2X7R 'membrane pore' activity

Cells in poly-L-lysine-coated black optical 96-well plates (Nunc, 165305) were placed in PSS containing 0–2 mM Ca^{2+} and 1 µM YO-PRO1 (Invitrogen). The plate was transferred to a FLUOstar Omega reader (BMG Labtech) equilibrated to 37°C and 5% CO_2. BzATP was injected to obtain a 0–500 µM final concentration (n=3) and fluorescence measured (4-mm orbital area) every 40 s for 30 min. Where indicated, cells were preincubated with 100 µM ^{10}Panx (Tocris) for 10 min or 10–100 µg/ml trovafloxacin (Sigma) for 30 min and stimulated in the presence of inhibitors. After normalization for well-specific fluorescence, the average YO-PRO1 fluorescence of unstimulated cells was subtracted from that of agonist-stimulated cells to correct for bleaching. Dye uptake rates were derived by linear regression of data from the initial 5 min.

$[Ca^{2+}]_i$ measurements in plate format

Cells (3×10^4 cells/well) in optical 96-well plates were loaded with Fluo-4-AM, washed and placed in fresh OptiMEM (90 µl/well). After measuring baseline fluorescence, different concentrations of BzATP (0–300 µM) or medium alone were injected (10 µl/well). Fluorescence changes were measured in well mode over 20 s, with 40 0.1-s intervals followed by 0.4-s intervals. Data from eight wells per condition were averaged. The fluorescence of the control was subtracted from data with agonist treatment to correct for bleaching. Data (F, fluorescence; t, time) for the first 10 s were fitted using Eqn 1 to estimate the maximal fluorescence value (F_{max}):

$$F = \frac{1 - e^{-(A-F_{max})kt}}{\frac{1}{F_{max}} - \frac{1}{A}e^{-(A-F_{max})kt}} + C, \quad (1)$$

whereby k is the association constant, A is a function of agonist concentration and C is a constant for baseline correction. The association constant obtained from

data fitting was k=1.8×10^{-6} M^{-1} s^{-1}. F_{max} was then plotted against the agonist concentration to derive a dose–response curve.

Membrane potential analysis

Voltage sensor probes, coumarin-labeled phospholipid CC2-DMPE (FRET donor) and oxonol dye DiSBAC$_2$(3) (acceptor) were from Invitrogen. Cells (3×10^4 cells/well) in optical 96-well plates were loaded with 10 µM CC2-DMPE in FRET buffer (10 mM Hepes-NaOH, pH 7.4, 160 mM NaCl, 0.9 mM $CaCl_2$, 1 mM $MgCl_2$, and 10 mM glucose) containing 200 µg/ml Pluronic F-127 for 30 min, washed and incubated in 100 µl 10 µM DiSBAC$_2$(3) in FRET buffer for 20 min. Tartrazine (1.2 mM final concentration) was added, and after 10 min, fluorescence measurements (λ_{ex} of 420 nm; λ_{em} of 460 nm and 550 nm; 10-nm bandpass filters) were conducted in well mode at 37°C and 5% CO_2. Gain was adjusted to yield similar baseline readings for each fluorophor at resting potential. Following baseline acquisition, 10 µl 0.82 M KCl, 1 mM BzATP or buffer control were injected while monitoring fluorescence. Following subtraction of signal without cells, the signal ratio (SR) before and at equilibrium after depolarization was calculated, and the response ratio (RR) derived as RR=SR^{depol}/SR^{pol}.

Statistics

One-way ANOVA was used and significance between groups determined with Tukey's post-test, whereby P<0.05 was considered significant.

Acknowledgements

We are grateful to Dr Lea Bauer and Ms Ana Mafalda dos Reis for technical assistance.

Competing interests

The authors declare no competing or financial interests.

Author contributions

D.A. conceived the study. M.A., R.G., S.D. and V.K. carried out the experiments. M.A. and D.A. analyzed all the experiments. M.A. and D.A. wrote the manuscript with input from all authors.

Funding

This work was supported by an Arthritis Research UK Center grant [grant number 18461 to D.A.] and Foundation Fellowship [grant number 20512 to M.A. and D.A.]; a Cardiff University PhD studentship (to M.A.) and President's research scholarship (to R.G.). Deposited in PMC for immediate release.

Supplementary information

Supplementary information available online at
http://jcs.biologists.org/lookup/suppl/doi:10.1242/jcs.175968/-/DC1

References

Adinolfi, E., Cirillo, M., Woltersdorf, R., Falzoni, S., Chiozzi, P., Pellegatti, P., Callegari, M. G., Sandonà, D., Markwardt, F., Schmalzing, G. et al. (2010). Trophic activity of a naturally occurring truncated isoform of the P2X7 receptor. *FASEB J.* **24**, 3393-3404.

Aeschlimann, D. and Paulsson, M. (1994). Transglutaminases: protein crosslinking enzymes in tissues and body fluids. *Thromb. Haemost.* **71**, 402-415.

Aeschlimann, D. and Thomazy, V. (2000). Protein crosslinking in assembly and remodelling of extracellular matrices: the role of transglutaminases. *Connect. Tissue Res.* **41**, 1-27.

Aeschlimann, D., Wetterwald, A., Fleisch, H. and Paulsson, M. (1993). Expression of tissue transglutaminase in skeletal tissues correlates with events of terminal differentiation of chondrocytes. *J. Cell Biol.* **120**, 1461-1470.

Aeschlimann, D., Kaupp, O. and Paulsson, M. (1995). Transglutaminase-catalyzed matrix cross-linking in differentiating cartilage: identification of osteonectin as a major glutaminyl substrate. *J. Cell Biol.* **129**, 881-892.

Allsopp, R. C. and Evans, R. J. (2015). Contribution of the juxtatransmembrane intracellular regions to the time course and permeation of ATP-gated P2X7 receptor ion channels. *J. Biol. Chem.* **290**, 14556-14566.

Antonyak, M. A., Li, B., Boroughs, L. K., Johnson, J. L., Druso, J. E., Bryant, K. L., Holowka, D. A. and Cerione, R. A. (2011). Cancer cell-derived microvesicles induce transformation by transferring tissue transglutaminase and fibronectin to recipient cells. *Proc. Natl. Acad. Sci. USA* **108**, 4852-4857.

Arlt, A., Kruse, M.-L., Breitenbroich, M., Gehrz, A., Koc, B., Minkenberg, J., Fölsch, U. R. and Schäfer, H. (2003). The early response gene IEX-1 attenuates NF-κB activation in 293 cells, a possible counter-regulatory process leading to enhanced cell death. *Oncogene* **22**, 3343-3351.

Balklava, Z., Verderio, E., Collighan, R., Gross, S., Adams, J. and Griffin, M. (2002). Analysis of tissue transglutaminase function in the migration of Swiss 3T3 fibroblasts: the active-state conformation of the enzyme does not affect cell motility but is important for its secretion. *J. Biol. Chem.* **277**, 16567-16575.

Bartlett, R., Stokes, L. and Sluyter, R. (2014). The P2X7 receptor channel: recent developments and the use of P2X7 antagonists in models of disease. *Pharmacol. Rev.* **66**, 638-675.

Belkin, A. M., Akimov, S. S., Zaritskaya, L. S., Ratnikov, B. I., Deryugina, E. I. and Strongin, A. Y. (2001). Matrix-dependent proteolysis of surface transglutaminase by membrane-type metalloproteinase regulates cancer cell adhesion and locomotion. *J. Biol. Chem.* **276**, 18415-18422.

Browne, L. E., Compan, V., Bragg, L. and North, R. A. (2013). P2X7 receptor channels allow direct permeation of nanometer-sized dyes. *J. Neurosci.* **33**, 3557-3566.

Burnstock, G. (2015). Physiopathological roles of P2X receptors in the central nervous system. *Curr. Med. Chem.* **22**, 819-844.

Cervetto, C., Alloisio, S., Frattaroli, D., Mazzotta, M. C., Milanese, M., Gavazzo, P., Passalacqua, M., Nobile, M., Maura, G. and Marcoli, M. (2013). The P2X7 receptor as a route for non-exocytotic glutamate release: dependence on the carboxyl tail. *J. Neurochem.* **124**, 821-831.

Chou, C.-Y., Streets, A. J., Watson, P. F., Huang, L., Verderio, E. A. M. and Johnson, T. S. (2011). A crucial sequence for transglutaminase type 2 extracellular trafficking in renal tubular epithelial cells lies in its N-terminal beta-sandwich domain. *J. Biol. Chem.* **286**, 27825-27835.

Cocucci, E., Racchetti, G. and Meldolesi, J. (2009). Shedding microvesicles: artefacts no more. *Trends Cell Biol.* **19**, 43-51.

Coddou, C., Yan, Z., Obsil, T., Huidobro-Toro, J. P. and Stojilkovic, S. S. (2011). Activation and regulation of purinergic P2X receptor channels. *Pharmacol. Rev.* **63**, 641-683.

Dubyak, G. R. (2012). P2X7 receptor regulation of non-classical secretion from immune effector cells. *Cell. Microbiol.* **14**, 1697-1706.

Garcia, M. and Knight, M. M. (2010). Cyclic loading opens hemichannels to release ATP as part of a chondrocyte mechanotransduction pathway. *J. Orthop. Res.* **28**, 510-515.

Gudipaty, L., Munetz, J., Verhoef, P. A. and Dubyak, G. R. (2003). Essential role for Ca2+ in regulation of IL-1β secretion by P2X7 nucleotide receptor in monocytes, macrophages, and HEK-293 cells. *Am. J. Physiol. Cell Physiol.* **285**, C286-C299.

Gulbransen, B. D., Bashashati, M., Hirota, S. A., Gui, X., Roberts, J. A., MacDonald, J. A., Muruve, D. A., McKay, D. M., Beck, P. L., Mawe, G. M. et al. (2012). Activation of neuronal P2X7 receptor–pannexin-1 mediates death of enteric neurons during colitis. *Nat. Med.* **18**, 600-604.

Han, B.-G., Cho, J.-W., Cho, Y. D., Jeong, K.-C., Kim, S.-Y. and Lee, B. I. (2010). Crystal structure of human transglutaminase 2 in complex with adenosine triphosphate. *Int. J. Biol. Macromol.* **47**, 190-195.

Hattori, M. and Gouaux, E. (2012). Molecular mechanism of ATP binding and ion channel activation in P2X receptors. *Nature* **485**, 207-212.

Honore, P., Donnelly-Roberts, D., Namovic, M. T., Hsieh, G., Zhu, C. Z., Mikusa, J. P., Hernandez, G., Zhong, C., Gauvin, D. M., Chandran, P. et al. (2006). A-740003 [N-(1-{[(cyanoimino)(5-quinolinylamino) methyl]amino}-2,2-dimethyl propyl)-2-(3,4-dimethoxyphenyl)acetamide], a novel and selective P2X7 receptor antagonist, dose-dependently reduces neuropathic pain in the rat. *J. Pharmacol. Exp. Ther.* **319**, 1376-1385.

Iismaa, S. E., Mearns, B. M., Lorand, L. and Graham, R. M. (2009). Transglutaminases and disease: Lessons from genetically engineered mouse models and inherited disorders. *Physiol. Rev.* **89**, 991-1023.

Jaeger, S. U., Schroeder, B. O., Meyer-Hoffert, U., Courth, L., Fehr, S. N., Gersemann, M., Stange, E. F. and Wehkamp, J. (2013). Cell-mediated reduction of human β-defensin 1: a major role for mucosal thioredoxin. *Mucosal Immunol.* **6**, 1179-1190.

Jiang, R., Taly, A. and Grutter, T. (2013). Moving through the gate in ATP-activated P2X receptors. *Trends Biochem. Sci.* **38**, 20-29.

Jin, X., Stamnaes, J., Klöck, C., DiRaimondo, T. R., Sollid, L. M. and Khosla, C. (2011). Activation of extracellular transglutaminase 2 by thioredoxin. *J. Biol. Chem.* **286**, 37866-37873.

Johnson, K. A. and Terkeltaub, R. A. (2005). External GTP-bound transglutaminase 2 is a molecular switch for chondrocyte hypertrophic differentiation and calcification. *J. Biol. Chem.* **280**, 15004-15012.

Kawate, T., Michel, J. C., Birdsong, W. T. and Gouaux, E. (2009). Crystal structure of the ATP-gated P2X(4) ion channel in the closed state. *Nature* **460**, 592-598.

Korponay-Szabó, I. R., Halttunen, T., Szalai, Z., Laurila, K., Király, R., Kovács, J. B., Fésüs, L. and Mäki, M. (2004). In vivo targeting of intestinal and extraintestinal transglutaminase 2 by coeliac autoantibodies. *Gut* **53**, 641-648.

Labasi, J. M., Petrushova, N., Donovan, C., McCurdy, S., Lira, P., Payette, M. M., Brissette, W., Wicks, J. R., Audoly, L. and Gabel, C. A. (2002). Absence of the P2X7 receptor alters leukocyte function and attenuates an inflammatory response. *J. Immunol.* **168**, 6436-6445.

Loof, T. G., Mörgelin, M., Johansson, L., Oehmcke, S., Olin, A. I., Dickneite, G., Norrby-Teglund, A., Theopold, U. and Herwald, H. (2011). Coagulation, an ancestral serine protease cascade, exerts a novel function in early immune defense. *Blood* **118**, 2589-2598.

Lorand, L. and Graham, R. M. (2003). Transglutaminases: crosslinking enzymes with pleiotropic functions. *Nat. Rev. Mol. Cell Biol.* **4**, 140-156.
Lortat-Jacob, H., Burhan, I., Scarpellini, A., Thomas, A., Imberty, A., Vivès, R. R., Johnson, T., Gutierrez, A. and Verderio, E. A. M. (2012). Transglutaminase-2 interaction with heparin: identification of a heparin binding site that regulates cell adhesion to fibronectin-transglutaminase-2 matrix. *J. Biol. Chem.* **287**, 18005-18017.
Lu, B., Nakamura, T., Inouye, K., Li, J., Tang, Y., Lundbäck, P., Valdes-Ferrer, S. I., Olofsson, P. S., Kalb, T., Roth, J. et al. (2012). Novel role of PKR in inflammasome activation and HMGB1 release. *Nature* **488**, 670-674.
Lucattelli, M., Cicko, S., Müller, T., Lommatzsch, M., De Cunto, G., Cardini, S., Sundas, W., Grimm, M., Zeiser, R., Dürk, T. et al. (2011). P2X7 receptor signaling in the pathogenesis of smoke-induced lung inflammation and emphysema. *Am. J. Respir. Cell Mol. Biol.* **44**, 423-429.
MacKenzie, A., Wilson, H. L., Kiss-Toth, E., Dower, S. K., North, R. A. and Surprenant, A. (2001). Rapid secretion of interleukin-1β by microvesicle shedding. *Immunity* **15**, 825-835.
Mackenzie, A. B., Young, M. T., Adinolfi, E. and Surprenant, A. (2005). Pseudoapoptosis induced by brief activation of ATP-gated P2X7 receptors. *J. Biol. Chem.* **280**, 33968-33976.
Mariathasan, S., Weiss, D. S., Newton, K., McBride, J., O'Rourke, K., Roose-Girma, M., Lee, W. P., Weinrauch, Y., Monack, D. M. and Dixit, V. M. (2006). Cryopyrin activates the inflammasome in response to toxins and ATP. *Nature* **440**, 228-232.
Mehta, K. and Lopez-Berestein, G. (1986). Expression of tissue transglutaminase in cultured monocytic leukemia (THP-1) cells during differentiation. *Cancer Res.* **46**, 1388-1394.
Muesch, A., Hartmann, E., Rohde, K., Rubartelli, A., Sitia, R. and Rapoport, T. A. (1990). A novel pathway for secretory proteins? *Trends Biochem. Sci.* **15**, 86-88.
Nickel, W. and Rabouille, C. (2009). Mechanisms of regulated unconventional protein secretion. *Nat. Rev. Mol. Cell Biol.* **10**, 148-155.
Nurminskaya, M. V. and Belkin, A. M. (2012). Cellular functions of tissue transglutaminase. *Int. Rev. Cell Mol. Biol.* **294**, 1-97.
Olson, K. R., McIntosh, J. R. and Olmsted, J. B. (1995). Analysis of MAP 4 function in living cells using green fluorescent protein (GFP) chimeras. *J. Cell Biol.* **130**, 639-650.
Pelegrín, P. (2011). Many ways to dilate the P2X7 receptor pore. *Br. J. Pharmacol.* **163**, 908-911.
Pelegrin, P. and Surprenant, A. (2007). Pannexin-1 couples to maitotoxin- and nigericin-induced interleukin-1beta release through a dye uptake-independent pathway. *J. Biol. Chem.* **282**, 2386-2394.
Pelegrin, P., Barroso-Gutierrez, C. and Surprenant, A. (2008). P2X7 receptor differentially couples to distinct release pathways for IL-1β in mouse macrophage. *J. Immunol.* **180**, 7147-7157.
Pfeiffer, Z. A., Aga, M., Prabhu, U., Watters, J. J., Hall, D. J. and Bertics, P. J. (2004). The nucleotide receptor P2X7 mediates actin reorganization and membrane blebbing in RAW 264.7 macrophages via p38 MAP kinase and Rho. *J. Leukoc. Biol.* **75**, 1173-1182.
Pinkas, D. M., Strop, P., Brunger, A. T. and Khosla, C. (2007). Transglutaminase 2 undergoes a large conformational change upon activation. *PLoS Biol.* **5**, e327.
Poon, I. K. H., Chiu, Y.-H., Armstrong, A. J., Kinchen, J. M., Juncadella, I. J., Bayliss, D. A. and Ravichandran, K. S. (2014). Unexpected link between an antibiotic, pannexin channels and apoptosis. *Nature* **507**, 329-334.
Rabouille, C., Malhotra, V. and Nickel, W. (2012). Diversity in unconventional protein secretion. *J. Cell Sci.* **125**, 5251-5255.
Rassendren, F., Buell, G. N., Virginio, C., Collo, G., North, R. A. and Surprenant, A. (1997). The permeabilizing ATP receptor, P2X7: Cloning and expression of a human cDNA. *J. Biol. Chem.* **272**, 5482-5486.
Riccardi, D. and Kemp, P. J. (2012). The calcium-sensing receptor beyond extracellular calcium homeostasis: conception, development, adult physiology, and disease. *Annu. Rev. Physiol.* **74**, 271-297.
Rodriguez-Larrea, D. and Bayley, H. (2014). Protein co-translocational unfolding depends on the direction of pulling. *Nat. Commun.* **5**, 4841.
Rubartelli, A., Bajetto, A., Allavena, G., Wollman, E. and Sitia, R. (1992). Secretion of thioredoxin by normal and neoplastic cells through a leaderless secretory pathway. *J. Biol. Chem.* **267**, 24161-24164.
Rumney, R. M. H., Sunters, A., Reilly, G. C. and Gartland, A. (2012). Application of multiple forms of mechanical loading to human osteoblasts reveals increased ATP release in response to fluid flow in 3D cultures and differential regulation of immediate early genes. *J. Biomech.* **45**, 549-554.
Scarpellini, A., Germack, R., Lortat-Jacob, H., Muramatsu, T., Billett, E., Johnson, T. and Verderio, E. A. M. (2009). Heparan sulfate proteoglycans are receptors for the cell-surface trafficking and biological activity of transglutaminase-2. *J. Biol. Chem.* **284**, 18411-18423.
Schachter, J. B., Sromek, S. M., Nicholas, R. A. and Harden, T. K. (1997). HEK293 human embryonic kidney cells endogenously express the P2Y1 and P2Y2 receptors. *Neuropharmacology* **36**, 1181-1187.
Siegel, M., Strnad, P., Watts, R. E., Choi, K., Jabri, B., Omary, M. B. and Khosla, C. (2008). Extracellular transglutaminase 2 is catalytically inactive, but is transiently activated upon tissue injury. *PLoS ONE* **3**, e1861.
Smart, M. L., Gu, B., Panchal, R. G., Wiley, J., Cromer, B., Williams, D. A. and Petrou, S. (2003). P2X7 receptor cell surface expression and cytolytic pore formation are regulated by a distal C-terminal region. *J. Biol. Chem.* **278**, 8853-8860.
Solle, M., Labasi, J., Perregaux, D. G., Stam, E., Petrushova, N., Koller, B. H., Griffiths, R. J. and Gabel, C. A. (2001). Altered cytokine production in mice lacking P2X(7) receptors. *J. Biol. Chem.* **276**, 125-132.
Sorge, R. E., Trang, T., Dorfman, R., Smith, S. B., Beggs, S., Ritchie, J., Austin, J.-S., Zaykin, D. V., Meulen, H. V., Costigan, M. et al. (2012). Genetically determined P2X7 receptor pore formation regulates variability in chronic pain sensitivity. *Nat. Med.* **18**, 595-599.
Stamnaes, J., Pinkas, D. M., Fleckenstein, B., Khosla, C. and Sollid, L. M. (2010). Redox regulation of transglutaminase 2 activity. *J. Biol. Chem.* **285**, 25402-25409.
Stegmayer, C., Kehlenbach, A., Tournaviti, S., Wegehingel, S., Zehe, C., Denny, P., Smith, D. F., Schwappach, B. and Nickel, W. (2005). Direct transport across the plasma membrane of mammalian cells of Leishmania HASPB as revealed by a CHO export mutant. *J. Cell Sci.* **118**, 517-527.
Stephens, P., Grenard, P., Aeschlimann, P., Langley, M., Blain, E., Errington, R., Kipling, D., Thomas, D. and Aeschlimann, D. (2004). Crosslinking and G-protein functions of transglutaminase 2 contribute differentially to fibroblast wound healing responses. *J. Cell Sci.* **117**, 3389-3403.
Stokes, L., Fuller, S. J., Sluyter, R., Skarratt, K. K., Gu, B. J. and Wiley, J. S. (2010). Two haplotypes of the P2X7 receptor containing the Ala-348 to Thr polymorphism exhibit a gain-of-function effect and enhanced interleukin-1β secretion. *FASEB J.* **24**, 2916-2927.
Strowig, T., Henao-Mejia, J., Elinav, E. and Flavell, R. (2012). Inflammasomes in health and disease. *Nature* **481**, 278-286.
Sun, C., Heid, M. E., Keyel, P. A. and Salter, R. D. (2013). The second transmembrane domain of P2X7 contributes to dilated pore formation. *PLoS ONE* **8**, e61886.
Surprenant, A., Rassendren, F., Kawashima, E., North, R. A. and Buell, G. (1996). The cytolytic P2Z receptor for extracellular ATP identified as a P2X receptor (P2X7). *Science* **272**, 735-738.
Thomas, H., Beck, K., Adamczyk, M., Aeschlimann, P., Langley, M., Oita, R., Thiebach, L., Hils, M. and Aeschlimann, D. (2013). Transglutaminase 6: A protein associated with central nervous system development and motor function. *Amino Acids* **44**, 161-177.
Tóth, B., Garabuczi, E., Sarang, Z., Vereb, G., Vámosi, G., Aeschlimann, D., Blaskó, B., Bécsi, B., Erdõdi, F., Lacy-Hulbert, A. et al. (2009). Transglutaminase 2 is needed for the formation of an efficient phagocyte portal in macrophages engulfing apoptotic cells. *J. Immunol.* **182**, 2084-2092.
Upchurch, H. F., Conway, E., Patterson, M. K., Jr., Birckbichler, P. J. and Maxwell, M. D. (1987). Cellular transglutaminase has affinity for extracellular matrix. *In Vitro Cell. Dev. Biol.* **23**, 795-800.
van den Akker, J., van Bavel, E., van Geel, R., Matlung, H. L., Guvenc Tuna, B., Janssen, G. M. C., van Veelen, P. A., Boelens, W. C., De Mey, J. G. R. and Bakker, E. N. T. P. (2011). The redox state of transglutaminase 2 controls arterial remodeling. *PLoS ONE* **6**, e23067.
Virginio, C., Church, D., North, R. A. and Surprenant, A. (1997). Effects of divalent cations, protons and calmidazolium at the rat P2X7 receptor. *Neuropharmacology* **36**, 1285-1294.
Virginio, C., MacKenzie, A., North, R. A. and Surprenant, A. (1999). Kinetics of cell lysis, dye uptake and permeability changes in cells expressing the rat P2X7 receptor. *J. Physiol.* **519**, 335-346.
Webber, J. and Clayton, A. (2013). How pure are your vesicles? *J. Extracell. Vesicles* **2**, 19681.
Wolff, C., Fuks, B. and Chatelain, P. (2003). Comparative study of membrane potential-sensitive fluorescent probes and their use in ion channel screening assays. *J. Biomol. Screen.* **8**, 533-543.
Yan, Z., Khadra, A., Sherman, A. and Stojilkovic, S. S. (2011). Calcium-dependent block of P2X7 receptor channel function is allosteric. *J. Gen. Physiol.* **138**, 437-452.
Zemskov, E. A., Mikhailenko, I., Hsia, R.-C., Zaritskaya, L. and Belkin, A. M. (2011). Unconventional secretion of tissue transglutaminase involves phospholipid-dependent delivery into recycling endosomes. *PLoS ONE* **6**, e19414.
Zone, J. J., Schmidt, L. A., Taylor, T. B., Hull, C. M., Sotiriou, M. C., Jaskowski, T. D., Hill, H. R. and Meyer, L. J. (2011). Dermatitis herpetiformis sera or goat anti-transglutaminase-3 transferred to human skin-grafted mice mimics dermatitis herpetiformis immunopathology. *J. Immunol.* **186**, 4474-4480.

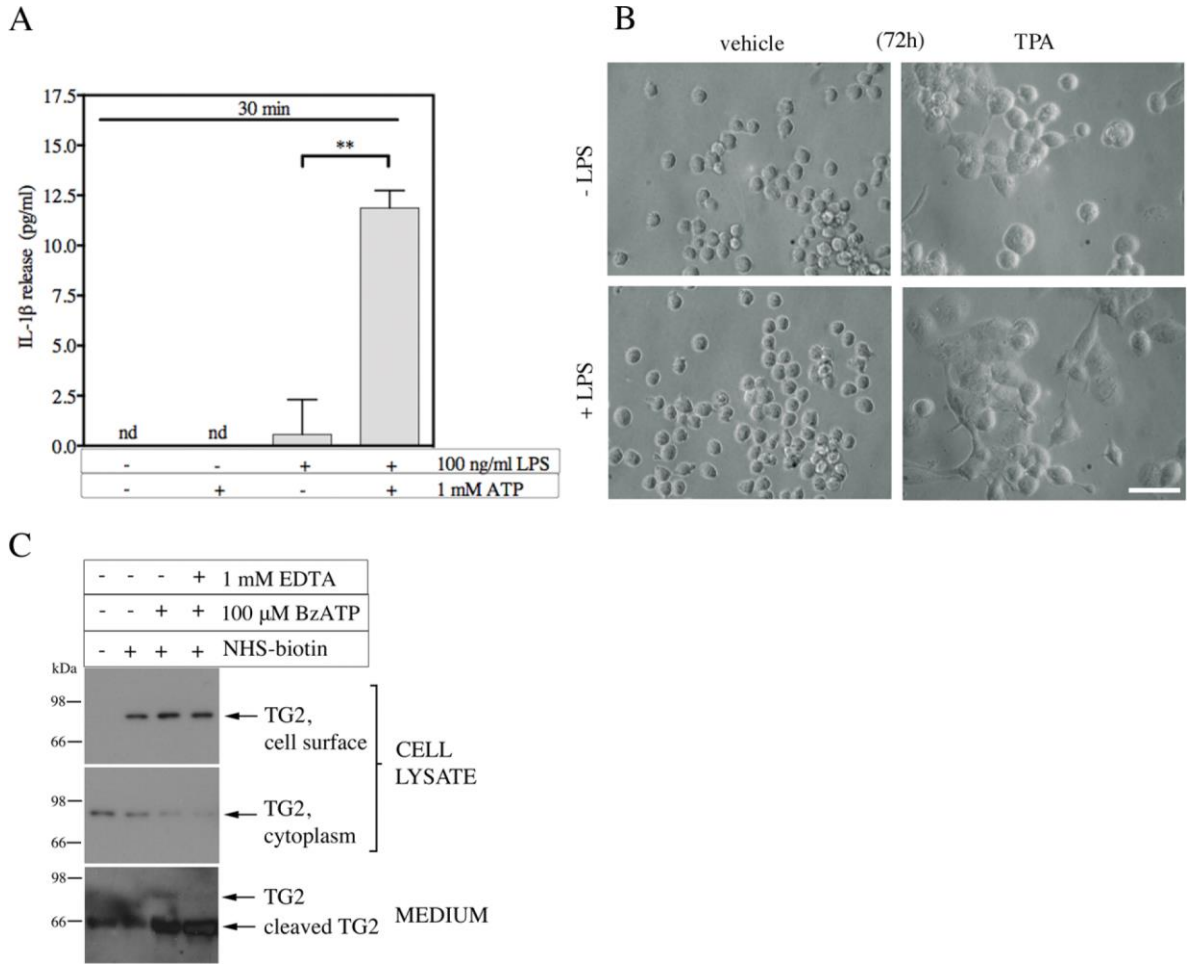

Fig. S1. Differentiation and IL-1β secretion of monocytes, and analysis of cell-associated TG2 in macrophages.

(A) P2X7R mediated IL-1β release. Untreated or LPS treated THP-1 cells were ATP stimulated in PSS for 30min as indicated, followed by analysis of cell free supernatants for secreted IL-1β by capture ELISA (mean±s.e.m., nd=not detectable; 2 independent experiments).

(B) Morphological changes confirm cell differentiation. Phase contrast images of THP-1 cells analysed in Fig. 1A are shown. THP-1 cells were differentiated for indicated time with 50ng/ml TPA and stimulated with 100ng/ml LPS as indicated. Bar=50μm.

(C) Detection of cell surface-associated TG2. *In vitro* differentiated primary human macrophages were stimulated with BzATP for 10min, followed by biotinylation of cell surface proteins prior to cell extraction. Biotinylated proteins were isolated from extracts on a NeutrAvidin-agarose matrix, and both unbound (cytoplasm) and bound (cell surface) proteins analysed for TG2 by Western blotting alongside the respective cell supernatants from stimulation (medium). The biotin-active ester was omitted from a parallel sample as indicated to corroborate specificity of the cell-surface protein isolation procedure. Note, only free but not cell-associated extracellular TG2 was cleaved, and cation chelation with EDTA during stimulation did not prevent TG2 processing indicating that it is not a metalloproteinase-mediated event.

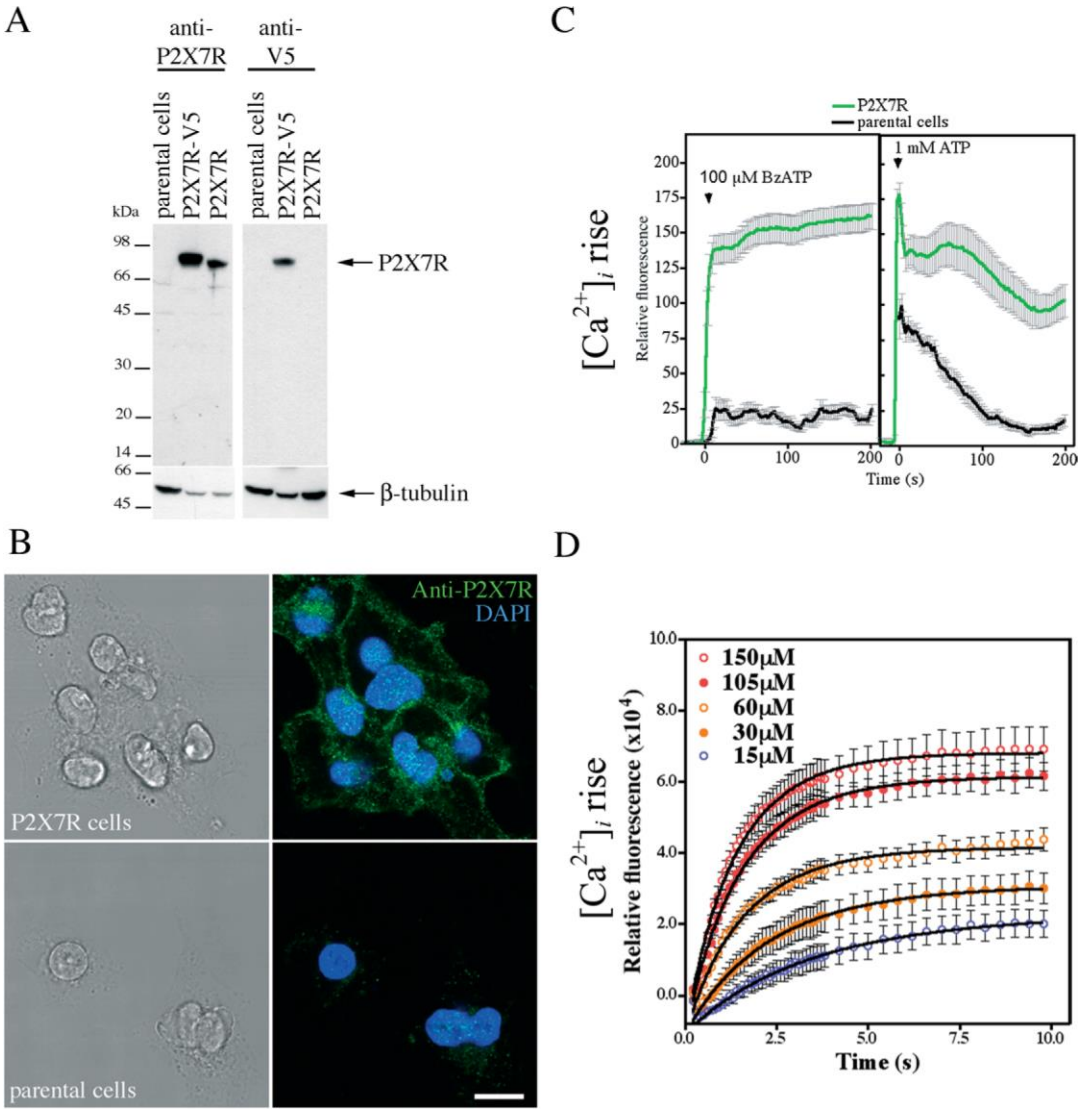

Fig. S2. Characterization of cells expressing P2X7R as a transgene.

(A) Expression of P2X7R in HEK293 cells. Cells stably expressing wild-type or V5-tagged P2X7R were extracted and proteins (25μg/lane) separated by SDS-PAGE under reducing conditions, followed by Western blotting using antibodies to P2X7R, to V5, or to β-tubulin as a loading control.

(B) Immunolocalization of P2X7R. P2X7R and parental cells were fixed, permeabilized and stained with anti-P2X7R antibodies recognizing the intracellular *C*-terminal domain as well as DAPI to highlight nuclei. Fluorescence images (right) representing an optical section acquired by confocal microscopy are shown alongside phase contrast images (left). Bar=10μm.

(C) Intracellular Ca^{2+} response in P2X7R and parental cells. Cells were loaded with Ca^{2+}-indicator Fluo-4-AM in OptiMEM for 20min prior to stimulation with ATP or BzATP as indicated. Fluorescence change in individual cells was monitored by confocal microscopy (λ_{Ex}=488nm, λ_{Em}=500-535nm) and is given as mean±s.e.m. (n=12) of a representative experiment. Note, ATP elicits P2Y receptor responses whereas BzATP is P2X receptor specific. Therefore, parental cells are not responsive to BzATP but respond to ATP stimulation with transient oscillations in $[Ca^{2+}]_i$ which is likely due to activation of P2Y1R or P2Y2R that are constitutively expressed in these cells (Schachter et al., 1997).

(D) Changes in intracellular free Ca^{2+} concentration in response to different concentrations of agonist in P2X7R cells. Fluo-4-AM loaded cells were stimulated with various concentrations of BzATP ranging from 15-300μM. For clarity, only selected concentrations of a representative experiment are shown. Data reflects the mean fluorescence (λ_{Ex}=485-12nm, λ_{Em}=520-10nm) of the cell layer from 8 wells after normalization for well-specific baseline fluorescence and subtraction of data from unstimulated control cells. For analysis, the initial 10s following stimulation were considered and data was fitted using second order kinetics as outlined in Materials and Methods. Note, BzATP concentrations <10μM were unable to elicit $[Ca^{2+}]_i$ changes.

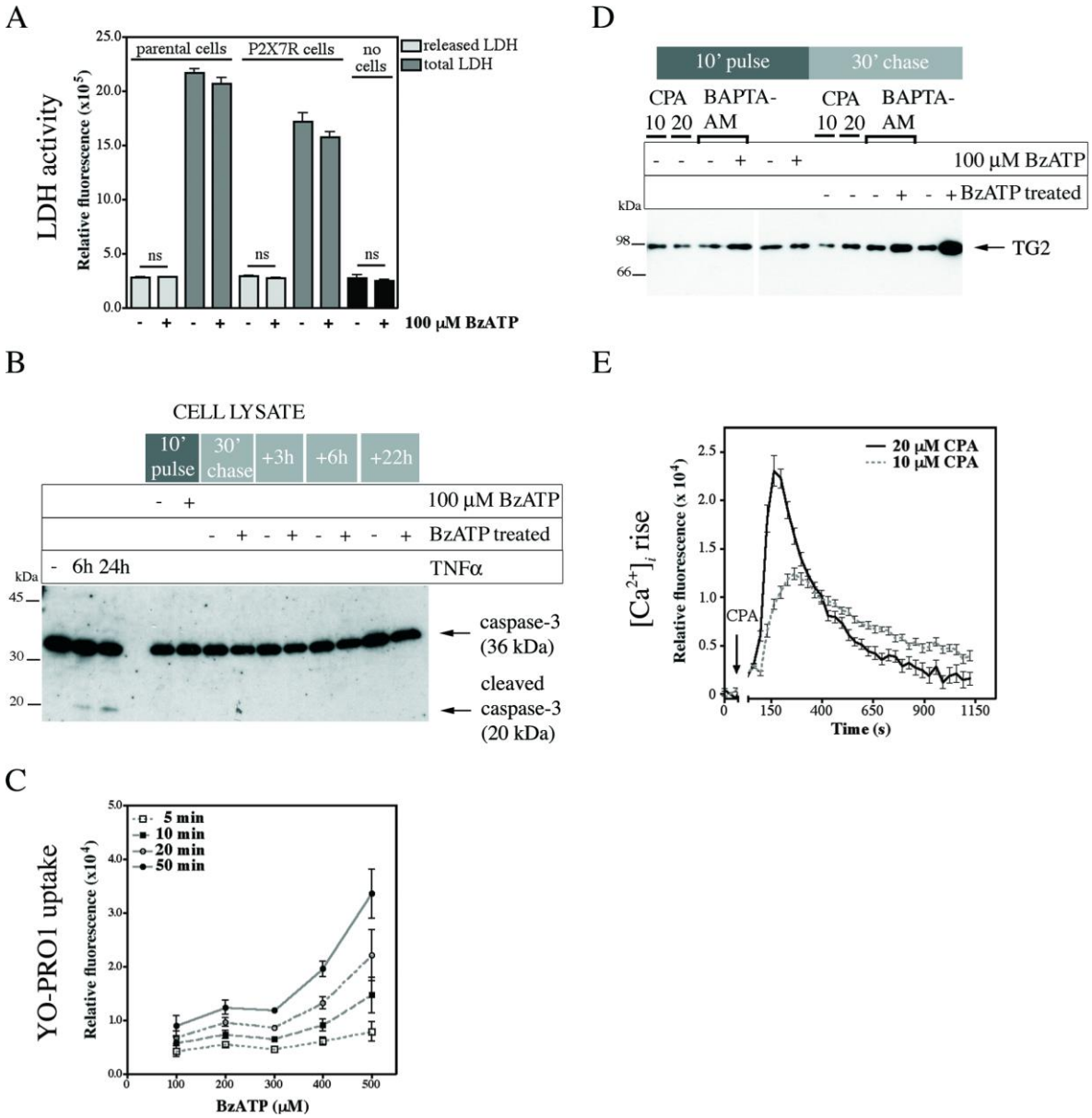

Fig. S3. P2X7R-mediated TG2 release is not due to compromised cell integrity or induction of cell death, and requires events beyond Ca^{2+} signaling.

(A) P2X7R activation is not compromising cell integrity. HEK293 P2X7R or parental cells were stimulated with BzATP for 10min as indicated, and then conditioned media assayed for LDH with (total LDH) or without (released LDH) prior cell lysis by measuring NADH-dependent resorufin fluorescence (λ_{Ex}=540-10nm, λ_{Em}=590-10nm) (mean±s.e.m., n=3; ns=not significant).

(B) P2X7R activation is not inducing apoptosis. P2X7R cells were BzATP stimulated and chased as before, and subsequently cultured in serum containing medium for up to 22h. Alternatively, apoptosis was induced with 20ng/ml TNFα for indicated time. Cell extracts were analysed by Western blotting for cleaved caspase-3.

(C) P2X7R-dependent "membrane pore" activity is characterized by two states induced at different agonist concentrations. P2X7R cells were stimulated with various concentrations of BzATP in PSS

containing YO-PRO1, and fluorescence changes over time upon continuous agonist stimulation monitored as outlined in Fig. 5C. Results are given as mean fluorescence±s.e.m. at different time points, and show that the cell response to different agonist concentrations displays a biphasic profile. This highlights firstly that for BzATP≤300μM, altering BzATP concentration relative to Ca^{2+} concentration does not alter dye uptake in line with changes in free nucleotide concentration and secondly, that the cellular response >300μM BzATP involves an additional mechanistic component with slower kinetics.

(D) Rise in intracellular Ca^{2+} concentration alone is not sufficient to induce TG2 secretion but is a necessary component. P2X7R cells expressing TG2 were treated with 10 or 20μM CPA in Ca^{2+}-free medium to release Ca^{2+} from intracellular stores. Alternatively, cells were washed with Ca^{2+}-free medium, pre-treated with 10μM cell permeable Ca^{2+}-chelator BAPTA-AM for 10min where indicated, and then BzATP stimulated for 10min as indicated. Cells were then chased for 30min in BzATP/CPA-free medium. Conditioned media were analyzed by Western blotting for TG2.

(E) Changes in $[Ca^{2+}]_i$ mediated by CPA. Change in fluorescence in Fluo-4-AM loaded cells in response to CPA relative to control was monitored (mean±s.e.m. of 8 replicate wells).

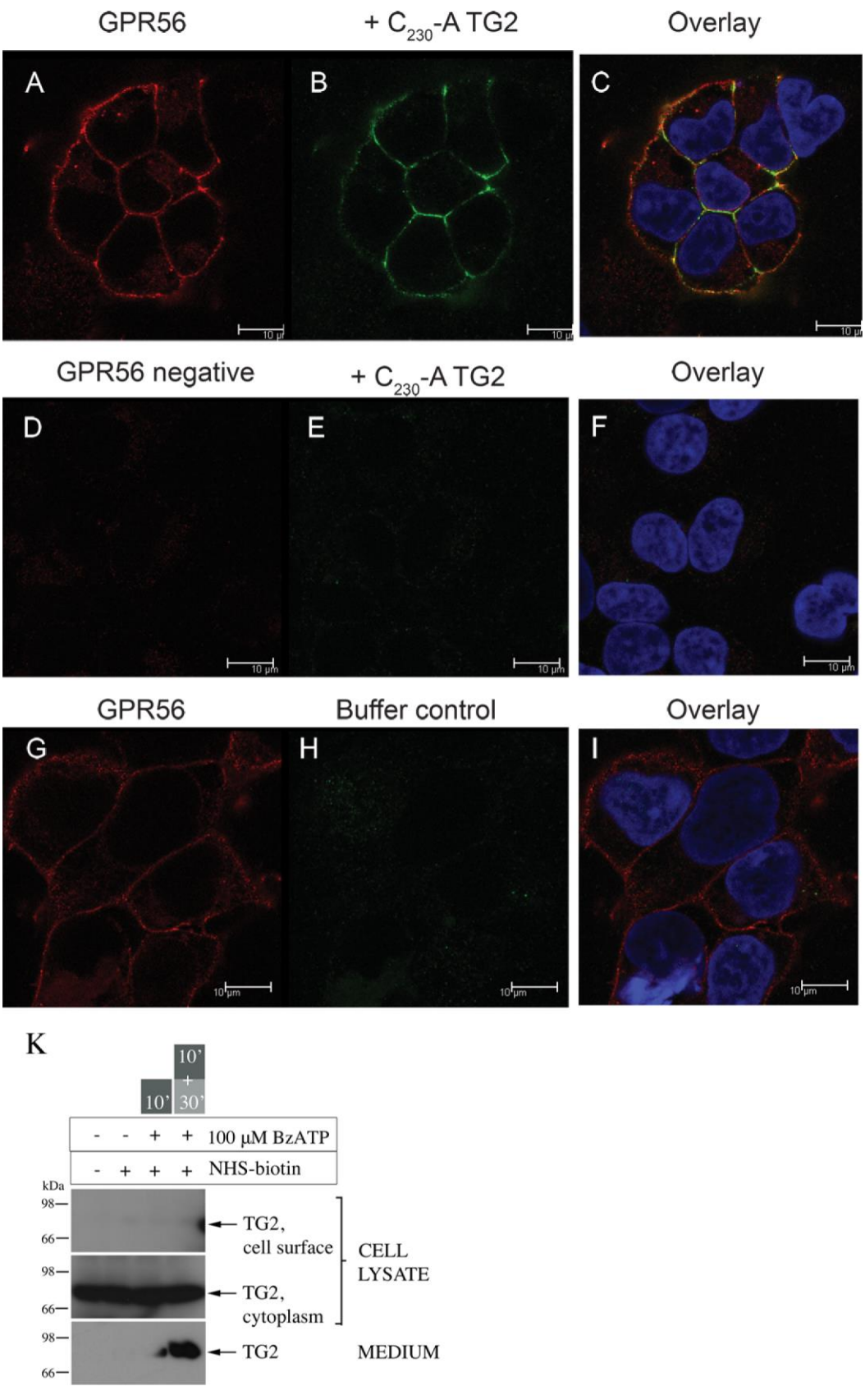

Fig. S4. TG2 is not sequestered to cell surface in HEK293 cells.

(A-I) HEK293 flp-in cells stably expressing the G-coupled receptor GPR56 under control of a tetracycline repressor sensitive promoter (T-REx system) were seeded onto poly-L-lysine coated coverslips and receptor expression induced with doxycycline for 48h (A-C, G-I) prior to treatment with 20μg/ml of the oxidation resistant TG2 C^{230}A mutant (A-C, D-F) or control buffer (G-I) for various times. Cells were fixed, permeabilised and stained with antibodies to the *N*-terminus of GPR56 (red) or to TG2 (green). Data shown reflects 5s after stimulation with TG2. In GPR56 negative cells, no cell surface association of TG2 was observed (E,F), and this remained unchanged even after prolonged incubation for up to 30min. In contrast, expression of one of the receptors, GPR56, known to interact with TG2 lead to rapid cell surface association of TG2 (B,C), and subsequent internalisation.

(K) To further confirm the absence of extracellular cell- or matrix-associated TG2, HEK293 P2X7R cells expressing wildtype TG2 were BzATP stimulated as before, and the cell layer biotinylated as in Fig. S1C either immediately after 10min of stimulation or following a 30min chase without agonist. Extracted unmodified proteins (cytoplasm) or proteins carrying biotin (cell-surface/matrix) were analysed for TG2 by Western blotting alongside media collected after pulse and chase, respectively. Virtually none of the externalized TG2 was associated with the cell layer in HEK293 cells in contrast to macrophages (compare to Fig. S1C) which are known to harbor active enzyme at the cell surface (Toth et al., 2009).

Table S1. Oligonucleotides used to generate expression constructs. Mutated nucleotides are shown in bold face.

cDNA Construct	Forward primer	Reverse primer
P2X7R	*5′-* TTAGGTACCTTCACCATGCCGGCC TGCTGC	*5′-* TTTCTCGAGTCAGTAAGGACTCTTGAAGCC ACTGTA
P2X7R-V5	see P2X7R	*5′-* TTTCTCGAGGTAAGGACTCTTGAAGCCACT GTACTG
P2X7R variant B	see P2X7R	*5′-* TTCTCGAGTTAGTCACTTCCTTCTCCAAAC CATTTTCCTAAAGCATGGAAAAGAGA
P2X7R $P^{451}L$	*5′-* GACACACCCC**T**GATTCCTGGAC	*5′-*CAGGAATC**A**GGGGTGTGTCATGG
P2X7R $A^{348}T$	*5′-*GTCTGGCC**A**CTGTGTTCATCG	*5′-*GAACACAG**T**GGCCAGACCGAAG

Table S2. Expression constructs for GFP-tagged human TG2 based on pRc/CMV vector[a]

Fusion protein	Sequence
TG2-GFP	atg... gcc-cccaagctt-atg... aaa-gcggccgctcgagcatgcatctag ^{1}M -*hTG2*- ^{687}A - P K L -^{1}M -*GFP*- ^{238}K - A A A R A C I
GFP-TG2	atg... aaa-gcggccgctcgagcagatcccgcggcc-atg... gcctaa ^{1}M -*GFP*- ^{238}K - A A A R A D P A A - ^{1}M -*hTG2*- ^{687}A

a; pRc/CMV-GFP vector was a kind gift of Dr Olmstedt, University of Rochester, New York , USA (Olson et al., 1995).